Fire Modeling Results for Sprinkler Trade-offs Related to Building Size/Egress, Unprotected Opening Areas and Fire Resistance Ratings for Selected R-2 Occupancies

by
Nicholas A. Dembsey
Brian J. Meacham
Honggang Wang
Praveen Kamath

Fire Protection Engineering
Worcester Polytechnic Institute

WPI

For
Project FAIL-SAFE
National Association of State Fire Marshals Fire Research & Education Foundation

Executive Summary

Three major sprinkler trade-offs including Egress, Unprotected Opening Area (UOA) and Fire Resistance Rating (FRR) are addressed in this report by computational modeling. Assumptions including initial and boundary conditions are made to provide a set of environmental conditions for computational modeling, which mainly focus on parameters of the fire, building type/materials and control logics.

The computational modeling addresses three building Configurations: Configuration I that does not have a sprinkler system by design, Configuration II that does have a sprinkler system by design and the sprinkler system functions well, and Configuration III that has a sprinkler system by design but the sprinkler system does not function. The third is further divided into Configuration III-A and III-B, with the former being a building Type VA and the latter being a building Type VB. Buildings of Configuration I is also called buildings without sprinkler trade-offs, whereas buildings of Configuration II and III-A/III-B are also called buildings with sprinkler trade-offs. Buildings of Configuration I and Configuration III-B are small in size, whereas buildings of Configuration II and III-A are in larger in size. From Configuration I to Configuration III-A the simulations of sprinkler trade-offs focus on the egress issues stemming from enlarged building size, from Configuration I to Configuration III-B the simulations of sprinkler trade-offs focus on the UOA and FRR issues.

For egress modeling, PATHFINDER is adopted to simulate the RSETs and FDS is adopted to simulate the ASETs, they together work out a set of egress safety factors which is the ratio of ASET and RSET given a specific scenario pair of fire and egress. Fire scenarios are varied by changing the fire Soot Yield from 0.052 to 0.1, fire HRR in a sprinkler controlled fire from 0.5MW to 1MW, fire growth rate from fast to Ultra-fast/slow, corridor door state from both open to one open/both closed. Egress scenarios are obtained by changing the corridor door state from open to close, the occupants state from all normal indicating a common walking speed to half normal indicating a discounted walking speed, the initial delay time or pre-movement time from zero to 90s/180s/300s, and the exits' state from available to disabled. Overall the egress scenarios are divided into three categories: Best, Worst and Mean. Best egress scenarios delegate the most advantageous situations that make the most use of ASET of each exit, whereas worst egress scenarios delegate the most adversary situations that make least use of ASET of each exit, mean egress scenarios are just between them. The most important conclusions from the egress modeling are: (a) If no corridor door is closed, although buildings with sprinkler trade-offs generally perform better than buildings without sprinkler trade-offs, the life risk of occupants is not negligible and increases quickly with the delay time; (b) If one corridor door is closed, buildings without sprinkler trade-offs generally performs as same as buildings with sprinkler trade-offs when sprinklers do function as design, but better when sprinklers do not function as design. If both corridor doors are closed, buildings without sprinkler trade-offs generally performs much better than that with sprinkler trade-offs, but in each case successful evacuations can be ensured because the safety factors are large enough..

For UOA modeling, FDS is adopted to simulate the radiation heat flux based on the four pairs of UOA and FSD allowed in the IBC Code. Fires in a standalone apartment that has all the openings connected directly to outside are discussed first, followed by fires in

building apartments that has part of the openings connected to a narrow corridor. The most important difference between these two cases is that the ventilation conditions of a standalone apartment fire is much better than that of a building apartment fire. The major conclusions of UOA modeling is that the minimum FSD should be kept no less than 6ft instead of 3ft listed in the IBC code.

For FRR modeling, a commonly used structural engineering software by practicing professionals, RISA software suite [1] is used. The two separate proprietary products from RISA suite, namely RISA-Floor [2] and RISA-3D [3] are adopted for the current work to carry out fire resistance rating studies. In this study, reduced cross-section modeling theory is adopted to simulate the loss of sectional capacity due to charring of wood framing members. The theory is extended to carry out a reduced section structural analysis on a single apartment unit using RISA software suite. The main findings of this study are: (a) The exterior wall panels on the shorter direction lose their axial capacity. (b) The Loss of axial capacity of the walls occurs quicker in Type VB buildings (with sprinklers not operational) than in type VA buildings (with no sprinklers). This is attributed to the use of 1 hour rated gypsum wall boards used in type VA buildings and an unrated gypsum wallboard (or 30 min. rated) in type VB buildings and no operational sprinklers. (c) RISA-3D model of a single apartment floor system shows that the load-redistribution occurs when a wall supporting the diaphragm loses its axial capacity and hence does not result in a localized failure of the diaphragm. (d) The failure of the floor system is likely to occur when more than 75% of the walls supporting the diaphragm lose their axial capacity. (e) The failure trends obtained from the reduced section analysis of a single apartment wall and floor system shows that the fire is likely to travel horizontally to the neighboring apartments on the same level before it spreads vertically in a well-contained apartment.

The accuracy of the results may be improved by excluding some of the assumptions made in the current analysis by: (a) Using localized char depths in members (differential char) to determine the local failures in wall and floor systems. (b) Assuming orthotropic properties of wood, which takes into account the true behavior of the material. (c) Conducting a detailed finite element analysis of wall system, floor system and an assembly of both systems for a single apartment building. This could be extended to large buildings. However, the analysis of a full-structure is computationally demanding. (d) Modeling the gypsum wallboard into the FE analysis to conduct a sequential thermos-mechanical analysis.

Potential future research topics are also proposed.

(1) Details on the apartment fire scenarios

1.1. Background

In the first phase report of this project*, A Literature Review of sprinkler trade-off*, three major sprinkler trade-offs were identified: building size, Unprotected Openings Area, and structural Fire Resistance Ratings. In the second phase, these three sprinklers trade-off were evaluated by computer modeling. This report centers on Fire Modeling results in R-2 buildings with three sprinkler Configurations:

- Configuration I

  A small Type VA building (3 stories) that does not have a sprinkler system by design
- Configuration II

  A large Type VA building (4 stories) that does have a sprinkler system by design and it does function
- Configuration III

  There are further two sub-Configurations:

  III-A: A large Type VA building (4 stories) that does have a sprinkler system by design but it does not function

  III-B: A small Type VB building that does have a sprinkler system by design but it does not function

During the modeling process, Configuration I works as a benchmark fire scenario to be compared with the other fire scenarios. Configuration II is compared with Configuration III-A during the egress analysis. From Configuration I to Configuration III-A, the sprinkler trade-offs focus on the increase in building size including foot plan area and the number of stories, and thus the computer modeling addresses egress concerns. Although the trade-offs on travel distance are clearly stated in the IBC Code, it is not easy to design two comparable buildings which cover exactly this kind of trade-off. Therefore building size is chosen as the basic factor affecting the egress process. From Configuration I to Configuration III-B, the sprinkler trade-offs focus on the reduction of Fire Resistance Ratings (FRRs) of the walls/ceiling/floor, and thus the computer modeling is designed to address the concerns of structural stability and fire spreading to neighboring buildings. A summary of building Configuration categories are shown in the following table:

Table 1 Descriptions about building Configurations*

building configuration	construction type	foot plan area(ft^2) real/limit in IBC code	Stories real/limit in IBC code	S	F	usage
Configuration I	Type VA	10,617/12,000	3/3	No	NA	benchmark
Configuration II	Type VA	32,668/36,000	4/4	Yes	Yes	egress analysis
Configuration III-A	Type VA	32,668/36,000	4/4	Yes	No	egress analysis
Configuration III-B	Type VB	10,617/21,000	3/3	Yes	No	FRR and UOA analysis

*S=Does the building has a sprinkler system by design? F=Does the sprinkler system function? NA= Not Applicable

The egress analysis includes two components: RSET analysis and ASET analysis. For RSET analysis, the following factors are considered:

1) The availability of each exit during the egress process. If one exit is unavailable or disabled, occupants will not use this exit during the egress process.

2) The state of corridor doors: mechanically held open or closed.

3) The walking speed of different occupants. Occupants are divided into two groups: normal with common walking speed and non-normal with 50% discounted walking speed.

4) The initial delay time or pre-movement time denoting the time between the establishment of a fire and the decision of occupants to begin move along a means of egress.

For ASET analysis, the following factors are investigated:

1) The Soot Yield. Based on the components of materials used as the fuel in our research, which is a combination of 50% wood and 50% polyurethane, the Soot Yield is calculated as 0.052 based on data from the SFPE Handbook. Under more adverse conditions the Soot Yield might rise to a higher level. A higher Soot Yield fraction of 0.1 is adopted in this report.

2) Maximum HRR achieved in a sprinkler controlled fire. Based on our calculations a sprinkler is likely to function when the fire HRR arrives at 500kW. Under some extreme conditions, it is also possible for HRR to go over 1MW. Therefore 1MW is set to be the maximum HRR that could occur in an apartment fire.

3) The Fire Growth Rate. Three Fire Growth Rates are considered in this report: Slow, Fast, and Ultra-fast, with more simulations about Ultra-fast fires since they represent more adversary conditions.

4) The state of corridor doors. Usually fire doors are kept closed when no one is passing through. In case of emergency, however, they might be held open intentionally or accidently. Some research shows that whether doors are kept closed during a fire incident has great influence on the ASET of a building [4]. In this report only the two corridor doors on the floor where a fire initiates are taken into account since they are the most important doors in the sense of smoke control, corridor doors on other floors have little effect on the ASET because occupants would have left the floor before they can be helpful. Three options of corridor door state are simulated in this report: both corridor doors closed, only one corridor door closed (more specifically it is the North corridor door which is close to the fire apartment), both corridor door open.

The UOA analysis has two ambient conditions for the apartments involved in fire: standalone apartment and building apartment. The ventilation conditions between standalone apartment fire and building apartment fire are different. Due to all the openings connected to the outside ambient, air supply in standalone apartment fire is much easier than that in building apartment fire where at least one openings have to connect to a narrow corridor. For building apartment fire, two fire scales are considered: one apartment being involved in fire and five apartments being involved in fire.

The simplified structural analysis for this study includes reduced section analysis of a single apartment building considering a uniform temperature distribution and a uniform charring of framing elements. The structural analysis was carried out using the RISA software suite (RISA-3D and RISA Floor). RISA Floor application was used to determine the loss of axial capacity of wood-framed walls whereas RISA-3D was used to determine the loss of flexural capacity of the dimensional lumber floor system for a single apartment unit. The apartment was loaded using the load combinations according to IBC2015 ASD. An additional point load and a moving load was also considered to account for the firefighter load. Different parameters associated with the structural behavior such as axial capacity of walls, member deflection, shear forces and bending moments of critical floor joists and plate stresses for the subfloor deck were studies at varying char depths. The results of the single apartment building were then extended to project the behavior of a multi-apartment building in the event of a fire spread.

1.2. Geometry model

In total four types of computational domain are presented below to deal with the simulations of FRR, egress, and UOA:

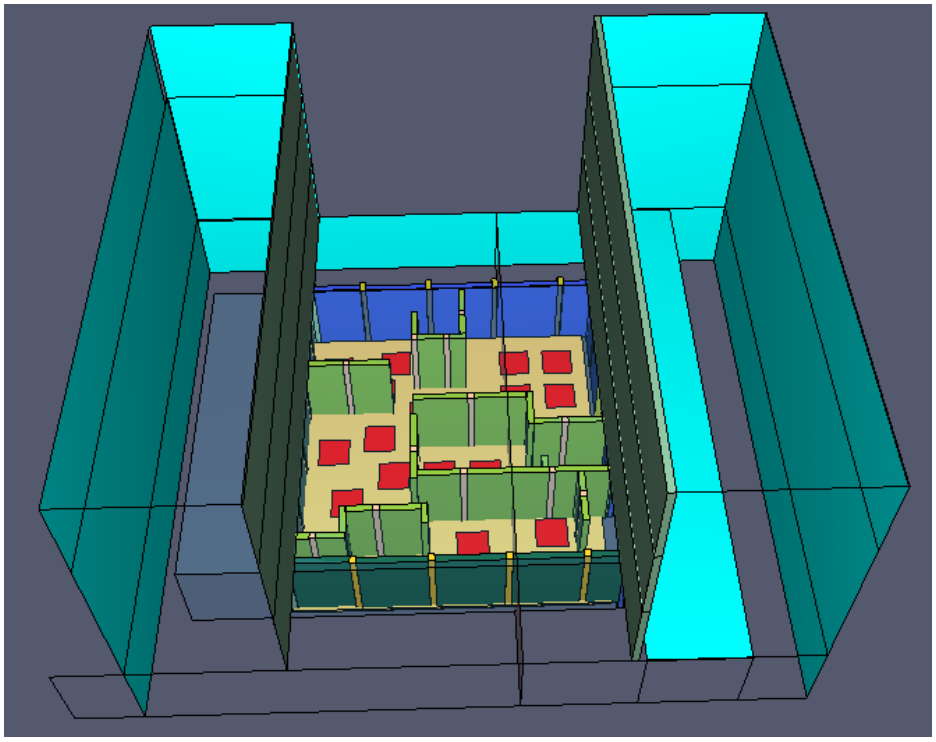

(a)Thermal model within an apartment

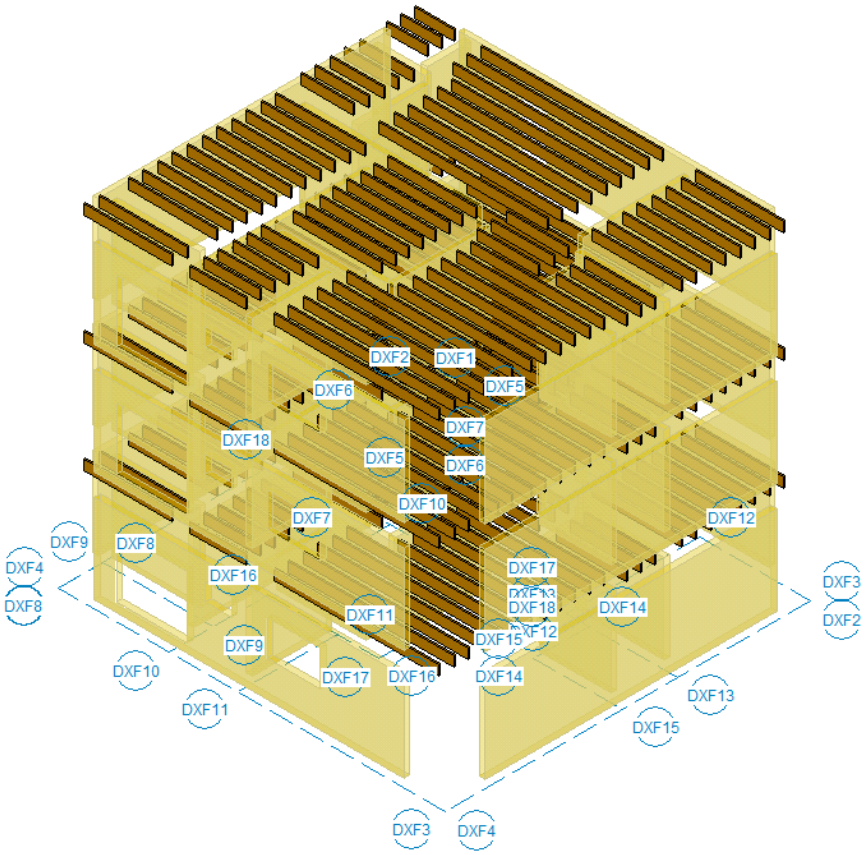

(b) structural model for 1 apartment,3 level

Figure 1 Computational domain for FRR analysis of Configuration I/III-B building

(for a), temperature curves developed through the walls/ceilings of Configuration I and Configuration III-B are compared; for b), degradation analysis/charring analysis of Configuration 1 and Configuration III-B based on the temperature rise curves are compared, and then structural stability analysis based on the reduced cross-section method are conducted)

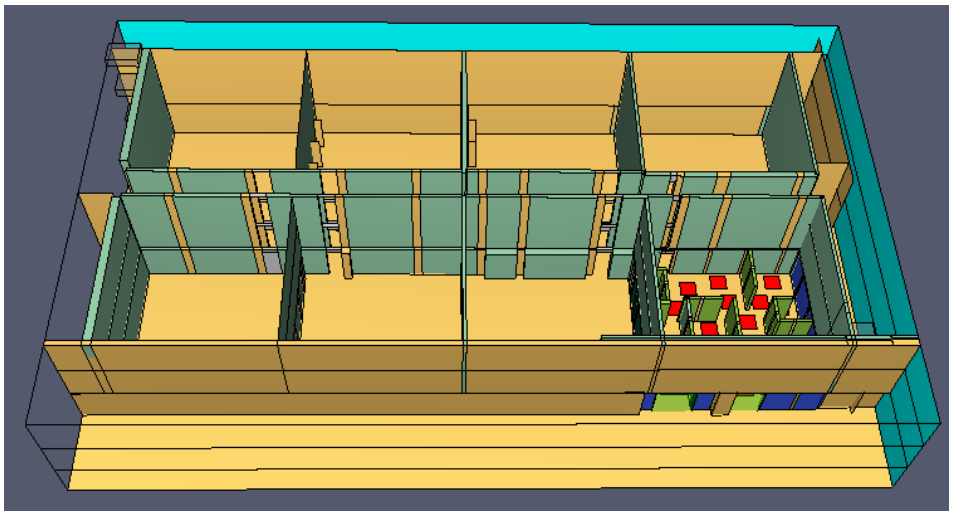

(a) Three-story building of Configuration I

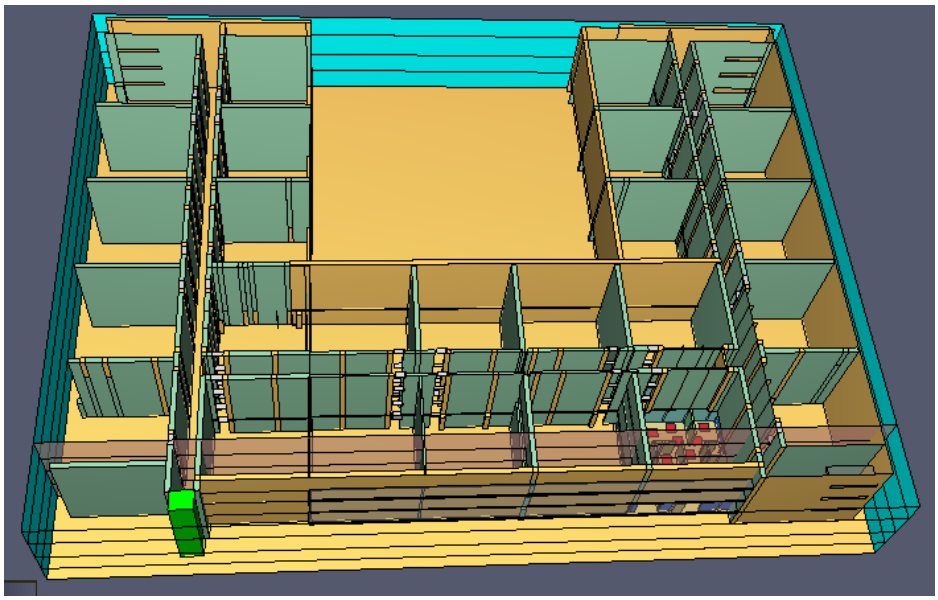

(b) Four-story building of Configuration II or III-A

Figure 2 Computational domains for egress analysis

(Available Safe Egress Times (ASETs) of Configuration I and Configuration II/III-A are simulated by FDS. Required Safe Egress Times (RSETs) are simulated by PATHFINDER)

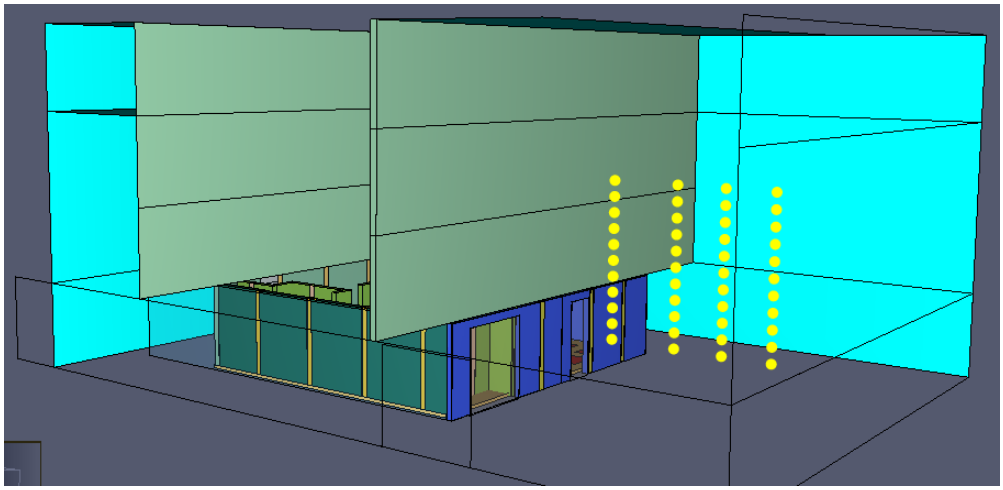

(a) Standalone apartment

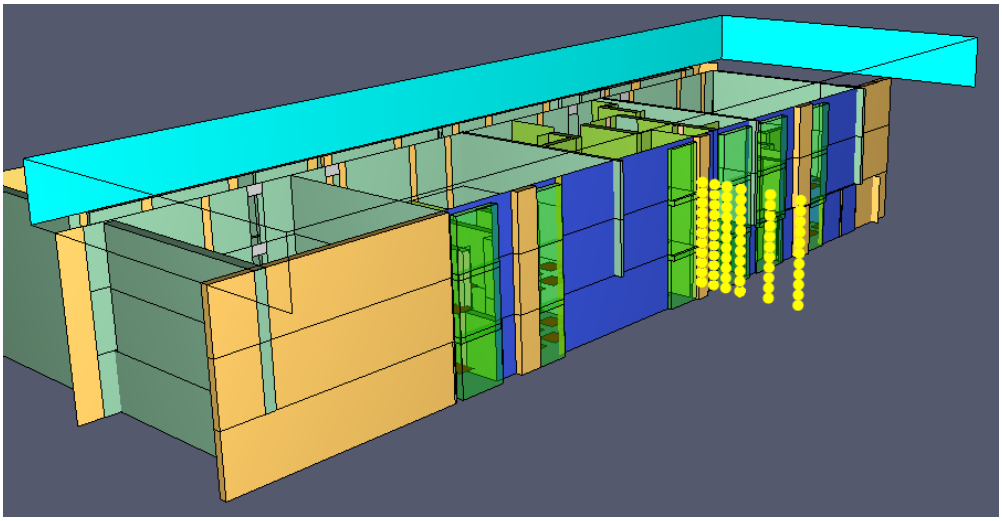

(b) Apartment building with three stories

Figure 3 Computational domain for UOA analysis

(Hazards of fire spreading to neighboring buildings are analyzed by setting various UOAs and observing heat fluxes in various locations from the fire façade. For (a), the distance from the four heat flux device trees to the façade are 3.8ft, 11.2ft, 16.5ft, and 21.8ft, as shown in (a) by yellow dots; For (b), the distance from the 6 heat flux device trees to the façade are 3.8ft, 5.6ft, 8.3ft,11.2ft,16.5ft, and 21.8ft, as shown in (b) by yellow dots)

Before starting comprehensive simulations, a cell size sensitivity analysis was conducted to select a cell size with both acceptable accuracy and plausibility. A cell size of 0.24mx0.40mx0.125m (NO.R6) was adopted for FRR analysis and UOA analysis. More details are presented in **APPENDIX 1.**

1.3. Physical model for the severe fire scenario

a) Basic assumptions for severe fire scenarios (more details of calculations are presented in **APPENDIX 3)** :

- Gas burner model

To simplify the simulation, a gas burner model is adopted which eliminates the ignition process.

- Adverse fire load density

A relatively higher fire load is adopted to simulate a worst condition, namely

$$F_L = 600 + 500 + 130 + 40 = 1270 MJ / m^2$$

where 600 is the average contents fire load density, 500 is the standard deviation of contents fire load density, 130 is the average fixed fire load density and 40 is the standard deviation of fixed fire load density[5]

- Fire duration

Based on our fire load density, the fire duration is calculated to be 65.2 minutes. In our simulation 70 minutes or 4200s is adopted as simulation time for structural analysis and 30 minutes or 1800s for egress analysis since all the occupants will definitely leave the building within 30 minutes.

- T-squared fire- fast fire

To simulate the fire spreading process, 20 gas burners are set in the apartment. Each burner will grow as a T-squared fire. To simulate a worse condition, a fast fire with t_g = 150 s, which means a burner will achieve 1MW in 150 seconds, is adopted as benchmark case in this report.

- Fuel

To be close to a real fire, a mixed fuel made from half polyurethane and half wood (oak) is used as the fuel with a soot yield of 0.052 which is calculated from combustion characteristics of each component of the mixed fuel.

- HRR in sprinkler controlled fires

It is assumed that the fire will stop growing at the time of one sprinkler's activation, after activation the fire will keep a steady HRR simulating a condition under which a sprinkler can only control the fire spreading process but cannot extinguish a fire. The steady HRR after activation of one sprinkler is set to 500KW for a relatively severe fire in our benchmark case, more details about the calculation can be found in APPENDIX 2.

In addition, to simulate a more severe condition, a HRR of 1MW is adopted in the cases of "other options".

- Ventilation controlled fire

The fire power is designed to ensure a ventilation controlled fire after flashover.

- Smoke movement after activation of a sprinkler

Generally the activation of a sprinkler will decrease the smoke temperature and thus weaken the moving potential of smoke. To simplify the simulation it is assumed that no cooling effects from activation of a sprinkler are taken into account.

- Untenable criteria

According to Chapter 6 of "The Modeling Plan for Sprinkler Trade-offs Related to Building Size/Egress, Unprotected Opening Areas and Fire Resistance Ratings", the visibility of 5m is chosen as the desirable tenability criteria in our modeling plan.

b) Boundary/initial conditions

- Ambient temperature

The ambient temperature is set to 20^{o}C.

- Walls/floor/ceiling

All the walls/floor/ceiling are non-adiabatic.

- Apartment openings

There are three openings, a door connecting the corridor and two windows. The door is always open from the very beginning, the windows will be opened once the temperature sensors set in the head of the windows were activated based on a critical temperature of 300^{o}C.

- Initial fire

The fire starts from the burner in the corner of the kitchen and then spreads to other burners.

- Pre-movement time

Usually it will take more or less seconds for a person to confirm the fire before he or she decides to egress. In this report, zero second of pre-movement time is used in the benchmark case, three non-zero pre-movement times of 90s, 180s and 300s are used in cases of "other options",

- Construction and materials

Generally two construction types are involved in this report: Type VA and Type VB. The materials and sizes we use to construct type VA or Type VB buildings are shown below:

Table 2 Construction materials and sizes*

construction members	Type VA	Type VB
West wall(corridor wall)	GWB(5/8 ins)+wood stud(2x4 ins)/Insulator(4 ins)+GWB(5/8 ins)	GWB(1/2 ins)+wood stud(2x4 ins)/Insulator(4 ins)+GWB(1/2 ins)
North exterior wall	GWB(5/8 ins)+wood stud(2x4 ins)/Insulator(4 ins)+Woodboard(7/16 ins)	GWB(1/2 ins)+wood stud(2x4 ins)/Insulator(4 ins)+Woodboard(7/16 ins)
East exterior wall	GWB(5/8 ins)+wood stud(2x4 ins)/Insulator(4 ins)+Woodboard(7/16 ins)	GWB(1/2 ins)+wood stud(2x4 ins)/Insulator(4 ins)+Woodboard(7/16 ins)
South wall(compartment separations)	GWB(5/8 ins) + woodboard(3/8 ins)+ wood stud(4 ins)/Insulator(4 ins) +Woodboard(3/8 ins) + GWB(5/8 ins)	GWB(1/2 ins) + woodboard(3/8 ins)+ wood stud(4 ins)/Insulator(4 ins) +Woodboard(3/8 ins) + GWB(1/2 ins)
Internal partition walls	GWB(1/2 ins)+wood stud(2x4 ins)/Insulator(4 ins)+GWB(1/2 ins)	GWB(1/2 ins)+wood stud(2x4 ins)/Insulator(4 ins)+GWB(1/2 ins)
Floor/Ceiling	GWB(5/8 ins) + wood joist (2x10 ins) + wood deck(3/4 ins)	GWB(1/2 ins) + wood joist (2x10 ins) + wood deck(3/4 ins)

* the wood studs are 16 inches centered, but in the FDS simulation due to limitation of minimum cell size, finally five studs are wrapped to occupy one cell.

The various walls listed in the above table are labeled in the following figure:

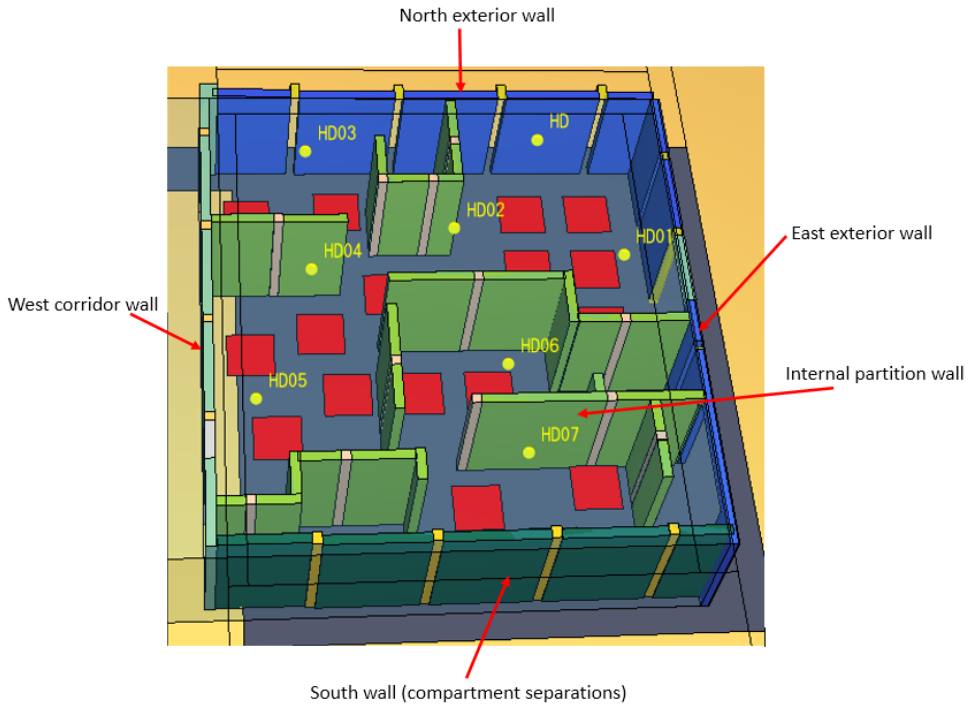

Figure 4 indication of various walls

c) Building Configurations for simulations of FRR, egress, and UOA

The occupancy group is R-2 based on the IBC code. The construction difference between a Type VA building and a Type VB building focuses on the thickness of Gypsum Wall Board (GWB).

- For FRR analysis

Two building Configurations are simulated for FRR analysis: Configuration I and Configuration III-B. It is assumed that no structural stability issues exist in a building that has a sprinkler system and it does function.

- For egress analysis

Three building Configurations are simulated for egress analysis: Configuration I, Configuration II, and Configuration III-A. It is assumed that no egress problems exist in a Type VB small apartment building that has a sprinkler system and it functions.

- For UOA analysis

Two building Configurations are simulated for UOA analysis: Configuration I and Configuration III-B. It is assumed that no hazards of fire spreading to a neighboring building exist in a building that has a sprinkler system and it does function.

Two ambient conditions are considered for apartment fire. In the first condition, the fire apartment is standalone with all the openings connected directly to the outside. In the second condition, the fire apartments are in an apartment building connected by corridors, leaving only the windows open to the outside. In the second condition, fire scenarios are divided into one apartment fire and five apartments fire, indicating a severe case and a more severe case.

d) Control logics

- Fire spreading control logic

The critical temperature for a neighboring burner to be ignited is set to 400 ^{o}C. This logic doesn't apply to UOA analysis in building apartments where the critical temperature is set to be only 100 ^{o}C to simplify the simulation process by reducing the time of fire spreading. This simplification is acceptable in that our main concern about UOA is during the stage of a post-flashover fire, leaving the fire spreading process less significant.

- Windows activation logic

The critical temperature for a window to be damaged and opened is set to 300 ^{o}C with a delay of 60s. With the same reason as above, this logic doesn't apply to UOA analysis in building apartments.

(2) Egress

2.1. Introduction to an analysis method based on egress safety factors

Based on the concept of egress safety factors, this section introduces an analysis method to assess the effects of sprinkler trade-offs on life risk of occupants

In real world, the egress progress of occupants and the smoke spreading process are interweaved together. The ways people use to egress are different. During the fire some people will choose to follow the directions of signs, some may use the exits they are most familiar with, the majority of the people may just follow others. Some exits may be available at the beginning but gradually lose their tenability as the smoke spreads. In other words different exits may provide different ASETs and people may use each exit until it becomes untenable.

In our work, however, the RSET and ASET simulations are separated and we have to set various egress scenarios to investigate the ratio of ASET to RSET, or the egress safety factor. Three egress scenarios are introduced here: best with highest probability (e.g. 90%), worst with lowest probability (e.g., 1%), and mean with considerable probability (e.g., 9%). In the best scenarios, we chose to close the exits with shorter ASET to work out the egress safety factors, ASET/RSET, which is physically reasonable. In the worst scenarios, we choose to close the exits with longer ASET, which is corresponding to the abnormal conditions, for example, that electrically controlled doors malfunction in case of emergency. Between them are the mean scenarios.

Factors that affect egress safety factors (ASET/RSET) can be classified into two categories: the ones influencing RSET and the ones influencing ASET. The former ones include Soot Yield, fire growth rate, the states of corridor doors (Open or Close) and Heat Release Rate (HRR) that can be achieved in a sprinkler controlled fire. The latter ones include states of occupants, availabilities of different exits, the states of corridor doors and the initial delay time before an egressing movement starts.

The analysis method follows the following steps to assess the effects of sprinkler trade-offs on life risk of occupants:

1) Assign a set of values to the environmental parameters that are needed by PATHFINDER to generate RSETs and by FDS to generate ASETs. These parameters are Soot Yield, Heat Release Rate(HRR) achieved in a sprinkler controlled fire, fire growth rate, states of corridor doors, states of occupants, and initial delay time before an evacuation action starts
2) Conduct the PATHFINDER and FDS simulation to determine the RSETs and ASETs
3) Pair the RSETs and ASETs and calculate the egress safety factor(ASET/RSET)
4) Based on the comparisons between safety factors of different building Configurations in different egress scenarios (Best, Worst, and Mean), discuss the advantages and disadvantages of sprinkler trade-offs.

2.2. Benchmark options

2.2.1. Explanation about the Benchmark options

In this chapter, some fundamental simulations are conducted. The following values are given to parameters used for RSET simulations in PATHFINDER:

1) Corridor door state: Both are open (All the other doors in floors other than the burning floor are open)
2) Occupants state: all are normal (means they can walk in a common speed)
3) Initial delay time (or pre-movement time): zero

The following values are given to parameters used for ASET simulations in FDS

1) Soot Yield (SY) : 0.052
2) Heat Release Rate in sprinkler controlled fires (or in a Configuration II building fire) : 0.5MW
3) Fire Growth Rate: Fast
4) Corridor door state: Both are open (All the other doors in floors other than the burning floor are open)

2.2.2. Building of Configuration I

This is a small foot print building (Figure 2 (a)), egress should not be a big concern but we should make it clear by FDS and PATHFINDER simulations.

a) RSET

PATHFINDER is employed to obtain the RSET under conditions of one exit or two exits available. Both SFPE hydraulic method and agent method (or steering method) are adopted.

The egress model in PATHFINDER is shown below:

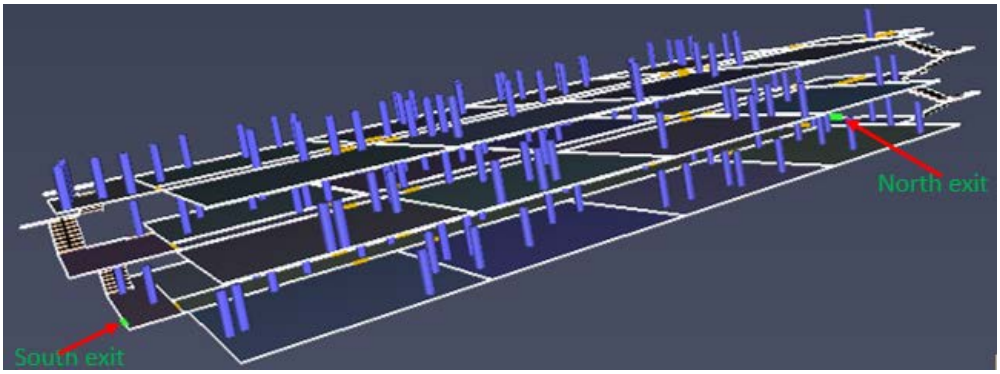

Figure 5 PATHFINDER egress model for building of Configuration I

Per IBC code, the occupancy load factor is 200ft^2/person for a R-2 occupancy group, therefore there are overall 157 persons in the building with total area of 31850 ft^2

There are two stairwells as exits. The two exits are just located in the two ends of the building.

The simulated RSETs under different conditions are shown below:

Table 3 RSETs under different conditions in Configuration I

Conditions	RSET(s)
South exit available, SFPE method	136
South exit available, steering method	147
North exit available, SFPE method	133
North exit available, steering method	153
Both exits available, SFPE method	87
Both exits available, steering method	93

b) ASET

FDS simulations are used to obtain the ASET. Each burner grows to 1MW in 150s following a T-squared curve, fire spreads to other burners when the critical temperature of 400 °C is met. Two sets of devices are installed in FDS model to record the visibility changes at the two exits located at the two ends of the building, as shown below:

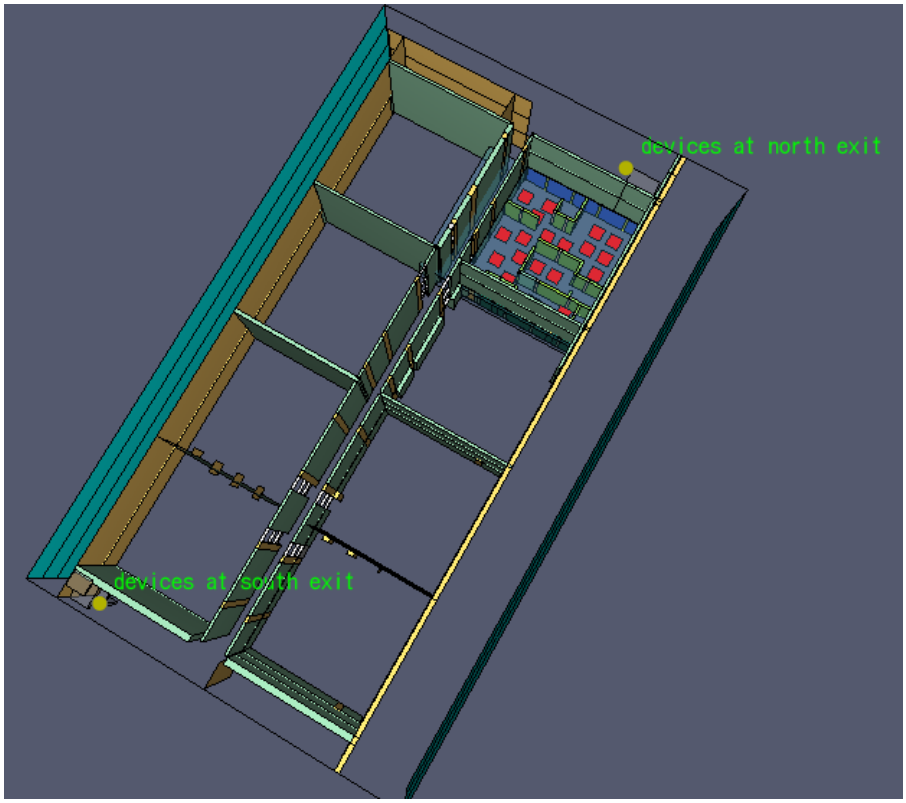

Figure 6 visibility devices at North and South exits

From FDS simulation, the HRR curves and the visibility curves at two exits are shown below:

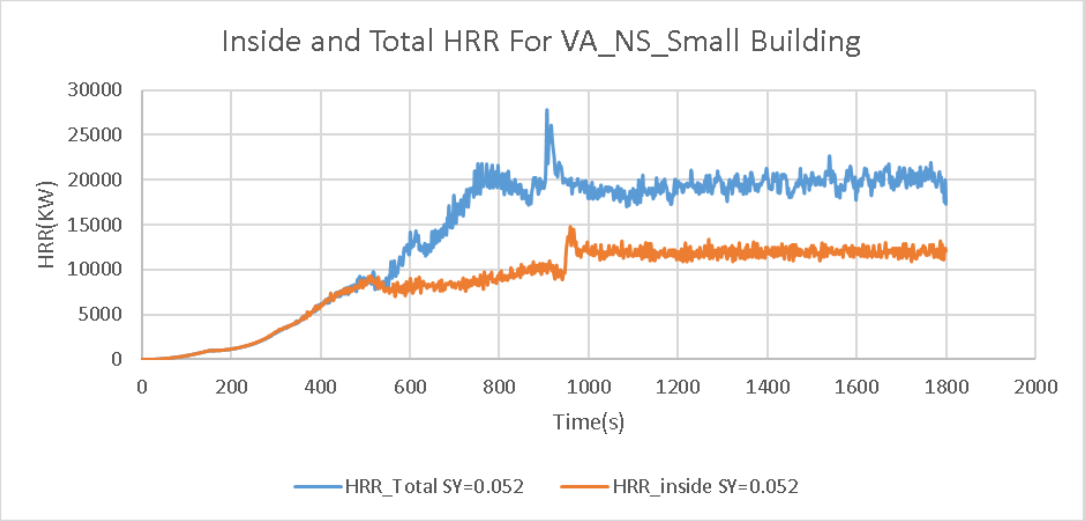

Figure 7 Total HRR and HRR inside the building of Configuration I

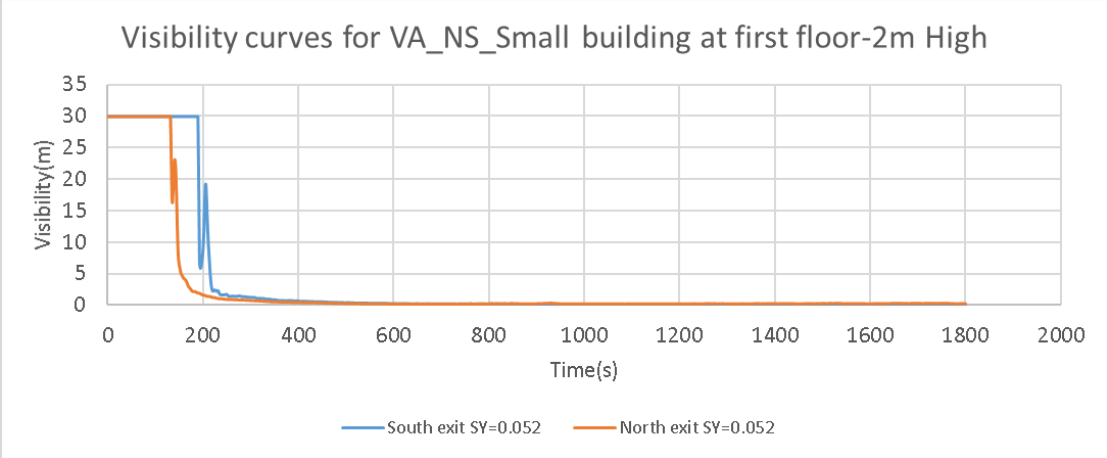

Figure 8 Visibility curves for the building of Configuration I at first floor

(Configuration I is "a Type VA small building that does not have a sprinkler system by design)

The above figure can be converted to the following ASETs table:

Table 4 ASETs provided by each exit in building of Configuration I

Exit	ASET(s)
South Exit	216
North Exit	155

2.2.3. Buildings of Configuration II or Configuration III-A

These are large foot print buildings (Figure 2 b)), egress should not be a big concern for building of Configuration II but we should make it clear by FDS and PATHFINDER simulations.

a) RSET

There are four PATHFINDER simulations employed to obtain the RSET under conditions of zero or one or two exits disabled. Both SFPE hydraulic method and agent method will be adopted

The egress model in PATHFINDER is shown below:

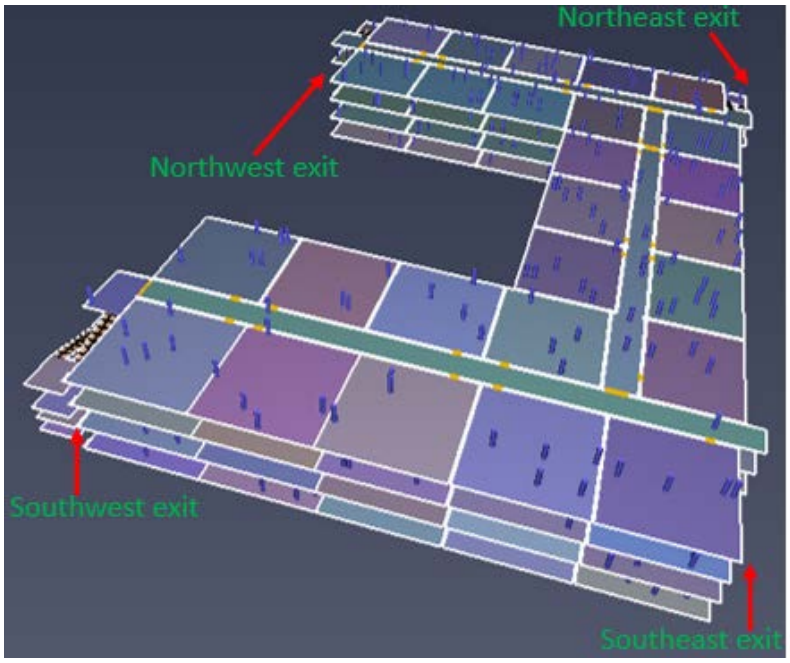

Figure 9 PATHFINDER egress model for building of Configuration II or III-A

(The occupancy load factor is 200 ft²/person, therefore there are overall 657 persons in the building with a total area of 130672 ft²)

There are three stairwells as exits. There is one more exit in the first floor mainly used for the elevators. The four exits are just located in the four corners of the building.

The simulated RSETs under different conditions are shown below:

Table 5 RSETs under different conditions in Configuration II and III-A

Conditions	RSET(s)
Southeast exit disabled, SFPE method	245
Southeast exit disabled, steering method	258
Northeast exit disabled, SFPE method	312
Northeast exit disabled, steering method	298
Northwest exit disabled, SFPE method	382
Northwest exit disabled, steering method	346
Southwest exit disabled, SFPE method	269
Southwest exit disabled, steering method	281
Both Southeast and Northeast exits disabled, SFPE method	312
Both Southeast and Northeast exits disabled, steering method	300
Both Northeast and Southwest exits disabled, SFPE method	433
Both Northeast and Southwest exits disabled, steering method	413
Both Northwest and Southeast disabled, SFPE method	382
Both Northwest and Southeast exits disabled, steering method	346
Both Southwest and Southeast disabled, SFPE method	299
Both Southwest and Southeast exits disabled, steering method	291
Zero exit disabled, SFPE method	245
Zero exit disabled, steering method	260

From this table some sensitivity analysis on different exits can be conducted. It shows that the RSET is not sensitive to the availability of Southeast exit but very sensitive to that of Northwest exit.

b) ASET

FDS simulations are used to obtain the ASET. Four sets of devises are installed in FDS model to record the visibility changes at the four exits located at the four corners of the building, as shown below:

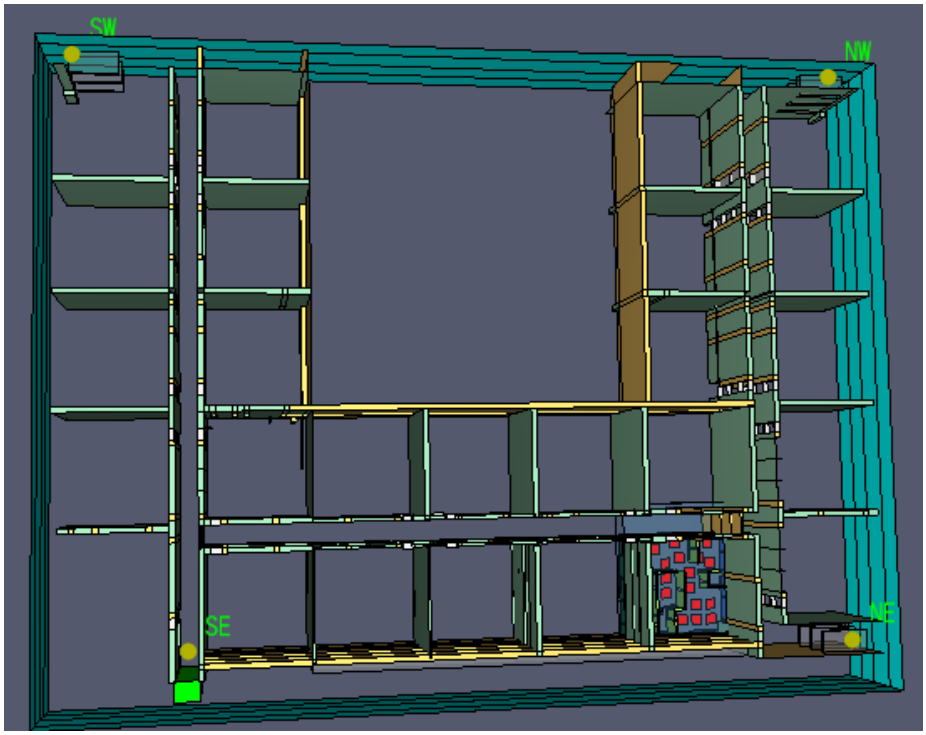

Figure 10 Visibility devices at four corner exits labeled as SW, SE, NE and NW

From FDS simulation, the HRR curves and visibility curves at four exits for building Configurations II are shown below:

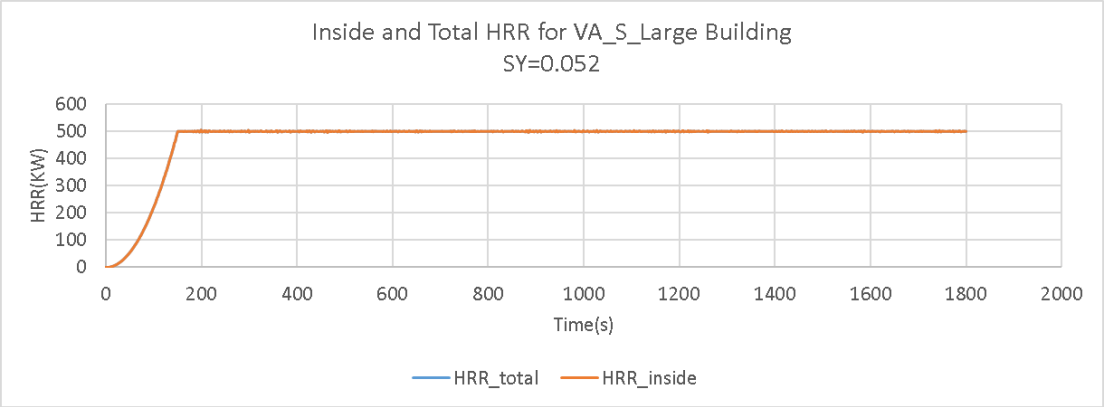

Figure 11 Total HRR and HRR inside the building of Configuration II

(*No HRR presents outside the building for a sprinkler controlled fire*)

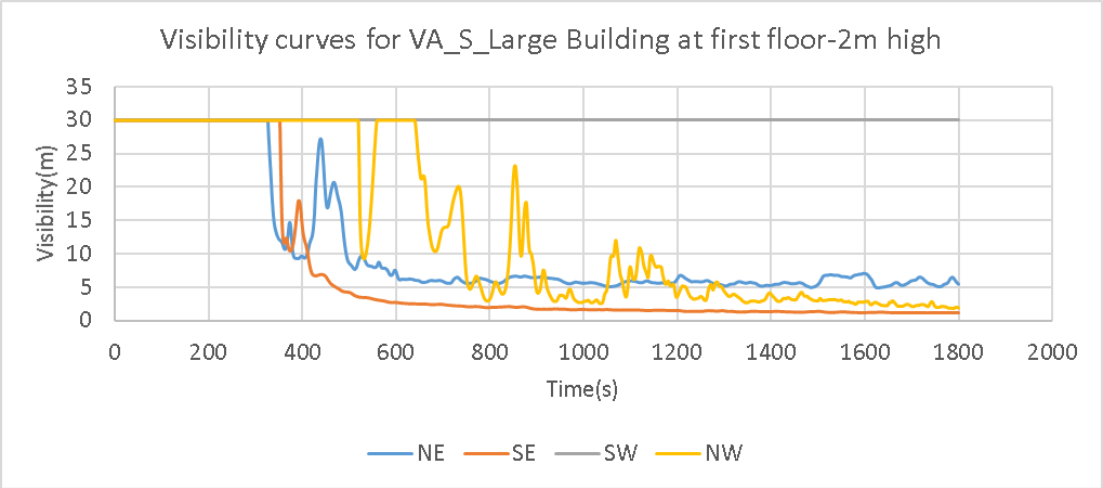

Figure 12 Visibility curves for building of Configuration II at the four corner exits

The above figure can be converted to the following ASETs table:

Table 6 ASETs provided by each exit in building of Configuration II

Exit	ASET(s)
Northeast	1490
Northwest	783
Southwest	>1800
Southeast	472

From FDS simulation, the HRR curves and visibility curves at four exits for building Configurations III-A are shown below:

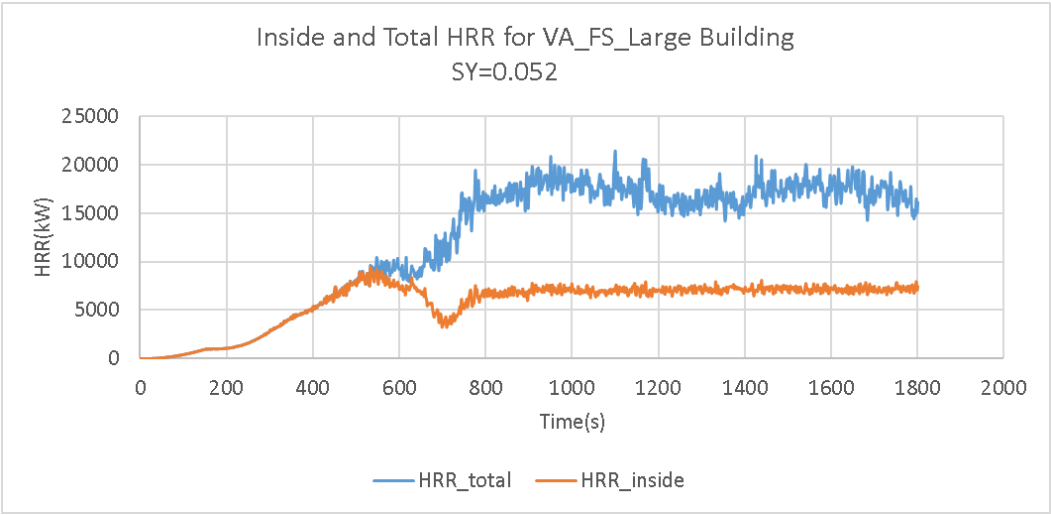

Figure 13 Total HRR and HRR inside the building of Configuration III-A

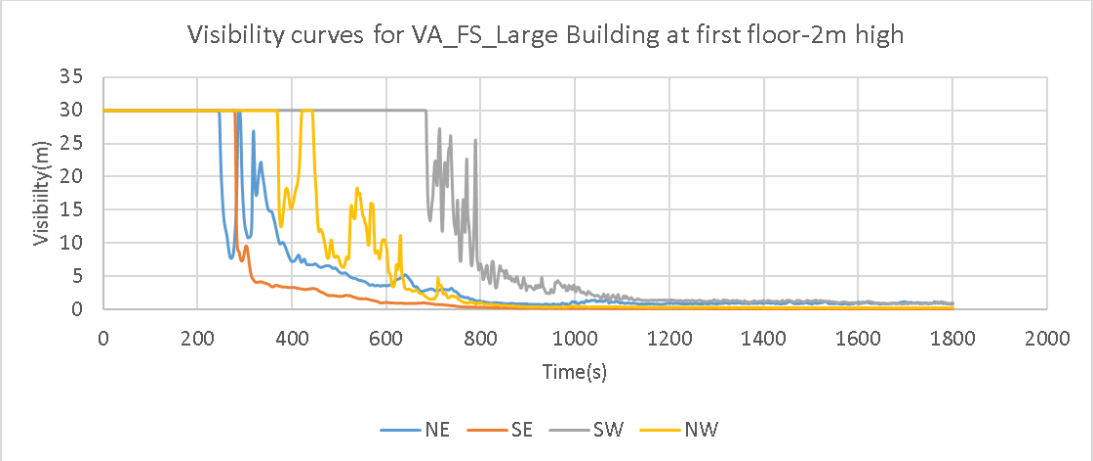

Figure 14 Visibility curves for building of Configuration III-A at the four corner exits

The above figure can be converted to the following ASETs table:

Table 7 ASETs provided by each exit in building of Configuration II

Exit	ASET(s)
Northeast	522
Northwest	608
Southwest	815
Southeast	320

2.2.4. Analysis on ASET/RSET

By integrating the RSETs and ASETs data in the above two sections, we have the following tables:

Table 8 Basic values of ASETs at various exits

Exit	ASET(s)
I- North exit	155
I- South exit	216
II-Northeast exit	1490
II-Northwest exit	783
II-Southwest exit	>1800
II-Southeast exit	472
III-A - Northeast exit	522
III-A - Northwest exit	608
III-A -Southwest exit	815
III-A - Southeast exit	320

Table 9 ASET/RSET changes in various building Configurations for best egress scenarios

building Configuration	ASET(s)	RSET(s)	Ratio of ASET/RSET
I- no exit disabled	155	93	1.67
I- North exit disabled	216	147	1.47
II-no exit disabled	472	260	1.82
II-Southeast exit disabled	783	258	3.03
II-Both Southeast and Northeast exits disabled	783	312	2.51
III-A - no exit disabled	320	260	1.23
III-A - Southeast exit disabled	522	258	2.02
III-A - Both Southeast and Northeast exits disabled	608	312	1.95

Table 10 ASET/RSET changes in various building Configurations for worst egress scenarios

building Configuration	ASET(s)	RSET(s)	Ratio of ASET/RSET
I- no exit disabled	155	93	1.67
I- South exit disabled	155	153	1.01
II-no exit disabled	472	260	1.82
II-Northwest exit disabled	472	382	1.24
II-Both Northeast and Southwest exits disabled	472	433	1.09
III-A - no exit disabled	320	260	1.23
III-A - Northwest exit disabled	320	382	0.84
III-A - Both Northeast and Southwest exits disabled	320	433	0.74

Table 11 ASET/RSET changes in various building Configurations for mean egress scenarios

building Configuration	ASET(s)	RSET(s)	Ratio of ASET/RSET
I- no exit disabled	155	93	1.67
I- North exit disabled	216	147	1.47
II-no exit disabled	472	260	1.82
II-Northwest exit disabled	472	382	1.24
II-Both Northwest and Southeast exits disabled	1490	382	3.90
III-A - no exit disabled	320	260	1.23
III-A - Northwest exit disabled	320	382	0.84
III-A - Both Northwest and Southeast exits disabled	522	382	1.37

In best scenarios, the ASETs of a building with one or two exits disabled are usually longer than that of the same building without disabled exits, the reason for this phenomenon is that we choose to disable the exit which becomes untenable sooner than others. This method is consistent with occupants' choice of escaping from untenable conditions during their egress progress.

A comparison of egress safety factors is shown in the following table:

Table 12 Changes of safety factors in various Configurations and scenarios

building Configuration	Ratio of ASET/RSET		
	B	W	M
I- no exit disabled	1.67	1.67	1.67
I- one exit disabled	1.47	1.01	1.47
II-no exit disabled	1.82	1.82	1.82
II-one exit disabled	3.03	1.24	1.24
II-two exits disabled	2.51	1.09	3.90
III-A - no exit disabled	1.23	1.23	1.23
III-A - one exit disabled	2.02	0.84	0.84
III-A - two exits disabled	1.95	0.74	1.37

*Yellow means the ratio is between 1.0 and 1.10, red means the ratio is less than one; B=Best, W=Worst, M=Mean

As stated at the beginning of this chapter, the best egress scenarios are the most common case with highest safety levels compared with the worst and mean case. The worst egress scenarios designate the extreme conditions when people have to go through the exits providing shortest ASETs. The mean egress scenarios do not mean that they could occur at an average probability but that the potential severity is between that of best and worst.

From **Table 12** we know that in most cases (namely the best scenarios) safety factors of Configuration II (sprinkler controlled fire) are higher than that of Configuration I (no sprinkler trade-offs). For Configuration III-A (sprinklered building but sprinklers do not function), two of the three scenarios have greater safety factors (2.02 and 1.95) than scenarios in Configuration I (1.67 and 1.47). Also for Configuration III-A, the scenario of “no exit disabled” has a lowest safety factor (the same phenomenon happens in other later sections of this chapter), which contradicts our common sense that more exits available means less risk. This contradiction stems from a characteristic of our method in which the ASET simulations are separated from the RSET ones. Therefore, although each red cell in the above table indicate ASET<RSET, it doesn’t mean that some occupants will be definitely trapped in smoke but that some occupants are still in the building when one exit initially available to them becomes untenable. Similarly, a yellow cell doesn’t necessarily mean the life risk is imminent but that the gap between the time when all occupants are successfully evacuated and that when one initially available exit becomes untenable is very narrow, or in other words, the safety margin is low.

In extreme cases (namely the worst scenarios), both Configuration I and II have one yellow cell indicating that the safety margin is low. The Configuration III has two red cells, indicating possible danger once some extreme conditions exist.

The safety factors in the mean scenarios are just between that in best and worst scenarios.

By combining these three scenarios, it seems that for our benchmark options the sprinkler trade-offs do not lower the egress safety level (the red cells happen in worst and mean scenarios which have much lower probability. More detailed analysis on benefits/costs of sprinkler trade-offs can be conducted by setting different weights and probabilities to the cells in the above table, which may present more interesting knowledge to deepen our understanding about sprinkler trade-offs.

In this chapter, the cells in Best cases with part exits disabled are illustrated in APPENDIX 4.

2.3. Influence of other options on egress safety factors

2.3.1. Soot Yield changing from 0.052 to 0.1

Based on the benchmark, which is SY=0.052, HRR=0.5MW for Configuration II, Fire Grow Rate = Fast, in this section only Soot Yield changes from 0.052 to 0.1.

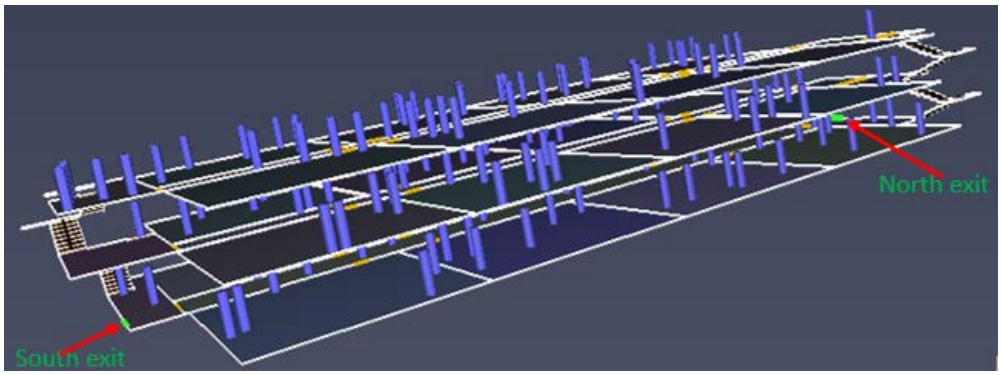

Figure 15 Locations of North and South exits for buildings of Configuration I

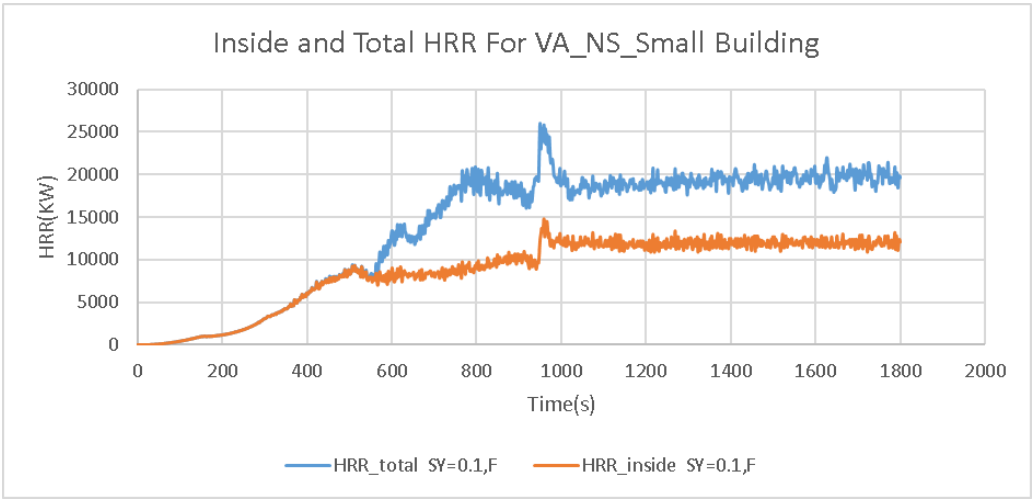

Figure 16 Total HRR and HRR inside the building of Configuration I

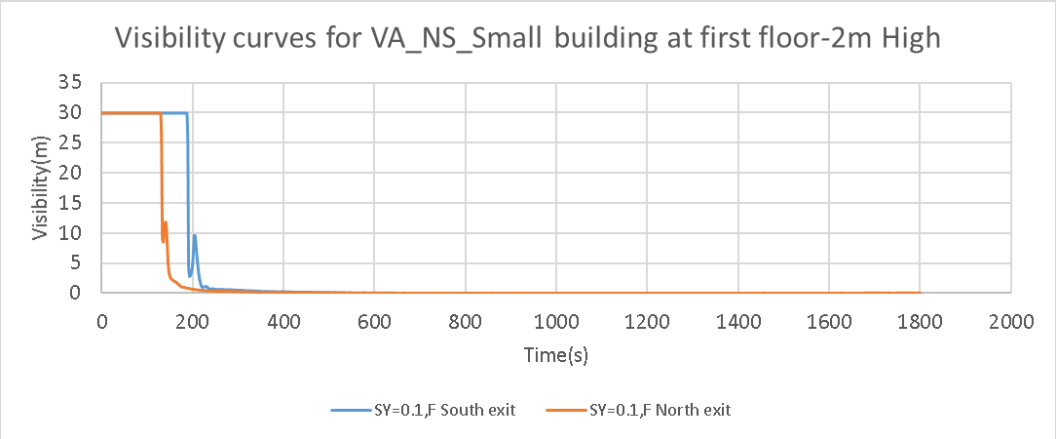

*SY=Soot Yield, F=Fast

Figure 17 visibility curves in a configruation I building

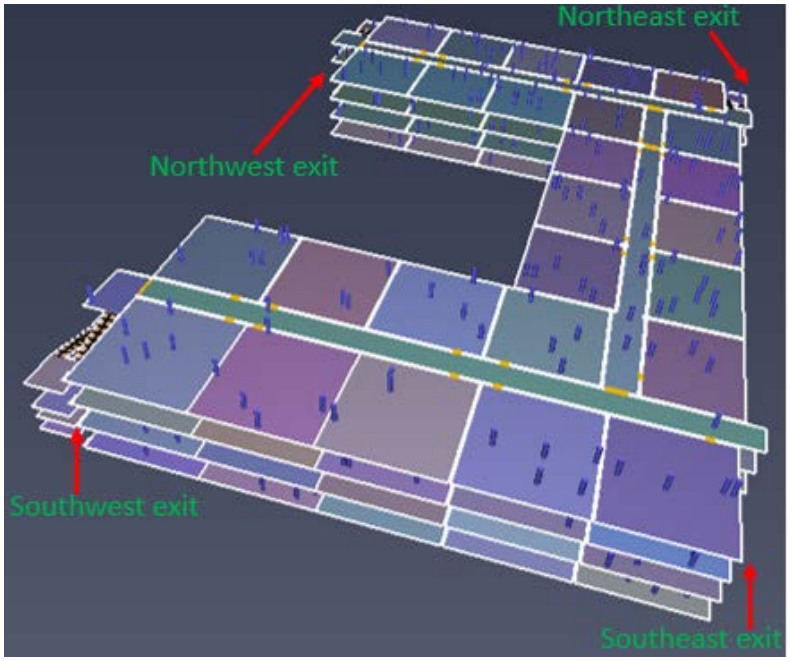

Figure 18 locations of four exits for buildings of Configuration II and III-A

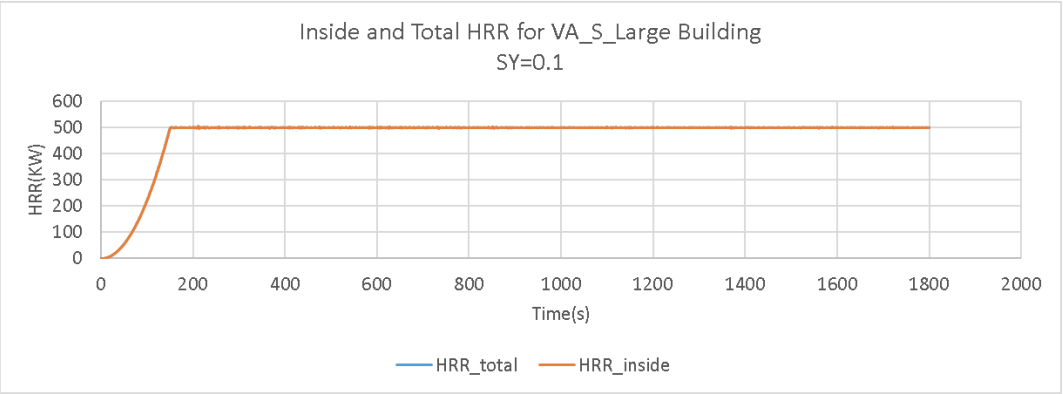

Figure 19 Total HRR and HRR inside the building of Configuration II

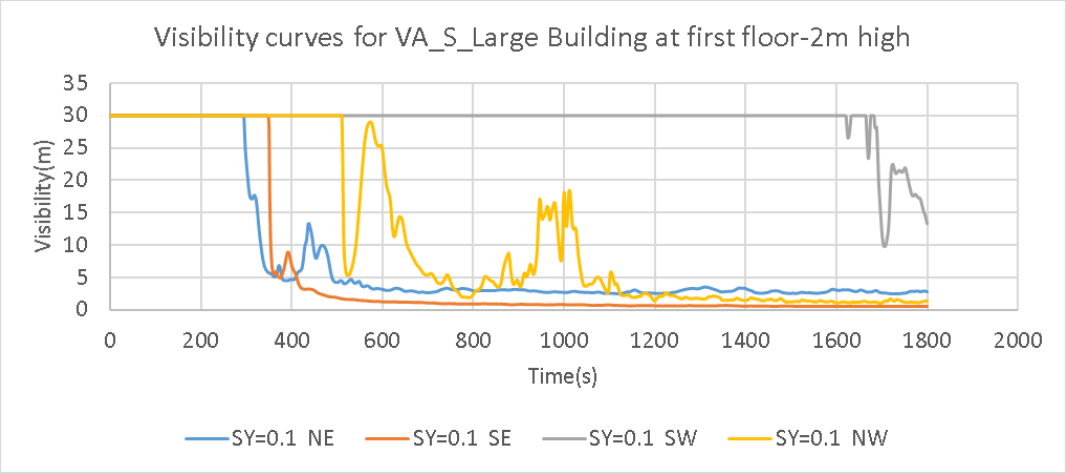

*SY=Soot Yield, NE= Northeast, SE=Southeast, SW=Southwest, NW=Northwest

Figure 20 visibility curves in a Configuration II building

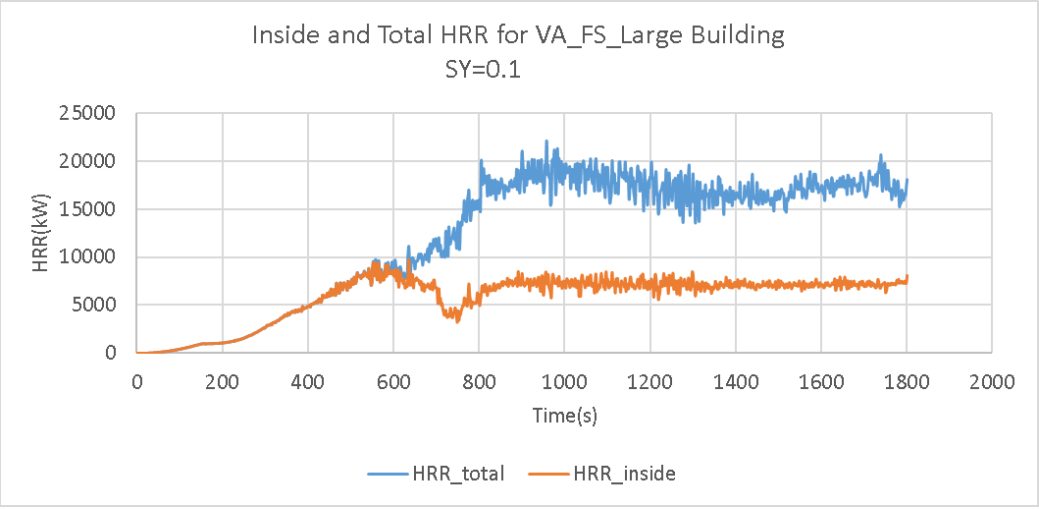

Figure 21 Total HRR and HRR inside the building of Configuration III-A

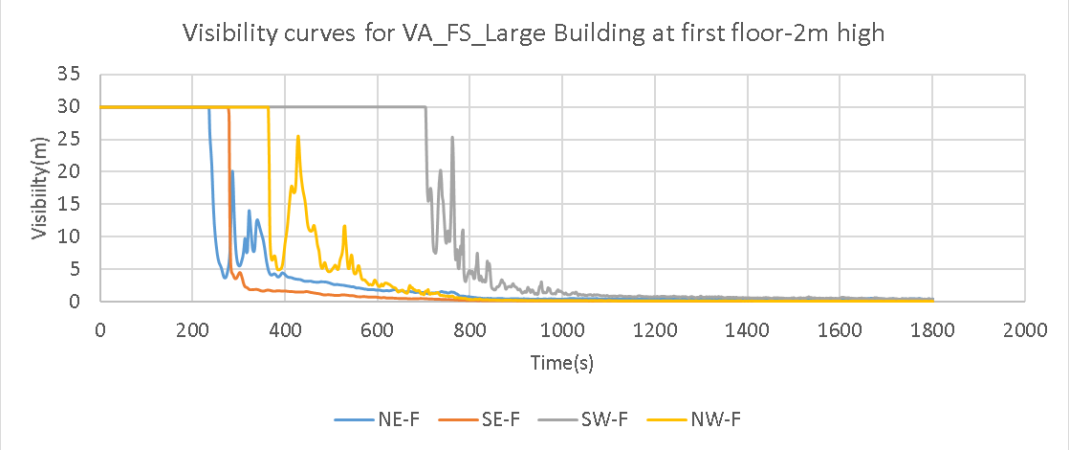

* NE= Northeast, SE=Southeast, SW=Southwest, NW=Northwest

Figure 22 visibility curves in a Configuration III-A building

Table 13 Basic values of ASETs at various exits for SY=0.1 compared with SY=0.052

Exit	ASET(s)	
	SY=0.1	SY=0.052
I- North exit	146	155
I- South exit	212	216
II-Northeast exit	490	1490
II-Northwest exit	716	783
II-Southwest exit	>1800	>1800
II-Southeast exit	412	472
III-A - Northeast exit	364	522
III-A - Northwest exit	549	608
III-A -Southwest exit	787	815
III-A - Southeast exit	284	320

The above table shows that a doubled soot yield may decrease the ASET of Configuration I, II, III-A by 3.5%, 23.5% and 10.8%, respectively, which means that the ASETs of buildings with sprinkler trade-offs are more sensitive to the change of soot yield than that of buildings without sprinkler trade-offs.

Table 14 ASET/RSET changes in various building Configurations for best egress scenarios-SY=0.1

building Configuration	ASET(s)	RSET(s)	Ratio of ASET/RSET
I- no exit disabled	146	93	1.57
I- North exit disabled	212	147	1.44
II-no exit disabled	412	260	1.58
II-Southeast exit disabled	716	258	2.78
II-Both Southeast and Northeast exits disabled	716	312	2.29
III-A - no exit disabled	284	260	1.09
III-A - Southeast exit disabled	364	258	1.41
III-A - Both Southeast and Northeast exits disabled	549	312	1.76

Table 15 ASET/RSET changes in various building Configurations for worst egress scenarios-SY=0.1

building Configuration	ASET(s)	RSET(s)	Ratio of ASET/RSET
I- no exit disabled	146	93	1.57
I- South exit disabled	146	153	0.95
II-no exit disabled	412	260	1.58
II-Northwest exit disabled	412	382	1.08
II-Both Northeast and Southwest exits disabled	412	433	0.95
III-A - no exit disabled	284	260	1.09
III-A - Northwest exit disabled	284	382	0.74
III-A - Both Northeast and Southwest exits disabled	284	433	0.66

Table 16 ASET/RSET changes in various building Configurations for mean egress scenarios-SY=0.1

building Configuration	ASET(s)	RSET(s)	Ratio of ASET/RSET
I- no exit disabled	146	93	1.57
I- North exit disabled	212	147	1.44
II-no exit disabled	412	260	1.58
II-Northwest exit disabled	412	382	1.08
II-Both Northwest and Southeast exits disabled	490	382	1.28
III-A - no exit disabled	284	260	1.09
III-A - Northwest exit disabled	284	382	0.74
III-A - Both Northwest and Southeast exits disabled	364	382	0.95

A comparison of egress safety factors are shown in the following table:

Table 17 comparison of safety factors in various Configurations and scenarios-SY

	SY=0.1			SY=0.052		
building configuration	B	W	M	B	W	M
I- no exit disabled	1.57	1.57	1.57	1.67	1.67	1.67
I- one exit disabled	1.44	0.95	1.44	1.47	1.01	1.47
II-no exit disabled	1.58	1.58	1.58	1.82	1.82	1.82
II-one exit disabled	2.78	1.08	1.08	3.03	1.24	1.24
II-two exits disabled	2.29	0.95	1.28	2.51	1.09	3.9
III-A - no exit disabled	1.09	1.09	1.09	1.23	1.23	1.23
III-A - one exit disabled	1.41	0.74	0.74	2.02	0.84	0.84
III-A - two exits disabled	1.76	0.66	0.95	1.95	0.74	1.37

*Yellow means the ratio is between 1.0 and 1.10, read means the ratio is less than one

The above table shows that when Soot Yield increases from 0.052 to 0.1, the safety factors of buildings with sprinkler trade-offs(Configuration II and III-A) drop faster than that of buildings without sprinkler trade-offs (Configuration I), indicating that buildings with sprinkler trade-offs are more sensitive to Soot Yield than buildings without sprinkler trade-offs.

2.3.2. HRR for sprinkler controlled fire changing from 0.5MW to 1MW

Based on the last section, which is SY=0.1, HRR=0.5MW for Configuration II, Fire Grow Rate = Fast, in this section only HRR for Configuration II, which is a sprinkler controlled fire, increase to 1MW.

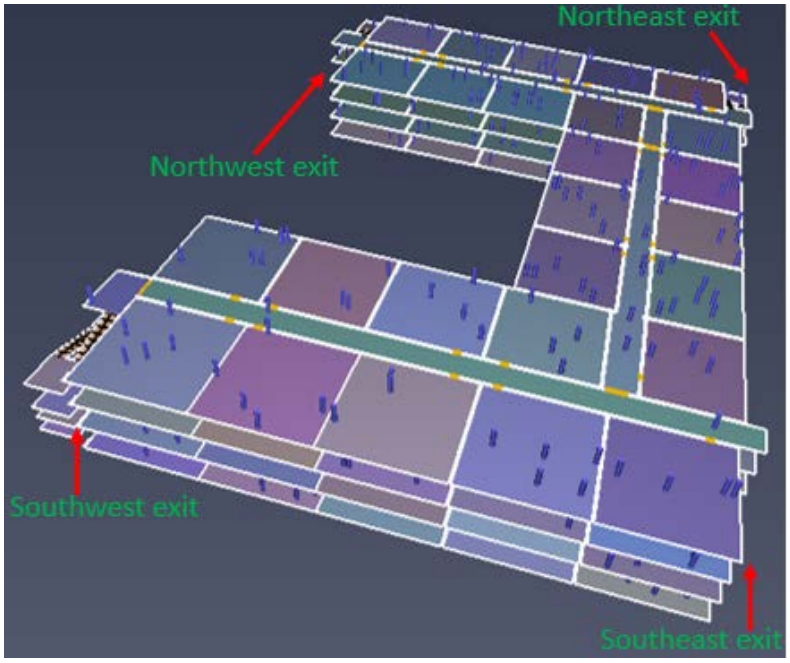

Figure 23 Locations of four exits for building of Configuration III-A

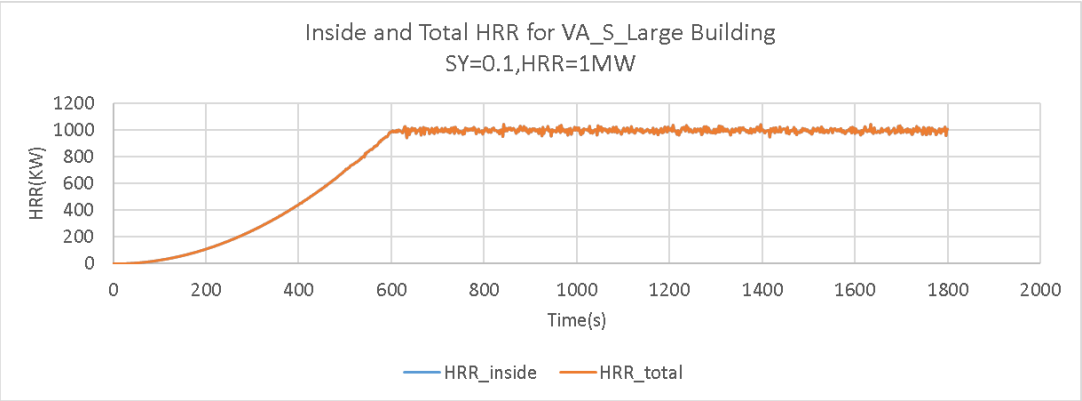

Figure 24 Total HRR and HRR inside the building of Configuration II

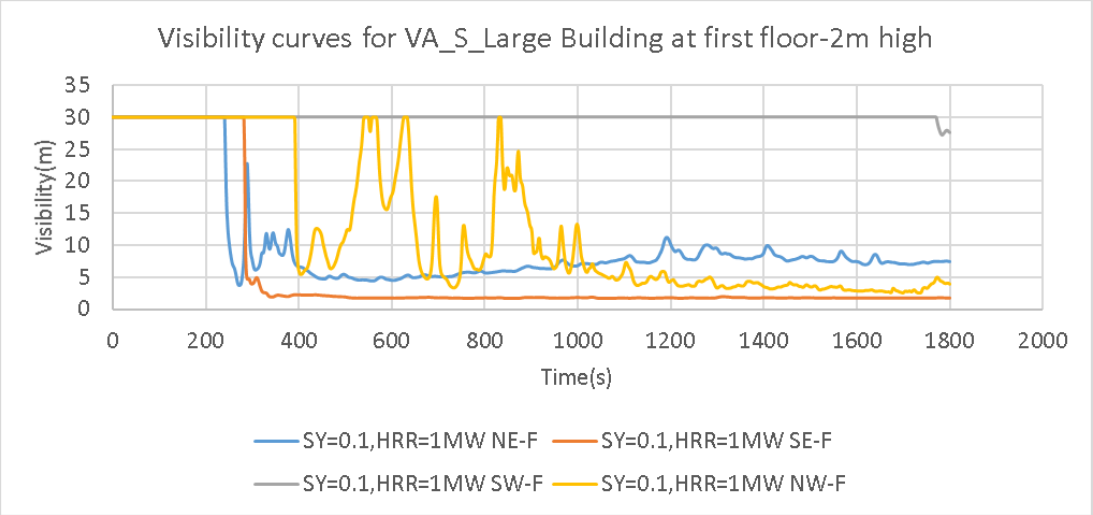

*SY=Soot Yield, NE= Northeast, SE=Southeast, SW=Southwest, NW=Northwest, HRR = Heat Release Rate of a sprinkler controlled fire

Figure 25 visibility curves in a Configuration II building

Table 18 Basic values of ASETs at various exits for HRR=1MW compared with HRR=0.5MW

Exit	ASET(s)	
	SY=0.1, HRR=1MW	SY=0.1, HRR=0.5MW
I- North exit	146	155
I- South exit	212	216
II-Northeast exit	443	490
II-Northwest exit	716	716
II-Southwest exit	>1800	>1800
II-Southeast exit	290	412
III-A - Northeast exit	364	522
III-A - Northwest exit	549	608
III-A - Southwest exit	787	815
III-A - Southeast exit	284	320

The maximum HRR achieved in a sprinkler controlled fire only affects the ASET in a building of Configuration II which by definition means a building with a functional sprinkler system. The above table

has been enlarged by including data from other Configurations in order to be conveniently compared with other options. In the above table, the Southeast and Northeast exits are more sensitive to the increase of HRR than the Northwest and Southwest exits (the Southeast exit loses 29.6% of its ASET and the Northeast exit loses 11.6% of its ASET as results of a doubled HRR achieved in a sprinkler controlled fire).

Table 19 ASET/RSET changes in various building Configurations for best egress scenarios-HRR=1MW

Building Configuration	ASET(s)	RSET(s)	Ratio of ASET/RSET
I- no exit disabled	146	93	1.57
I- North exit disabled	212	147	1.44
II-no exit disabled	290	260	1.12
II-Southeast exit disabled	716	258	2.78
II-Both Southeast and Northeast exits disabled	716	312	2.29
III-A - no exit disabled	284	260	1.09
III-A - Southeast exit disabled	364	258	1.41
III-A - Both Southeast and Northeast exits disabled	549	312	1.76

Table 20 ASET/RSET changes in various building Configurations for worst egress scenarios-HRR=1MW

building Configuration	ASET(s)	RSET(s)	Ratio of ASET/RSET
I- no exit disabled	146	93	1.57
I- South exit disabled	146	153	0.95
II-no exit disabled	290	260	1.12
II-Northwest exit disabled	290	382	0.76
II-Both Northeast and Southwest exits disabled	290	433	0.67
III-A - no exit disabled	284	260	1.09
III-A - Northwest exit disabled	284	382	0.74
III-A - Both Northeast and Southwest exits disabled	284	433	0.66

Table 21 ASET/RSET changes in various building Configurations for mean egress scenarios- HRR=1MW

building Configuration	ASET(s)	RSET(s)	Ratio of ASET/RSET
I- no exit disabled	146	93	1.57
I- North exit disabled	212	147	1.44
II-no exit disabled	290	260	1.12
II-Northwest exit disabled	290	382	0.76
II-Both Northwest and Southeast exits disabled	443	382	1.16
III-A - no exit disabled	284	260	1.09
III-A - Northwest exit disabled	284	382	0.74
III-A - Both Northwest and Southeast exits disabled	364	382	0.95

A comparison of egress safety factors is shown in the following table:

Table 22 comparison of safety factors in various Configurations and scenarios-HRR

	SY=0.1, HRR=0.5MW			SY=0.1, HRR=1MW		
building configuration	B	W	M	B	W	M
I- no exit disabled	1.57	1.57	1.57	1.57	1.57	1.57
I- one exit disabled	1.44	0.95	1.44	1.44	0.95	1.44
II-no exit disabled	1.58	1.58	1.58	1.12	1.12	1.12
II-one exit disabled	2.78	1.08	1.08	2.78	0.76	0.76
II-two exits disabled	2.29	0.95	1.28	2.29	0.67	1.16
III-A - no exit disabled	1.09	1.09	1.09	1.09	1.09	1.09
III-A - one exit disabled	1.41	0.74	0.74	1.41	0.74	0.74
III-A - two exits disabled	1.76	0.66	0.95	1.76	0.66	0.95

*Yellow means the ratio is between 1.0 and 1.10, read means the ratio is less than 1

The above table shows that with the doubled HRR in a sprinkler controlled fire, considerable drop of safety factors only occurs in worst and mean scenarios.

2.3.3. Fire Growth Rate changing from Fast to Ultra-fast/Slow

Based on the last section, which is SY=0.1, HRR=1MW for Configuration II, Fire Grow Rate = Fast, in this section only Fire Growth Rate changes from Fast to Ultra-fast/Slow. The following figures show how visibility limits are reached in different Configurations for an Ultra-fast/Slow fire.

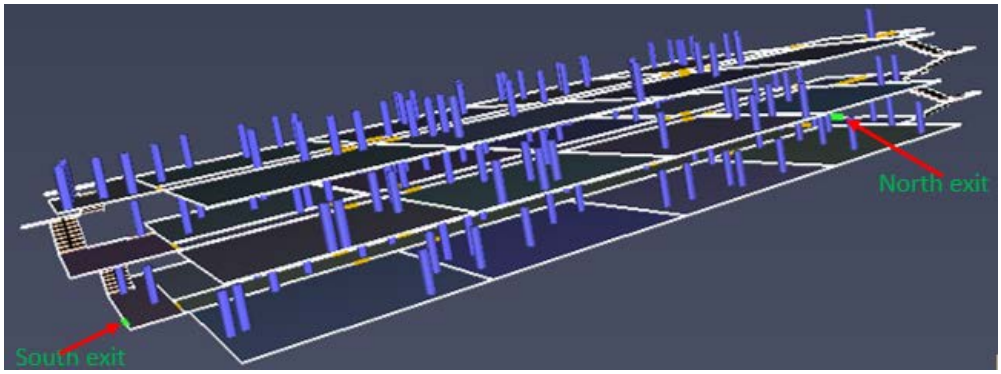

Figure 26 Locations of North and South exits for building of Configuration I

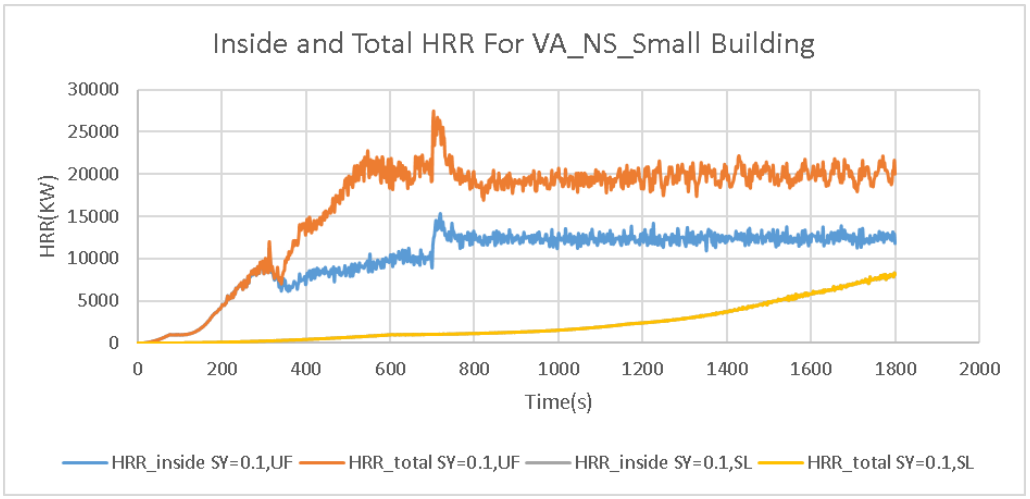

Figure 27 Total HRR and HRR inside the building of Configuration I for Slow fire and Ultra-fast fire

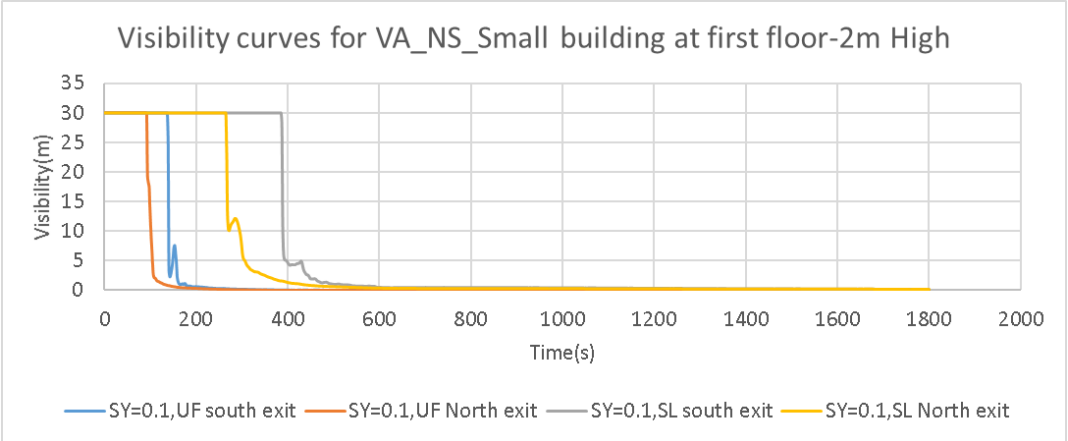

*SY=Soot Yield, NE= Northeast, SE=Southeast, SW=Southwest, NW=Northwest, UF = Ultra-fast (fire), SL=Slow (fire)

Figure 28 visibility curves in a Configuration I building for Slow fire and Ultra-fast fire

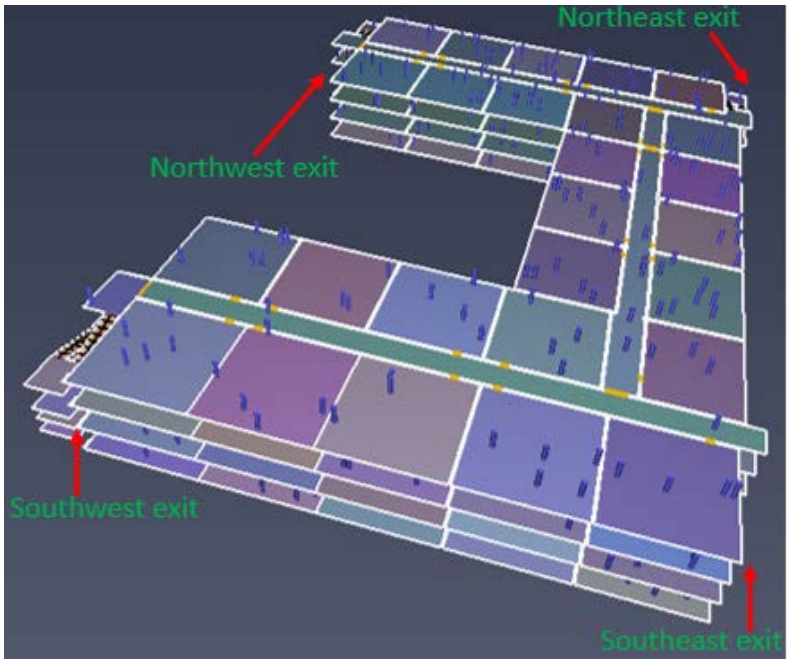

Figure 29 Locations of four exits for buildings of Configuration II and III-A

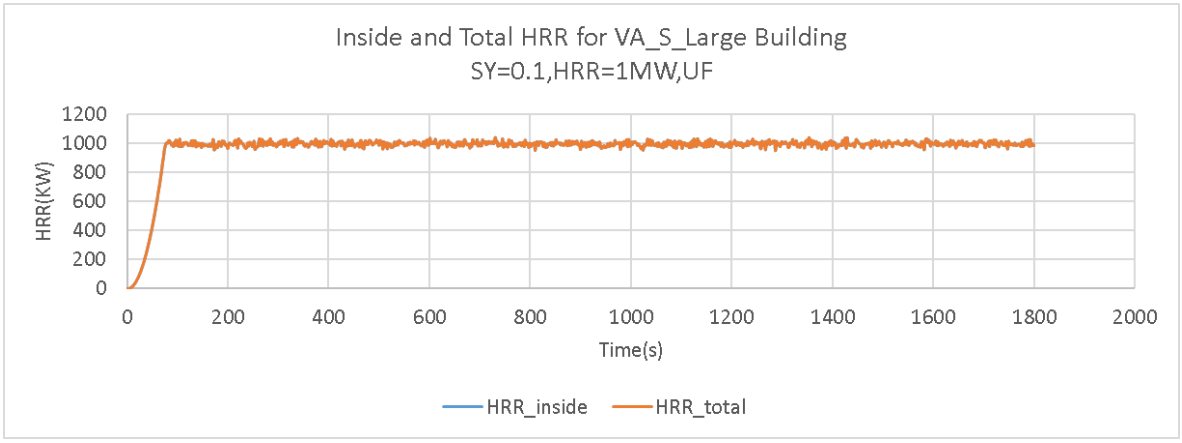

Figure 30 Total HRR and HRR inside the building of Configuration II for Ultra-fast fire

(No HRR presents outside the building)

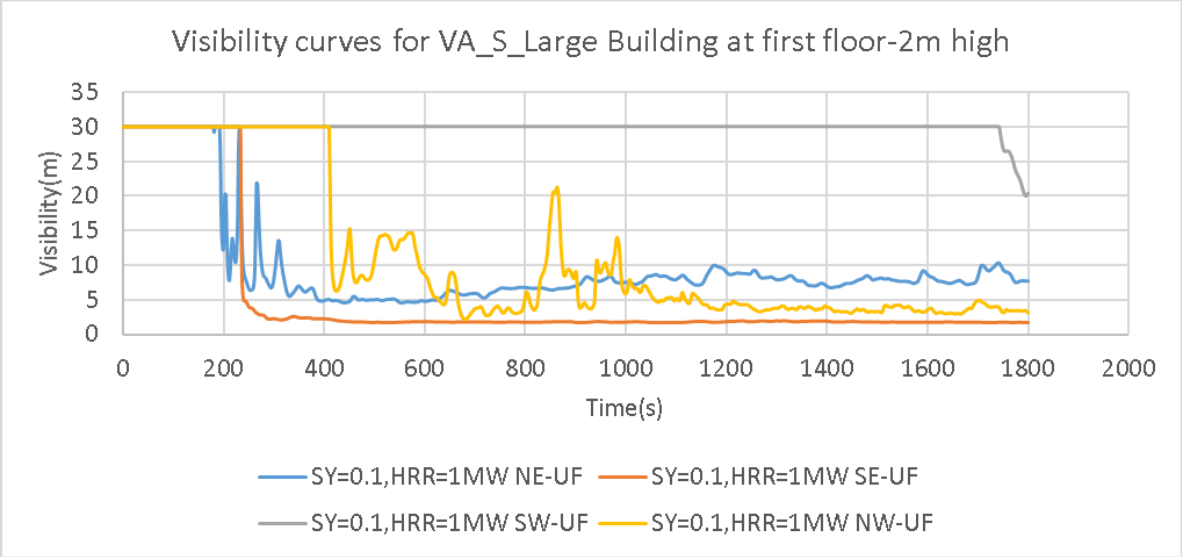

*SY=Soot Yield, NE= Northeast, SE=Southeast, SW=Southwest, NW=Northwest, UF=Ultra-fast

Figure 31 visibility curves in a Configuration II building

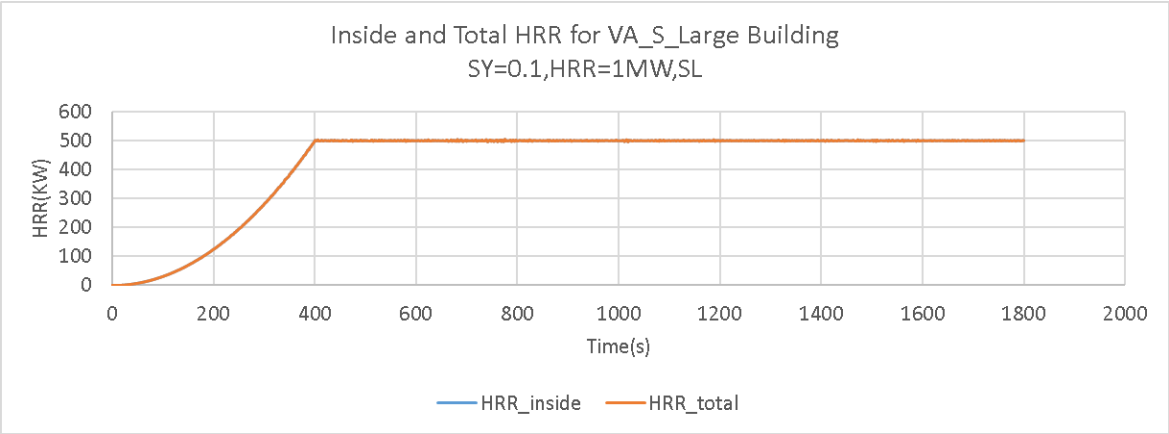

Figure 32 Total HRR and HRR inside the building of Configuration II for Slow fire

(No HRR presents outside the building)

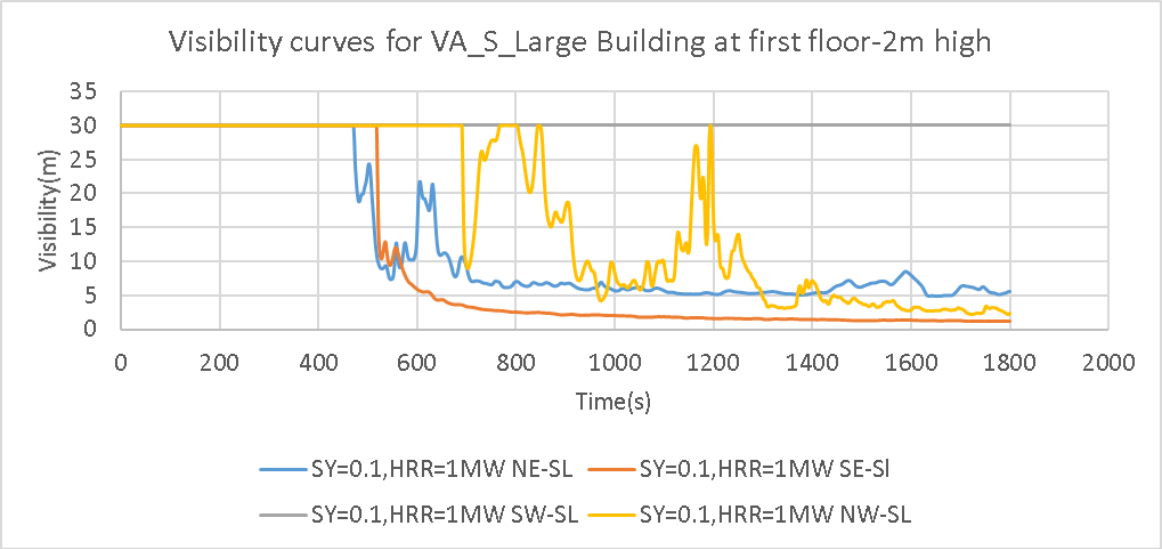

*SY=Soot Yield, NE= Northeast, SE=Southeast, SW=Southwest, NW=Northwest, SL=Slow (fire)

Figure 33 visibility curves in a Configuration II building

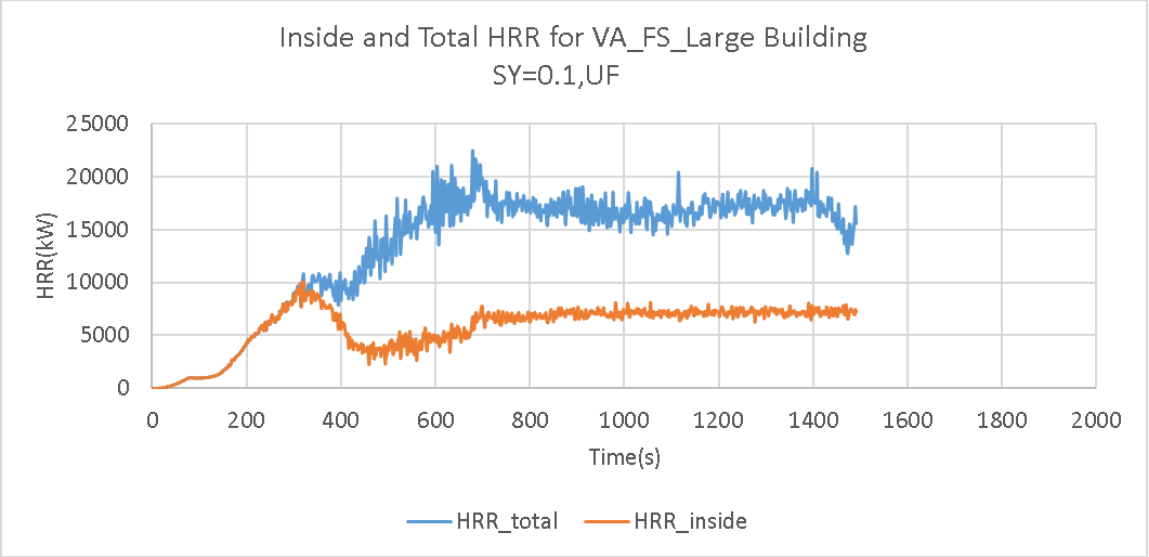

Figure 34 Total HRR and HRR inside the building of Configuration III-A for Slow fire

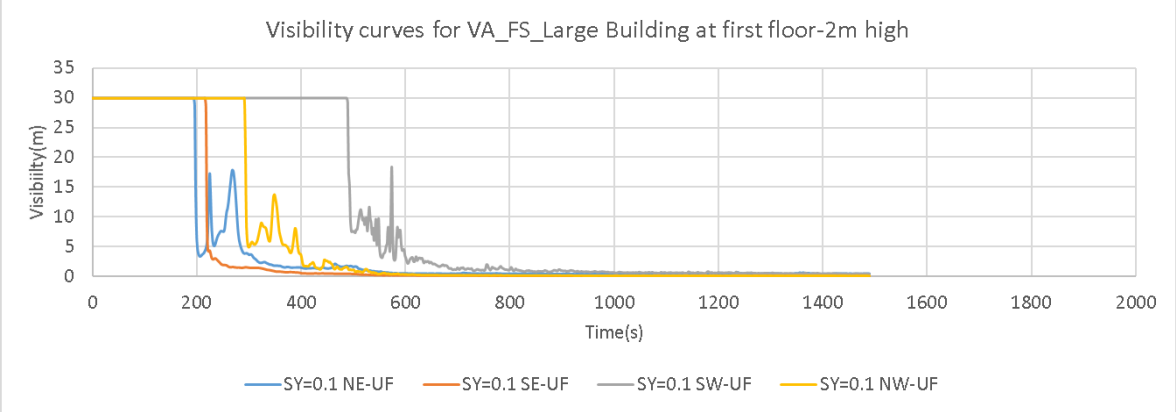

*SY=Soot Yield, NE= Northeast, SE=Southeast, SW=Southwest, NW=Northwest, UF=Ultra-fast

Figure 35 visibility curves in a Configuration III-A building

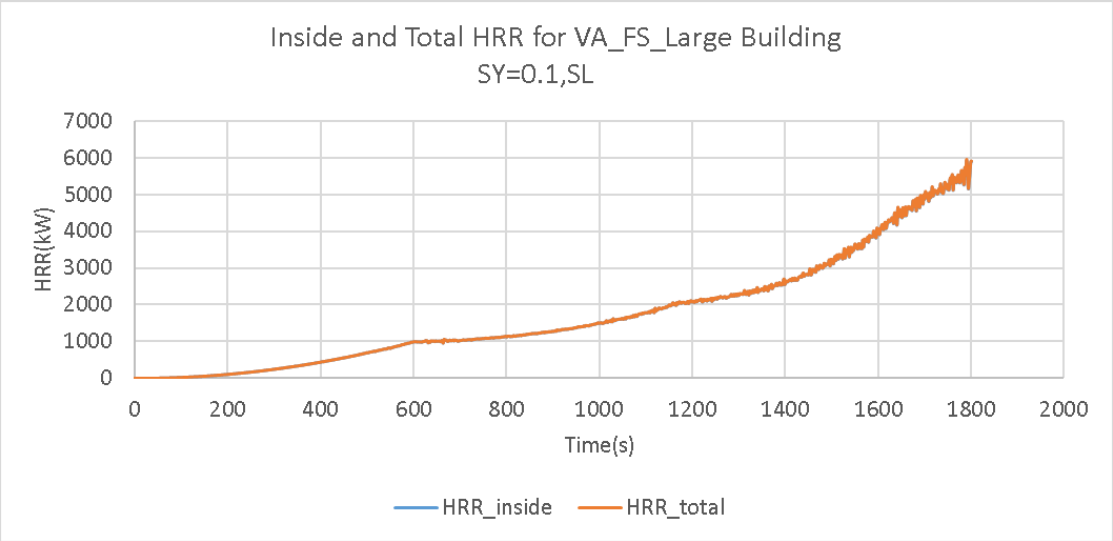

Figure 36 Total HRR and HRR inside the building of Configuration III-A for Slow fire

(No HRR presents outside the building)

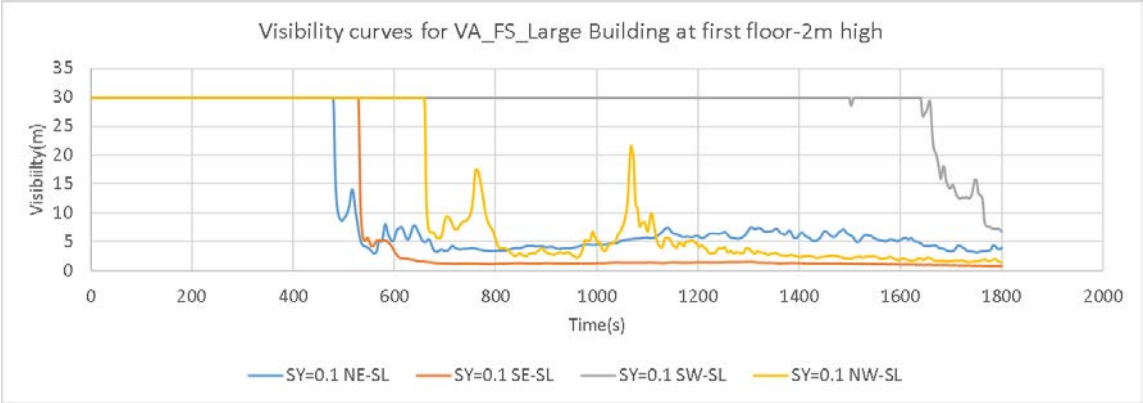

*SY=Soot Yield, NE= Northeast, SE=Southeast, SW=Southwest, NW=Northwest, SL=Slow (fire)

Figure 37 visibility curves in a Configuration III-A building

Table 23 Basic values of ASETs at various exits for Ultra-fast fire and Slow fire compared with Fast fire

Exit	ASET(s)			
	SY=0.1, HRR=1MW, Slow fire	SY=0.1, HRR=1MW, Ultra-fast fire	SY=0.1, HRR=1MW, Fast fire	SY=0.1, HRR=0.5MW, Fast fire
I- North exit	306	104	146	155
I- South exit	398	157	212	216
II-Northeast exit	1372	389	443	490
II-Northwest exit	968	668	716	716
II-Southwest exit	>1800	>1800	>1800	>1800
II-Southeast exit	632	241	290	412
III-A - Northeast exit	535	284	364	522
III-A - Northwest exit	803	394	549	608
III-A -Southwest exit	>1800	551	787	815
III-A - Southeast exit	551	221	284	320

The above table shows that an Ultra-fast fire may on average decrease the ASETs of Configuration I, II, III-A by 27.1%, 3.1% and 23.7%, respectively, a slow fire may on average increase the ASETs of Configuration I, II, III-A by 96.6%, 36.3% and 72.5%, respectively. These results mean that the ASETS of buildings with sprinkler trade-offs are less sensitive to the change of fire growth rate than that of buildings without sprinkler trade-offs.

Table 24 ASET/RSET changes in various building Configurations for best egress scenarios-Ultra-fast/Slow fire

building Configuration	ASET(s)		RSET(s)	Ratio of ASET/RSET	
	UF	SL		UF	SL
I- no exit disabled	104	306	93	1.12	3.29
I- North exit disabled	157	398	147	1.07	2.71
II-no exit disabled	241	632	260	0.93	2.43
II-Southeast exit disabled	668	968	258	2.59	3.75
II-Both Southeast and Northeast exits disabled	668	968	312	2.14	3.10
III-A - no exit disabled	221	535	260	0.85	2.06
III-A - Southeast exit disabled	284	535	258	1.10	2.07
III-A - Both Southeast and Northeast exits disabled	394	803	312	1.26	2.57

Table 25 ASET/RSET changes in various building Configurations for worst egress scenarios-Ultra-fast/Slow fire

building Configuration	ASET(s)		RSET(s)	Ratio of ASET/RSET	
	UF	SL		UF	SL
I- no exit disabled	104	306	93	1.12	3.29
I- South exit disabled	104	306	153	0.68	2.00
II-no exit disabled	241	632	260	0.93	2.43
II-Northwest exit disabled	241	632	382	0.63	1.65
II-Both Northeast and Southwest exits disabled	241	632	433	0.56	1.46
III-A - no exit disabled	221	535	260	0.85	2.06
III-A - Northwest exit disabled	221	535	382	0.58	1.40
III-A - Both Northeast and Southwest exits disabled	221	551	433	0.51	1.27

Table 26 ASET/RSET changes in various building Configurations for mean egress scenarios-Ultra-fast/Slow

building Configuration	ASET(s)		RSET(s)	Ratio of ASET/RSET	
	UF	SL		UF	SL
I- no exit disabled	104	306	93	1.12	3.29
I- North exit disabled	157	398	147	1.07	2.71
II-no exit disabled	241	632	260	0.93	2.43
II-Northwest exit disabled	241	632	382	0.63	1.65
II-Both Northwest and Southeast exits disabled	389	1342	382	1.02	3.51
III-A - no exit disabled	221	535	260	0.85	2.06
III-A - Northwest exit disabled	221	535	382	0.58	1.40
III-A - Both Northwest and Southeast exits disabled	284	535	382	0.74	1.40

A comparison of egress safety factors are shown in the following table:

Table 27 comparison of safety factors in various Configurations and scenarios-Ultra-fast/Slow fire

building configuration	SY=0.1, HRR=1MW, Ultra Fast fire			SY=0.1, HRR=1MW Fast fire			SY=0.1, HRR=1MW Slow fire		
	B	W	M	B	W	M	B	W	M
I- no exit disabled	1.12	1.12	1.12	1.57	1.57	1.57	3.29	3.29	3.29
I- one exit disabled	1.07	0.68	1.07	1.44	0.95	1.44	2.71	2	2.71
II-no exit disabled	0.93	0.93	0.93	1.12	1.12	1.12	2.43	2.43	2.43
II-one exit disabled	2.59	0.63	0.63	2.78	0.76	0.76	3.75	1.65	1.65
II-two exits disabled	2.14	0.56	1.02	2.29	0.67	1.28	3.1	1.46	3.51
III-A - no exit disabled	0.85	0.85	0.85	1.09	1.09	1.09	2.06	2.06	2.06
III-A - one exit disabled	1.1	0.58	0.58	1.41	0.74	0.74	2.07	1.4	1.4
III-A - two exits disabled	1.26	0.51	0.74	1.76	0.66	0.95	2.57	1.27	1.4

*Yellow means the ratio is between 1.0 and 1.10, read means the ratio is less than one

The above table shows that with the increase of fire growth rate, safety factors of buildings with sprinkler trade-offs (Configuration II and III-A) drop slower than that of buildings without sprinkler trade-offs.

2.3.4. Corridor door type changing from mechanically held open to closed

In the above three sections we focus on the variation of fire parameters, like HRR, Soot Yield and Fire Growth Rate, these factors can mainly change the ASET but has little influence on the RSET because in our case we ignore the interaction between egress process and smoke spreading process. This section we try to investigate the effects of corridor door type on both RSET and ASET.

The issues about “the types of the doors” concentrate on one question: Is a door mechanically held open? If the answer is Yes, the effective width of the door will not be compromised. If the answer is No, it is more reasonable to reduce the effective width of the door to the shoulder width of a person due to the need for a person to hold the leaf open. A maximum flow rate of 50 persons/min/door is suggested for doors that are not mechanically held open as a result of a reduced door width [6]. Here we assume that apartment doors on each floor and the corridor doors not on the first floor are mechanically held open, both North and South corridor doors in the first floor can be mechanically held open or not. This assumption takes into account the fact that the corridor doors on the fire initial floor are the most important smoke barriers maintaining the tenable conditions of stair exits. The locations of the two corridor doors are shown in the following two figures:

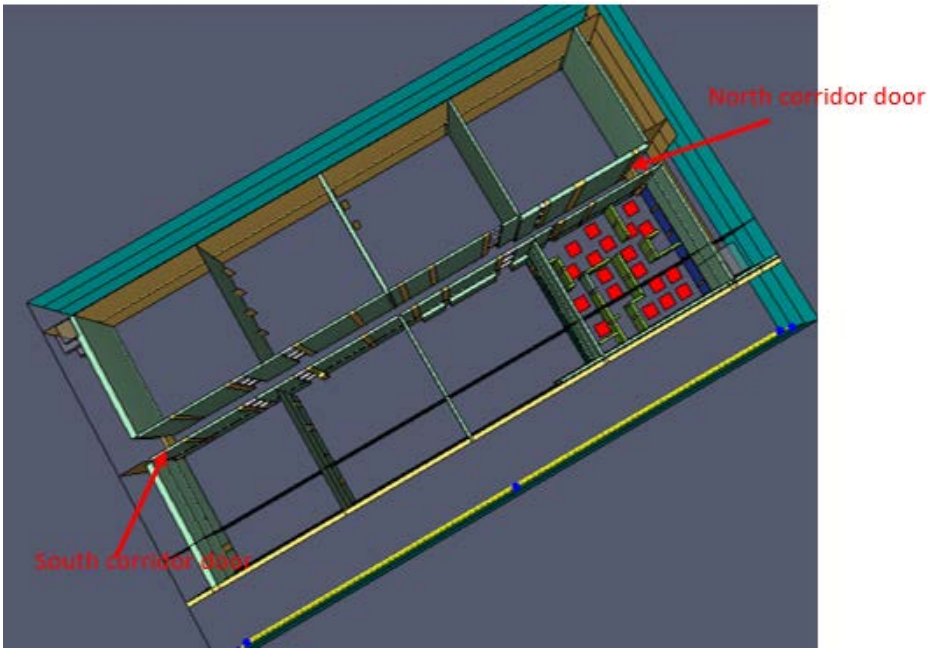

Figure 38 Locations of two corridor doors for building of Configuration I

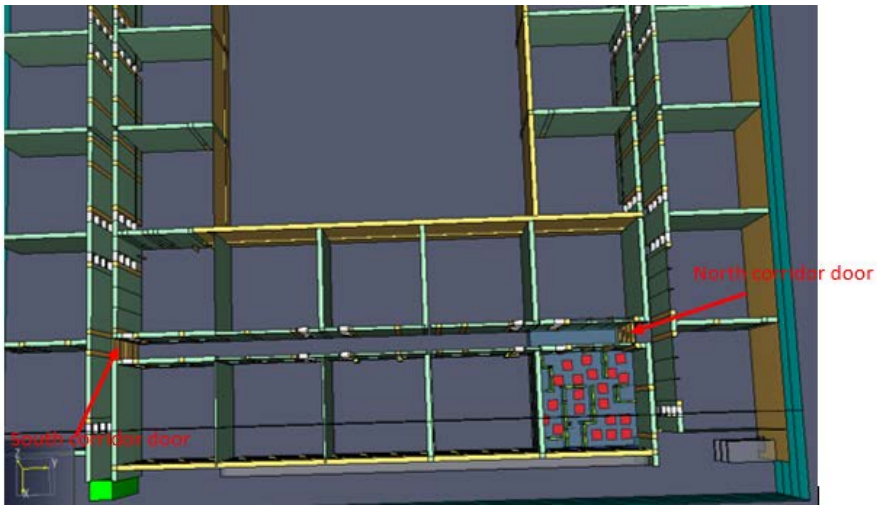

Figure 39 Locations of two corridor doors for buildings of Configuration II and III-A

a) RSET

The locations of exits are shown in the following two figures which are the same as before and repeated here just for convenience:

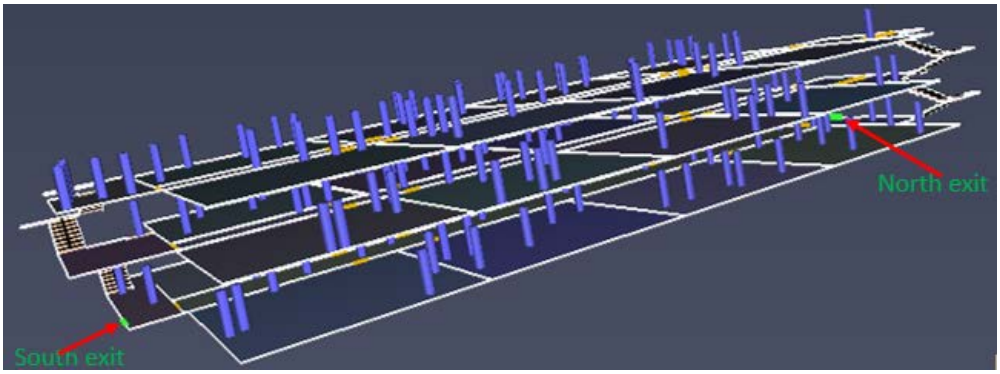

Figure 40 locations of North and South exits for building of Configuration I

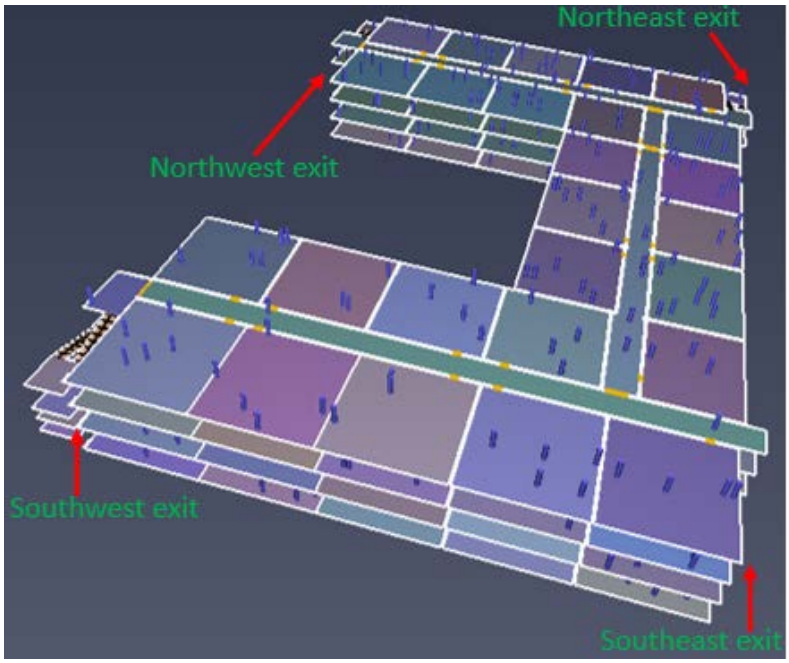

Figure 41 Locations of four exits for buildings of Configuration II and III-A

In PATHFINDER, a corridor door is assigned a maximum flow rate of 50 persons/min to simulate the doors not mechanically held open, the results are shown in the following tables:

Table 28 effects of corridor door on RSET in Configuration I

Conditions	RSET(s)	
	Open	close
South exit available, SFPE method	136	136
South exit available, steering method	147	148
North exit available, SFPE method	133	132
North exit available, steering method	153	153
Both exits available, SFPE method	87	87
Both exits available, steering method	93	94

Table 29 effects of corridor door on RSET in Configuration II and III-A

Conditions	RSET(s)	
	Open	close
Southeast exit disabled, SFPE method	245	255
Southeast exit disabled, steering method	258	270
Both Southeast and Northeast exits disabled, SFPE method	312	317
Both Southeast and Northeast exits disabled, steering method	300	304
Zero exit disabled, SFPE method	245	255
Zero exit disabled, steering method	260	270

From the above tables it can be concluded that whether corridor doors are mechanically held open or not has very tiny influence on the RSET (<3%).

b) ASET

Having the North corridor door closed, three simulations are conducted to seek the ASET of each exit. The results are shown in the following three figures:

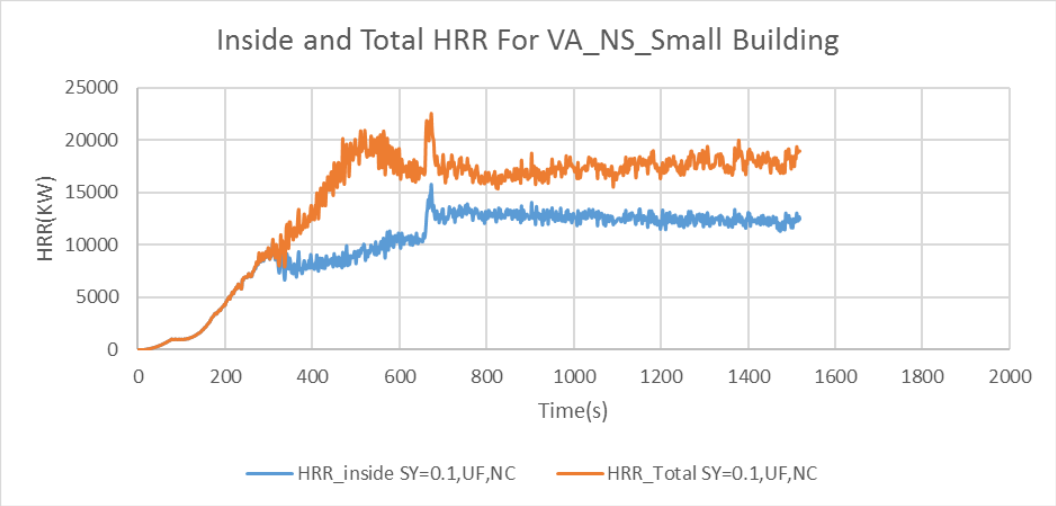

Figure 42 Total HRR and HRR inside the building of Configuration I with North corridor door closed

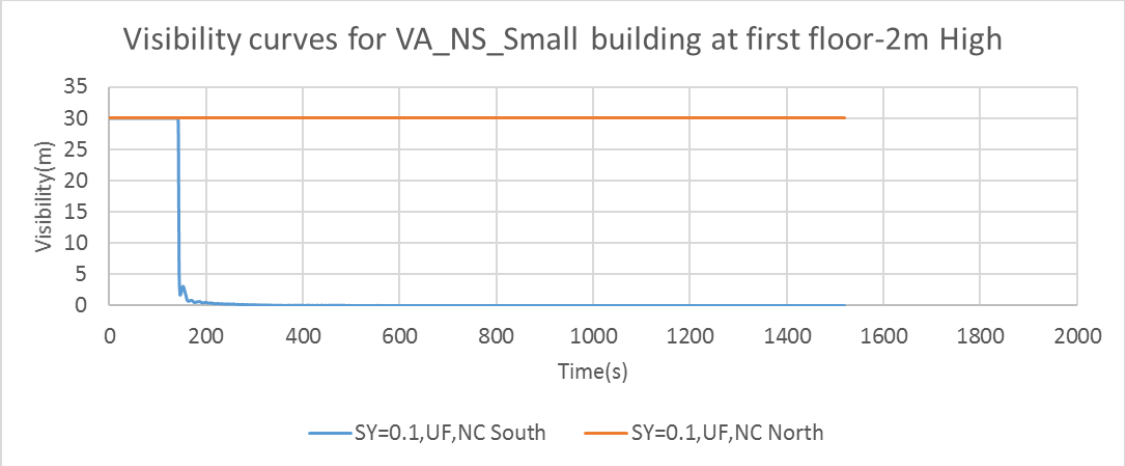

*SY=Soot Yield, UF=Ultra-fast (fire), NC= North corridor door (closed)

Figure 43 visibility curves in a Configuration I building

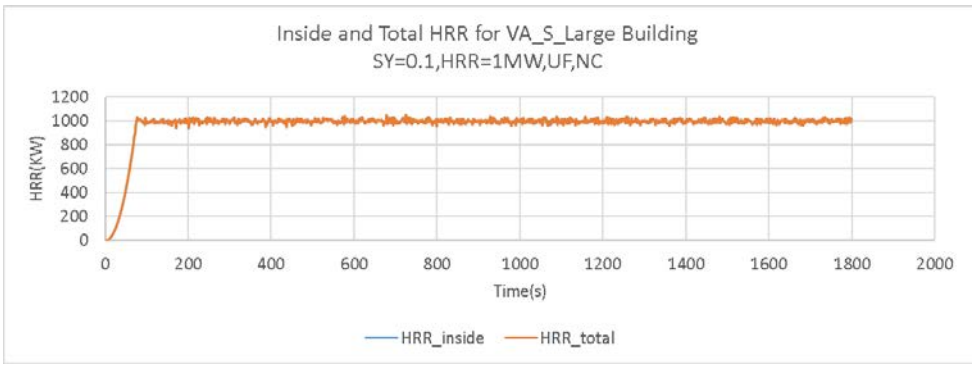

Figure 44 Total HRR and HRR inside the building of Configuration II with North corridor door closed

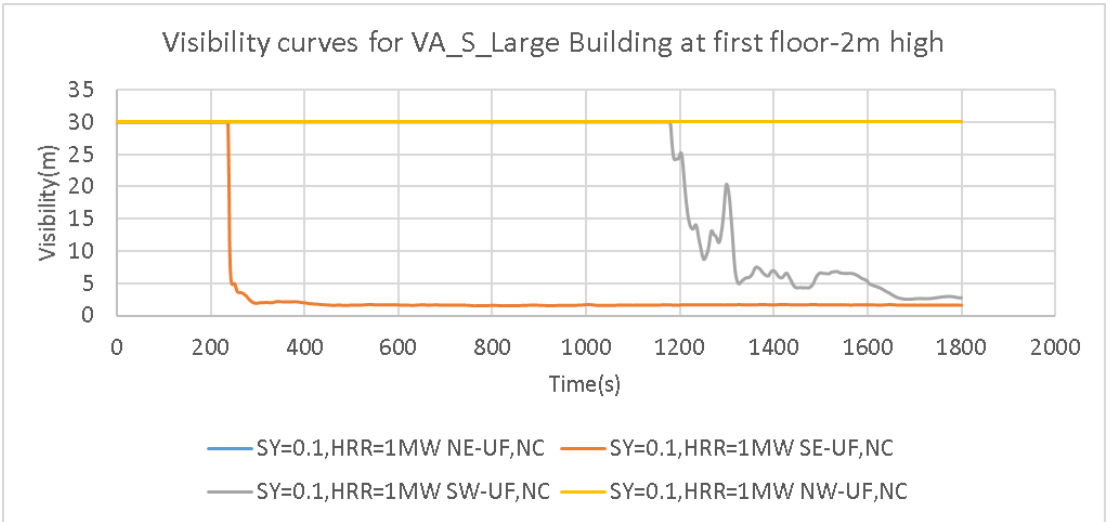

*SY=Soot Yield, NE= Northeast, SE=Southeast, SW=Southwest, NW=Northwest, NC = North corridor door (closed), UF = Ultra-fast (fire)

Figure 45 visibility curves in a Configuration II building

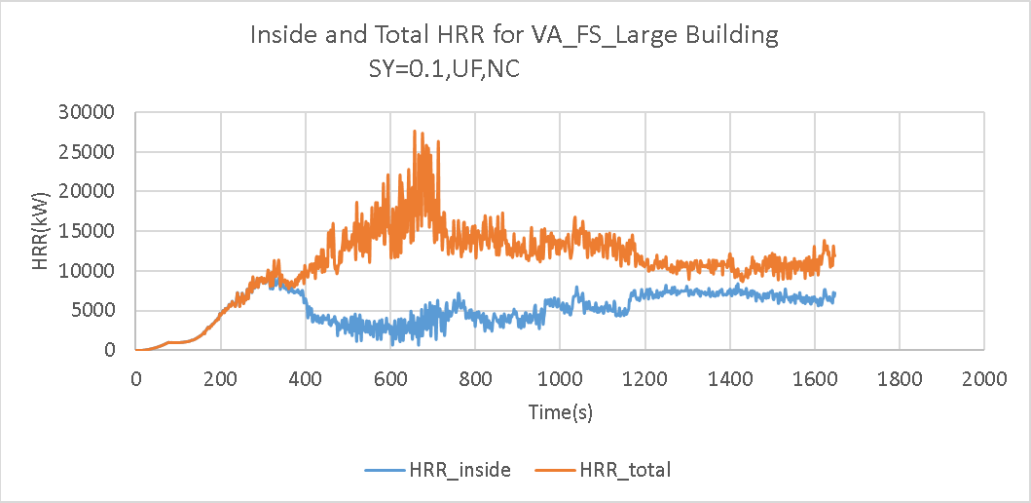

Figure 46 Total HRR and HRR inside the building of Configuration II with North the corridor door closed

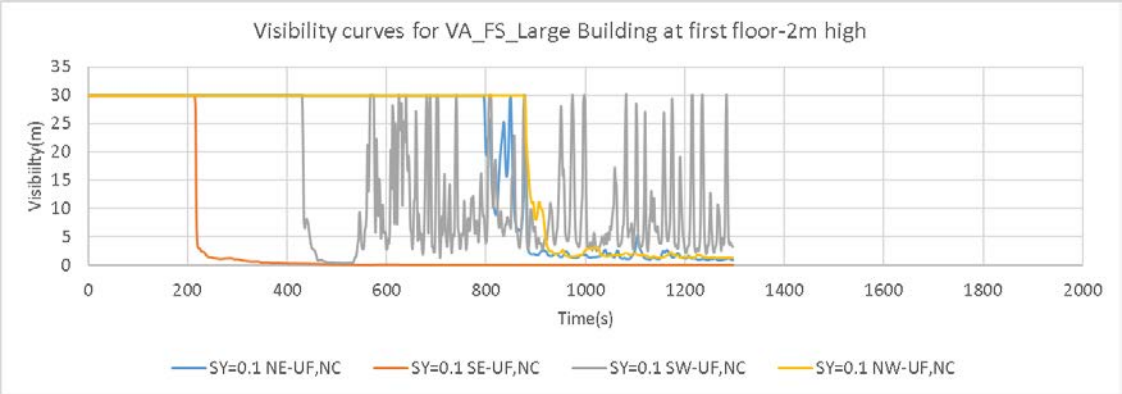

*SY=Soot Yield, NE= Northeast, SE=Southeast, SW=Southwest, NW=Northwest, NC = North corridor door (closed), UF = Ultra-fast (fire)

Figure 47 visibility curves in a Configuration III-A building

Having both the North corridor door and the South corridor closed, three simulations are conducted to seek the ASETs of each exit, as shown in the following three figures:

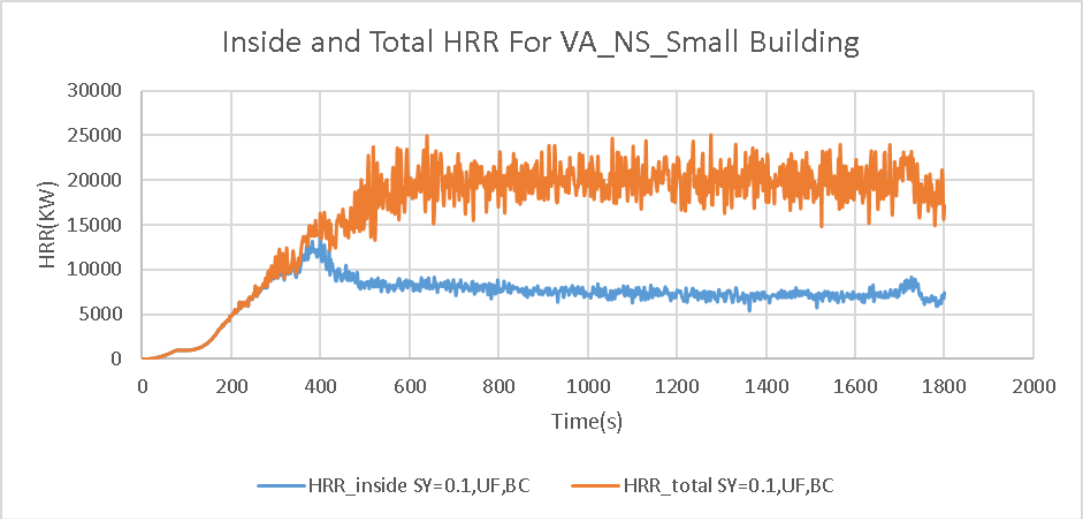

Figure 48 Total HRR and HRR inside the building of Configuration I with both corridor doors closed

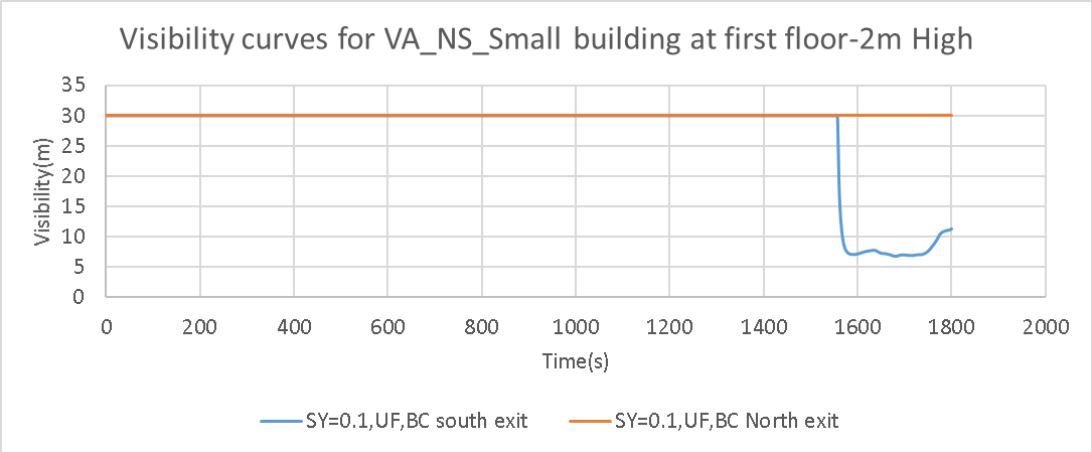

*SY=Soot Yield, UF=Ultra-fast (fire), BC = both corridor doors closed

Figure 49 visibility curves in a Configuration I building

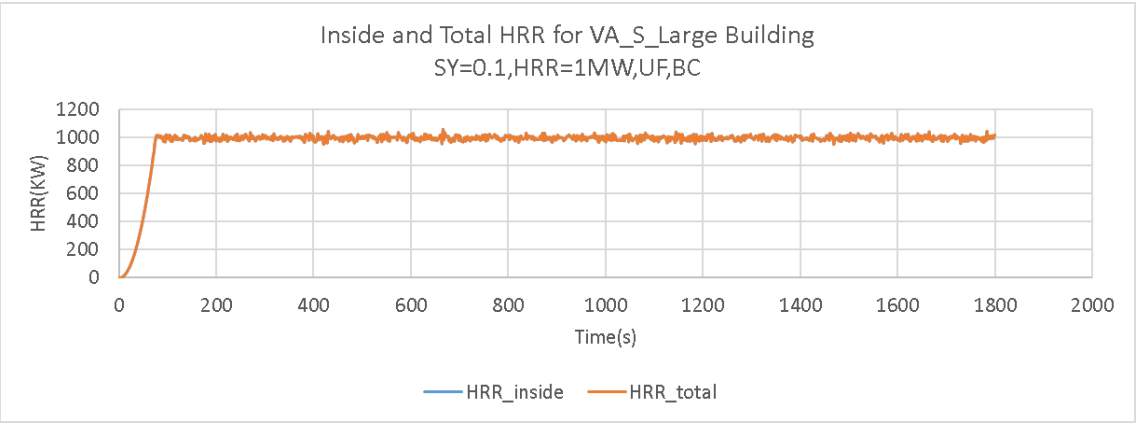

Figure 50 Total HRR and HRR inside the building of Configuration II with both corridor doors closed

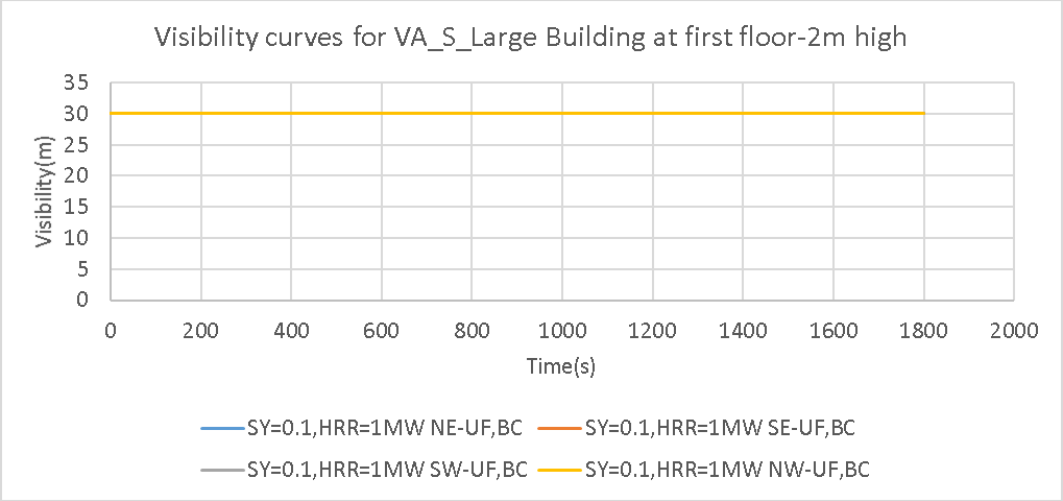

*SY=Soot Yield, NE= Northeast, SE=Southeast, SW=Southwest, NW=Northwest, BC = Both corridor doors (closed), UF = Ultra-fast (fire)

Figure 51 Visibility curves in a Configuration I building

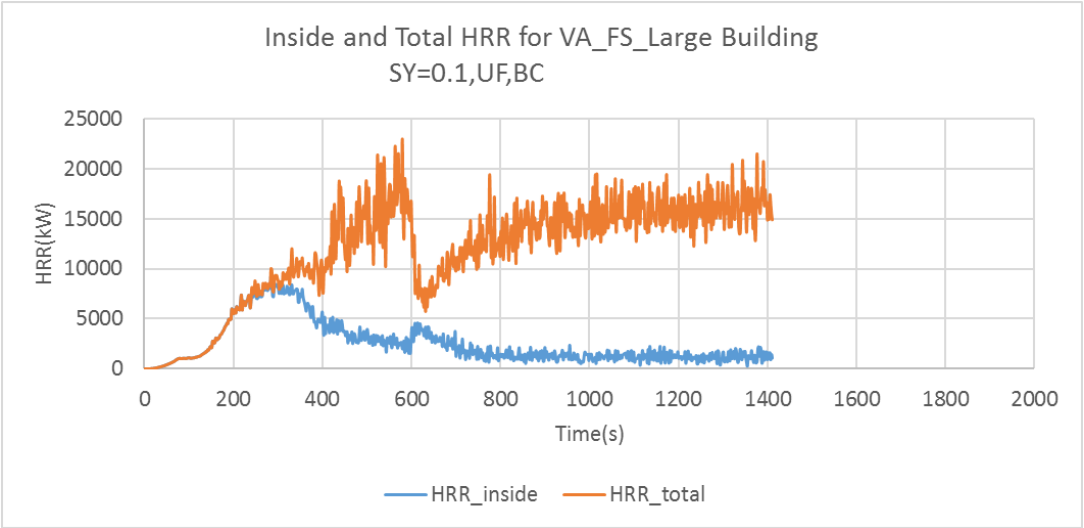

*SY=Soot Yield, UF=Ultra Fast, BC = Both corridor doors (closed)

Figure 52 Total HRR and HRR inside the building of Configuration IIL-A with both corridor doors closed

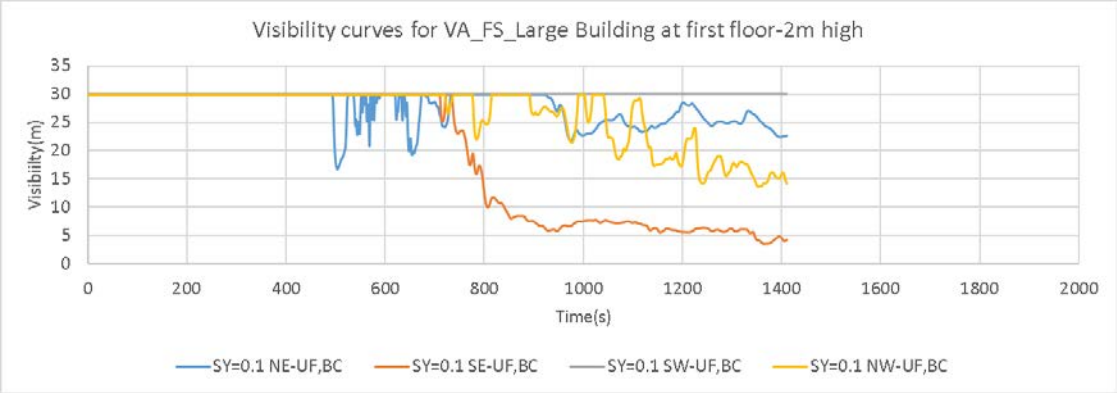

*SY=Soot Yield, NE= Northeast, SE=Southeast, SW=Southwest, NW=Northwest, BC = Both corridor doors (closed), UF = Ultra-fast (fire)

Figure 53 Visibility curves in a Configuration I building

From the above figures, a summary about the ASETs is given in the following table:

Table 30 Basic values of ASETs at various exits when North corridor door is closed compared with when it is open*

Exit	ASET(s) for SY=0.1,HRR=1MW,UF		
	Both corridor doors open	North corridor door closed	Both corridor doors closed
I- North exit	104	>1800	>1800
I- South exit	157	144	>1800
II-Northeast exit	389	>1800	>1800
II-Northwest exit	668	>1800	>1800
II-Southwest exit	>1800	1440	>1800
II-Southeast exit	241	247	>1800
III-A - Northeast exit	284	884	>1400
III-A - Northwest exit	394	920	>1400
III-A - Southwest exit	551	446	>1400
III-A - Southeast exit	221	220	1346

*SY=Soot Yield, UF=Ultra-fast (fire)

The above table shows that one closed North corridor door may on average increase the ASETs of Configuration I, II, III-A by 779.3%, 70.5% and 118.6%, respectively. Both closed North and South corridor doors may on average averagely increase the ASETs of Configuration I, II, III-A by 1150.2%, 82.1% and 204.9%, respectively. These results mean that buildings with sprinkler trade-offs are less sensitive to the states of corridor doors than buildings without sprinkler trade-offs.

The egress safety factors for three egress scenarios are shown in the following tables:

Table 31 ASET/RSET changes in various building Configurations for best egress scenarios-Ultra-fast with one or two corridor doors closed

building Configuration	ASET(s),SY=0.1,HRR=1MW,Ultra-fast fire		RSET (s)	Ratio of ASET/RSET	
	North corridor door closed	Both corridor doors closed		North corridor door closed	Both corridor doors closed
I- no exit disabled	144	>1800	93	1.55	>19.36
I- South exit disabled	>1800	>1800	153	>11.76	>11.76
II-no exit disabled	247	>1800	260	0.95	>6.92
II-Southeast exit disabled	1440	>1800	258	5.58	>6.98
II-Both Southeast and Southwest exits disabled	>1800	>1800	312	>5.77	>5.77
III-A - no exit disabled	220	1346	260	0.85	5.18
III-A - Southeast exit disabled	446	>1400	258	1.73	>5.43
III-A - Both Southeast and Southwest exits disabled	884	>1400	299	2.96	>4.68

Table 32 ASET/RSET changes in various building Configurations for worst egress scenarios-Ultra-fast with zero, one or two corridor doors closed

building Configuration	ASET(s), SY=0.1, HRR=1MW, Ultra-fast fire		RSET (s)	Ratio of ASET/RSET	
	North corridor door closed	Both corridor doors closed		North corridor door closed	Both corridor doors closed
I- no exit disabled	144	>1800	93	1.55	>19.36
I- North exit disabled	144	>1800	147	0.98	>12.24
II-no exit disabled	247	>1800	260	0.95	>6.92
II-Northwest exit disabled	247	>1800	382	0.96	>4.71
II-Both Northeast and Southwest exits disabled	247	>1800	433	0.79	>4.16
III-A - no exit disabled	220	1346	260	0.85	5.18
III-A - Northwest exit disabled	220	1346	382	0.58	3.52
III-A - Both Northeast and Southwest exits disabled	220	1346	433	0.51	3.11

Table 33 ASET/RSET changes in various building Configurations for mean egress scenarios-Ultra-fast with one or two corridor doors closed

building Configuration	ASET(s), SY=0.1, HRR=1MW, Ultra-fast fire		RSET (s)	Ratio of ASET/RSET	
	North corridor door closed	Both corridor doors closed		North corridor door closed	Both corridor doors closed
I- no exit disabled	144	>1800	93	1.55	>19.36
I- North exit disabled	144	>1800	147	0.98	>12.24
II-no exit disabled	247	>1800	260	0.95	>6.92
II-Northwest exit disabled	247	>1800	382	0.65	>4.71
II-Both Northwest and Southeast exits disabled	1440	>1800	382	3.77	>4.71
III-A - no exit disabled	220	1346	260	0.85	5.18
III-A - Northwest exit disabled	220	1346	382	0.58	3.52
III-A - Both Northwest and Southeast exits disabled	446	>1400	382	1.17	>3.66

A comparison of egress safety factors is shown in the following table:

Table 34 comparison of safety factors in various Configurations and scenarios- Ultra-fast with zero, one or two corridor doors closed

building configuration	SY=0.1,HRR=1MW, UF,Both corridor doors open			SY=0.1,HRR=1MW, UF, North corridor door closed			SY=0.1,HRR=1MW, UF, Both corridor doors closed		
	B	W	M	B	W	M	B	W	M
I- no exit disabled	1.12	1.12	1.12	1.55	1.55	1.55	19.36	19.4	19.36
I- one exit disabled	1.07	0.68	1.07	11.76	0.98	0.98	11.76	12.2	12.24
II-no exit disabled	0.93	0.93	0.93	0.95	0.95	0.95	6.92	6.92	6.92
II-one exit disabled	2.59	0.63	0.63	5.58	0.65	0.65	6.98	4.71	4.71
II-two exits disabled	2.14	0.56	1.02	6.02	0.57	3.77	6.02	4.16	4.71
III-A - no exit disabled	0.85	0.85	0.85	0.85	0.85	0.85	5.18	5.18	5.18
III-A - Northwest exit disabled	1.1	0.58	0.58	1.73	0.58	0.58	5.43	3.52	3.52
III-A – two exits disabled	1.26	0.51	0.74	2.96	0.51	1.17	4.68	3.11	3.66

*Yellow means the ratio is between 1.0 and 1.10, read means the ratio is less than one

The above table clearly shows that even under a worst fire condition (SY=0.1, HRR=1MW, Ultra-fast fire), if one corridor door is closed occupants can egress successfully in most of the best egress scenarios but will fail in the worst or mean egress scenarios. If both the North and South corridor doors are closed, the occupants can egress successfully in any Configuration under any egress scenarios. Buildings without sprinkler trade-offs are safer than that with sprinkler trade-offs if at least one corridor door is closed (the reason is that, although the ASET of a non-sprnklered building is shorter than that of a sprinklered building, the RSET of a non-sprinklered building is much shorter than that of a sprinklered building if no delay time is taken into account, delivering a higher safety factor for a non-sprinklered building than for a sprinklered building). Without any closed corridor doors, buildings with sprinkler trade-offs are safer than that without sprinkler trade-offs but still cannot remove the life risks of occupants to the degree as closed corridor doors do. The great performance of corridor doors in improving egress safety factors comes from two mechanisms: 1) it can physically prevent the propagation of smoke; 2) it can reduce the supply of fresh air, finally resulting in a weaker fire.

2.3.5. Occupants' state changes from all healthy to half-healthy

The occupants' state mainly means their ability to move freely. A healthy person means one can move at a common person's speed, an unhealthy person means one can only move at a discounted speed (50% of the normal speed in our case).

It is reasonable to assume that the changes of occupants' state can only change the RSET because in our research the ASET is exclusively determined by non-person factors like HRR, Soot Yield and fire growth rate.

By using PATHFINDER, the results of simulations are shown in the following tables:

Table 35 effects of occupants' state on RSET in Configuration I

Conditions	RSET(s)		Rising rate(%)
	All healthy	Half healthy	
South exit available, SFPE method	136	175	28.68
South exit available, steering method	147	169	14.97
North exit available, SFPE method	133	176	32.33
North exit available, steering method	153	183	19.61
Both exits available, SFPE method	87	108	24.14
Both exits available, steering method	93	115	23.66

Table 36 effects of occupants' state on RSET in Configuration II and III-A

Conditions	RSET(s)		Rising rate(%)
	All healthy	Half healthy	
Southeast exit disabled, SFPE method	245	319	30.20
Southeast exit disabled, steering method	258	295	14.34
Both Southeast and Northeast exits disabled, SFPE method	312	416	33.33
Both Southeast and Northeast exits disabled, steering method	300	392	30.67
Zero exit disabled, SFPE method	245	320	30.61
Zero exit disabled, steering method	260	295	13.46

From the above tables it can be concluded that the occupants' state has considerable influence on the RSET. When half of the occupants become unhealthy, the RSET will on average averagely increase 25%. Consequently all the egress safety factors will averagely drop by 20%, indicating high life risks in egress scenarios other than a slow fire and without closed corridor doors. For a slow fire or non-slow fires but with corridor doors closed, the safety factors are large enough to survive a 20% discount.

2.3.6. Initial delay time

a) introduction

Usually the required safe egress time (RSET) includes three time components, namely, detection time, pre-movement time and movement time [7].

In the above sections we don't address the effects of delay time (detection time plus pre-movement time) on the safety factors, which means the RSET only includes the movement time.

If smoke detectors are adopted, the following equation can be adopted to estimate the detection time:

$$t_u = exp(\lambda + \delta ln a_f)$$

Where λ, δ are the regression coefficients, a_f is fire growth rate. The mean values of λ, δ are 3.02 and -0.31, respectively (SFPE handbook, the 5th edition, page 3234). Therefore for a slow, medium, fast, Ultra-fast fire, the detection time is 117s, 77s, 51s and 34s.

In residential occupancies, the pre-movement time has a range of 60 to 1200 seconds and usually form a log-normal distribution (SPFE, 5th , table 64.6, and page 2124). Therefore the range of detection time is much smaller than that of pre-movement time, which means pre-movement time usually takes up most of the delay time. In our work, three delay times with log-normal distribution are adopted, the mean values are 90s, 180s and 300s, each having a standard deviation of 30s. By running PATHFINDER, the RSETs with different delay times are shown in the following tables:

Table 37 RSETs under different delay times in Configuration I

Conditions	RSET(s)			
	Delay=0	Delay=90	Delay =180	Delay=300
South exit available, SFPE method	136	211	304	422
South exit available, steering method	147	218	307	425
North exit available, SFPE method	133	215	298	417
North exit available, steering method	153	220	313	431
Both exits available, SFPE method	87	198	287	405
Both exits available, steering method	93	201	290	408

Table 38 RSETs under different delay times in Configuration II and III-A

Conditions	RSET(s)			
	Delay =0s	Delay= 90s	Delay= 180s	Delay= 300
Southeast exit disabled, SFPE method	245	325	415	534
Southeast exit disabled, steering method	258	336	425	545
Northeast exit disabled, SFPE method	312	378	469	588
Northeast exit disabled, steering method	298	369	456	576
Northwest exit disabled, SFPE method	382	444	534	651
Northwest exit disabled, steering method	346	411	505	620
Southwest exit disabled, SFPE method	269	354	441	562
Southwest exit disabled, steering method	281	359	454	572
Both Southeast and Northeast exits disabled, SFPE method	312	362	453	573
Both Southeast and Northeast exits disabled, steering method	300	353	441	560
Both Northeast and Southwest exits disabled, SFPE method	433	498	589	708
Both Northeast and Southwest exits disabled, steering method	413	480	571	687
Both Northwest and Southeast disabled, SFPE method	382	444	534	651
Both Northwest and Southeast exits disabled, steering method	346	411	503	623
Both Southwest and Southeast disabled, SFPE method	299	374	462	584
Both Southwest and Southeast exits disabled, steering method	291	381	466	590
Zero exit disabled, SFPE method	245	326	415	536
Zero exit disabled, steering method	260	339	423	542

Accordingly, **Table 27** and **Table 34** are converted to the following tables based on different delay time.

b) Delay time = 90s

Table 39 comparison of safety factors in various Configurations and scenarios-Ultra-fast/Slow fire with both corridor doors open

building configuration	SY=0.1, HRR=1MW, Ultra Fast fire			SY=0.1, HRR=1MW Fast fire			SY=0.1, HRR=1MW Slow fire		
	B	W	M	B	W	M	B	W	M
I- no exit disabled	0.52	0.52	0.52	0.73	0.73	0.73	1.52	1.52	1.52
I- one exit disabled	0.72	0.48	0.72	0.97	0.67	0.97	1.81	1.4	1.81
II-no exit disabled	0.71	0.71	0.71	0.86	0.86	0.86	1.86	1.86	1.86
II-one exit disabled	1.99	0.54	0.54	2.13	0.65	0.65	2.88	1.42	1.42
II-two exits disabled	1.85	0.48	0.88	1.98	0.58	1	2.56	1.27	3.02
III-A - no exit disabled	0.65	0.65	0.65	0.84	0.84	0.84	1.58	1.58	1.58
III-A - one exit disabled	0.85	0.5	0.5	1.08	0.64	0.64	1.59	1.2	1.2
III-A - two exits disabled	1.09	0.44	0.64	1.52	0.57	0.82	2.12	1.11	1.2

*Yellow means the ratio is between 1.0 and 1.10, red means the ratio is less than one

Generally, with 90s delay time, the above table tells us that if both corridor doors are open buildings with sprinkler trade-offs outperform that without sprinkler trade-offs no matter what fire growth rates are.

Table 40 comparison of safety factors in various Configurations and scenarios- Ultra-fast with zero, one or two corridor doors closed

building configuration	SY=0.1,HRR=1MW, UF fire,Both corridor doors open			SY=0.1,HRR=1MW, UF, North corridor door closed			SY=0.1,HRR=1MW, UF, Both corridor doors closed		
	B	W	M	B	W	M	B	W	M
I- no exit disabled	0.52	0.52	0.52	0.72	0.72	0.72	8.96	8.96	8.96
I- one exit disabled	0.72	0.48	0.71	8.26	0.65	0.65	8.26	8.18	8.18
II-no exit disabled	0.71	0.71	0.71	0.73	0.73	0.73	5.31	5.31	5.31
II-one exit disabled	1.99	0.54	0.54	4.29	0.56	0.56	5.36	4.05	4.05
II-two exits disabled	1.85	0.48	0.88	4.81	0.5	3.24	4.81	3.61	4.05
III-A - no exit disabled	0.65	0.65	0.65	0.65	0.65	0.65	3.97	3.97	3.97
III-A - one exit disabled	0.85	0.5	0.5	1.33	0.5	0.5	4.17	3.03	3.03
III-A – two exits disabled	1.09	0.44	0.64	2.36	0.44	1	3.74	2.7	3.15

*Yellow means the ratio is between 1.0 and 1.10, red means the ratio is less than one

For an Ultra-fast fire, the above table tells us that if an evacuation action has 90s delay the buildings with sprinkler trade-offs perform better than that without sprinkler trade-offs do when both corridor doors are open. When one corridor door is closed, the performances of the buildings with sprinkler trade-offs and without sprinkler trade-offs are almost same if sprinklers function as design. But if the sprinklers don't function as design, the buildings with sprinkler trade-offs perform worse than that without sprinkler trade-offs do. When both corridor doors are closed, buildings without sprinkler trade-offs have higher safety factors than that with sprinkler trade-offs, but actually in every case successful egress can be guaranteed since the safety factors are high enough.

c) Delay time = 180s

Table 41 comparison of safety factors in various Configurations and scenarios-Ultra-fast/Slow fire with both corridor doors open

building configuration	SY=0.1, HRR=1MW, Ultra Fast fire			SY=0.1, HRR=1MW Fast fire			SY=0.1, HRR=1MW Slow fire		
	B	W	M	B	W	M	B	W	M
I- no exit disabled	0.36	0.36	0.36	0.5	0.5	0.5	1.06	1.06	1.06
I- one exit disabled	0.51	0.33	0.51	0.69	0.47	0.69	1.3	0.98	1.3
II-no exit disabled	0.57	0.57	0.57	0.69	0.69	0.69	1.49	1.49	1.49
II-one exit disabled	1.57	0.45	0.45	1.68	0.54	0.54	2.28	1.18	1.18
II-two exits disabled	1.42	0.41	0.73	1.53	0.49	0.83	2.06	1.07	2.51
III-A - no exit disabled	0.52	0.52	0.52	0.67	0.67	0.67	1.26	1.26	1.26
III-A - one exit disabled	0.67	0.41	0.41	0.86	0.53	0.53	1.26	1	1
III-A - two exits disabled	0.84	0.38	0.53	1.17	0.48	0.68	1.71	0.94	1

*Yellow means the ratio is between 1.0 and 1.10, red means the ratio is less than one

With 180s delay time, the above table tells us that if both corridor doors are open buildings with sprinkler trade-offs outperform that without sprinkler trade-offs no matter what fire growth rates are.

Table 42 comparison of safety factors in various Configurations and scenarios- Ultra-fast with zero, one or two corridor doors closed

building configuration	SY=0.1,HRR=1MW, Ultra Fast fire,Both corridor doors open			SY=0.1,HRR=1MW, UF, North corridor door closed			SY=0.1,HRR=1MW, UF, Both corridor doors closed		
	B	W	M	B	W	M	B	W	M
I- no exit disabled	0.36	0.36	0.36	0.5	0.5	0.5	6.21	6.21	6.21
I- one exit disabled	0.51	0.33	0.51	5.75	0.47	0.47	5.75	5.86	5.86
II-no exit disabled	0.57	0.57	0.57	0.58	0.58	0.58	4.26	4.26	4.26
II-one exit disabled	1.57	0.45	0.45	3.39	0.46	0.46	4.24	3.37	3.37
II-two exits disabled	1.42	0.41	0.73	3.9	0.42	2.7	3.84	3.06	3.37
III-A - no exit disabled	0.52	0.52	0.52	0.52	0.52	0.52	3.18	3.18	3.18
III-A - one exit disabled	0.67	0.41	0.41	1.05	0.41	0.41	3.29	2.52	2.52
III-A – two exits disabled	0.84	0.38	0.53	1.91	0.37	0.84	3.03	2.29	2.62

*Yellow means the ratio is between 1.0 and 1.10, read means the ratio is less than one

For an Ultra-fast fire, the above table tells us that if an evacuation action has 180s delay the buildings with sprinkler trade-offs perform better than that without sprinkler trade-offs do when both corridor doors are open. When one corridor door is closed, the performance of the buildings with sprinkler trade-offs and without sprinkler trade-offs are almost the same if sprinklers function as designed. But if the sprinklers don't function as designed, the buildings with sprinkler trade-offs on average perform worse than that without sprinkler trade-offs do. When both corridor doors are closed, buildings without sprinkler trade-offs have higher safety factors than that with sprinkler trade-offs, but actually in every case successful egress can be guaranteed since the safety factors are high enough.

d) Delay time = 300s

Table 43 comparison of safety factors in various Configurations and scenarios-Ultra-fast/Slow fire with both corridor doors open

building configuration	SY=0.1,HRR=1MW, Ultra Fast fire			SY=0.1,HRR=1MW Fast fire			SY=0.1,HRR=1MW Slow fire		
	B	W	M	B	W	M	B	W	M
I- no exit disabled	0.25	0.25	0.25	0.36	0.36	0.36	0.75	0.75	0.75
I- one exit disabled	0.37	0.24	0.37	0.5	0.34	0.5	0.94	0.71	0.94
II-no exit disabled	0.44	0.44	0.44	0.54	0.54	0.54	1.17	1.17	1.17
II-one exit disabled	1.23	0.37	0.37	1.31	0.45	0.45	1.78	0.97	0.97
II-two exits disabled	1.14	0.34	0.6	1.22	0.41	0.68	1.65	0.89	2.06
III-A - no exit disabled	0.41	0.41	0.41	0.52	0.52	0.52	0.99	0.99	0.99
III-A - one exit disabled	0.52	0.34	0.34	0.67	0.44	0.44	0.98	0.82	0.82
III-A – two exits disabled	0.67	0.31	0.44	0.93	0.4	0.56	1.37	0.78	0.82

*Yellow means the ratio is between 1.0 and 1.10, read means the ratio is less than one

With 300s delay time, the above table tells us that if both corridor doors are open buildings with sprinkler trade-offs outperform that without sprinkler trade-offs no matter what fire growth rates are.

Table 44 comparison of safety factors in various Configurations and scenarios- Ultra-fast with zero, one or two corridor doors closed

building configuration	SY=0.1,HRR=1MW, Ultra Fast fire,Both corridor doors open			SY=0.1,HRR=1MW, UF, North corridor door closed			SY=0.1,HRR=1MW, UF, Both corridor doors closed		
	B	W	M	B	W	M	B	W	M
I- no exit disabled	0.25	0.25	0.25	0.35	0.35	0.35	4.41	4.41	4.41
I- one exit disabled	0.37	0.24	0.37	4.18	0.34	0.34	4.18	4.24	4.24
II-no exit disabled	0.44	0.44	0.44	0.46	0.46	0.46	3.32	3.32	3.32
II-one exit disabled	1.23	0.37	0.37	2.64	0.38	0.38	3.3	2.76	2.76
II-two exits disabled	1.14	0.34	0.6	3.08	0.35	2.21	3.06	2.54	2.76
III-A - no exit disabled	0.41	0.41	0.41	0.41	0.41	0.41	2.48	2.48	2.48
III-A - one exit disabled	0.52	0.34	0.34	0.82	0.34	0.34	2.57	2.07	2.07
III-A – two exits disabled	0.67	0.31	0.44	1.51	0.31	0.69	2.4	1.9	2.15

*Yellow means the ratio is between 1.0 and 1.10, read means the ratio is less than one

For an Ultra-fast fire, the above table tells us that if an evacuation action has 300s delay the buildings with sprinkler trade-offs perform better than that without sprinkler trade-offs do when both corridor doors are open. When one corridor door is closed, the performances of the buildings with sprinkler trade-offs and without sprinkler trade-offs are almost same if sprinklers function as design. But if the sprinklers don't function as design, the buildings with sprinkler trade-offs averagely perform worse than that without sprinkler trade-offs do. When both corridor doors are closed, buildings without sprinkler trade-offs have higher safety factors than that with sprinkler trade-offs, but actually in every case successful egress can be guaranteed since the safety factors are high enough.

2.4. Conclusions and discussions

From the figures and tables in this chapter, the following conclusions are made:

1) In buildings with sprinkler trade-offs (Configuration II and III-A), the RSET is not sensitive to the availability of the Southeast exit but very sensitive to that of the Northwest exit

2) For our benchmark options (SY=0.052, HRR=0.5MW, Fast fire, all occupants normal, both corridor doors open, zero delay time), the sprinkler trade-offs do not increase the life risk of occupants.

3) The ASETs of buildings with sprinkler trade-offs (Configuration II and III-A) are more sensitive to the change of soot yield than that of buildings without sprinkler trade-offs (Configuration I)

4) As far as the life risk of occupants is concerned, buildings without sprinkler trade-offs outperform that with sprinkler trade-offs when Soot Yield increases.

5) The Southeast and Northeast exits are more sensitive to the increase of HRR than the Northwest and Southwest exits (as results of a doubled HRR achieved in a sprinkler controlled fire, the Southeast exit loses 29.6% of its ASET and the Northeast exit loses 11.6% of its ASET, whereas the Southwest and Northwest exits suffer little).

6) The increase of HRR from 0.5MW to 1MW makes the safety factor of a Configuration II building to decrease by (2.12-1.96)/2.12-1 =7.5%

7) The ASETS of buildings with sprinkler trade-offs are less sensitive to the change of fire growth rate than that of buildings without sprinkler trade-offs.

8) In a fast fire or Ultra-fast fire without any closed corridor doors and any delay times, life risk of occupants in Configuration I buildings is lower than that in Configuration III-A buildings (sprinklers don't function) but higher than that in Configuration II buildings (sprinklers do function). In a slow fire without any closed corridor doors and any delay times, buildings without sprinkler trade-offs perform at least as well as buildings with sprinkler trade-offs do. If the delay time is 90s or more, buildings of both Configuration II and III-A perform better than that of Configuration I, but even so life risk of occupants is of greater concern as compared to when corridor doors are closed.

9) From slow fire to fast fire and Ultra-fast fire, buildings with sprinkler trade-offs gain more benefits than that without sprinkler trade-offs if no corridor doors are closed.

10) Whether corridor doors are mechanically held open or not has very tiny influence on the RSET (<3%) in occupant loads of 200ft^2/person.

11) For any delay time, closed corridor doors have very significant effects on the improvement of ASET no matter what type the building is. If one corridor door is closed, buildings without sprinkler trade-offs are as safe as that with sprinkler trade-offs when sprinklers do function as design but safer when sprinklers do not function as design. If both corridor doors are closed, buildings without sprinkler trade-offs generally performs much better than that with sprinkler trade-offs, but in each case successful evacuations can be ensured because the safety factors are large enough.

12) The occupants' state has considerable influence on the RSET. When half of the occupants become half unhealthy, the RSET will averagely increase 25%. Consequently all the egress safety factors will averagely drop by 20%, indicating high life risks in fast or Ultra-fast fires without closed corridor doors. For a slow fire or non-slow fires but with corridor doors closed, the safety factors are large enough to survive a 20% discount

Two of the most important findings are

1) If no corridor door is closed, although buildings with sprinkler trade-offs generally perform better than buildings without sprinkler trade-offs, the life risk of occupants increases quickly with the delay time.

2) If one corridor door is closed, buildings without sprinkler trade-offs generally performs as same as buildings with sprinkler trade-offs when sprinklers do function as design, but better when sprinklers do not function as design. If both corridor doors are closed, buildings without sprinkler trade-offs generally perform much better than that with sprinkler trade-offs, but in each case successful evacuations can be ensured because the safety factors are large enough.

2.5. Comments about code changes

For a long time, HRR has been considered a primary hazard criteria to characterize a fire. Consequently sprinkler trade-offs on building size have been widely adopted in building codes due to the significant effect of a functional sprinkler system on the reduction of HRR in most fires. As to the issue of successful egress, however, measures, to reduce the spreading speed of smoke, for example mechanically closed doors, perform better than sprinklers that only reduce the HRR.

This report shows that, without the help of closed corridor doors, sprinklers alone cannot provide a maximal safety level for occupants. In buildings with enlarged size as a result of sprinkler trade-offs, the successful evacuation of occupants depends not on whether the sprinklers do a good job but on whether the mechanically closed doors are reliable. As far as the evacuation of occupants is concerned, buildings with sprinkler trade-offs of enlarged size (Configuration II and III-A) perform better than that without sprinkler trade-offs of enlarged size (Configuration I) only when all the corridor doors are mechanically held open (or the mechanically held closed doors have considerably low reliabilities that leave many doors open under fire conditions). But even in this better case the life risk of occupants still cannot be decreased to an ignorable level. Since all fire doors in a means of egress shall close or be closed in case of fire [8], the reliabilities of these doors are important to the safety level of occupants. Therefore, high reliability of fire doors should be paid more attention even in buildings with sprinklers.

2.6. Possible future work

In the above sections of this chapter, life risk of occupants is mentioned several times with some qualitative wards like “considerable”, etc. Although a quantitative description about the life risk of occupants is obviously more helpful, the detail data for us to arrive at this quantitative level is currently unavailable. Probability information necessary to achieve a quantitative risk analysis includes probability distributions of:

1) Sprinklers’ effectiveness;
2) Fires with various grow rates (slow, medium, fast, Ultra-fast);
3) Fires with various soot yields;
4) Fire doors’ reliability;
5) Occupants with different walking speeds;
6) Initial delay time or pre-movement time of occupants.
7) Fire frequencies of Configuration I, II, III-A buildings (fire frequency in a building increases with the total building area)
8) The number of fatalities in fires of Configuration I, II, III-A buildings (possibly Configuration II < Configuration I < Configuration III-A)

With these distributions, Monte-Carlo simulations can be employed to work out a more detail map about the life risk of occupants in different buildings.

(3) UOA

3.1. Introduction

Ventilation conditions are very important in that they affect how a fire initiated from an apartment develops by limiting the make-up air that could potentially be entrained into the fire. The way for entrained air to affect the risk of fire spreading to a neighboring building is not straightforward. Generally the heat flux imposed on an area of façade in the neighboring building comes from the UOA itself and the size of the flame standing out of the UOA. As far as the apartment temperature is concerned, a higher amount of entrained air can on one hand increase the HRR within the fire apartment, meanwhile on the other hand increase the convection heat transfer to outside ambient air. The two effects are opposite to each other and the final temperature changes depend on the phase of the fire. Theoretically, in the fuel-rich side the first effect is greater than the second and the apartment temperature keeps rising with the increase of entrained air. In the fuel lean side, the first effect is ignorable and the apartment temperature keeps dropping with the increase of entrained air. Actually, even if the entrained air is enough for complete combustion, incomplete burning will still occur due to the radical flow field carrying some unburned components out, therefore the temperature will first increase and then drop quickly as the UOA increases. As to the size of flames extending outside the UOA, a higher amount of entrained air will reduce the unburned fuel in the smoke that can burn outside when meeting fresh air, thus decrease the size of flames extending out of the UOA.

Note that ventilation conditions can change from building to building even though they have the same UOA. The specific locations of the UOA do matter. The ventilation conditions of a standalone apartment are significantly different from that of a building apartment, with both having the same UOA. In a standalone apartment, all the openings connect directly to outside environment, whereas in a building apartment some openings have to connect to a narrow corridor, deteriorating the ventilation conditions. Although the case of building apartments are more realistic than that of standalone apartments, the research of the latter is helpful to better understand the fire behavior of the former and can also provide realistic insight as a limit to ventilation. So we will begin our discussion with the standalone apartment case.

The overall FDS model for UOA analysis is shown in Figure 3. Four levels of sprinkler trade-offs adopted in IBC Code are investigated in this report.

To help readers to feel better about the modeling results, some post-flashover fire pictures extracted from simulations are available in APPENDIX 4.

3.2. Heat flux fields from various UOA - standalone compartment case

3.2.1. Fire Separation Distance(FSD) between 3 to 10 ft

In the IBC Code, the UOA is allowed to increase from 10% to 25% due to introduction of sprinkler trade-offs for Fire Separation Distance (FSD) between 3 to 10 ft. There are two scenarios: One

has 10% of UOA in a Configuration I compartment, the other has 25% of UOA in Configuration III-B compartment.

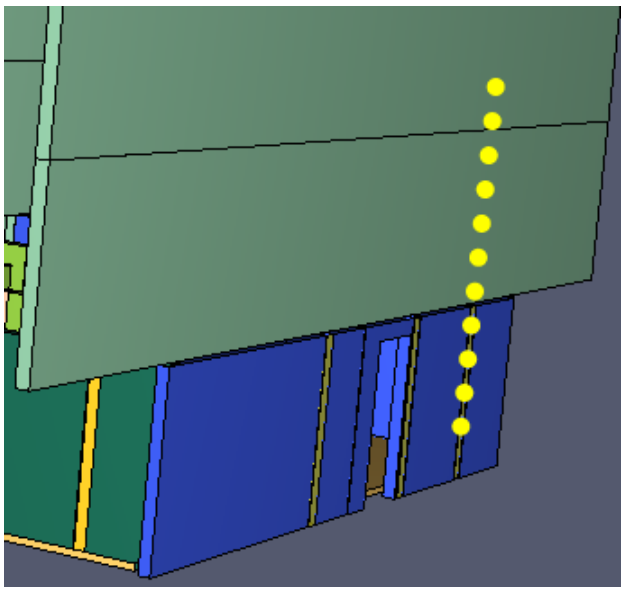

Figure 54 10% of UOA in a building of Configuration I

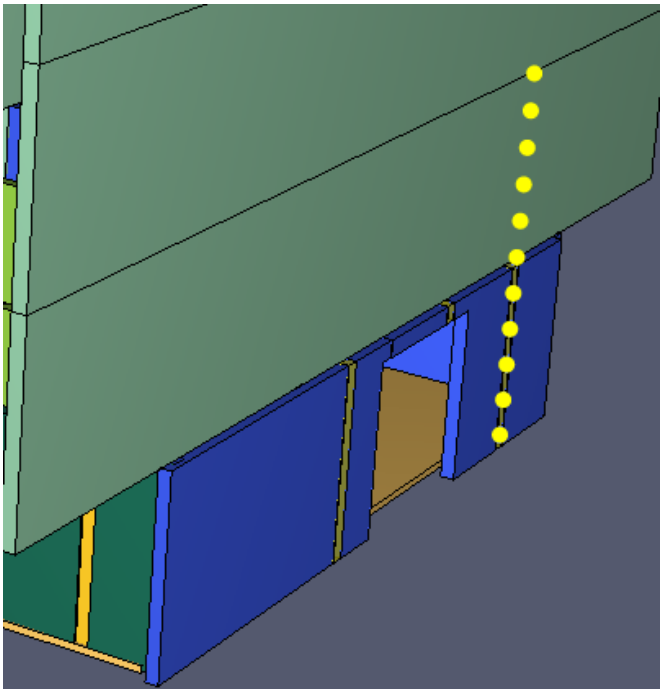

Figure 55 25% of UOA in building of Configuration III-B

The simulations results are shown in the following figures:

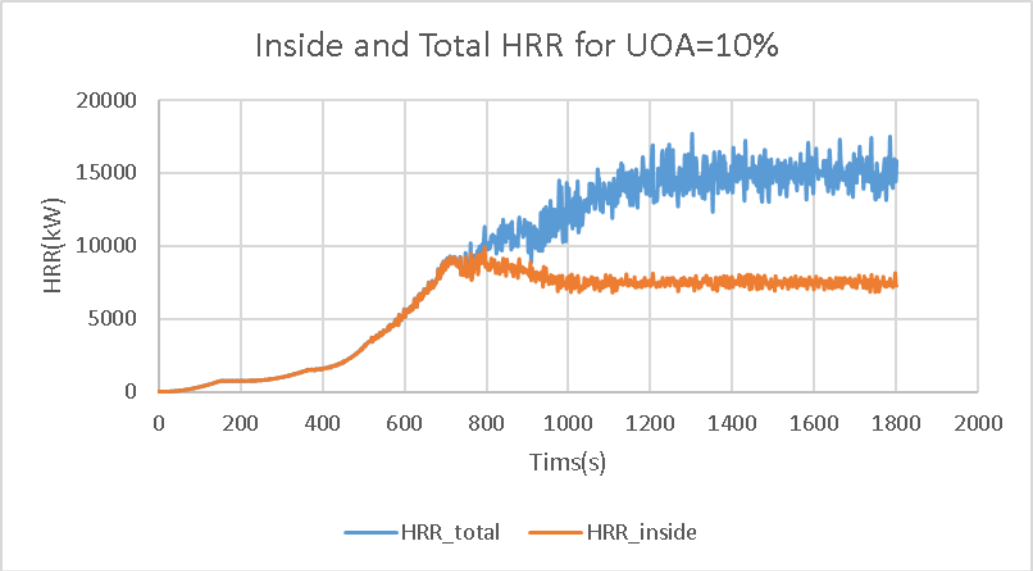

Figure 56 Relationship of total HRR and HRR inside the apartment for UOA =10%

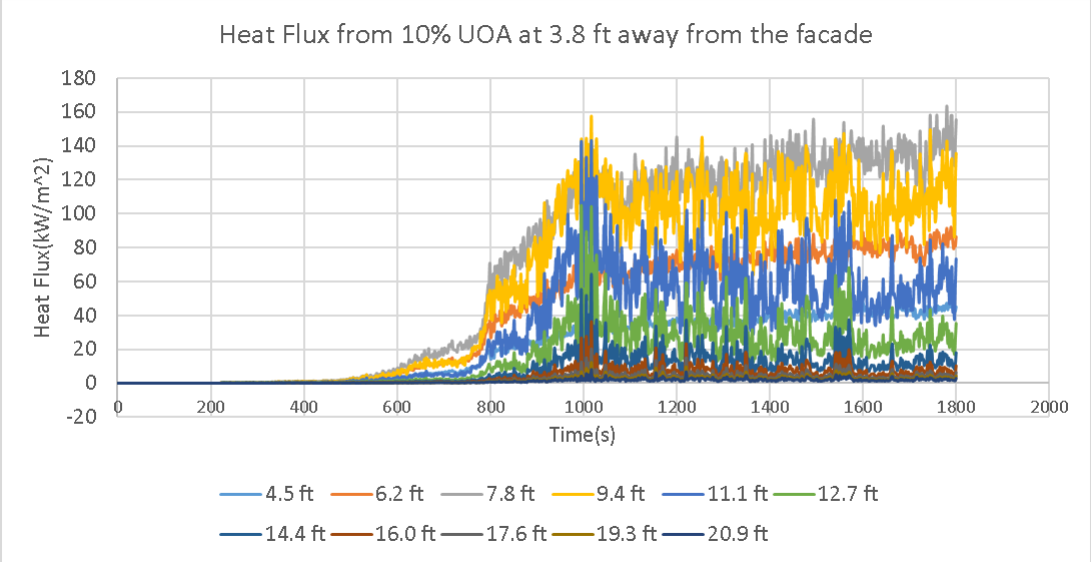

Figure 57 Heat flux from a 10% UOA, Configuration I compartment, at 3.8ft (1.14m) away from the façade

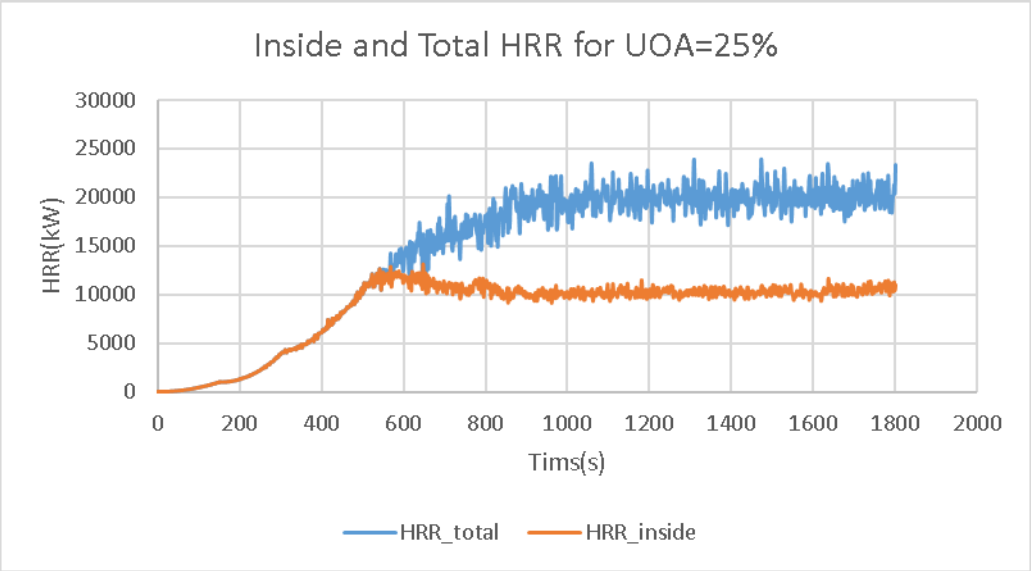

Figure 58 Relationship of total HRR and HRR inside the Type VB apartment for UOA =25%

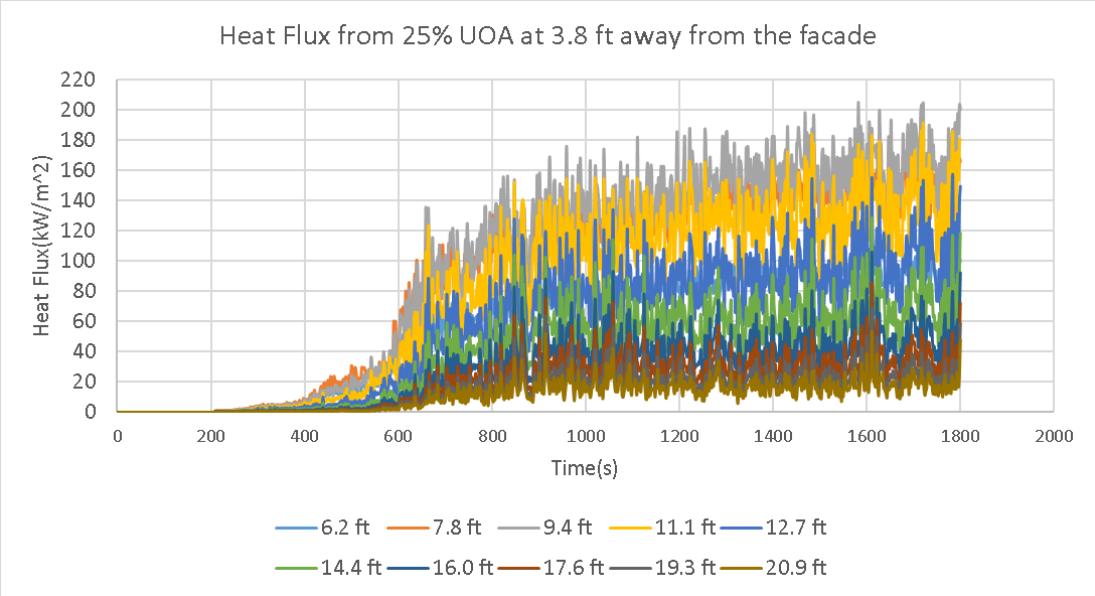

Figure 59 Heat flux from a 25% UOA, Configuration III-B compartment at 3.8ft (1.14m) away from the façade

From the above figures we know that:

1) For the 10% UOA in Configuration I compartment the highest heat flux is around 164kW/m^2, whereas for the 25% UOA in a Configuration III-B compartment the highest heat flux is around 205kw/m^2.
2) The Highest heat flux point moves from 7.8ft (2.375m) in 10% UOA scenario to 9.4ft (2.875m) in 25% UOA scenario.
3) The ignitable area (Radiation Heat Flux > 12.5kW/m^2) for the 10% UOA, Configuration I compartment is below 17.6ft (5.375m), whereas the ignitable area for the 25% UOA, Configuration III-B compartment is beyond 20.9ft (6.375m).

4) At a FSD of 3.8ft (1.14m) the hazards of fire spreading to neighboring buildings are considerably high even if the UOA is kept as low as 10%.

3.2.2. FSD between 10 to 15 ft

In the IBC Code, the UOA is allowed to rise from 15% to 45% due to introduction of sprinkler trade-offs for FSD between 10 to 15 ft. There are two scenarios: One has 15% of UOA in a Configuration I compartment, the other has 45% of UOA in a Configuration III-B compartment

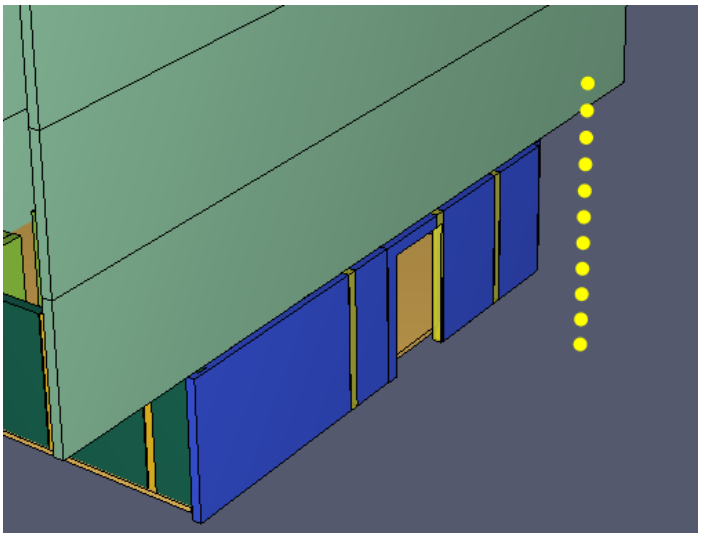

Figure 60 15% of UOA in a Configuration I compartment

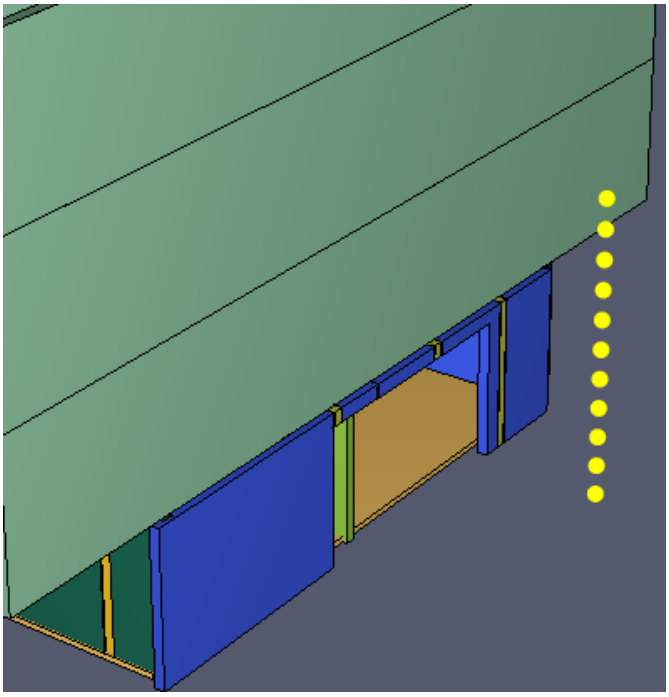

Figure 61 45% of UOA in Configuration III-B compartment

The simulation results are shown in the following figures:

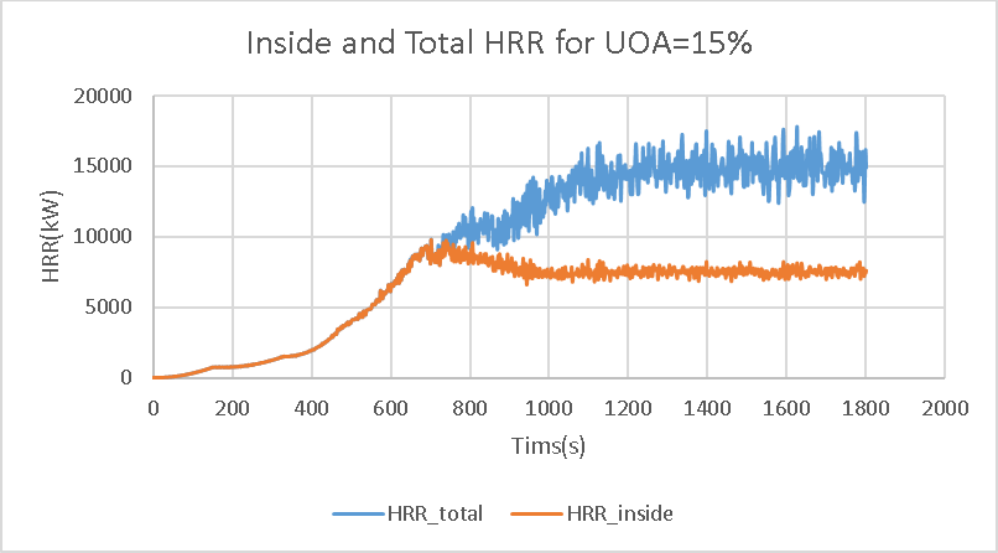

Figure 62 Relationship of total HRR and HRR inside the apartment for UOA =15%

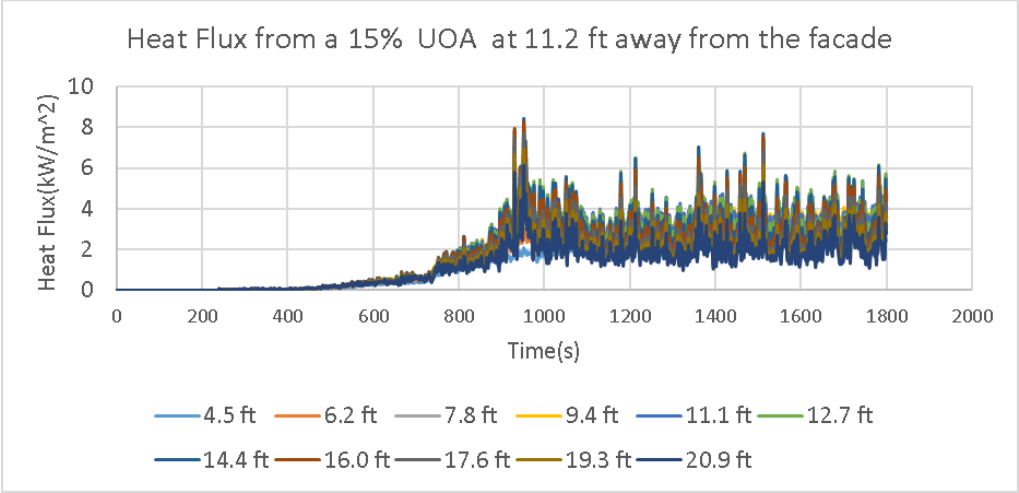

Figure 63 Heat flux from a 15% UOA, Configuration I compartment at 11.2ft (3.36m) away from the façade

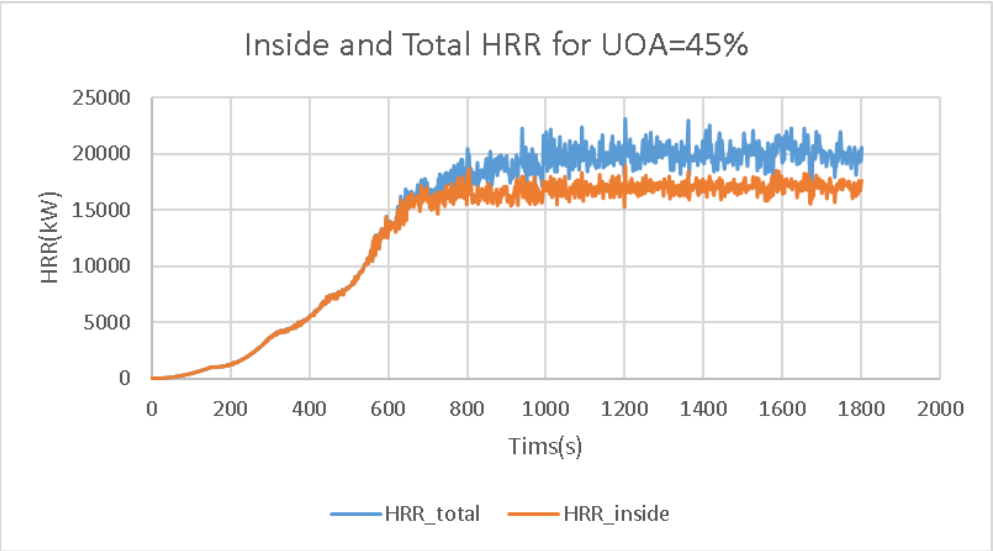

Figure 64 Relationship of total HRR and HRR inside the apartment for UOA =45%

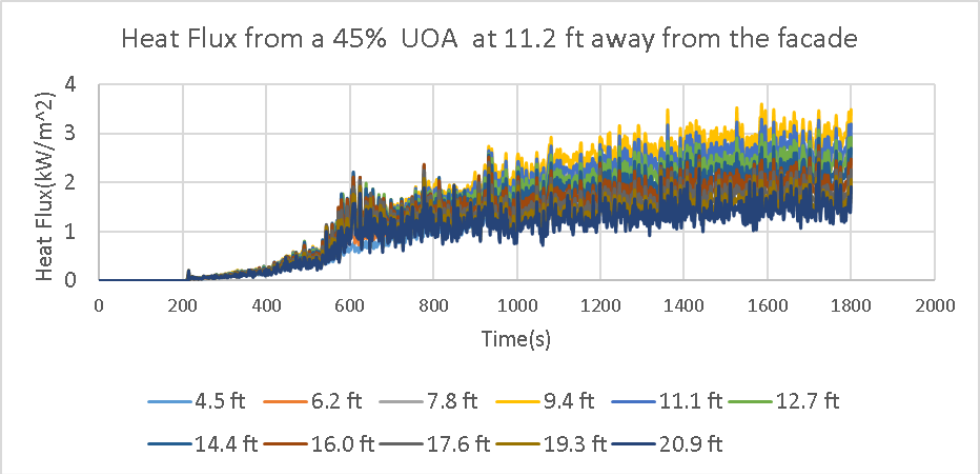

Figure 65 Heat flux from a 45% UOA, Configuration III-B compartment at 11.2 ft (3.36m) away from the facade

From the above two figures we know that:

1) For the 15% UOA in a Configuration I compartment the highest heat flux is around 8.3kW/m^2, whereas for the 25% UOA of a Configuration III-B compartment the highest heat flux is around 3.6 kw/m^2.
2) At a FSD of 11.2 ft (3.36m), there is little chance for fire to spreading to neighboring buildings even if the UOA is enlarged from 15% to 45%.

3.2.3. UOA changing from 25% to 75% due to introduction of sprinkler trade-offs for FSD between 15 to 20ft

In the IBC Code, the UOA is allowed to rise from 25% to 75% due to introduction of sprinkler trade-offs for FSD between 15 to 20 ft. There are two scenarios: One has 25% of UOA in Configuration I compartment, the other has 75% of UOA in a Configuration III-B compartment.

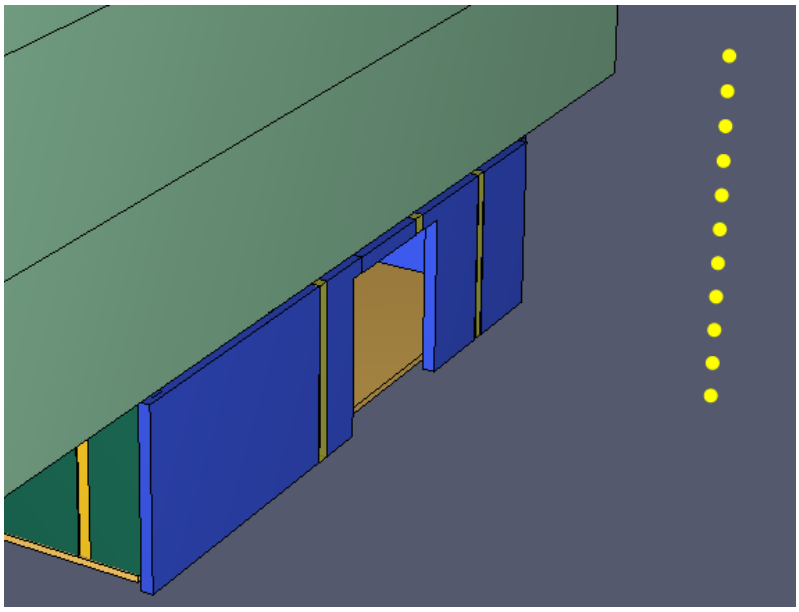

Figure 66 25% of UOA in a Configuration I compartment

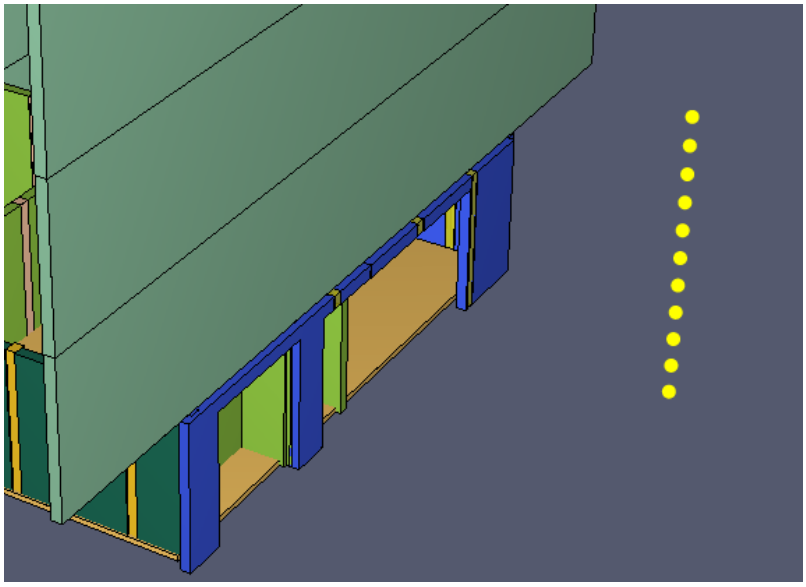

Figure 67 75% of UOA in a Configuration III-B compartment

The simulations results are shown in the following figures:

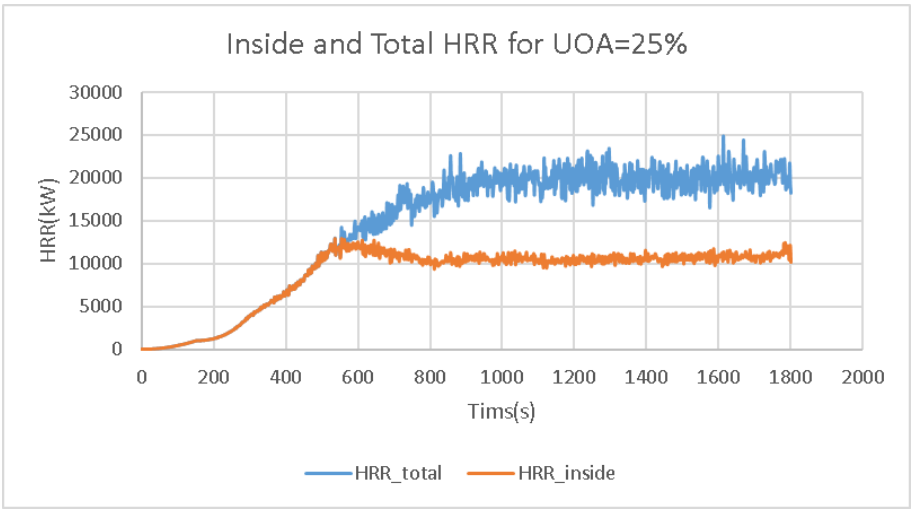

Figure 68 Relationship of total HRR and HRR inside the Type VA apartment for UOA =25%

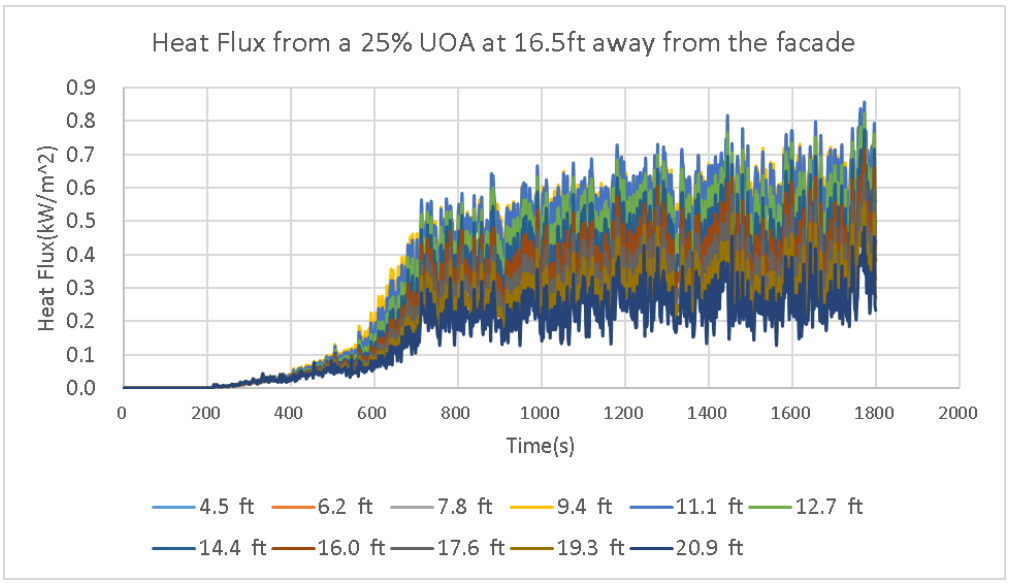

Figure 69 Heat flux from a 25% UOA, Configuration I compartment at 16.5 ft (4.95m) away from the façade

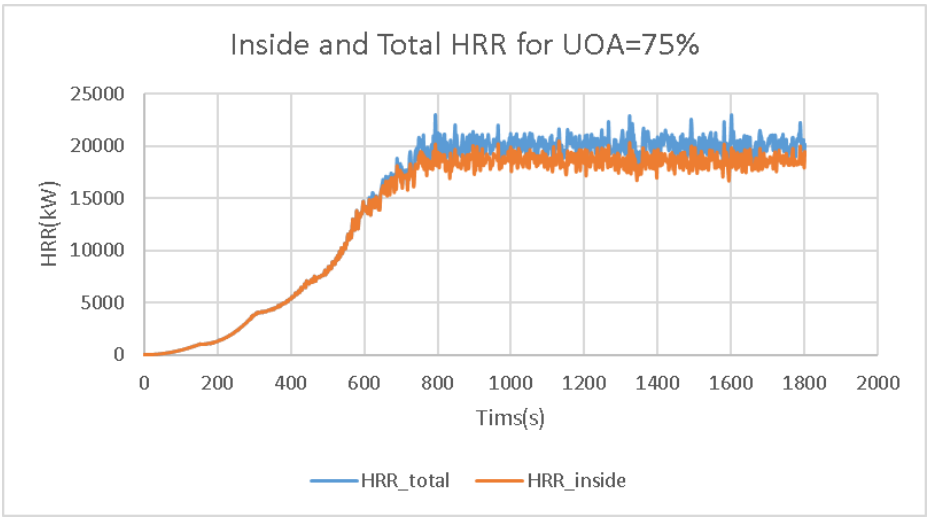

Figure 70 Relationship of total HRR and HRR inside the Type VB apartment for UOA =25%

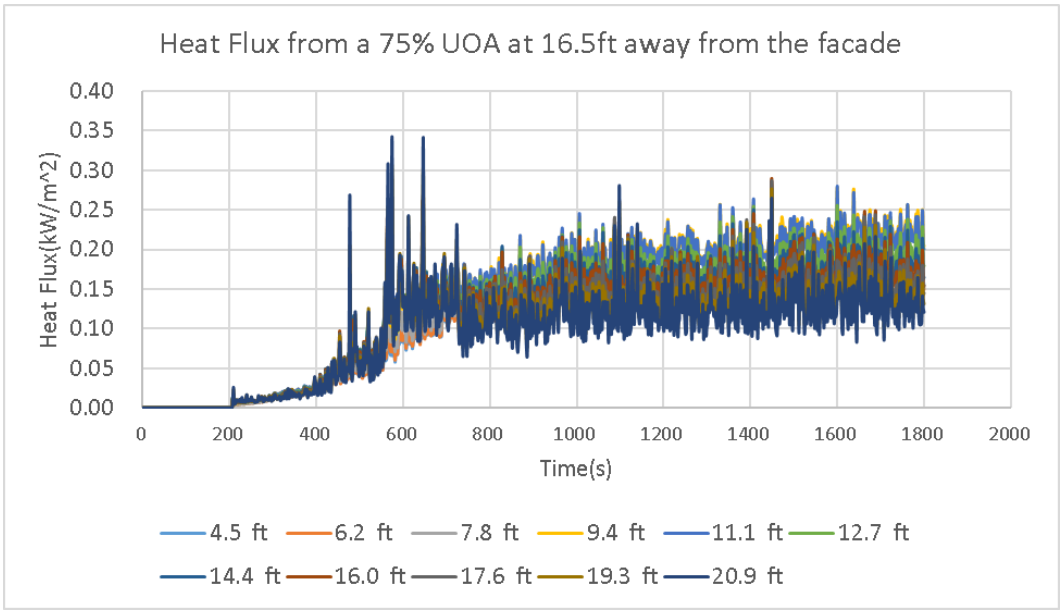

Figure 71 Heat flux from a 75% UOA, Configuration III-B compartment at 16.5ft (4.95m) away from the facade

From the above two figures we know that:

1) For the 25% UOA in a Configuration I compartment the highest heat flux is around 0.8kW/m^2, whereas for the 75% UOA in a Configuration III-B compartment the highest heat flux is around 0.3 kw/m^2.
2) At a FSD of 16.5ft (4.95m), there is little chance for fire to spreading to neighboring buildings even if the UOA is enlarged from 25% to 75%.

3.2.4. UOA changing from 70% to 100% due to introduction of sprinkler trade-offs for FSD greater than 20ft

In the IBC Code, the UOA is allowed to rise from 70% to 100% due to introduction of sprinkler trade-offs for FSD beyond 20 ft. There are two scenarios: One has 70% of UOA in a Configuration I compartment, the other has 100% of UOA in a Configuration III-B compartment.

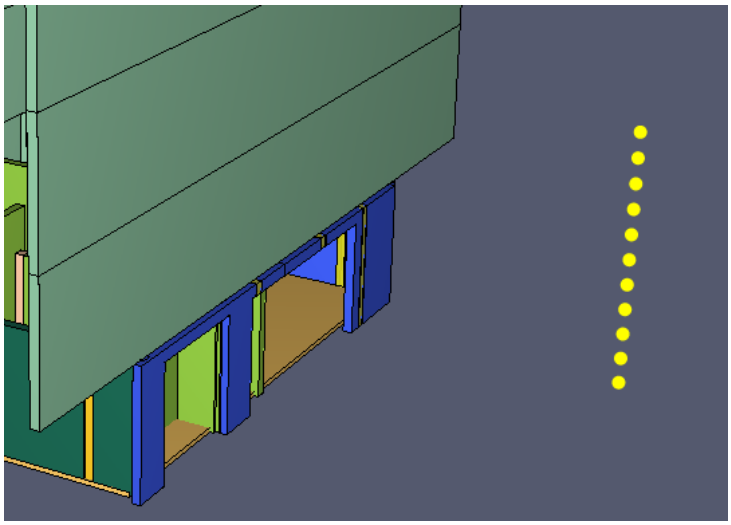

Figure 72 70% of UOA in a Configuration I compartment

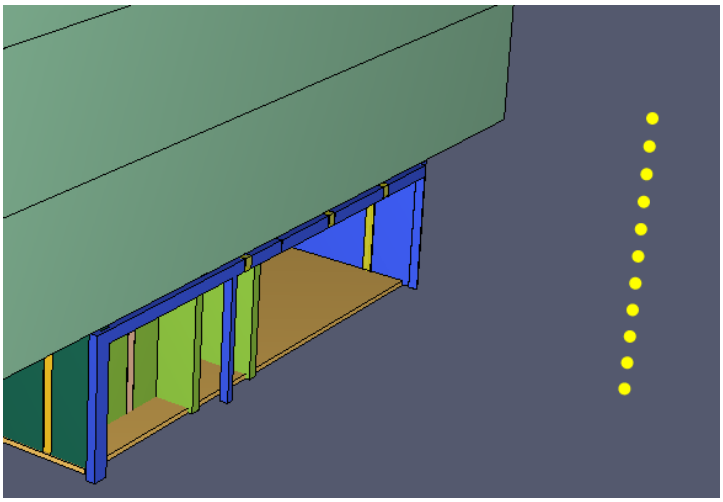

Figure 73 100% of UOA in Configuration III-B compartment

The simulations results are shown in the following figures:

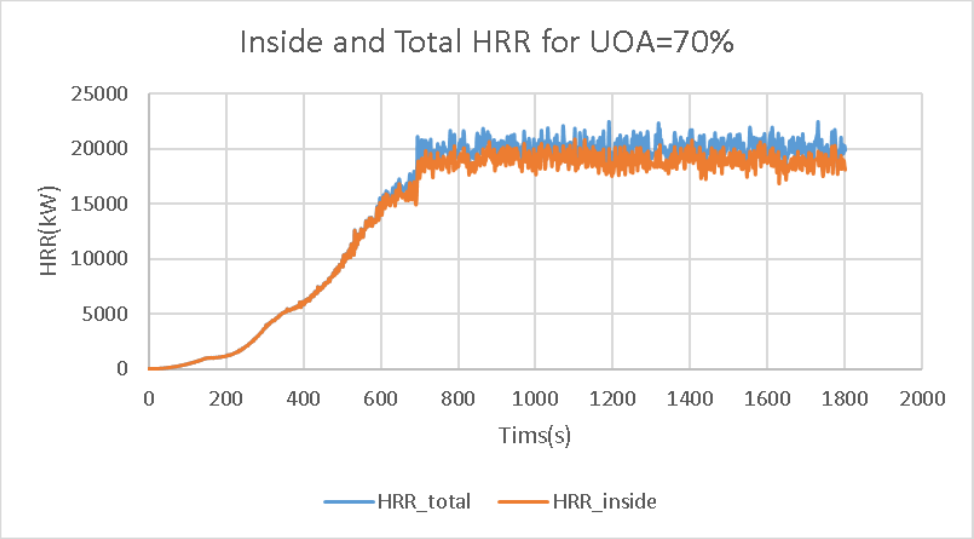

Figure 74 Relationship of total HRR and HRR inside the Type VA apartment for UOA =70%

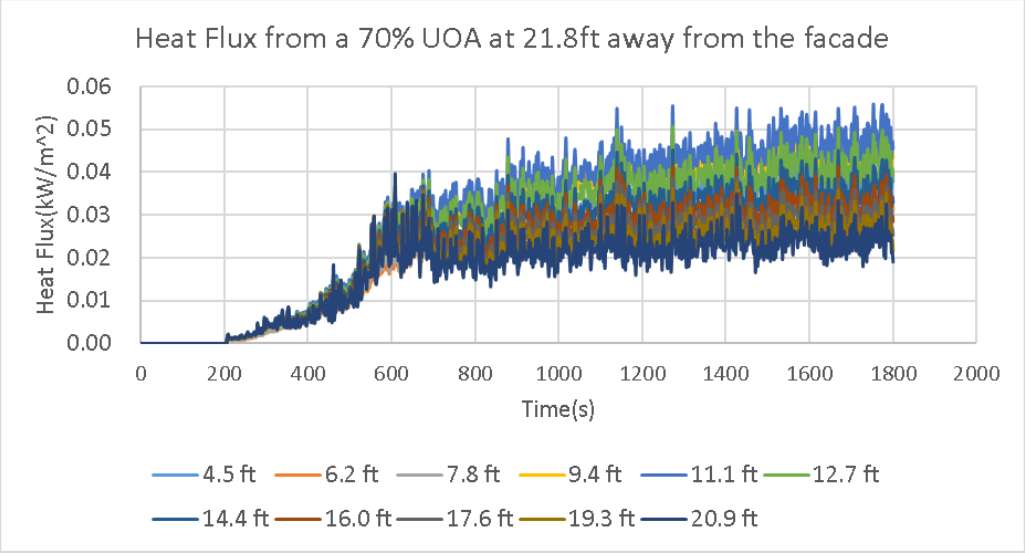

Figure 75 Heat flux from a 70% UOA, Configuration I compartment at 21.8 ft (6.54m) away from the façade

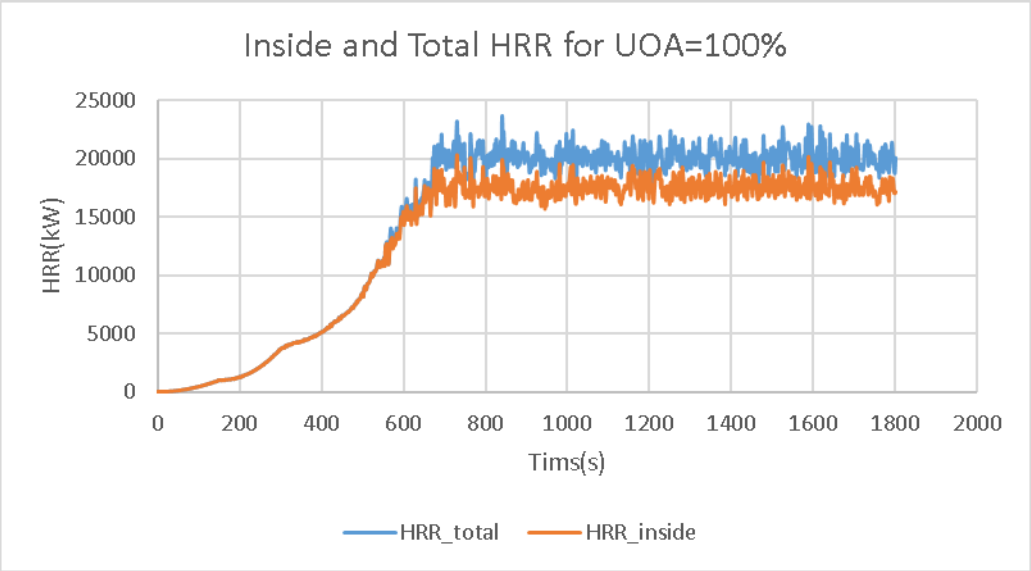

Figure 76 Relationship of total HRR and HRR inside the Type VB apartment for UOA =100%

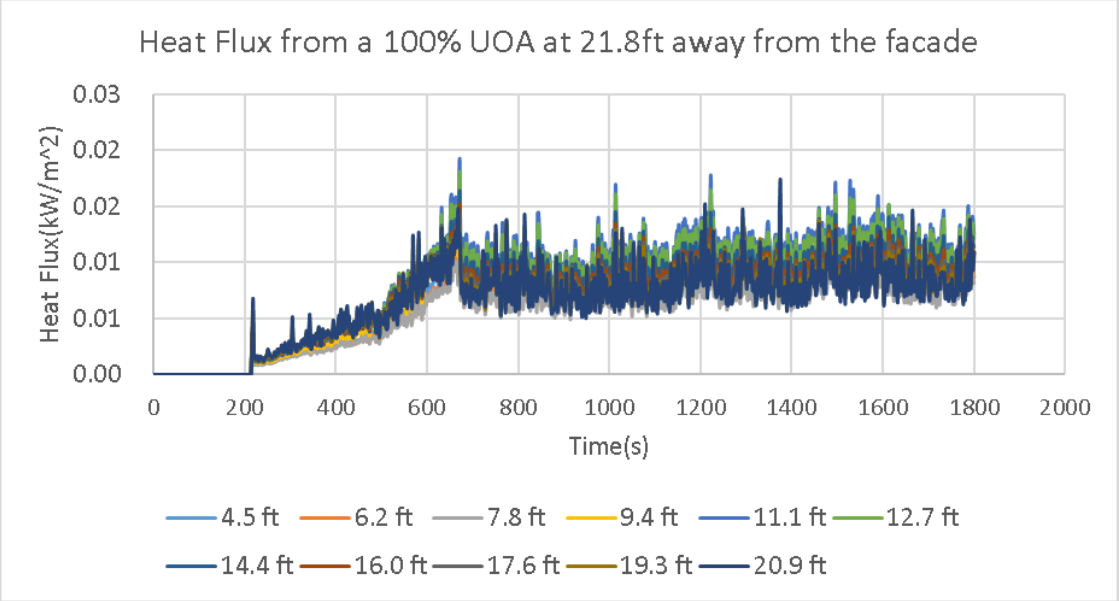

Figure 77 Heat flux from a 100% UOA, Configuration III-B compartment at 21.8ft (6.54m) away from the facade

From the above two figures we know that:

1) For the 70% UOA in a Configuration I compartment the highest heat flux is around 0.04kW/m^2, whereas for the 100% UOA in a Configuration III-B compartment the highest heat flux is around 0.01 kw/m^2.
2) At a FSD of 21.8ft (6.54m), there is little chance for fire to spreading to neighboring buildings even if the UOA is enlarged from 70% to 100%.
3) A summary about FSD, UOA and radiation Heat Flux is shown in the following table:

Table 45 summary about FSD, UOA and Heat Flux for standalone apartment fire

FSD(ft)	UOA(%)	Max Heat Flux(MHF,kW/ m^2)	Elevation of MHF point(ft)	Ignitable range(ft)
3.8	10	164	7.8	4.5~17.6
	25	205	9.4	4.5~20.9
11.2	15	8.3	16	null
	45	3.6	9.4	null
16.5	25	0.8	12.7	null
	75	0.3	20.9	null
21.8	70	0.04	20.9	null
	100	0.01	20.9	null

An ignitable range in the above table (and similar tables later) means the elevation range in façade of the neighboring building that is ignitable (namely, Heat Flux >12.5kW/m^2).

3.3. Heat flux fields from various UOA-Building apartment case

3.3.1. Background

The behavior of a standalone apartment fire differs from that of a building apartment fire in that an apartment in a building with corridors connecting apartments and stairwells connecting floors has less make-up air than a standalone apartment. In the last section our discussion centered on a standalone apartment fire, whereas in this section we will focus on a apartment fire in a building.

Compared to the single standalone apartment fire, two more detector trees, which are 5.3 feet and 8.6 feet from the façade, are shown:

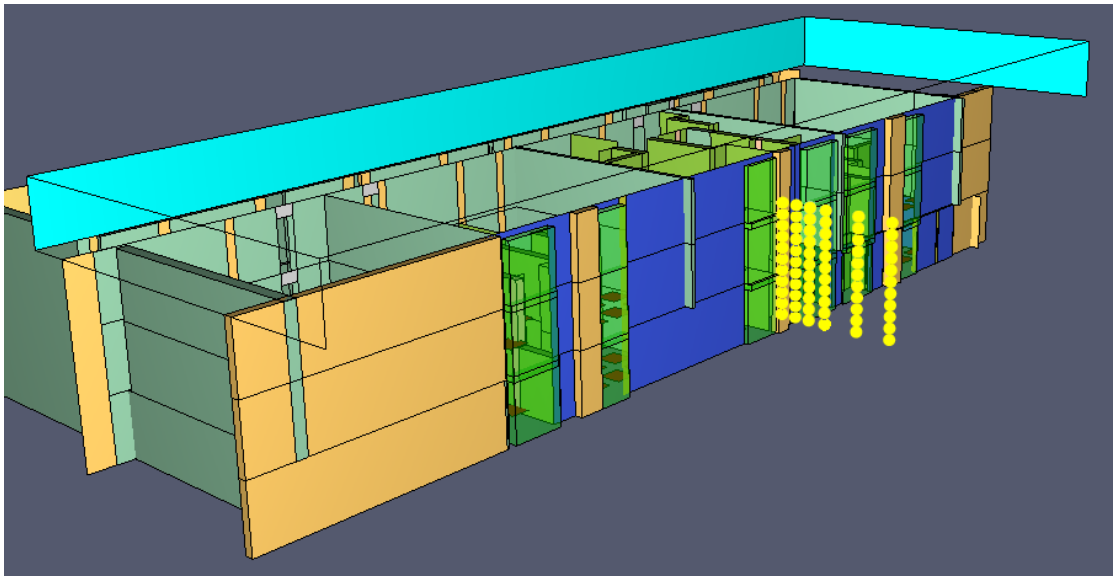

Figure 78 building compartments and detector trees of radiation heat flux

3.3.2. Fire Separation Distance(FSD) between 3 to 10 ft

In the IBC Code, the UOA is allowed to rise from 10% to 25% due to introduction of sprinkler trade-offs for Fire Separation Distance (FSD) between 3 to 10 ft. There are two scenarios: One has 10% of UOA in a Configuration I compartment, the other has 25% of UOA in Configuration III-B compartment.

a) If one compartment is involved in fire, the simulations results are shown in the following figures:

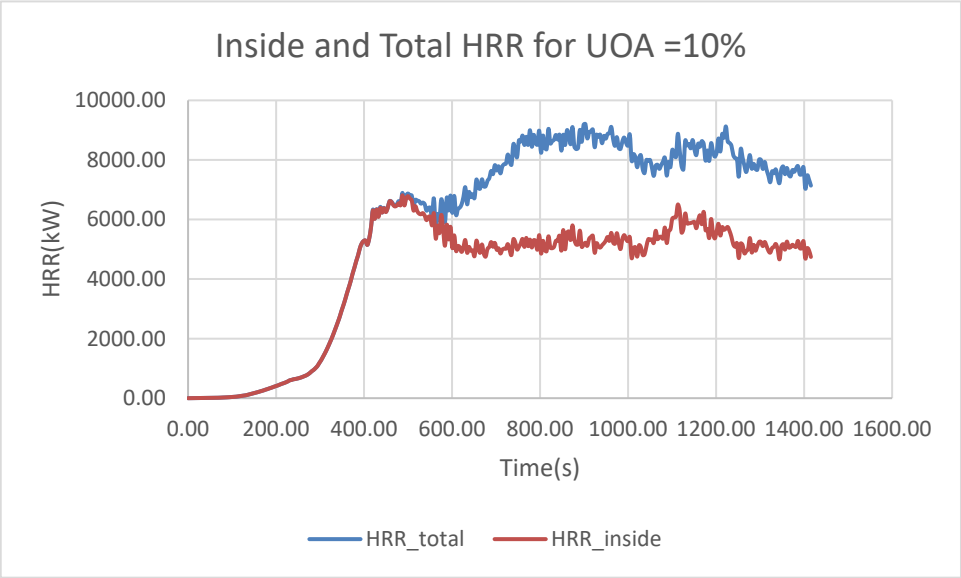

Figure 79 Relationship of total HRR and HRR inside the building for UOA =10%

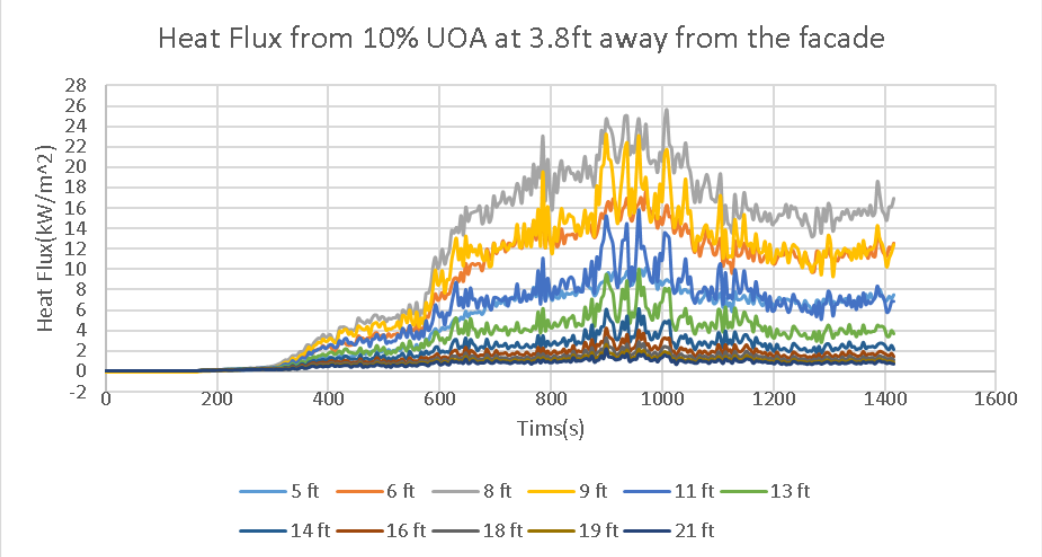

Figure 80 Heat flux from a 10% UOA, Configuration I compartment, at 3.8ft (1.14m) away from the façade

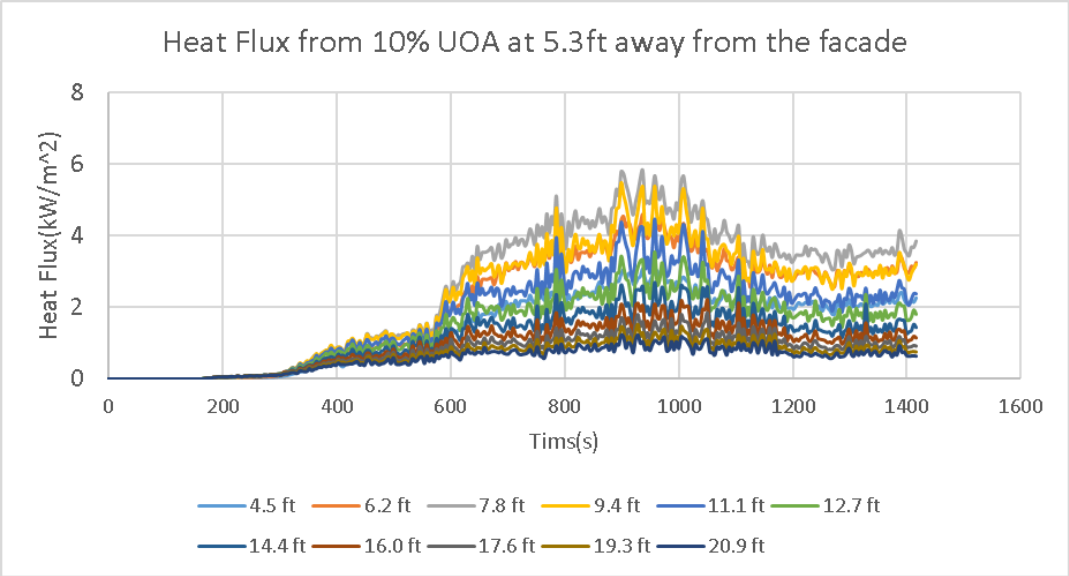

Figure 81 Heat flux from a 10% UOA, Configuration I compartment, at 5.3ft (1.59m) away from the façade

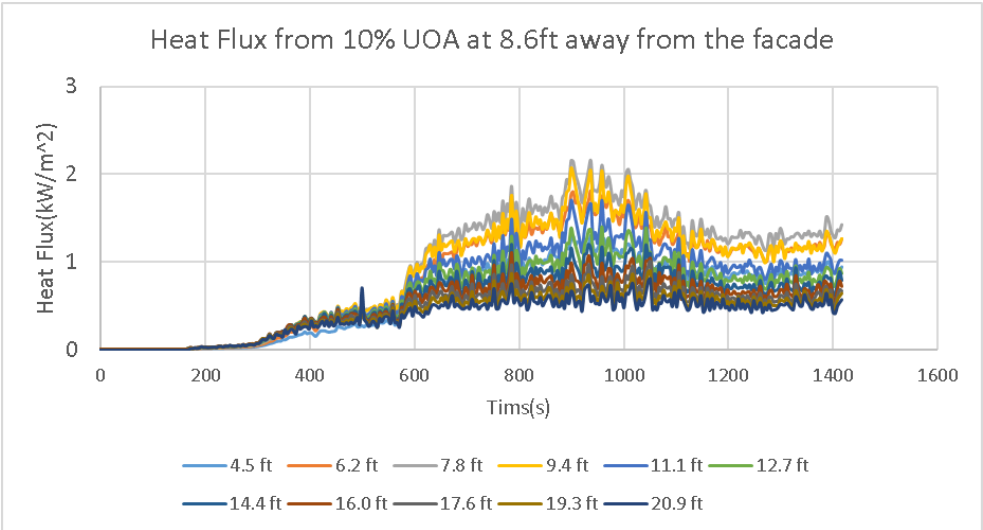

Figure 82 Heat flux from a 10% UOA, Configuration I compartment, at 8.6ft (2.58m) away from the façade

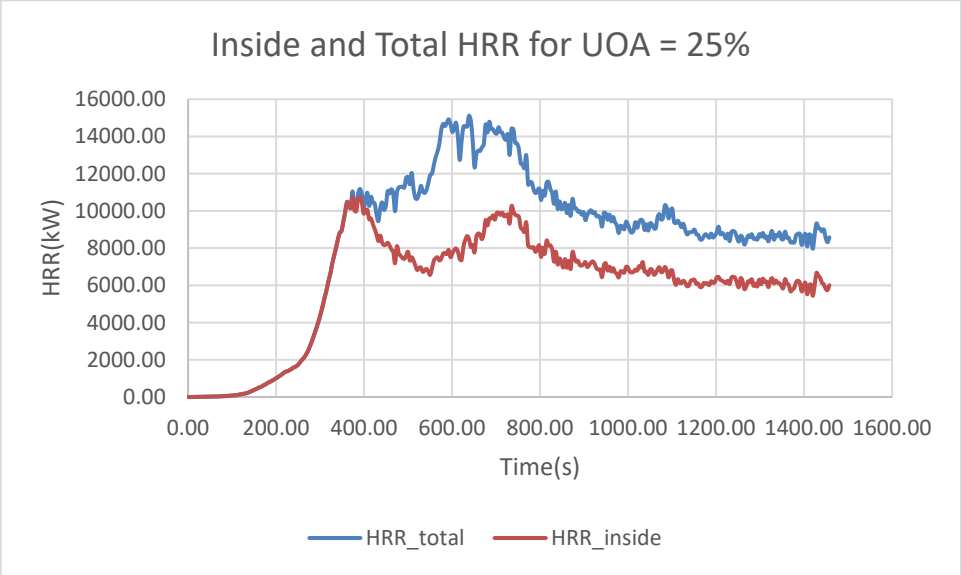

Figure 83 Relationship of total HRR and HRR inside the building for UOA =25%

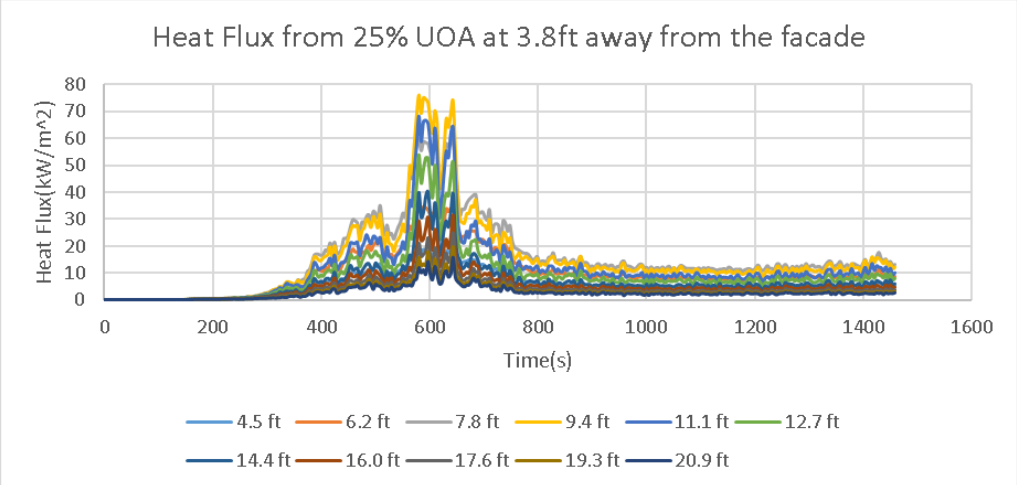

Figure 84 Heat flux from a 25% UOA, Configuration III-B compartment, at 3.8ft (1.14m) away from the façade

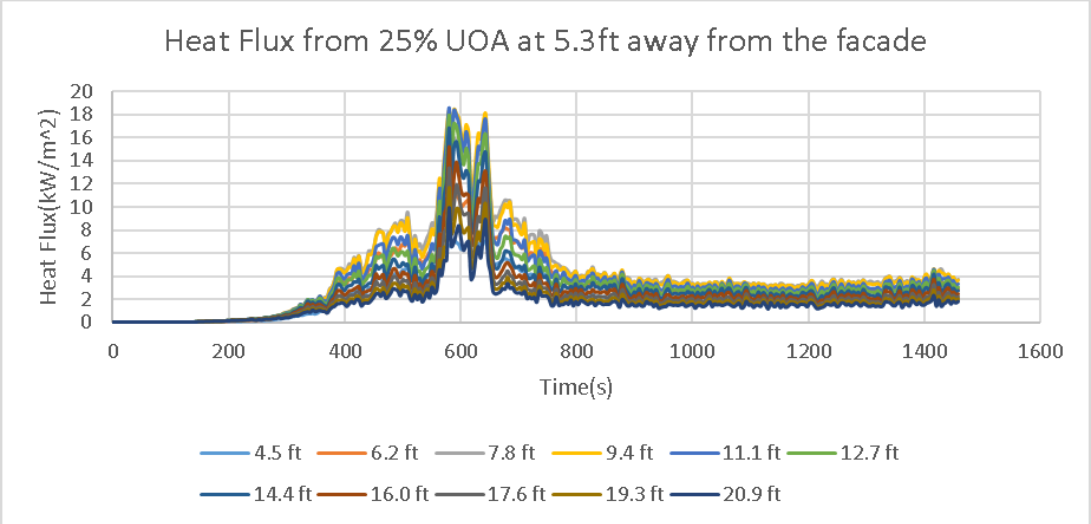

Figure 85 Heat flux from a 25% UOA, Configuration III-B compartment, at 5.3ft (1.59m) away from the façade

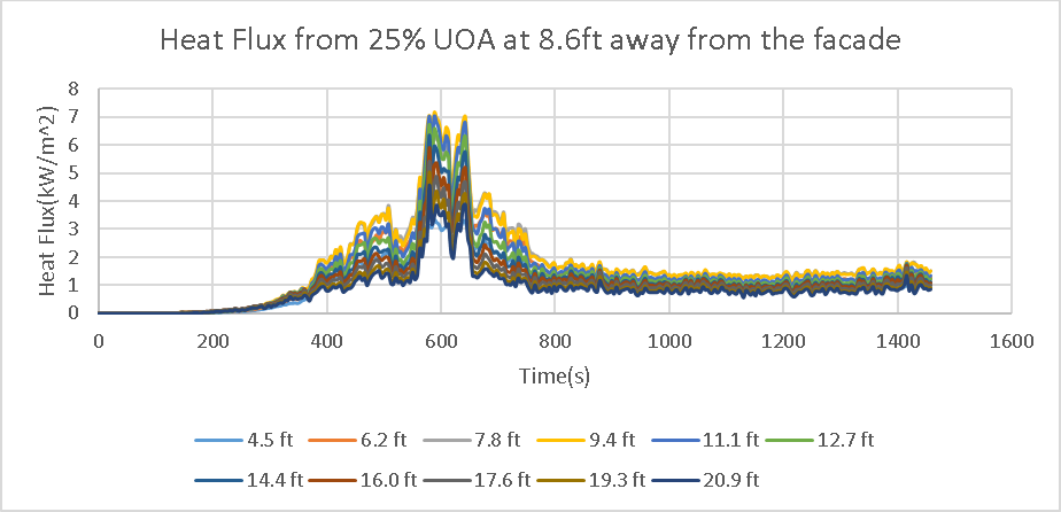

Figure 86 Heat flux from a 25% UOA, Configuration III-B compartment, at 8.6ft (2.58m) away from the façade

b) If five compartments are involved in fire, the simulations results are shown in the following figures:

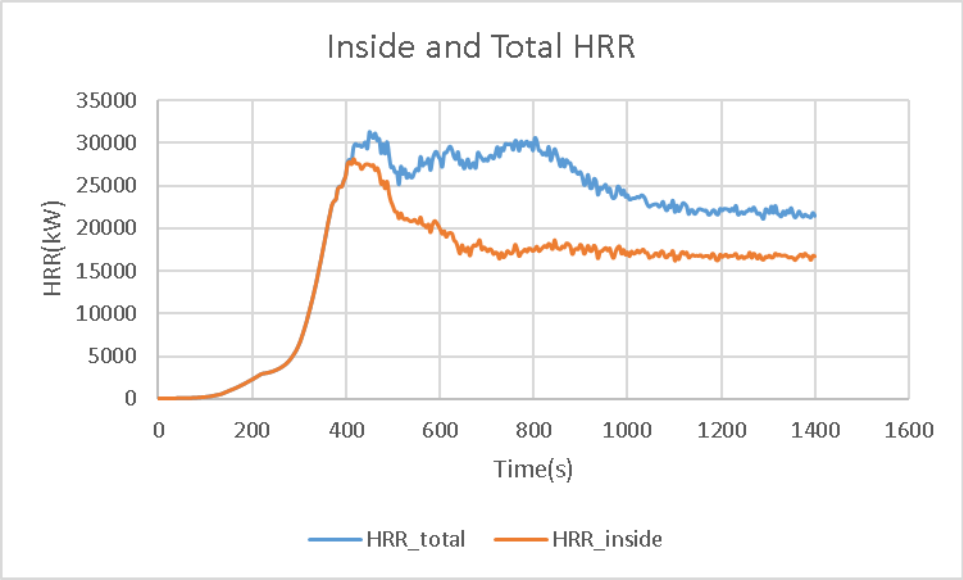

Figure 87 Relationship of total HRR and HRR inside the building for UOA =10% (5 apartments fire)

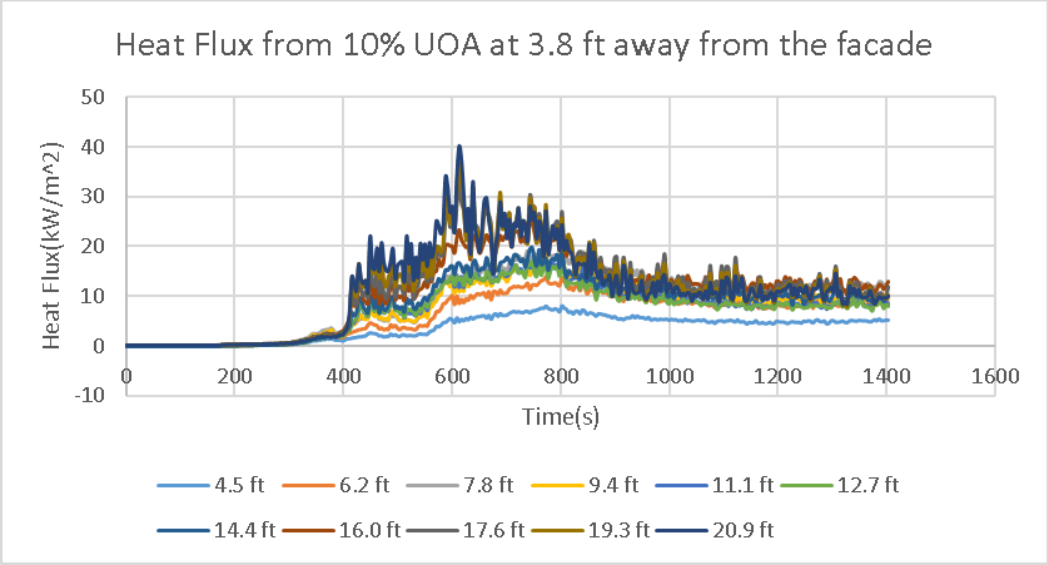

Figure 88 Heat flux from a 10% UOA, Configuration I compartment, at 3.8ft (1.14m) away from the façade

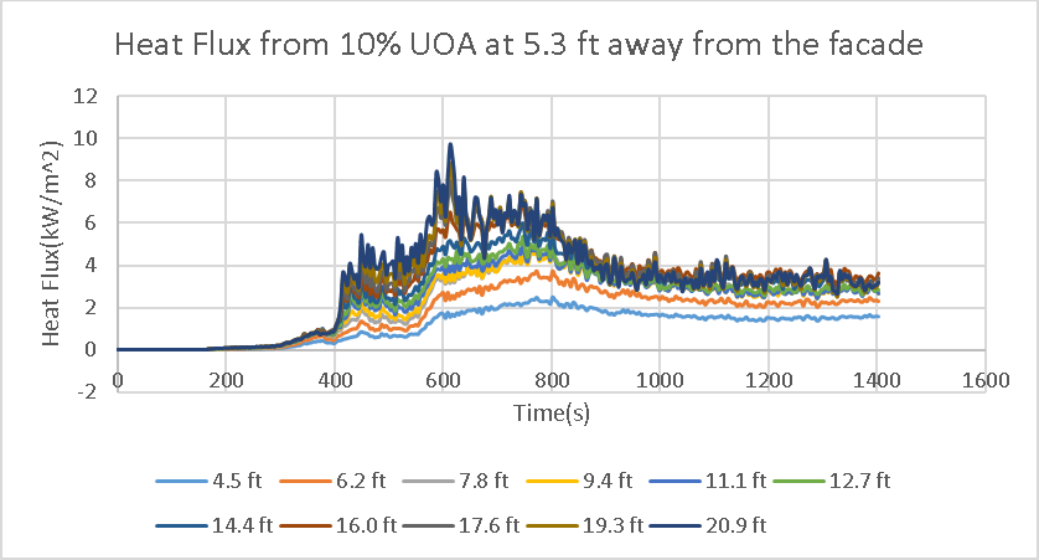

Figure 89 Heat flux from a 10% UOA, Configuration I compartment, at 5.3ft (1.59m) away from the façade

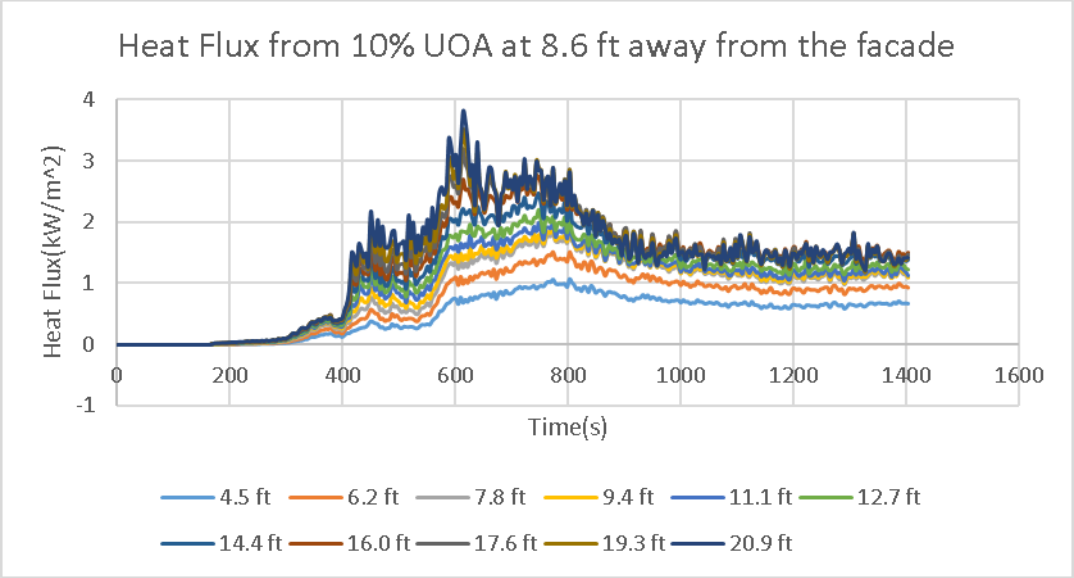

Figure 90 Heat flux from a 10% UOA, Configuration I compartment, at 8.6ft (2.58m) away from the façade

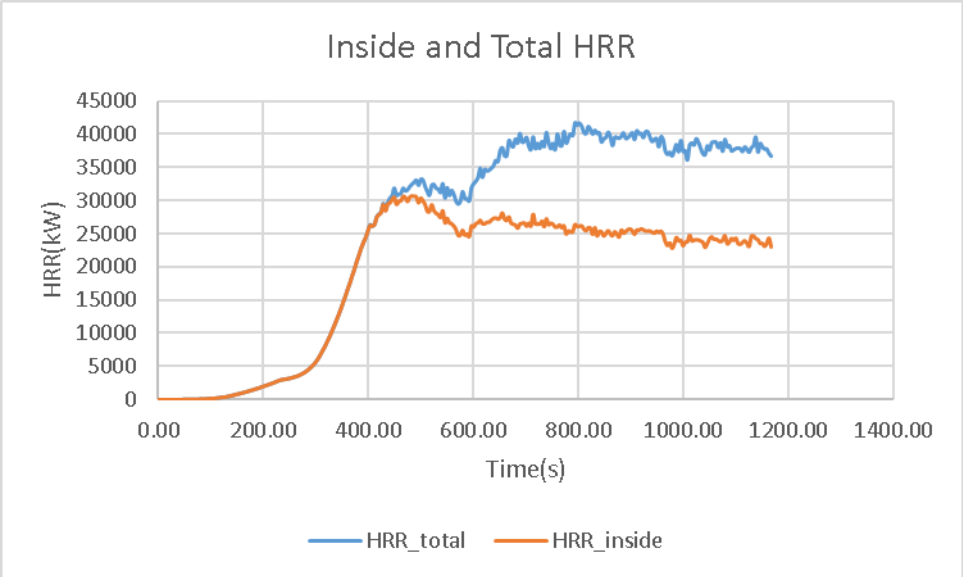

Figure 91 Relationship of total HRR and HRR inside the building for UOA =25% (5 apartments fire)

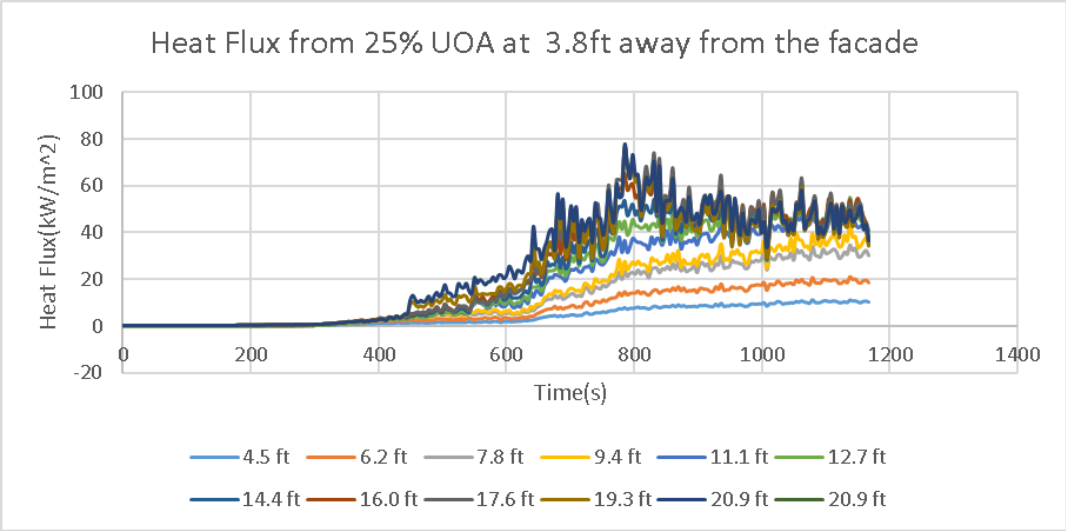

Figure 92 Heat flux from a 25% UOA, Configuration III-B compartment, at 3.8ft (1.14m) away from the façade

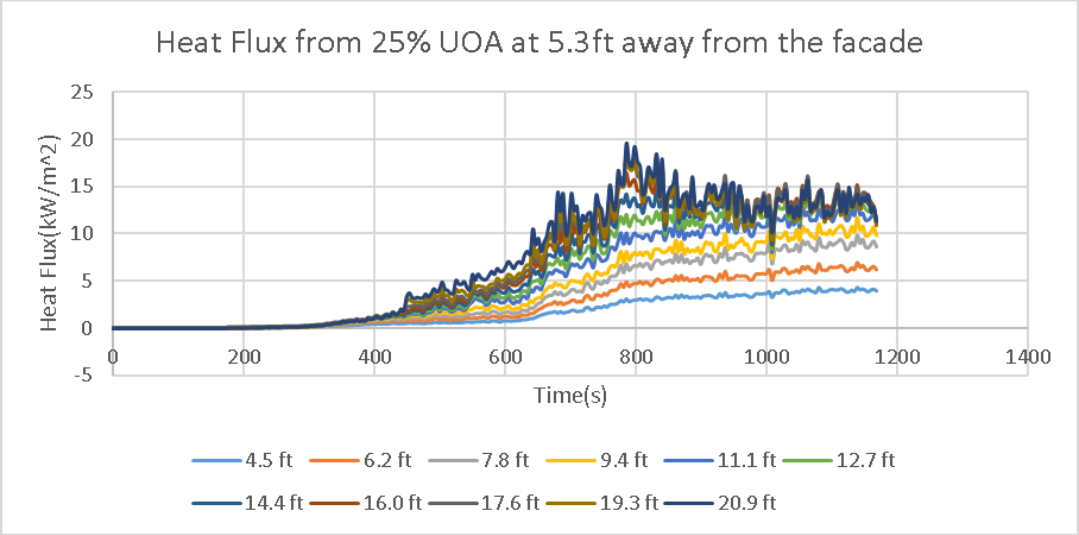

Figure 93 Heat flux from a 25% UOA, Configuration III-B compartment, at 5.3ft (1.59m) away from the façade

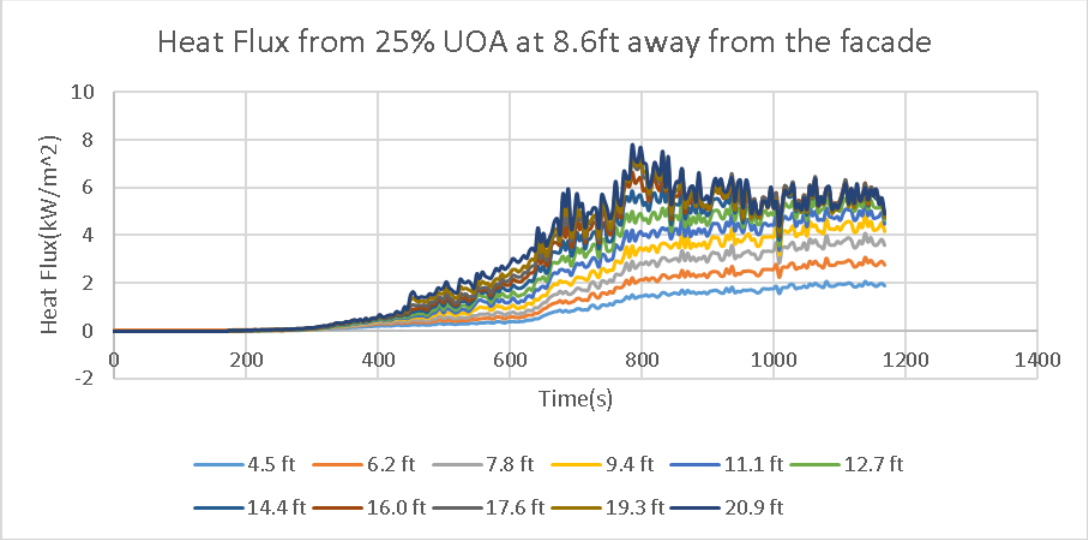

Figure 94 Heat flux from a 25% UOA, Configuration III-B compartment, at 8.6ft (2.58m) away from the façade

The following 2 tables show the summary of the above figure where the ignitable criteria means Radiation Heat Flux >12.5kW/ m^2:

Table 46 summary about FSD, UOA and Heat Flux for one apartment involved in fire

FSD(ft)	UOA(%)	Max Heat Flux(MHF,kW/ m^2)	Elevation of MHF point(ft)	Ignitable range(ft)
3.8	10	25	7.8	6.2~11.1
	25	75	9.4	4.5~20.9
5.3	10	5.8	7.8	null
	25	18.5	11.1	6.2~19.3
8.6	10	2.2	7.8	null
	25	7.2	9.4	null

Table 47 summary about FSD, UOA and Heat Flux for five apartment involved in fire

FSD(ft)	UOA(%)	Max Heat Flux(MHF,kW/ m^2)	Elevation of MHF point(ft)	Ignitable range(ft)
3.8	10	40	20.9	>6.2
	25	77.4	20.9	>6.2
5.3	10	9.7	20.9	null
	25	19.5	20.9	>11.2
8.6	10	3.8	20.9	null
	25	7.8	20.9	null

From the above 2 tables it is clear that at a FSD of 3.8ft the hazards of fire spreading to neighboring buildings are considerably high even if the UOA is kept as low as 10% with only one apartment being involved in fire.

3.3.3. Fire Separation Distance(FSD) between 10 to 15 ft

In the IBC Code, the UOA is allowed to rise from 15% to 45% due to introduction of sprinkler trade-offs for Fire Separation Distance (FSD) between 10 to 15 ft. There are two scenarios: One has 15% of UOA in a Configuration I compartment, the other has 45% of UOA in Configuration III-B compartment.

a) If one compartment is involved in fire, the simulations results are shown in the following figures:

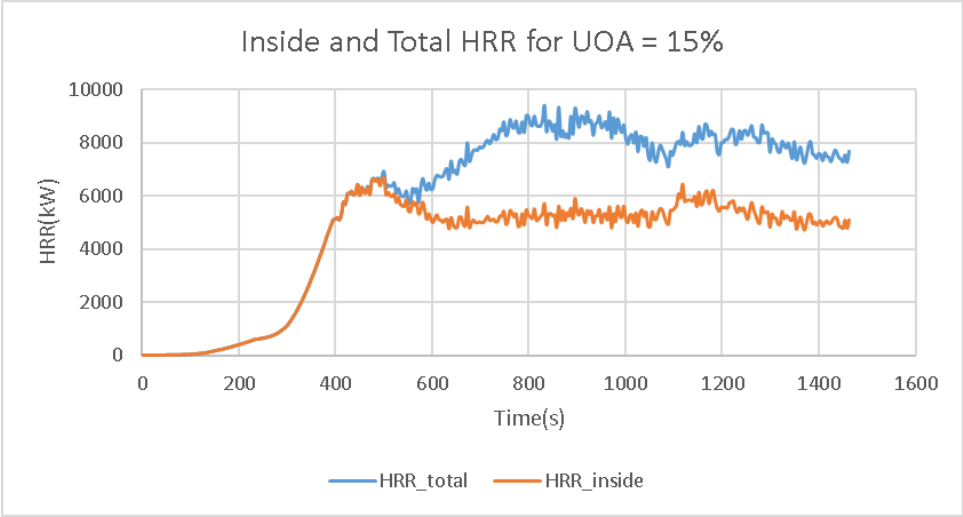

Figure 95 Relationship of total HRR and HRR inside the building for UOA =15% (1 apartment involved in fire)

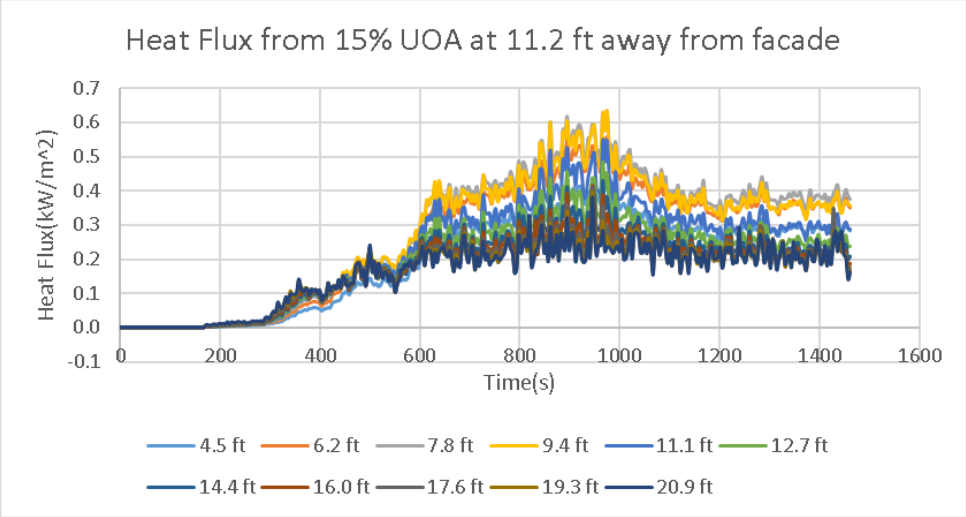

Figure 96 Heat flux from a 15% UOA, Configuration I compartment, at 11.2ft (3.36m) away from the façade (1 apartment involved in fire)

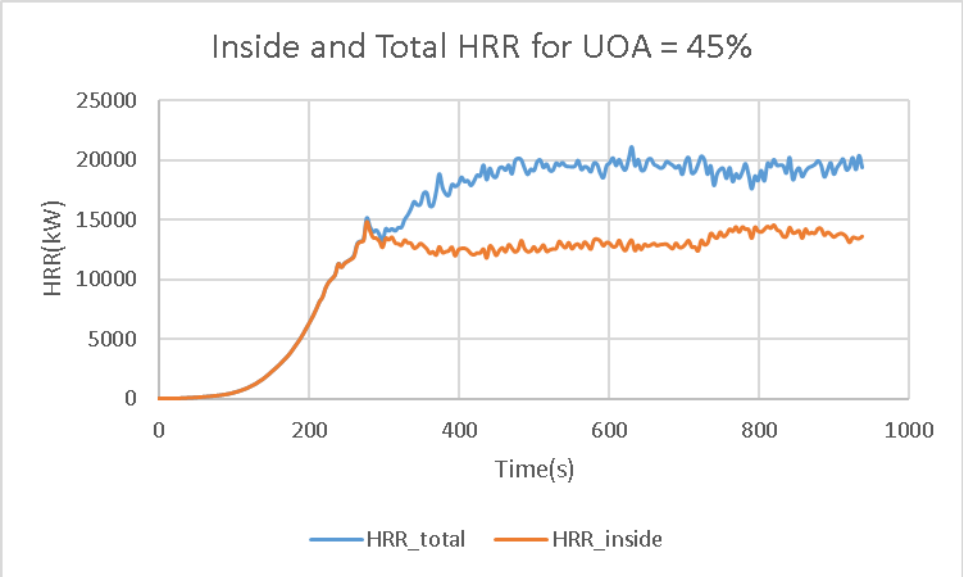

Figure 97 Relationship of total HRR and HRR inside the building for UOA =45% (1 apartment involved in fire)

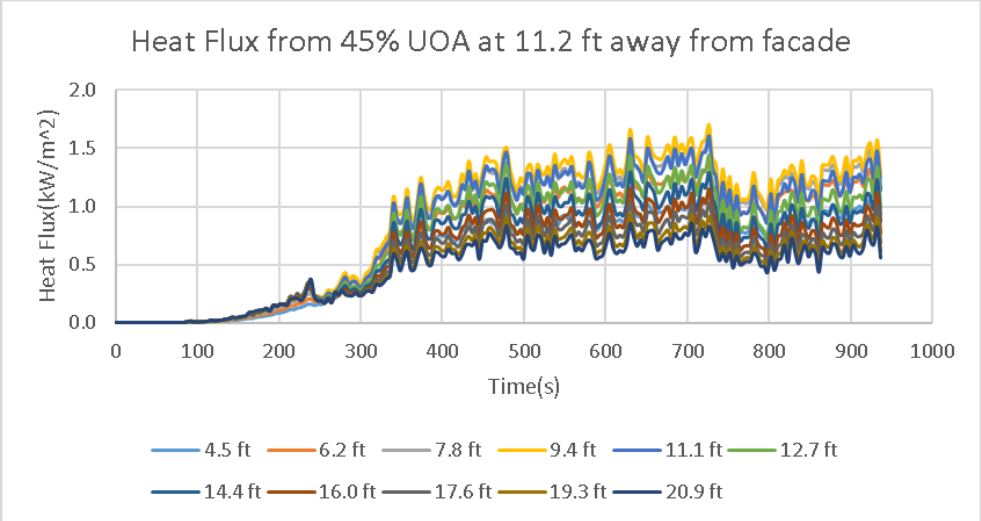

Figure 98 Heat flux from a 45% UOA, Configuration III-B compartment, at 11.2ft (3.36m) away from the façade (1 apartment involved in fire)

b) If five compartments are involved in fire, the simulation results are shown below:

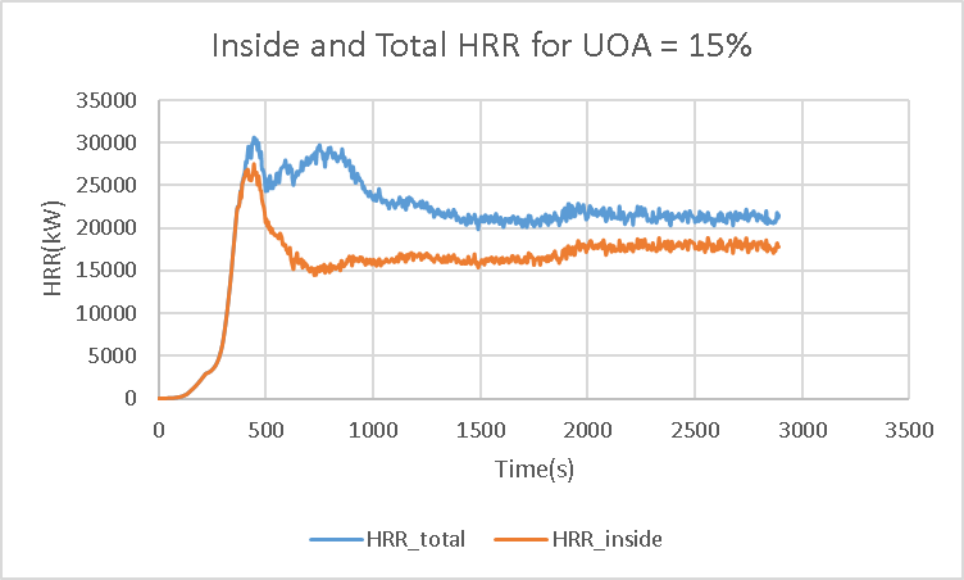

Figure 99 Relationship of total HRR and HRR inside the building for UOA =15% (5 apartments fire)

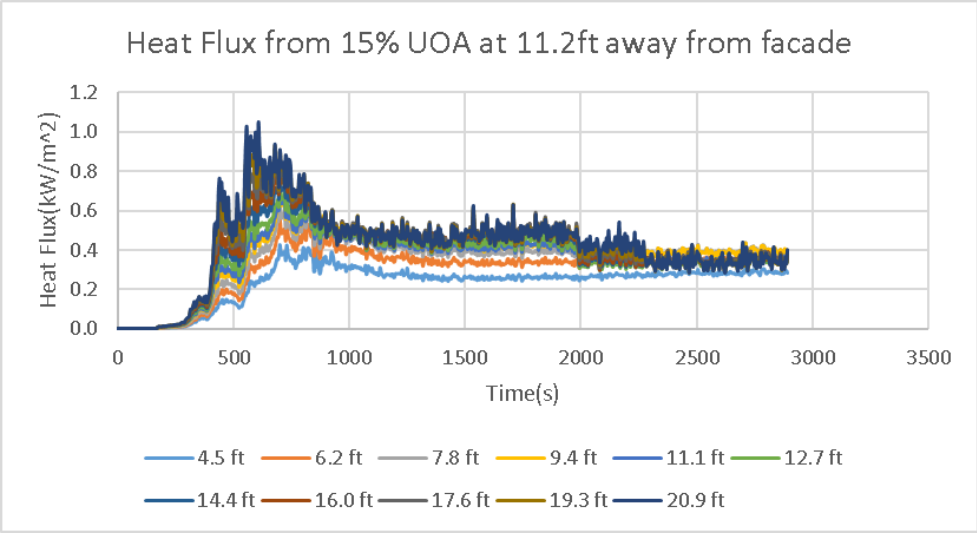

Figure 100 Heat flux from a 15% UOA, Configuration I compartment, at 11.2ft (3.36m) away from the façade

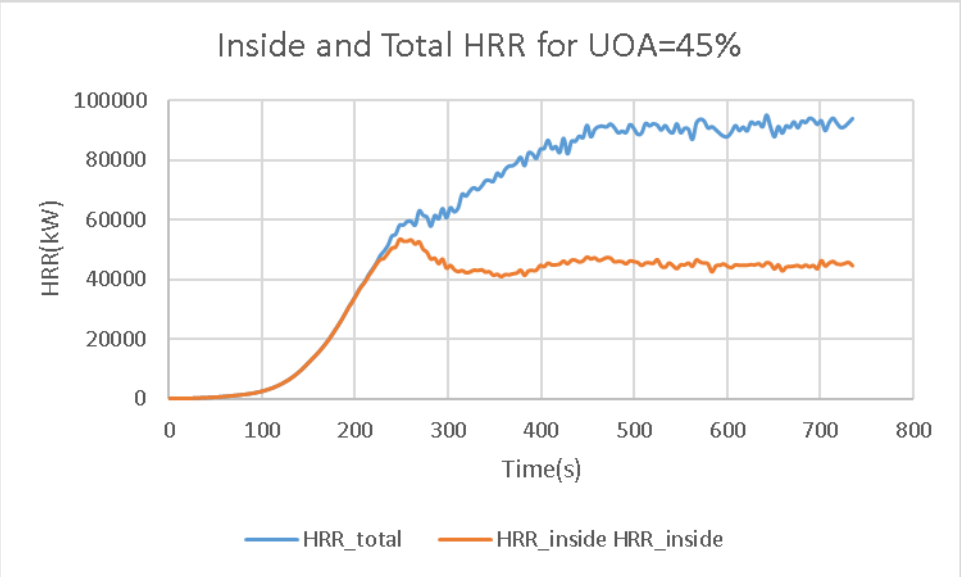

Figure 101 Relationship of total HRR and HRR inside the building for UOA=45% (5 apartments fire)

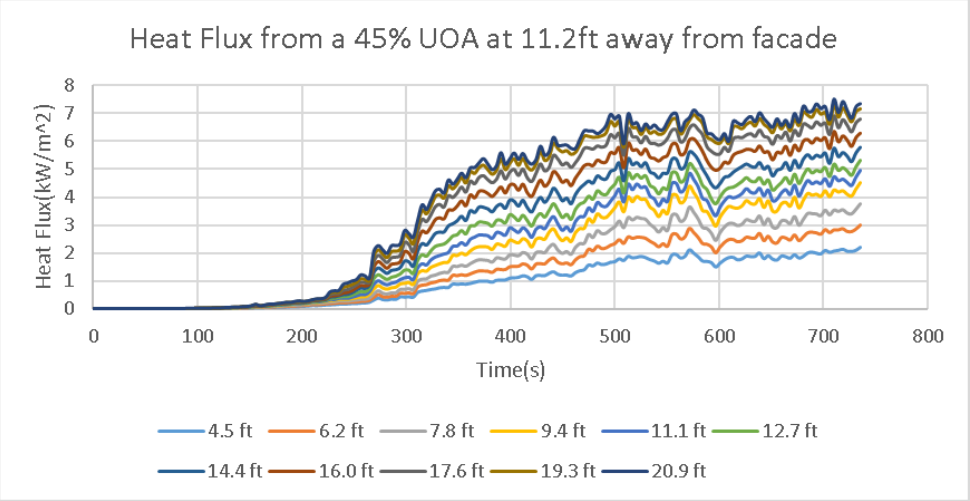

Figure 102 Heat flux from a 45% UOA, Configuration I compartment, at 11.2ft (3.36m) away from the façade

Table 48 summary about FSD, UOA and Heat Flux for one apartment involved in fire

FSD(ft)	UOA(%)	Max Heat Flux(MHF,kW/ m^2)	Elevation of MHF point(ft)	Ignitable range(ft)
11.2	15	0.63	9.4	null
	45	1.7	9.4	null

Table 49 summary about FSD, UOA and Heat Flux for five apartment involved in fire

FSD(ft)	UOA(%)	Max Heat Flux(MHF,kW/m^2)	Elevation of MHF point(ft)	Ignitable range(ft)
11.2	15	1.05	20.9	null
	45	7.51	20.9	null

From the above two tables it is clear that even if there are five apartments involved in fire, the heat flux at FSD=11.2ft from 45% UOA is less than the commonly used critical limit of 12.5kW/m^2. It is likely that the neighboring building will not be ignited.

3.3.4. Fire Separation Distance(FSD) between 15 to 20 ft

In the IBC Code, the UOA is allowed to rise from 25% to 75% due to introduction of sprinkler trade-offs for Fire Separation Distance (FSD) between 15 to 20 ft. There are two scenarios: One has 25% of UOA in a Configuration I compartment, the other has 75% of UOA in Configuration III-B compartment.

a) If one compartment is involved in fire, the simulations results are shown in the following figures:

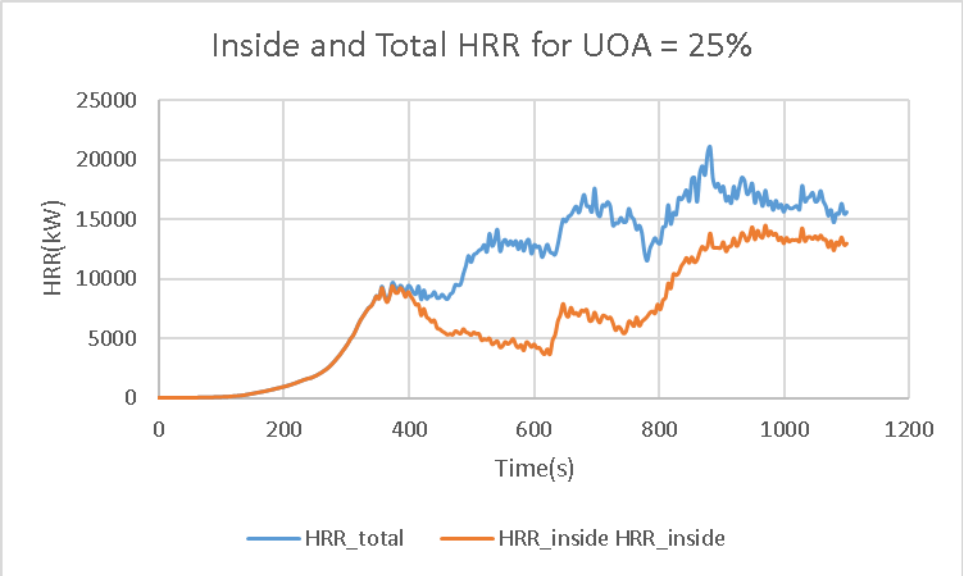

Figure 103 Relationship of total HRR and HRR inside the building for UOA =25% (one apartment involved in fire)

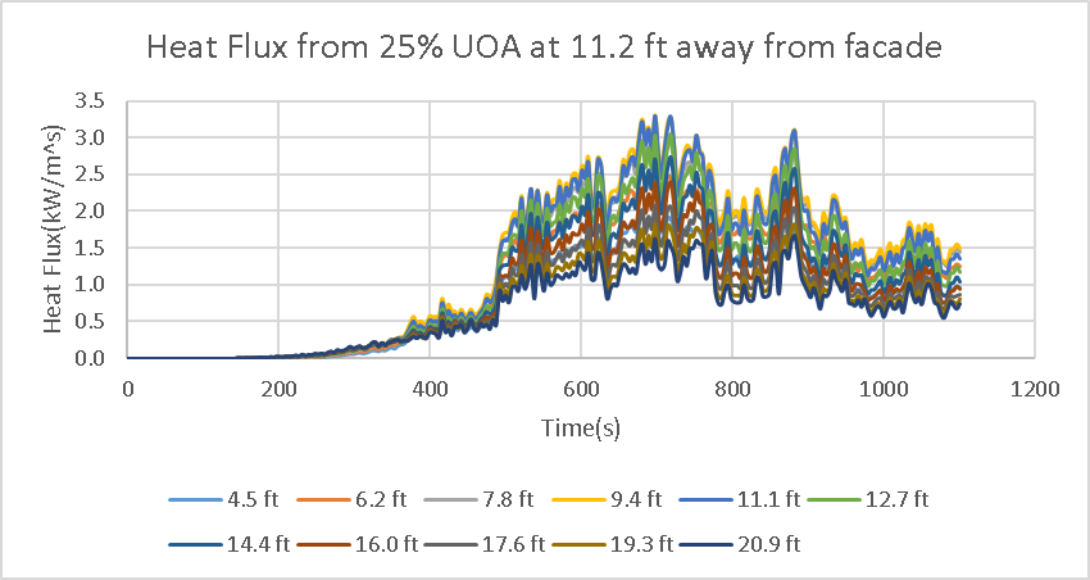

Figure 104 Heat flux from a 25% UOA, Configuration I compartment, at 11.2ft (3.36m) away from the façade (one apartment involved in fire)

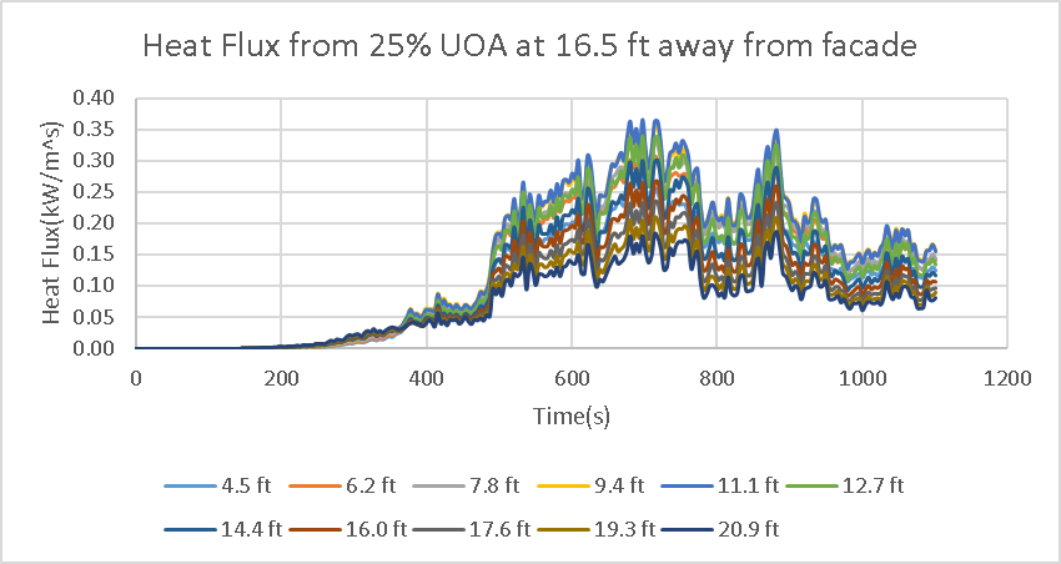

Figure 105 Heat flux from a 25% UOA, Configuration I compartment, at 16.5ft (4.95m) away from the façade (one apartment involved in fire)

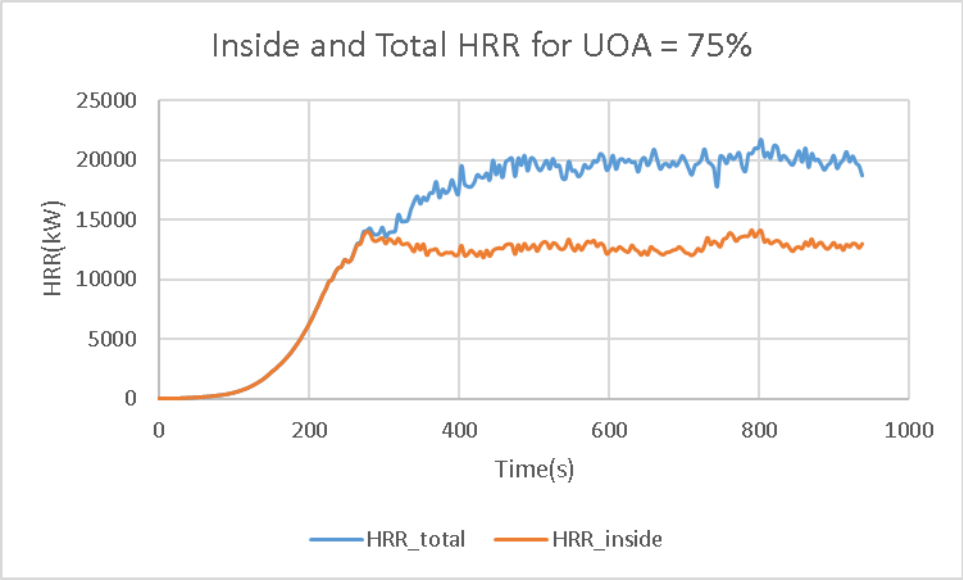

Figure 106 Relationship of total HRR and HRR inside the building for UOA =75% (one apartment involved in fire)

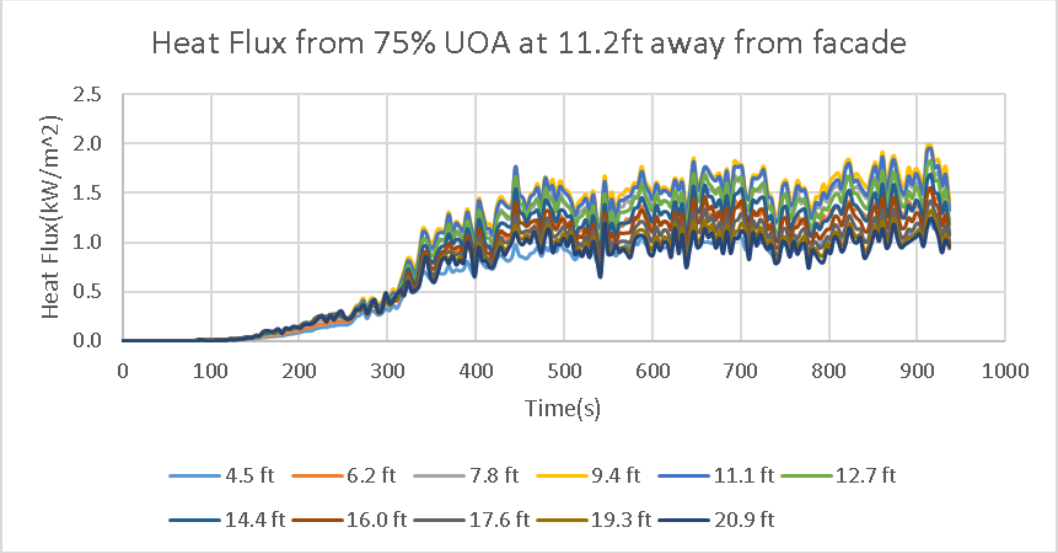

Figure 107 Heat flux from a 75% UOA, Configuration I compartment, at 11.2ft (3.36m) away from the façade (one apartment involved in fire)

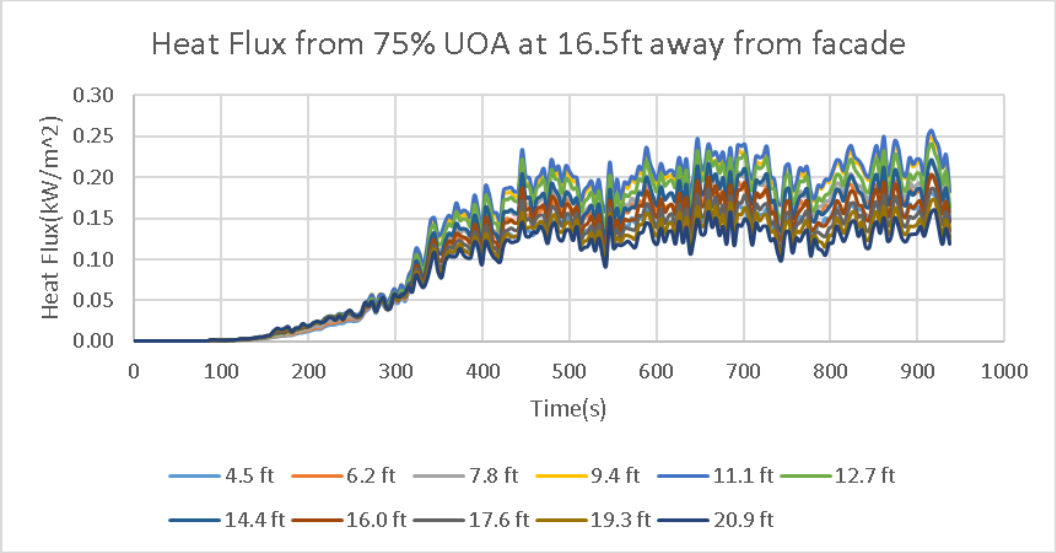

Figure 108 Heat flux from a 75% UOA, Configuration I compartment, at 11.2ft (3.36m) away from the façade (one apartment involved in fire)

b) If five compartments are involved in fire, the simulation results are shown below:

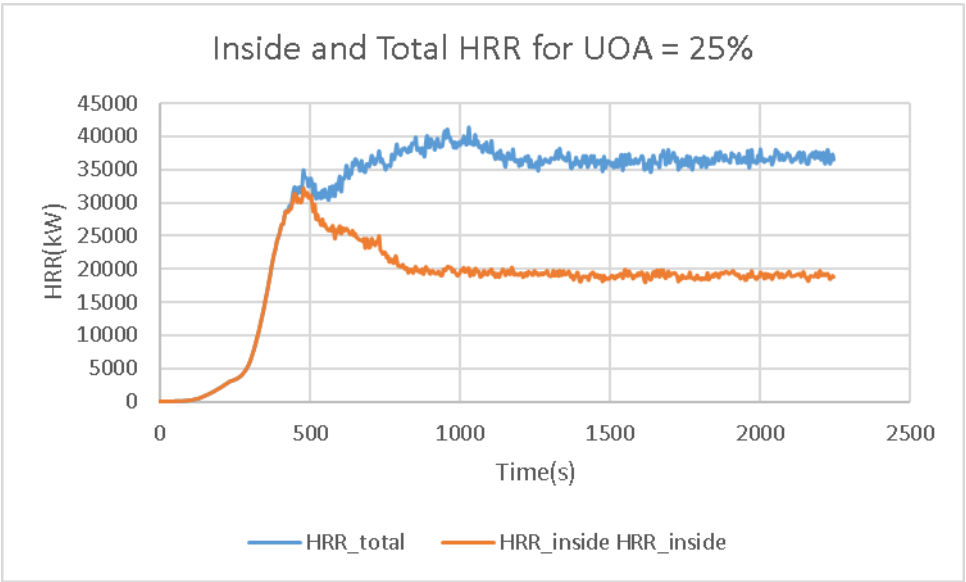

Figure 109 Relationship of total HRR and HRR inside the building for UOA =25% (5 apartment involved in fire)

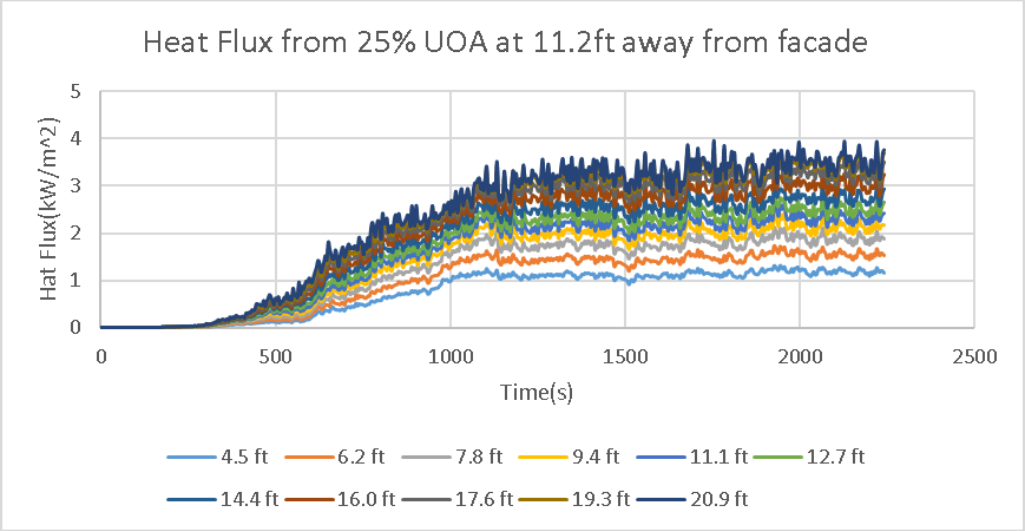

Figure 110 Heat flux from a 25% UOA, Configuration I compartment, at 11.2ft (3.36m) away from the façade (5 apartments involved in fire)

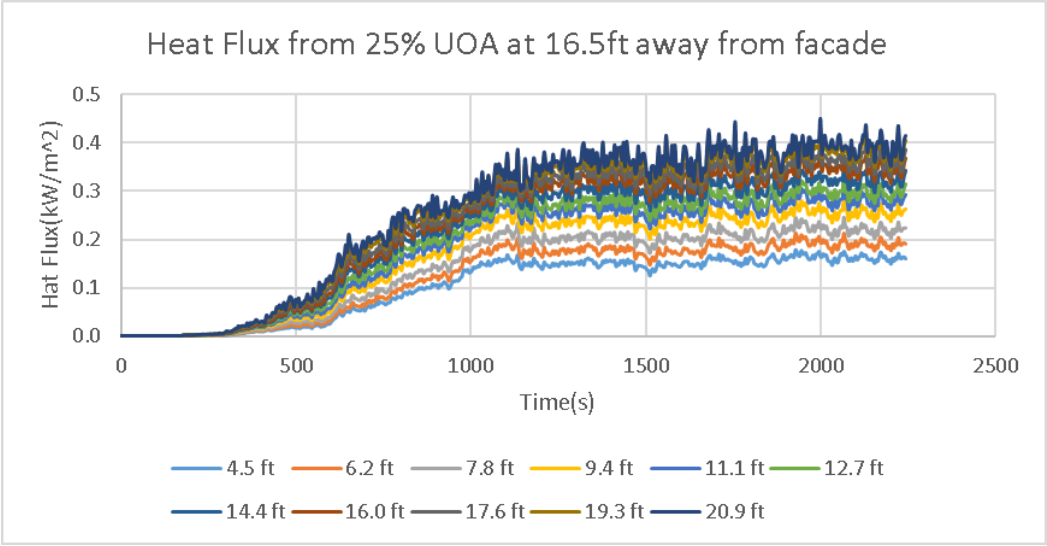

Figure 111 Heat flux from a 25% UOA, Configuration I compartment, at 16.5ft (4.95m) away from the façade (5 apartments involved in fire)

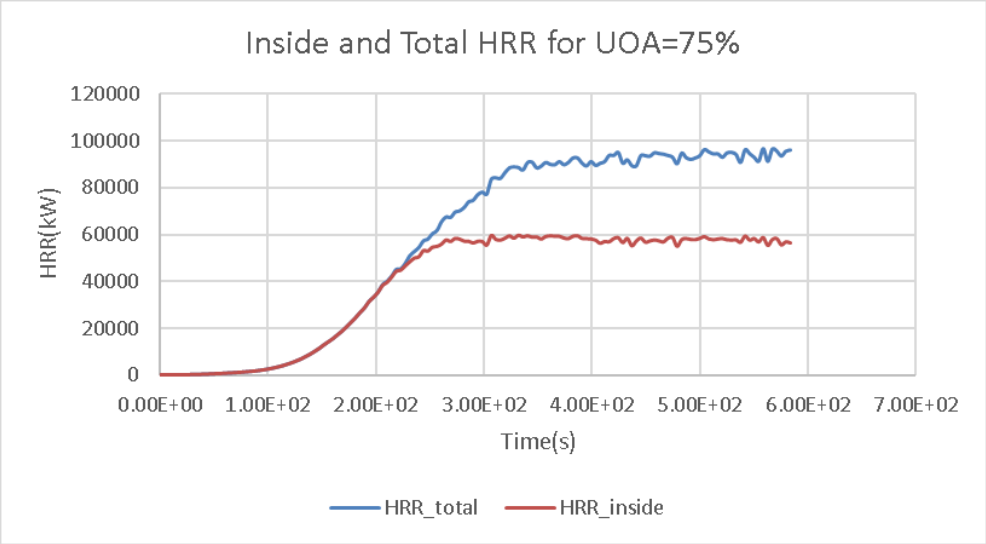

Figure 112 Relationship of total HRR and HRR inside the building for UOA =75% (5 apartments involved in fire)

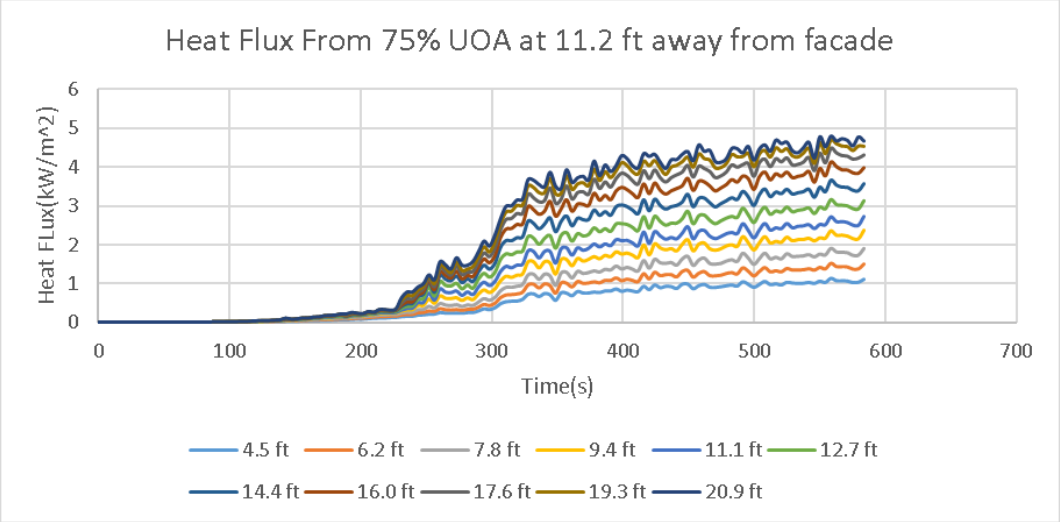

Figure 113 Heat flux from a 75% UOA, Configuration III-B compartment, at 11.2ft (3.36m) away from the façade (5 apartments involved in fire)

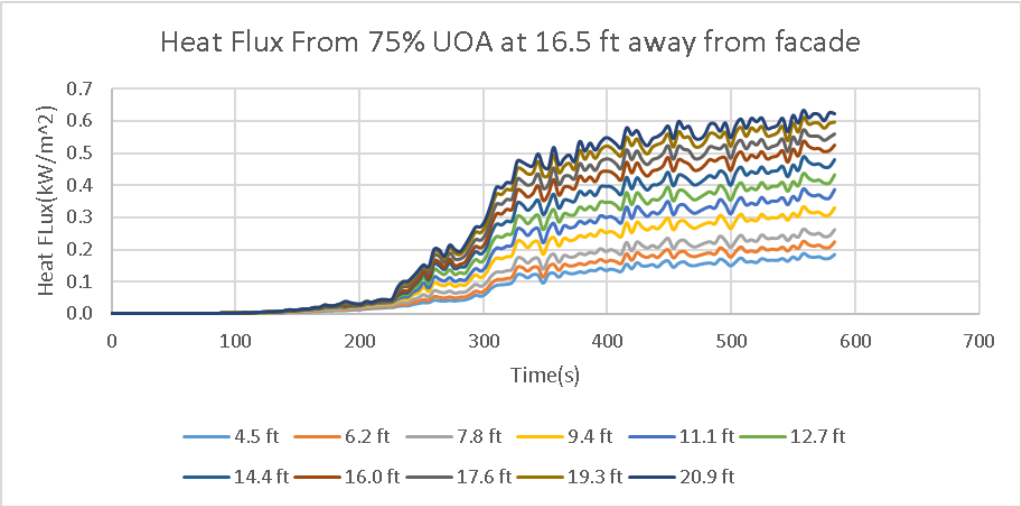

Figure 114 Heat flux from a 75% UOA, Configuration III-B compartment, at 16.5ft (4.95m) away from the façade (5 apartments involved in fire)

Table 50 summary about FSD, UOA and Heat Flux for one apartment involved in fire

FSD(ft)	UOA(%)	Max Heat Flux(MHF,kW/ m^2)	Elevation of MHF point(ft)	Ignitable range(ft)
11.2	25	3.29	11.1	null
	75	1.95	11.1	null
16.5	25	0.36	11.1	null
	75	0.26	11.1	null

Table 51 summary about FSD, UOA and Heat Flux for five apartment involved in fire

FSD(ft)	UOA(%)	Max Heat Flux(MHF,kW/ m^2)	Elevation of MHF point(ft)	Ignitable range(ft)
11.2	25	3.84	20.9	null
	75	4.67	20.9	null
16.5	25	0.45	20.9	null
	75	0.62	20.9	null

The above two tables show that even if the UOA is enlarged to 75% and with 5 apartments being involved in a fire, the radiation heat flux at FSD =11.2ft is much less than the critical limit of 12.5kW/m , let alone at FSD = 16.5ft.

3.3.5. Fire Separation Distance(FSD) greater than 20ft

In the IBC Code, the UOA is allowed to rise from 70% to 100% due to introduction of sprinkler trade-offs for Fire Separation Distance (FSD) greater than ft. There are two scenarios: One has 70% of UOA in a Configuration I compartment, the other has 100% of UOA in Configuration III-B compartment.

a) If one compartment is involved in fire, the simulations results are shown in the following figures:

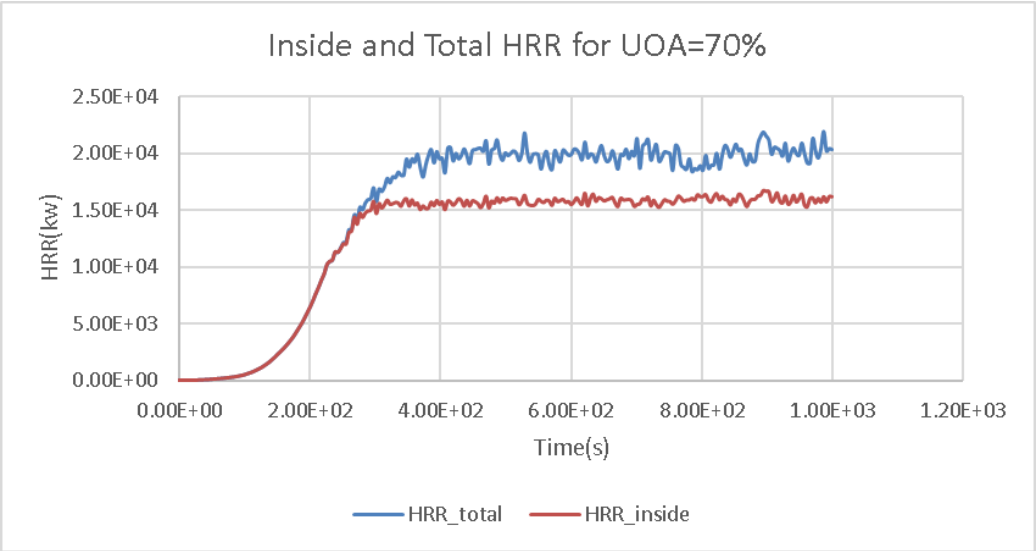

Figure 115 Relationship of total HRR and HRR inside the building for UOA =70% (1 apartment involved in fire)

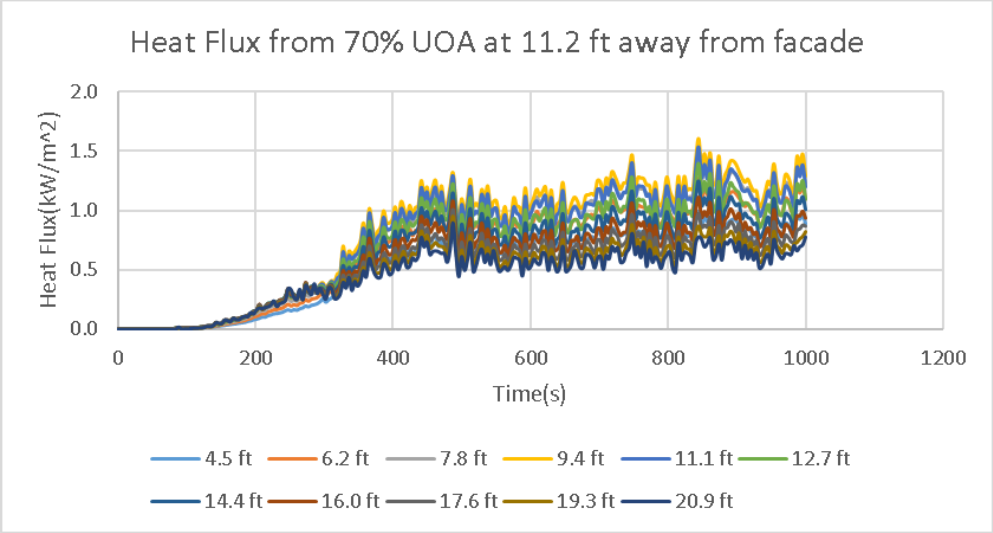

Figure 116 Heat flux from a 70% UOA, Configuration I compartment, at 11.2ft (3.36m) away from the façade (one apartment involved in fire)

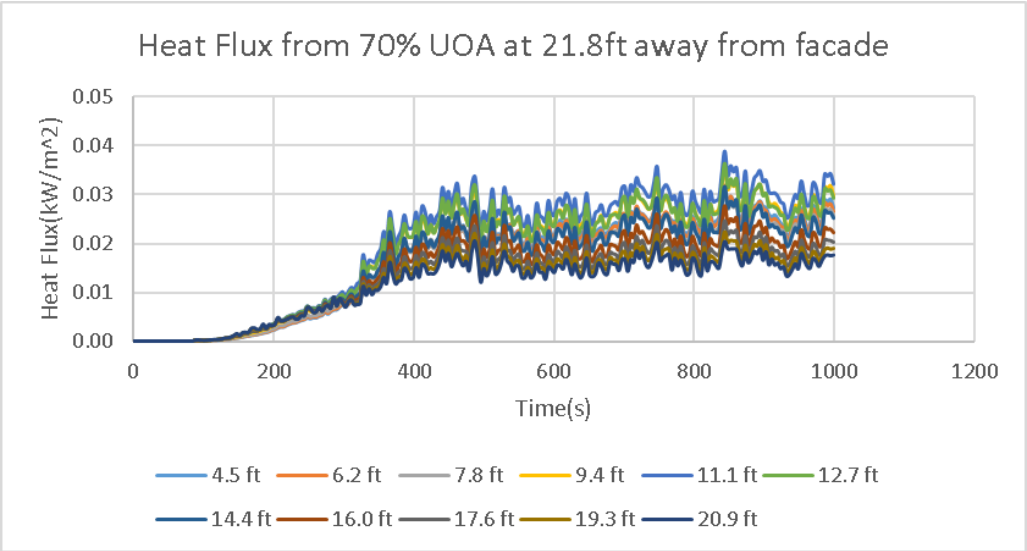

Figure 117 Heat flux from a 70% UOA, Configuration I compartment, at 21.8ft (6.58m) away from the façade (one apartment involved in fire)

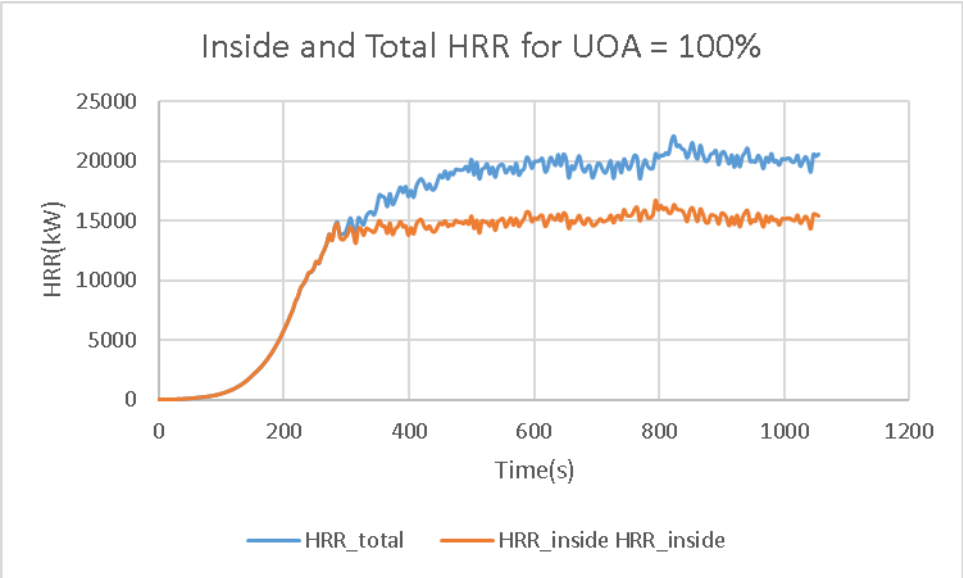

Figure 118 Relationship of total HRR and HRR inside the building for UOA =100% (one apartment involved in fire)

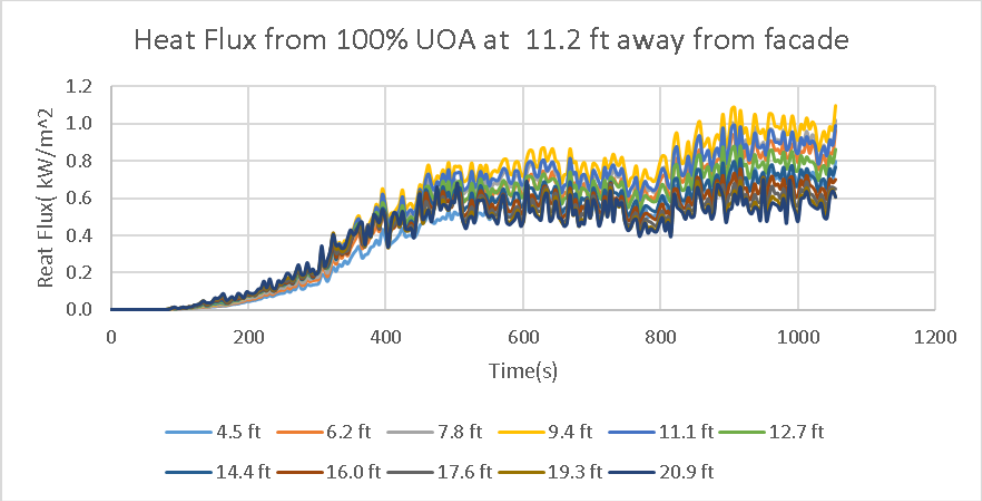

Figure 119 Heat flux from a 100% UOA, Configuration III-B compartment, at 11.2ft (3.36m) away from the façade (one apartment involved in fire)

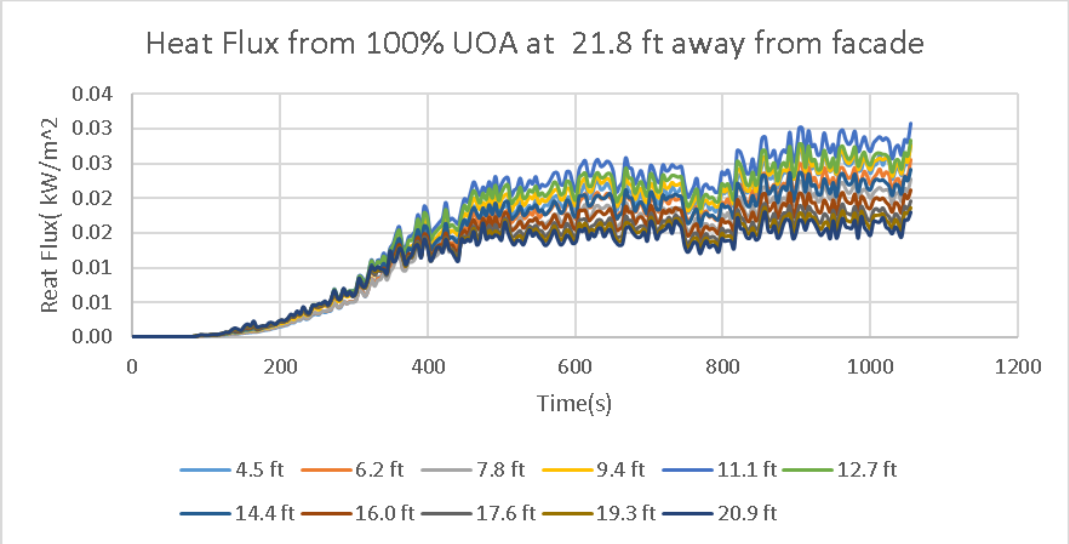

Figure 120 Heat flux from a 100% UOA, Configuration III-B compartment, at 21.8ft (6.58m) away from the façade (one apartment involved in fire)

b) If five apartments are involved in fire, the simulation results are shown below:

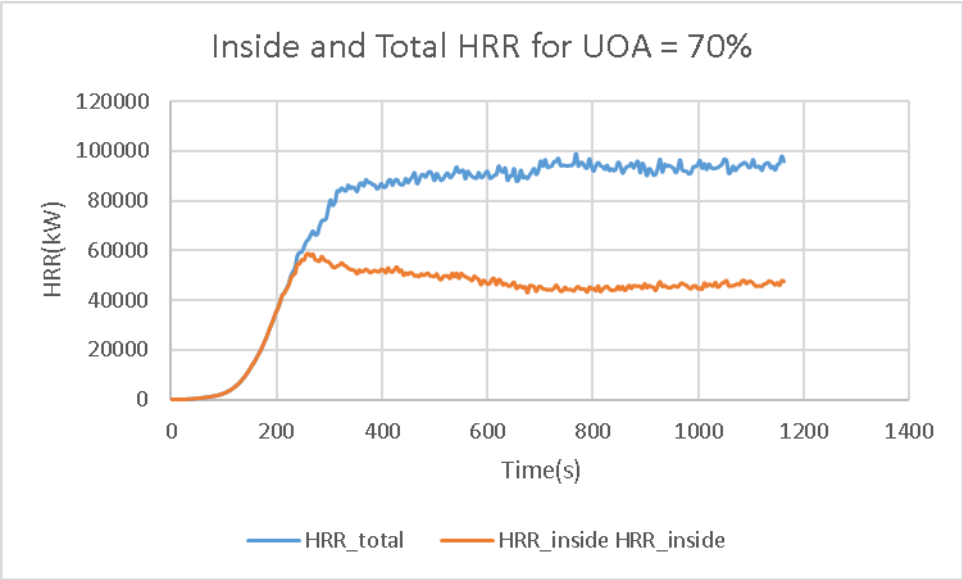

Figure 121 Relationship of total HRR and HRR inside the building for UOA =70% (5 apartments involved in fire)

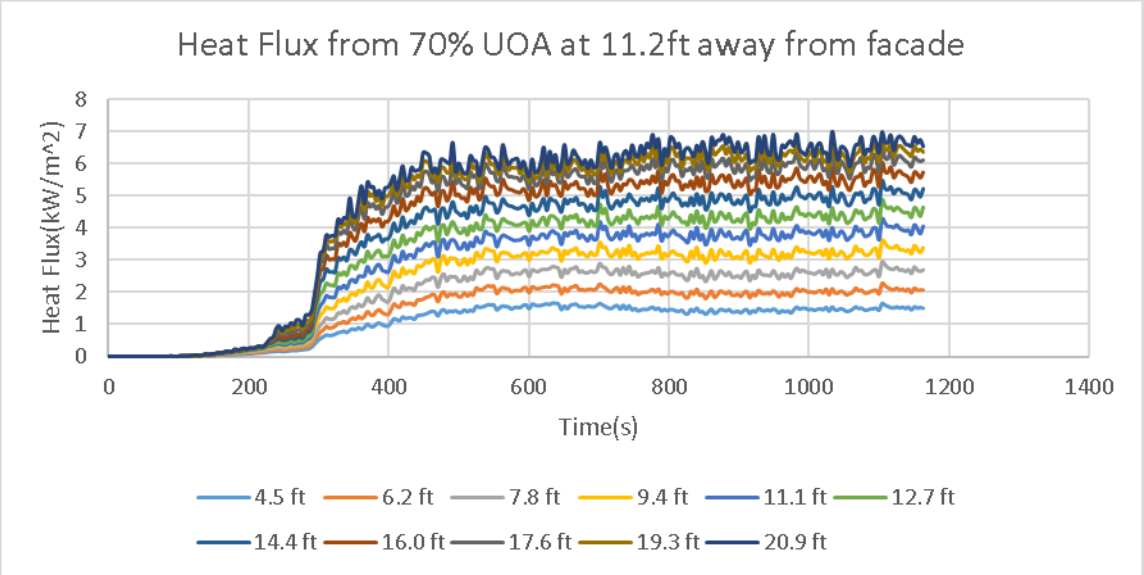

Figure 122 Heat flux from a 70% UOA, Configuration I compartment, at 11.2ft (3.36m) away from the façade (5 apartments involved in fire)

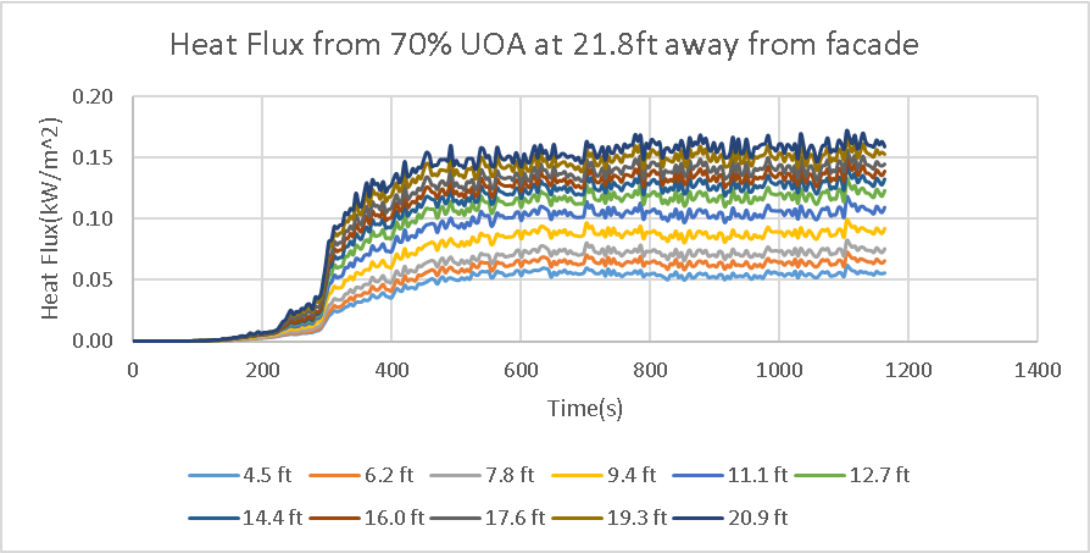

Figure 123 Heat flux from a 70% UOA, Configuration I compartment, at 21.8ft (6.58m) away from the façade (5 apartments involved in fire)

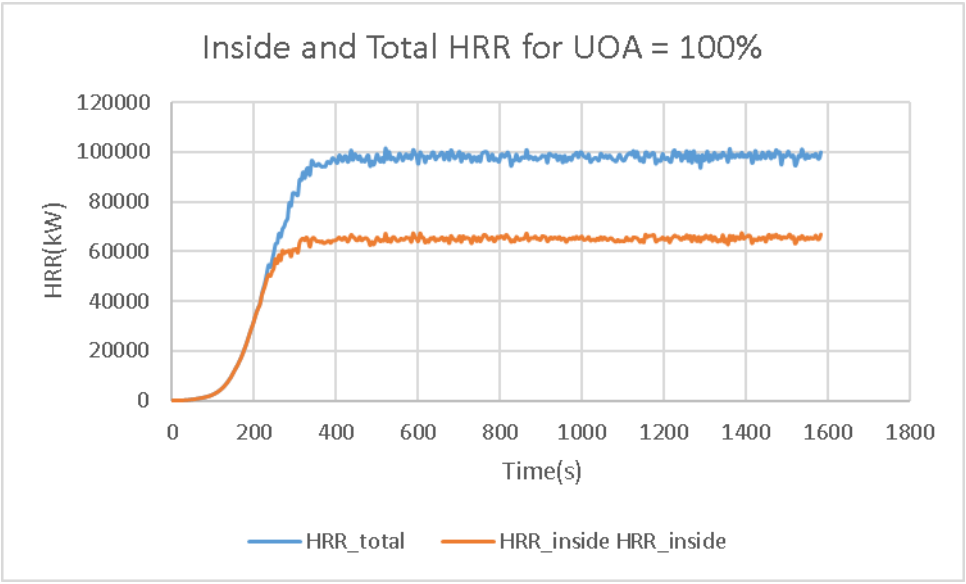

Figure 124 Relationship of total HRR and HRR inside the building for UOA =100% (five apartments involved in fire)

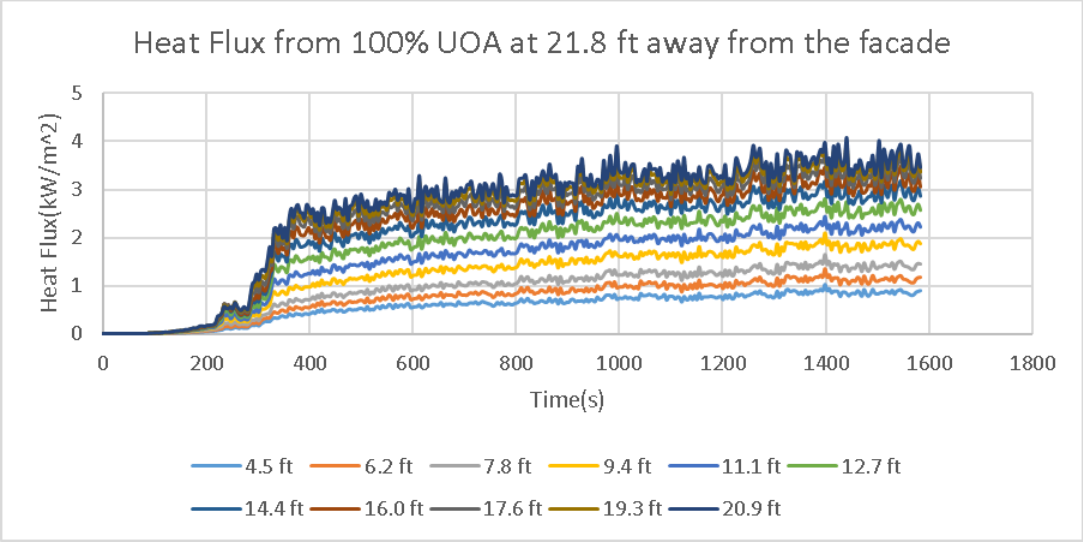

Figure 125 Heat flux from a 100% UOA, Configuration III-B compartment, at 11.2ft 3.36m) away from the façade (5 apartments involved in fire)

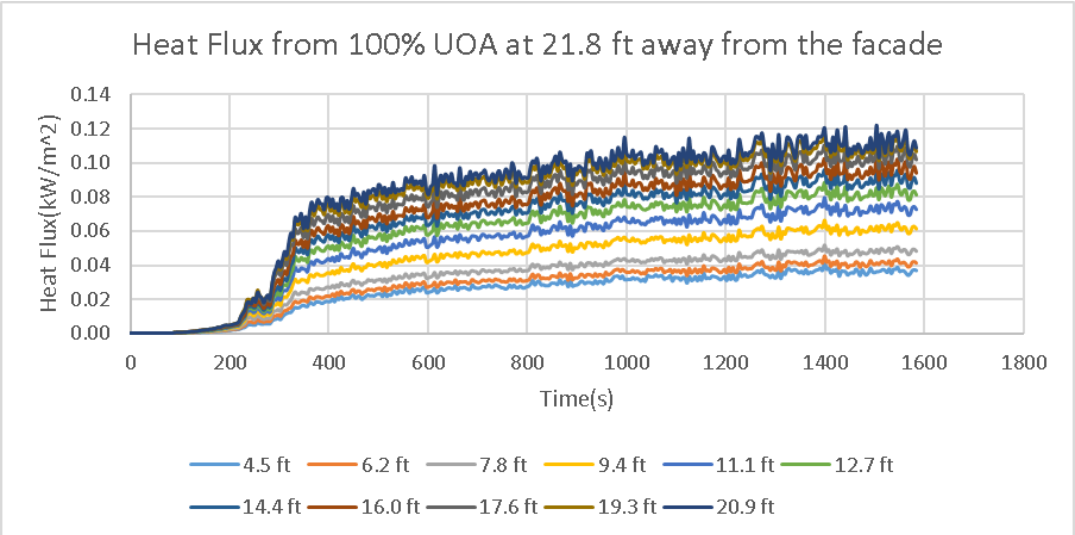

Figure 126 Heat flux from a 100% UOA, Configuration III-B compartment, at 21.8ft (6.58m) away from the façade (5 apartments involved in fire)

Table 52 summary about FSD, UOA and Heat Flux for one apartment involved in fire

FSD(ft)	UOA(%)	Max Heat Flux(MHF, kW/ m^2)	Elevation of MHF point(ft)	Ignitable range(ft)
11.2	70	1.54	11.1	null
	100	1.09	9.4	null
21.8	70	0.04	12.7	null
	100	0.03	11.1	null

Table 53 summary about FSD, UOA and Heat Flux for five apartment involved in fire

FSD(ft)	UOA(%)	Max Heat Flux(MHF,kW/ m^2)	Elevation of MHF point(ft)	Ignitable range(ft)
11.2	70	6.97	20.9	null
	100	4.08	20.9	null
21.8	70	0.12	20.9	null
	100	0.62	20.9	null

The above two tables show that even if the UOA is enlarged to 100% and with 5 apartments being involved in a fire, the radiation heat flux at FSD =11.2ft (3.36m) is much less than the critical limit of 12.5kW/m , let alone at FSD = 21.8ft (6.58m).

3.4. Conclusions and discussions

1) Although the enlargement of UOA can increase the effective area of the radiation source, the compartment temperature as a radiation source may drop due to increasingly cooling effects from more entrained air. The combined effects of increased radiation area and decreased radiation temperature depend on which factor dominates the radiation heat transfer in a specific problem. The compartment temperature changes due to the increase of UOA is shown below:

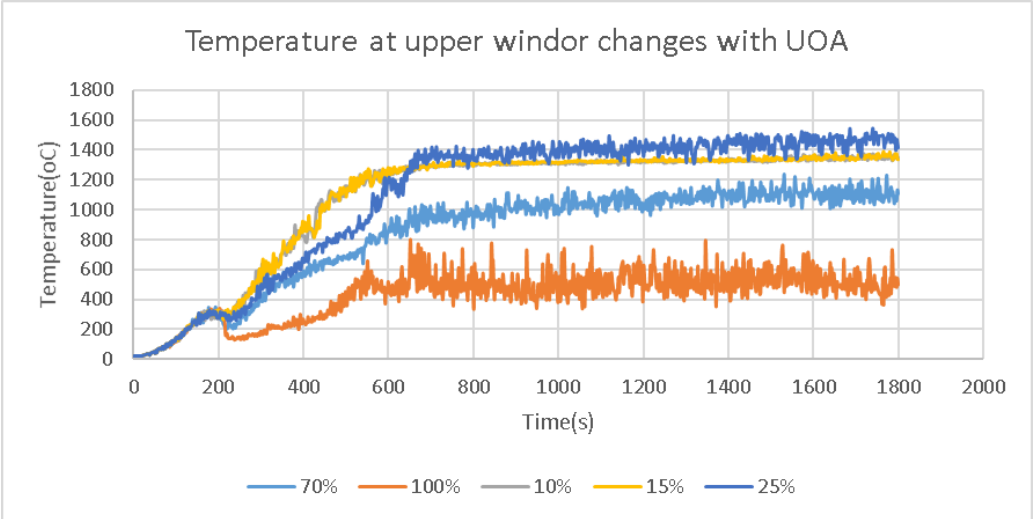

Figure 127 Temperature at upper window for different UOAs

(Before the steady state, the smaller the UOA is, the higher the temperature is; in the steady state, the temperature in 25% UOA compartment is the highest but just a little bit higher than that in 10% or 15% UOA compartment. For UOAs larger than 25%, the temperatures in the compartment decreases with the increase of UOA.)

2) The IBC Code requirements for FSD/UOA pairs are very risky when FSD is short (<3.8ft (1.14m)) and somehow conservative when FSD is long (>10ft (3m)).

3) The construction type has some effects on the radiation heat transfer. The following figure shows that a 25% UOA in Type VB building yields a higher radiation heat flux level than a 25% UOA in Type VA building does:

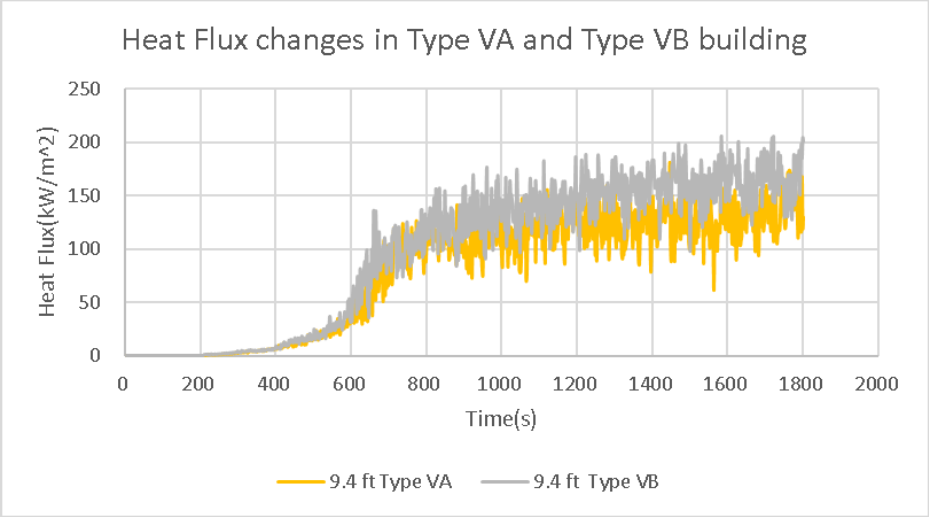

Figure 128 Heat flux changes in Type VA and Type VB building with FSD=3.8ft (1.14m)

4) A summary of the simulation results is shown in the following table:

Table 54 Relationships between UOA and FSD – single separated apartment

UOA	FIRE TYPE	FSD(ft)	Maximum Heat Flux(kW/m^2)
10% -Type VA	Standalone apartment fire	3.8	164
	One apartment fire	3.8	25
		5.3	5.8
		8.6	2.2
	Five apartments fire	3.8	40
		5.3	9.7
		8.6	3.8
25% - type VB	Standalone apartment fire	3.8	205
	One apartment fire	3.8	75
		5.3	18.5
		8.6	7.2
	Five apartments fire	3.8	77.4
		5.3	19.5
		8.6	7.8
15% -Type VA	Standalone apartment fire	11.2	8.3
	One apartment fire	11.2	0.63
	Five apartments fire	11.2	1.05
45% - Type VB	Standalone apartment fire	11.2	3.6
	One apartment fire	11.2	1.7
	Five apartments fire	11.2	7.51
25% - Type VA	Standalone apartment fire	16.5	0.8
	One apartment fire	11.2	3.29
		16.5	0.36
	Five apartments fire	11.2	3.84
		16.5	0.45
75% - Type VB	Standalone apartment fire	16.5	0.3
	One apartment fire	11.2	1.95
		16.5	0.26
	Five apartments fire	11.2	4.67
		16.5	0.62
70% - Type VA	Standalone apartment fire	21.8	0.04
	One apartment fire	11.2	1.54
		21.8	0.04
	Five apartments fire	11.2	6.97
		21.8	0.12
100%-Type VB	Standalone apartment fire	21.8	0.01
	One apartment fire	11.2	1.09
		21.8	0.03
	Five apartments fire	11.2	4.08
		21.8	0.62

5) In a standalone fire, all the openings are connected to the outside directly and thus fresh air is entrained by the fire, whereas in apartment fires within a building, the apartment doors are connected to a linear corridor and thus fresh air entrained by the fire is not as easily available. Due to the higher volume of make-up air entrained by the fire, a fire in a standalone apartment is usually more powerful than that in building apartments.

6) Although the gap of heat flux between a fire involving one apartment and a fire involving five apartments is not very big , the area exposed to the same level of heat flux may differ significantly. This indicates a possible higher fire risk given the assumption that the risk for a fire in one building to spread to another neighboring building is proportional to the area exposed to a critical heat flux.

3.5. Comments on code changes

For a long time people have believed that the risk for a fire in one building to spread to another neighboring one depends on the size of UOA, and therefore in building codes FSD are limited according to the size of UOA. In fact, radiation from a fire in one building comes from two components: that from the UOA itself and that from the flame extending out of the UOA. On the other hand, an average decreased temperature inside the fire apartment exists when the UOA is enlarged. Therefore, the magnitude of radiation heat flux depends on three factors: the size of UOA, the size of the flame envelop extending out of the UOA, and the temperature inside the fire apartment. Given the geometry of a building, the first factor is easily determined, but the determination of the latter two demands more specific data about the possible fire scenarios. Generally, the resistance for fresh air to enter into a fire apartment and to be consumed dominates the size of the flame extending out of the UOA, and the resistance for heat inside a fire apartment to transfer outside dominates the temperature that could be achieved inside the fire apartment. In the case of small UOA, the ventilation condition becomes very important.

The following figure describes a recommended code change (shown as future code) to building code (e.g., IBC code).

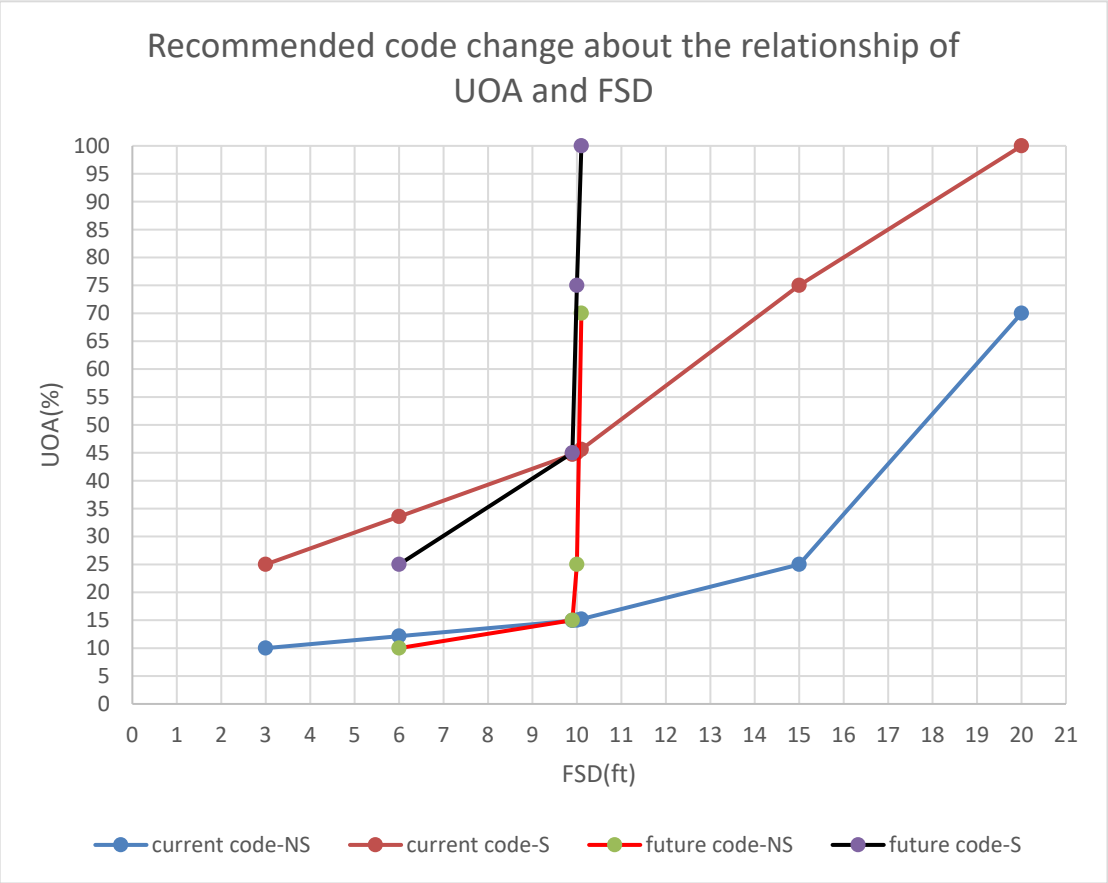

*NS: no sprinkler trade-offs applied, S: sprinkler trade-offs applied

Figure 129 provisions on UOA/FSD for current code and recommended future code

The recommendation in the above figure is that the FSD between two buildings should be kept at least 6ft (1.8m), meanwhile the maximum of FSD can be reduced to 10ft (3m) without introducing higher risk of fire spreading to another building by radiation heat transfer.

Note that the above recommend code change is a result of taking into account only radiation heat transfer under conditions of quiet ambient atmosphere. If strong wind exists during the fire, the flame standing out of the UOA may deflect to some extent, shrinking the real FSD and thus increasing the radiation level received by an exposed building façade. A strong wind can also facilitate the traveling of embers in some case, posing higher risk of pilot ignition on another neighboring building. Consequently, for the sake of safety, only the left end of the recommended curve in the above figure is proposed, which is to increase the minimum FSD from 3ft to 6ft.

3.6. Possible future work

In the above sections of this chapter, a qualitative risk analysis of fire propagation from one building to another is conducted, stating that the risk of fire spreading to another building is high when FSD is shorter than 6ft no matter what size of UOA a building has. Quantitative risk analysis of this type for a given combination of FSD and UOA is possible given that the following information is available:

1) The probability distribution of the number of apartments being involved in fire
2) The probability distribution of temperatures achieved inside the fire apartments
3) The probability distribution of flame size out of the UOA
4) The probability distribution of wind speed in a specific area

The possible analysis results may be figures plotting UOA and fire propagation risks for different FSD and wind speed, something like the following figure:

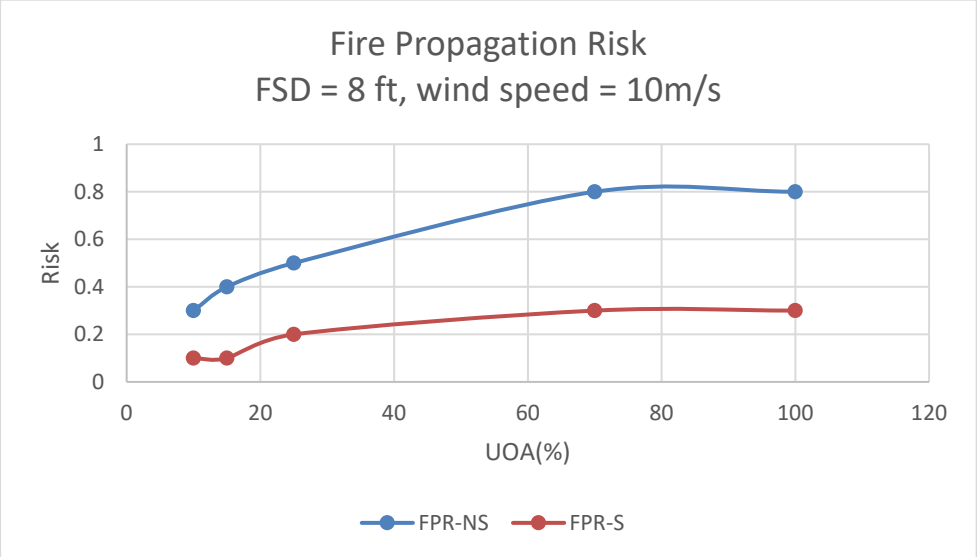

*NS=non sprinklered building, S=sprinklered building, FPR=Fire Propagation Risk

Figure 130 schematic figure of fire propagation risk (theoretical example, not real data)

(4) -Structural fire analysis

4.1. Introduction

To conduct a structural fire analysis for lightweight wood construction, the following steps are needed:

1) The thermal analysis to determine the temperatures in gas phase and solid phase.
2) Adopting charring rate as a methodology to account for the effect of fire on the structure.
3) Structural analysis of the apartment using reduced member cross-sections of wood studs/joists to account for charring.

The first step can be achieved by FDS simulation, for the second step, National Design Specification for Wood Construction (NDS) 2015 methodology is adopted and the third step is addressed by using the products of the well-recognized structural analysis software suite, RISA.

Some post-flashover pictures extracted from our simulations are included in APPENDIX 4.

4.2. The development of temperatures inside the walls/floor/ceiling and the compartment

It is assumed that for a Type VB small building that has a sprinkler system that functions as designed there will be no structural issues since flashover will not happen. To simplify the establishment of the FDS model, four studs are grouped together in our model to make “larger width studs” which then appear on the computational grid.

4.2.1. Distribution of temperature devices/profiles

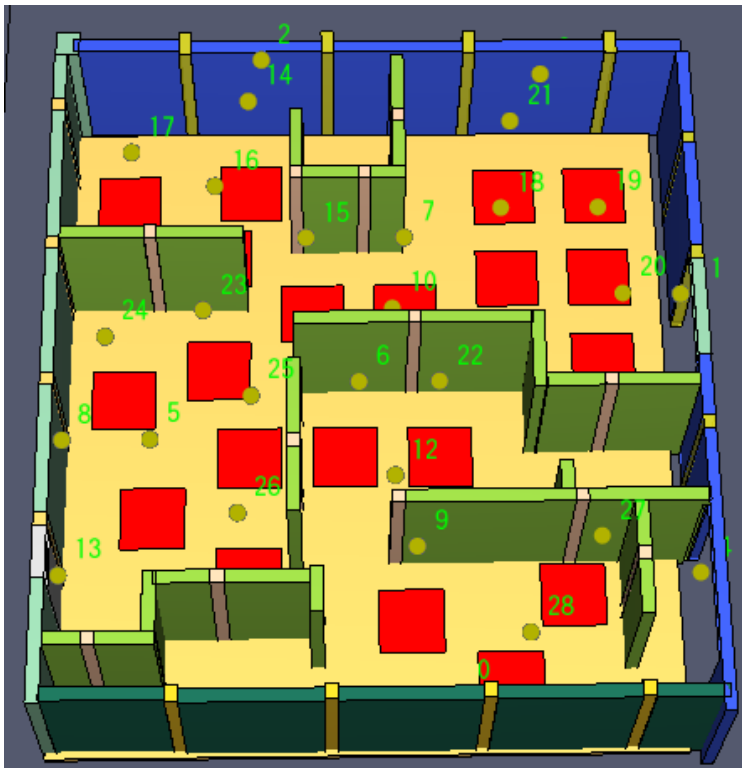

Figure 131 An overall figure of the apartment with temperature devices

The following devices/profiles are set in the above apartment:

1) In the North wall, a pair of devices (one is attached to the surface, the other is at the connection of gypsum wall board (GWB) and stud) is set at top and middle of each collected stud.

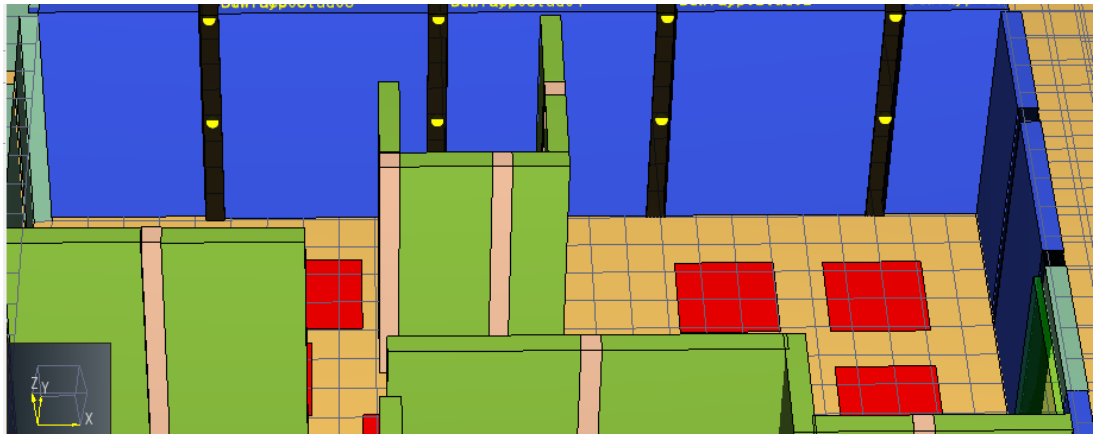

Figure 132 Eight pairs of devices are set in 4 collected studs in the North wall

2) In the ceiling, a pair of devices (one is attached to the inner surface, the other is at the connection of GWB and stud) is set just above each of the gas burner centers.

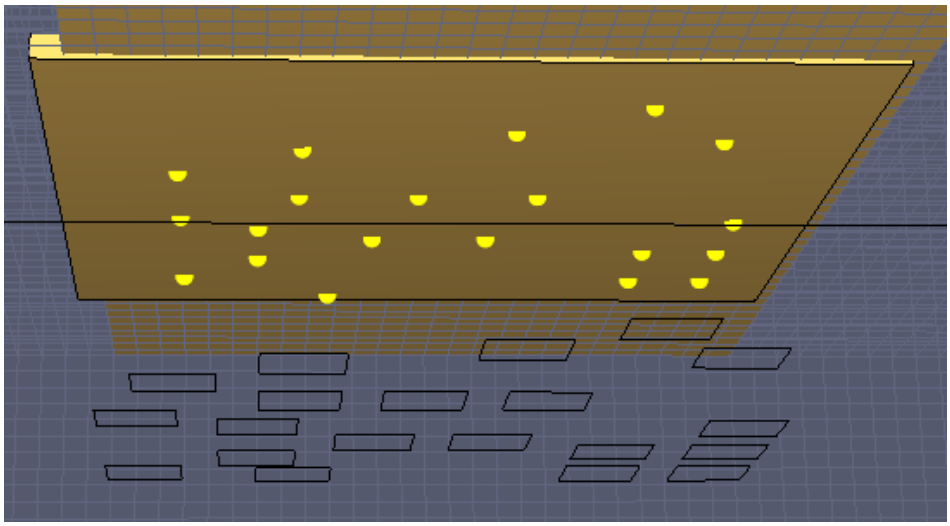

Figure 133 Ceiling devices deployment

3) For each collected stud, a pair of profiles are assigned (one is at the top, the other at the middle).

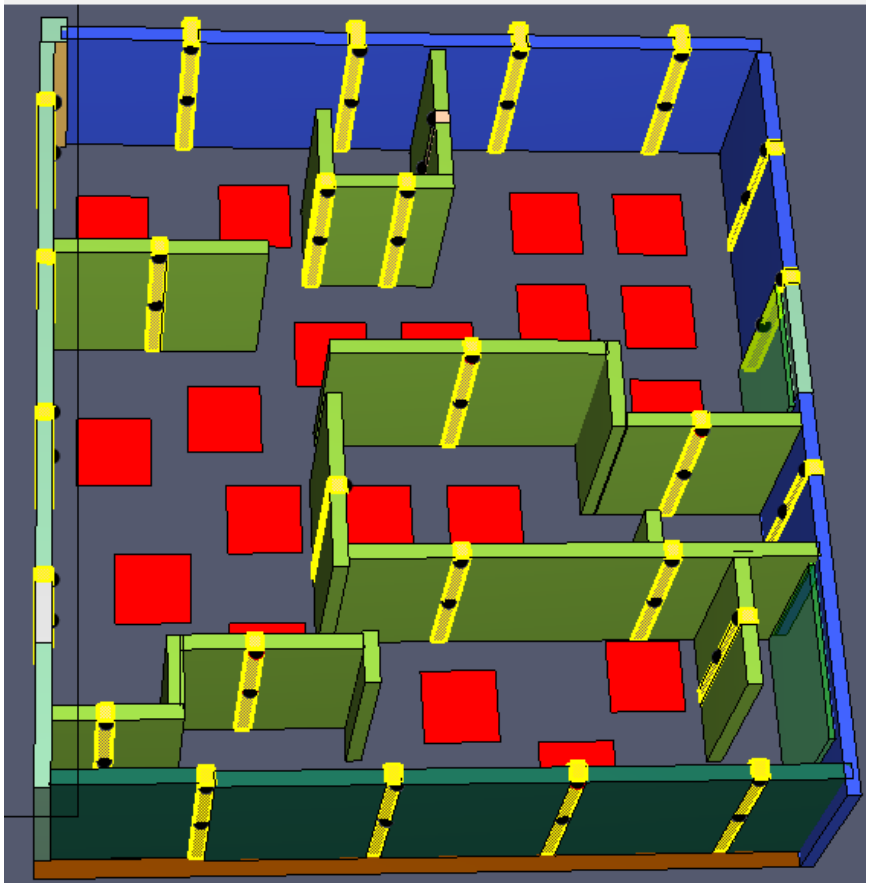

Figure 134 temperature profiles deployment-wood studs

4) For each panel (between two collected studs), set a pair of profile (one is at the top, the other at the middle).

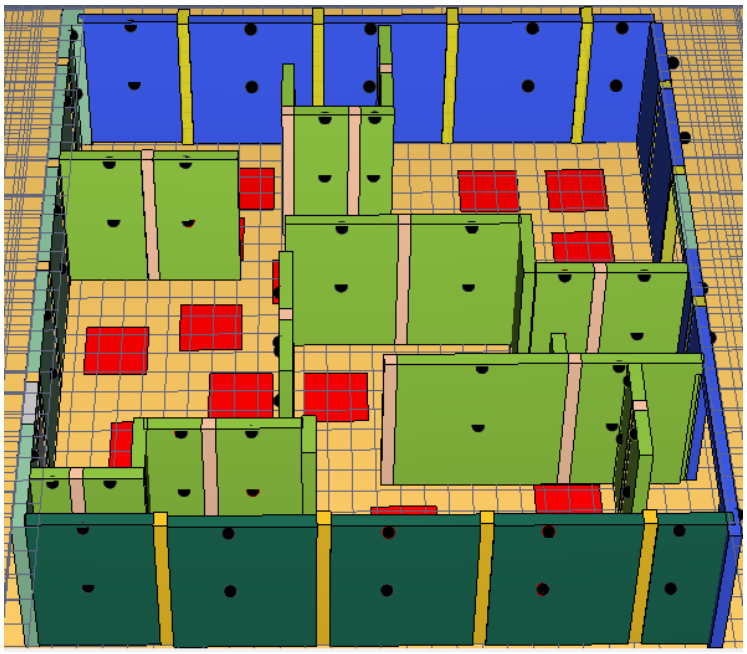

Figure 135 temperature profiles deployment-panel

5) Start from the point 0.2m far from the wall, set a gas temperature device tree, each tree includes 3 devices with heights of 0.5m,1.5m,2.5m, respectively. In total there are 11x10=110 device trees and 110x3=330 devices.

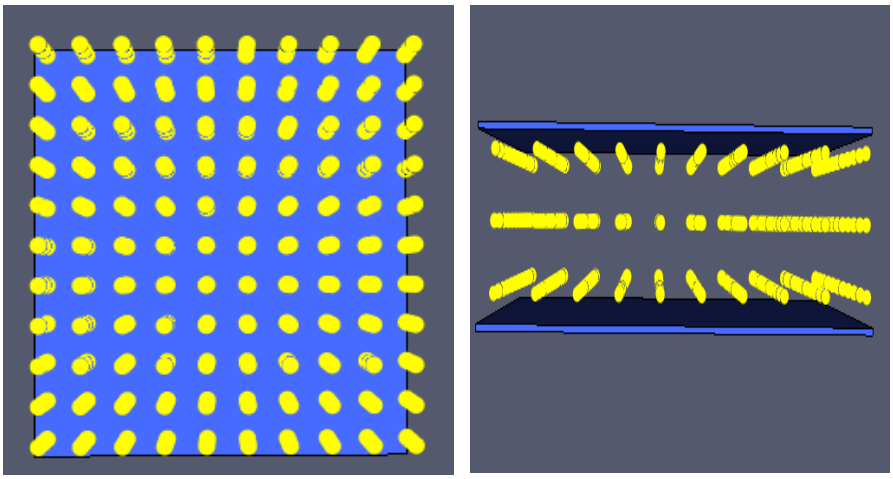

a) Plan view b) elevation view

Figure 136 Gas Temperature devices within the apartment

4.2.2. Simulation results

For structural safety analysis under fire effects, the weakest points are these with highest temperatures. Therefore, only locations with highest temperatures are investigated.

1) The stud's temperature curves

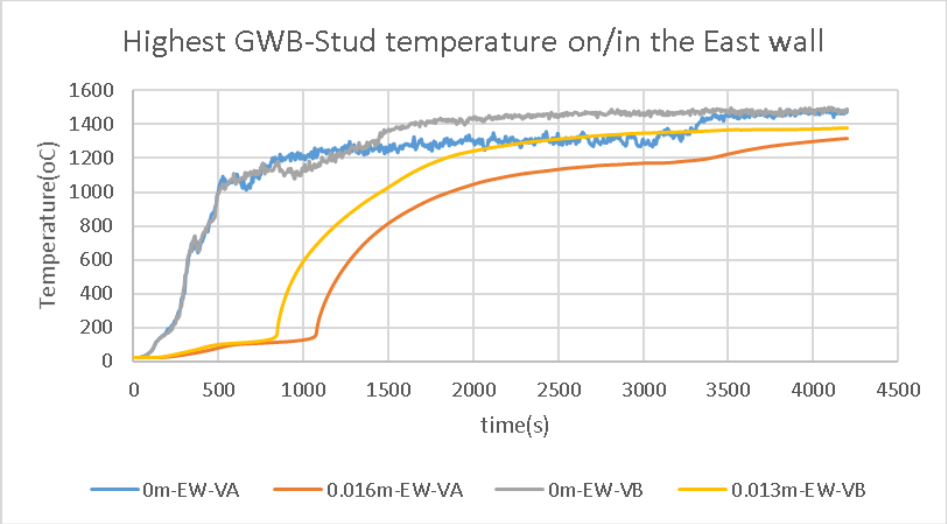

Figure 137 Comparison of highest temperatures on/in the east wall (GWB + Stud +GWB)

(This stud in the east wall is close to the first burner in the Northeast corner)

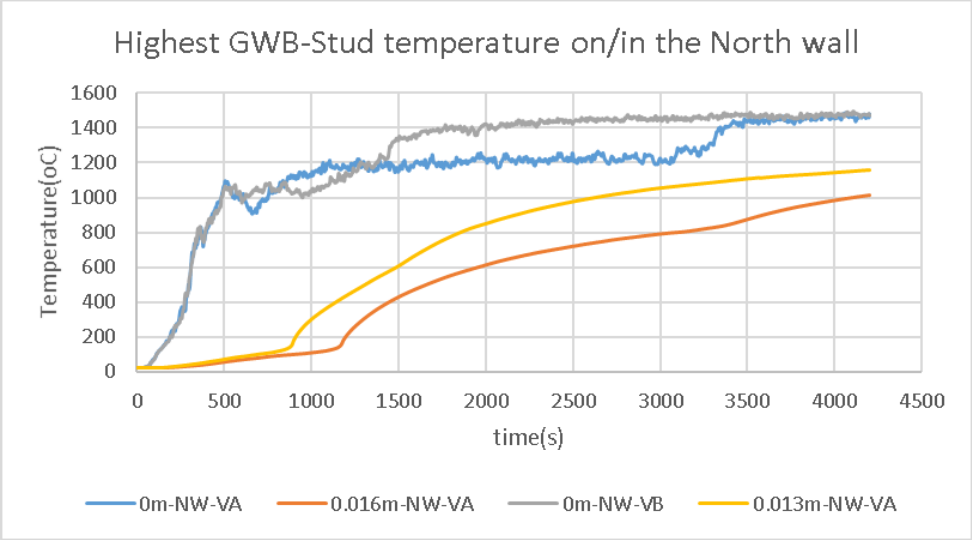

Figure 138 Comparison of highest temperatures on/in the North wall (GWB + Stud +GWB)

(This stud in the North wall is close to the first burner in the Northeast corner)

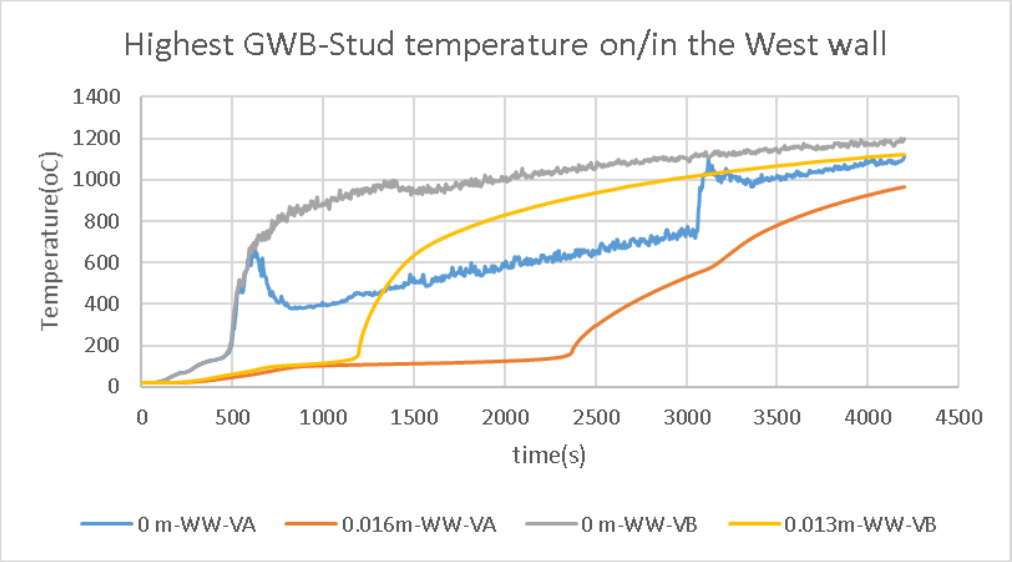

Figure 139 Comparison of highest temperatures on/in the West wall (GWB + Stud +GWB)
(This stud is close to the corridor door where radical fire plume turbulence exists in Type VA compartment due to the longer activation time for South window than in Type VB compartment, more details can be found in the conclusion paragraph of this section)

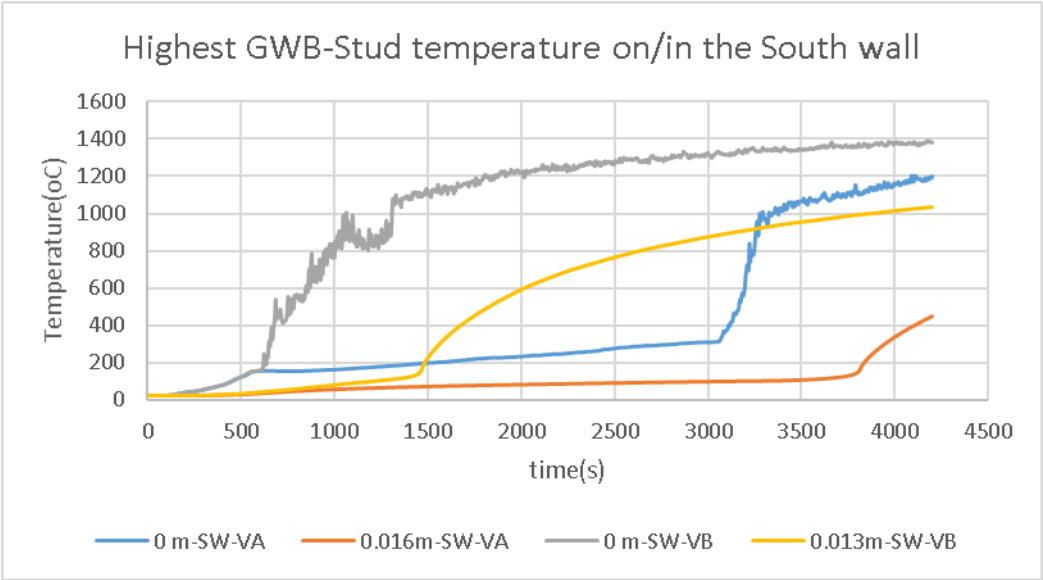

Figure 140 Comparison of highest temperatures on/in the West wall (GWB + Stud +GWB)
(This stud is close to the middle of the South wall)

2) The panel's temperature curves

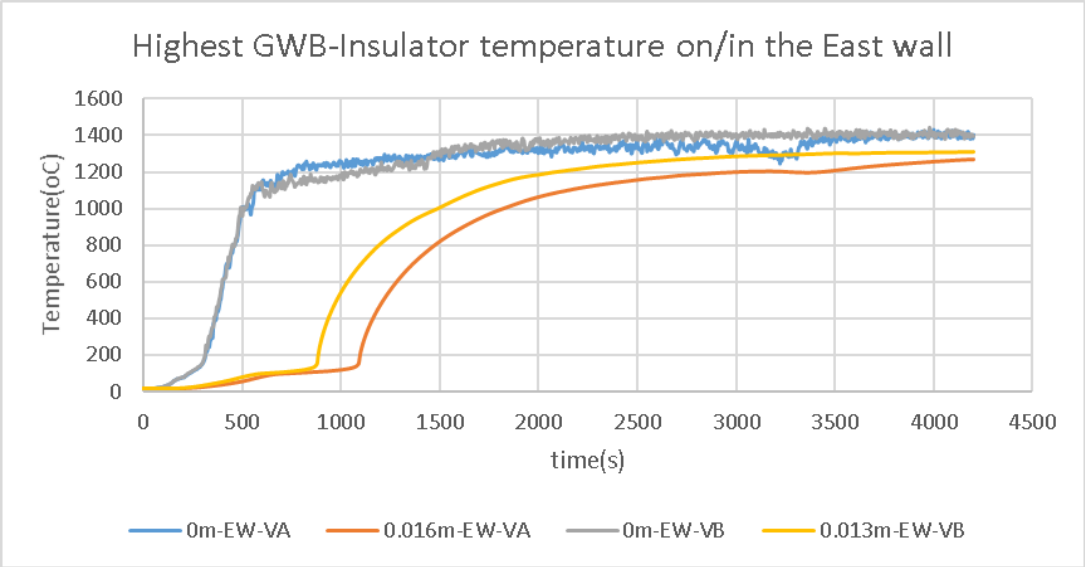

Figure 141 Comparison of highest temperatures on/in the east wall (GWB + Insulator+GWB)

(This panel in the east wall is close to the first burner in the Northeast corner)

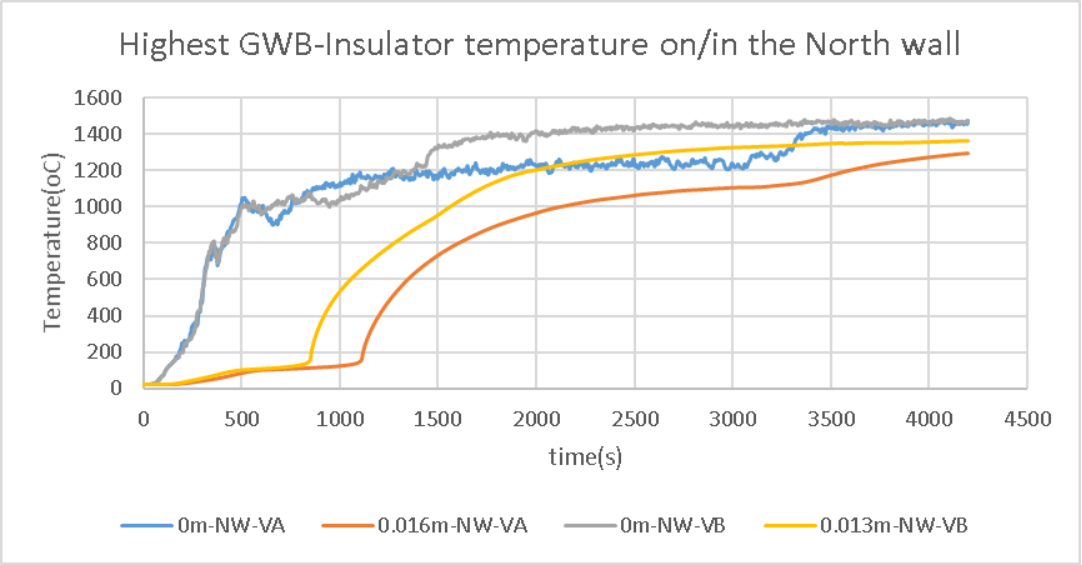

Figure 142 Comparison of highest temperatures on/in the North wall (GWB + Insulator+GWB)

(This panel in the North wall is close to the first burner in the Northeast corner)

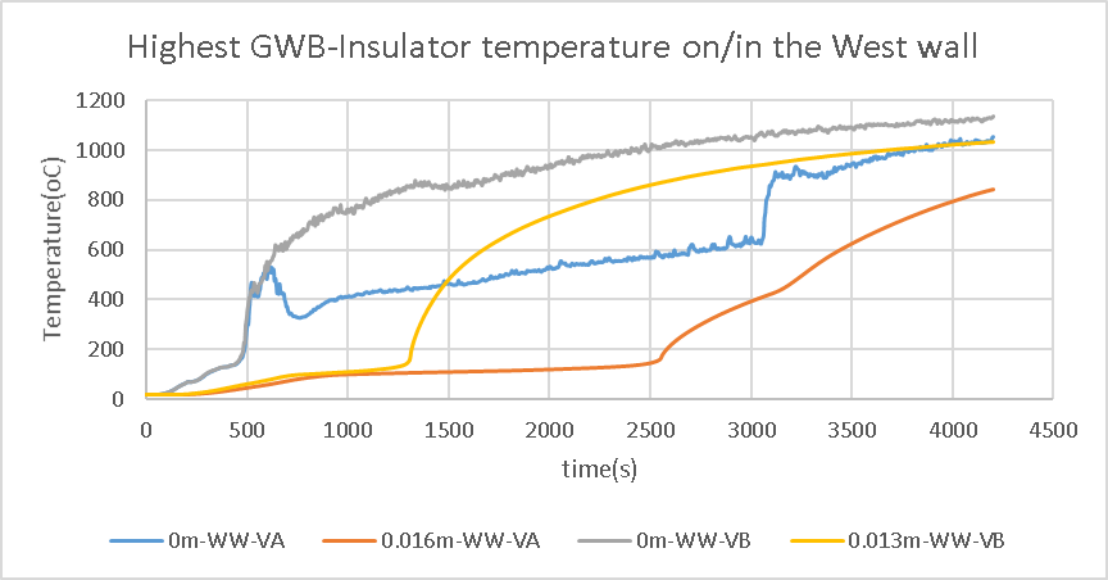

Figure 143 Comparison of highest temperatures on/in the West wall (GWB + Insulator+GWB)

(This panel is connected to the corridor door)

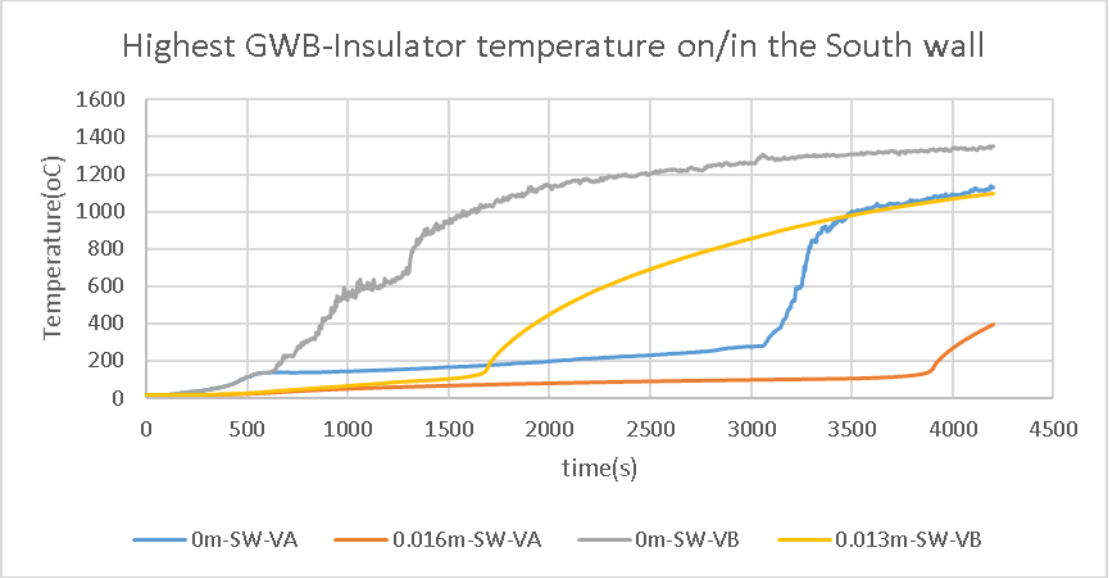

Figure 144 Comparison of highest temperatures on/in the South wall (GWB + Insulator+GWB)

(This panel is in the middle of the South wall)

3) The partition walls' temperature

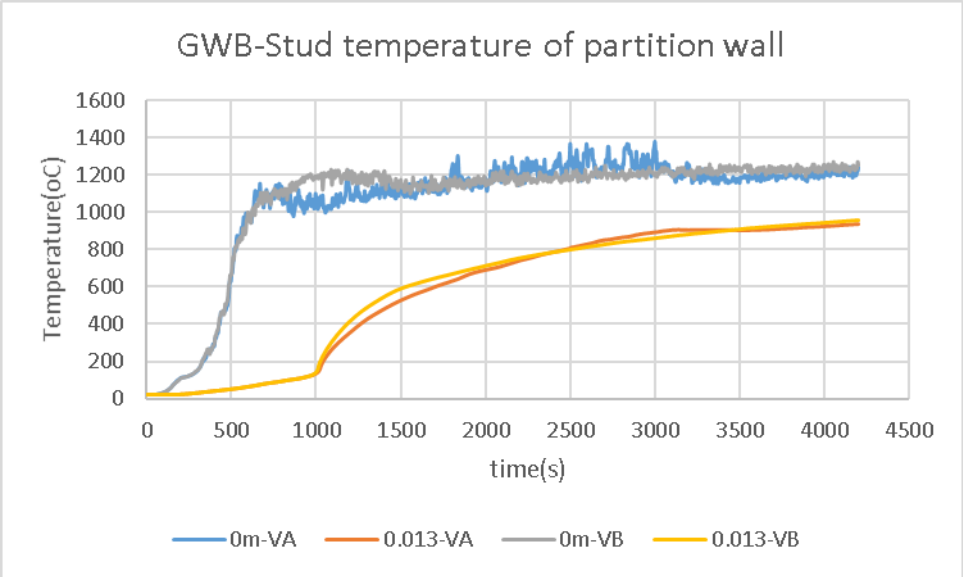

Figure 145 Comparison of highest temperatures on/in the partition wall (GWB + Stud +GWB)

(This stud is in the partition wall close to the North window)

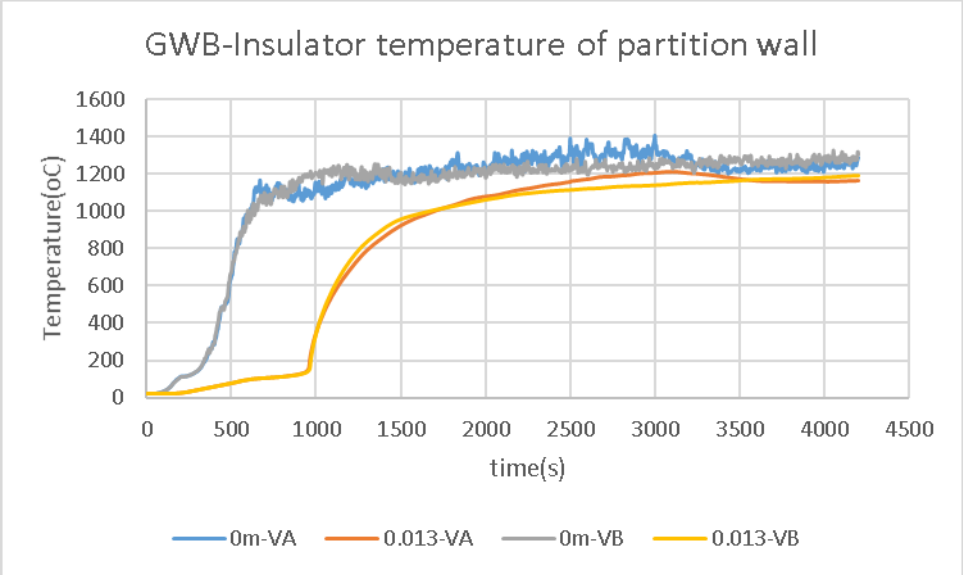

Figure 146 Comparison of highest temperatures on/in the partition wall (GWB + Insulator +GWB)

(This panel is in the partition wall close to the North window)

4) The Ceiling's temperature curves

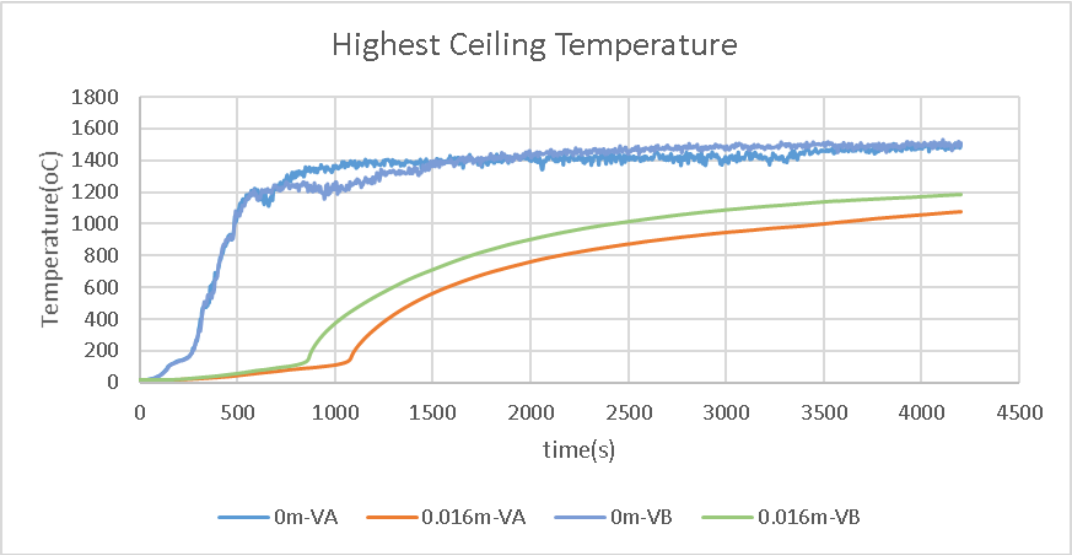

Figure 147 Comparison of highest temperatures on/in the ceiling

(This location is just above the burner close to the North window)

5) The compartment temperature curves

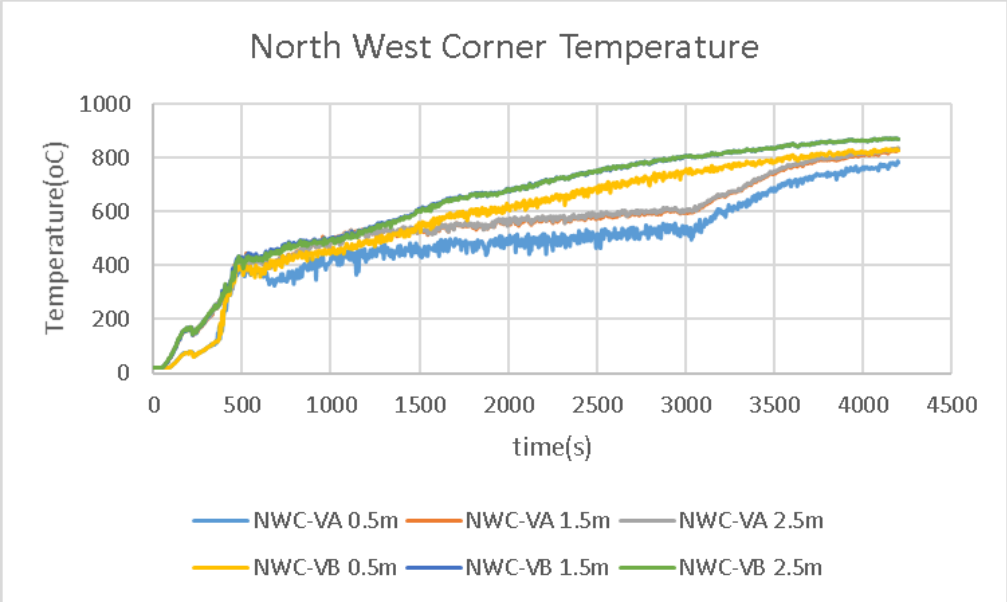

Figure 148 Comparison of Northwest Corner Temperatures in VA and VB compartment

(Temperatures at 1.5m and 2.5m are very close therefore are indiscernible)

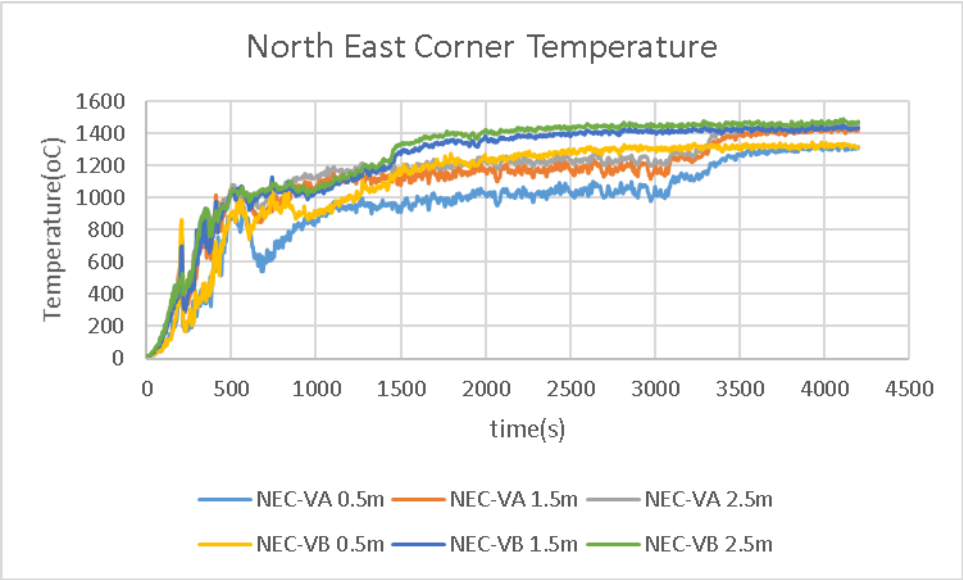

Figure 149 Comparison of Northeast Corner Temperatures in VA and VB compartment

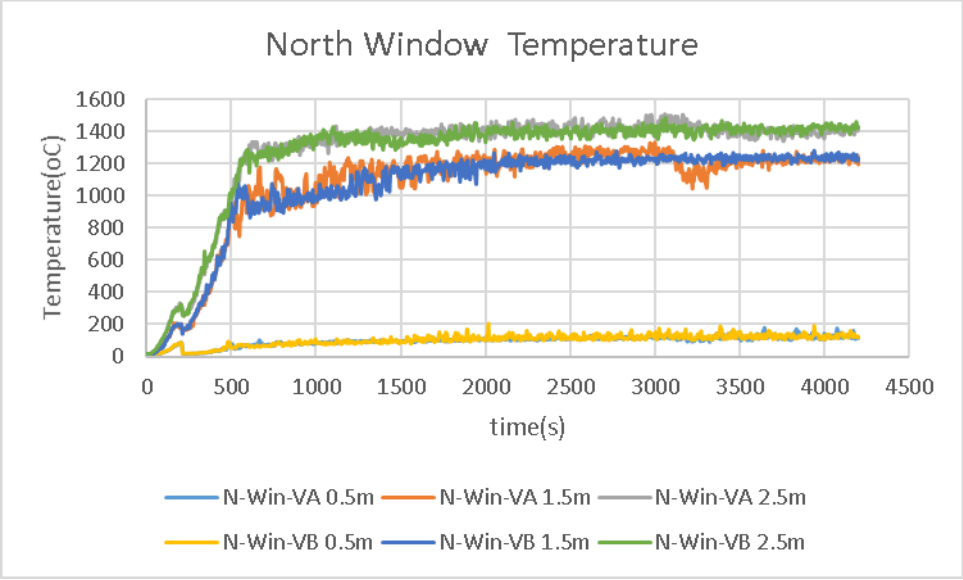

Figure 150 Comparison of North Window Temperatures in VA and VB compartment

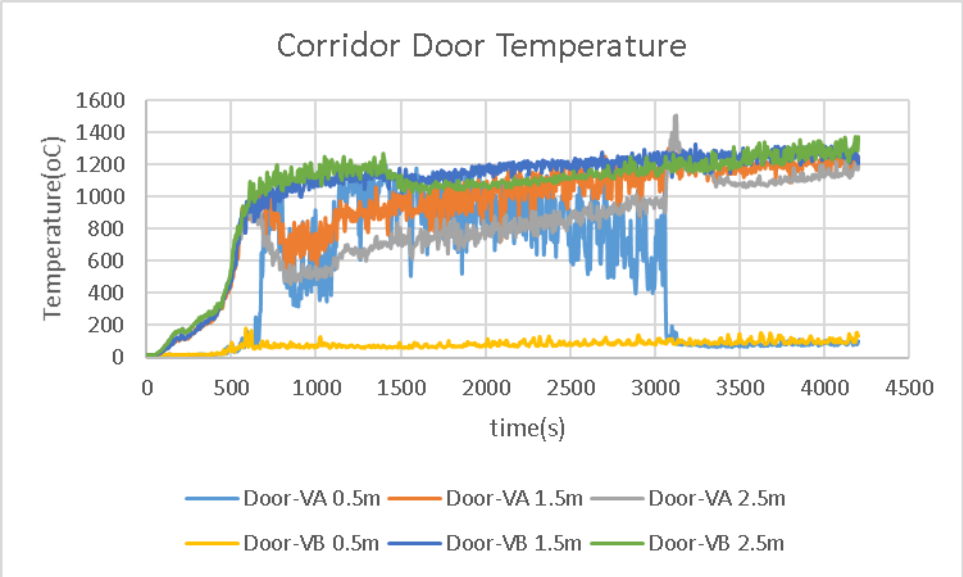

Figure 151 Comparison of corridor door Temperatures in VA and VB compartment

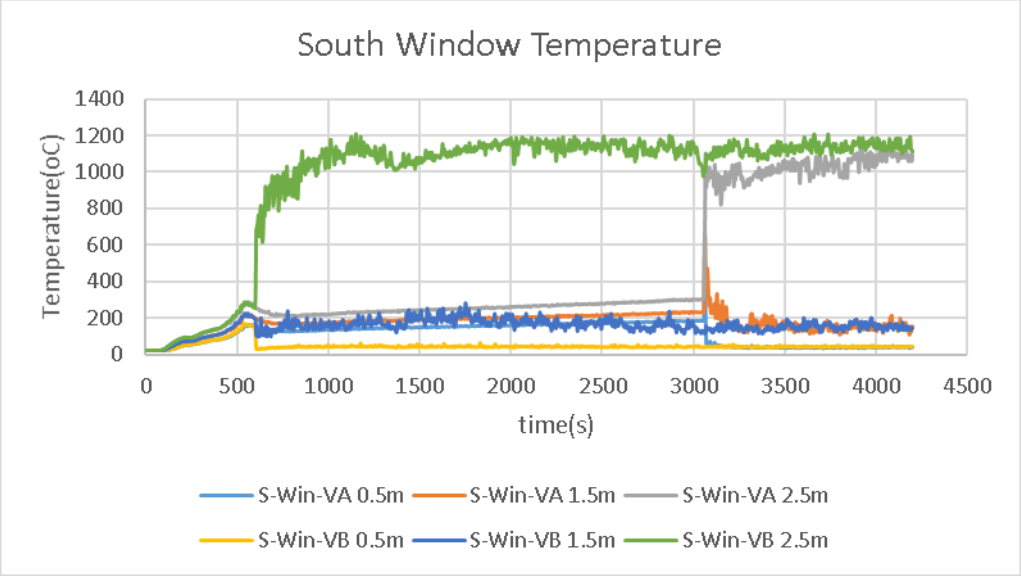

Figure 152 Comparison of South window Temperatures in VA and VB compartment

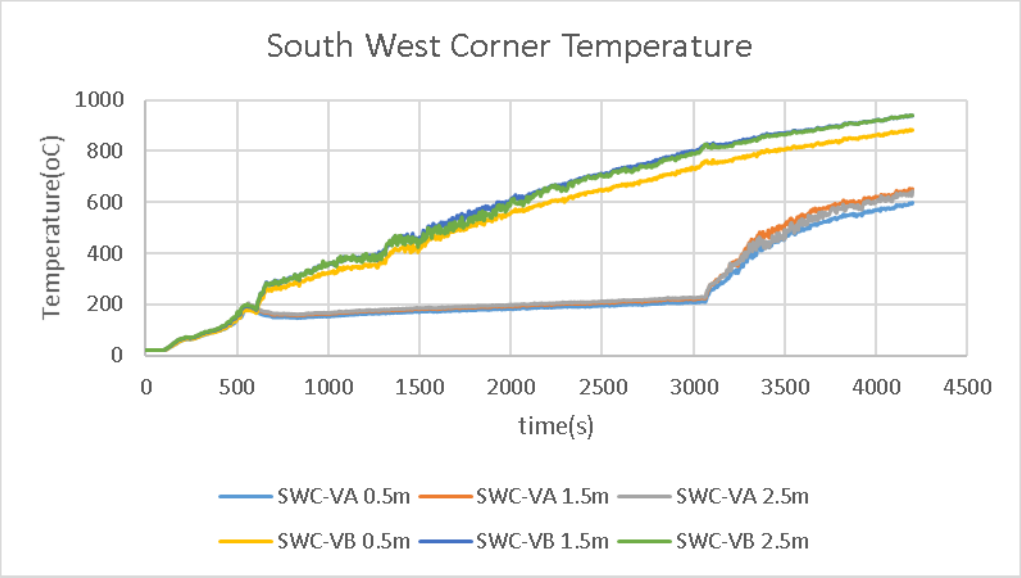

Figure 153 Comparison of Southwest corner Temperatures in VA and VB compartment

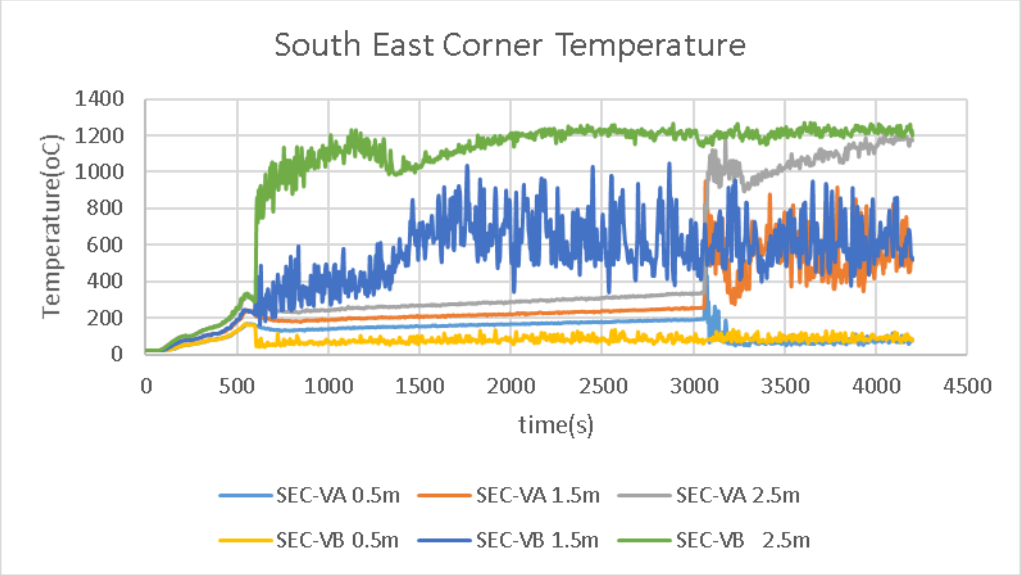

Figure 154 Comparison of Southeast corner Temperatures in VA and VB compartment

4.2.3. Conclusions

1) For solid phase temperatures, inside the walls/ceiling the temperatures in Type VB compartment are generally higher than in Type VA compartment. On the surface, the former is also greater than the latter after 1300s.
2) For gas phase temperature, except for the places near the openings, the temperature difference along vertical direction are small, the temperatures in Type VB apartment are generally higher than that in Type VA compartment.
3) The reason for higher temperatures on the surface of walls/ceiling and inside the compartment of Type VB is that the South window is opened much earlier in Type VB compartment than in Type VA compartment due to a small temperature change in type VA that delays the activation of South window, the increased air from the

failed window further increases the temperature on the surface of walls/ceiling and inside the compartment of Type VB by supplying more fresh air to the fire.

4) The reason for radical fire plume turbulence near the openings is that the slightly reduced temperatures developed in a Type VA compartment fire may have considerable influences on the operation of openings and thus the fire spreading processes if the temperature changes are just around the critical temperature used to remove a window. As a result, the fire spreading process is delayed to some extent in Type VA compartment fire, which can be shown in the following figures about differences of Heat Release Rates (HRRs) developed inside the compartment:

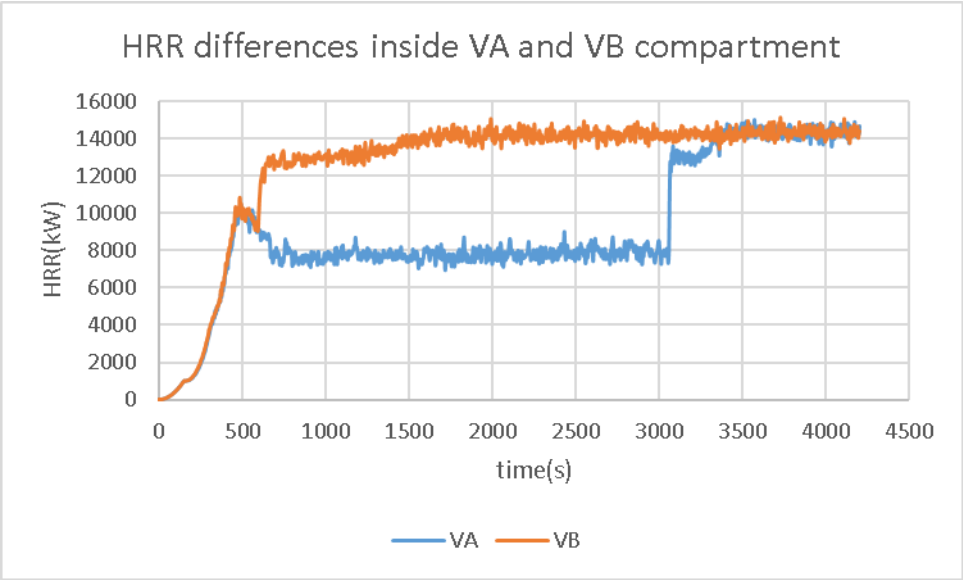

Figure 155 Different HRR developed in Type VA/VB compartment due to slightly changed compartment temperatures during the fire-growing phase

4.3. Structure stability analysis based on degradation/charring of walls/floor

4.3.1. Introduction

It is assumed that for Type VB building that has a functioning sprinkler system will have no structural issues since the fire is inhibited by the activated sprinklers from reaching a post-flashover phase. The basic conceptual flowchart for calculating the load-carrying capacity of wood structural elements is shown in the following figure:

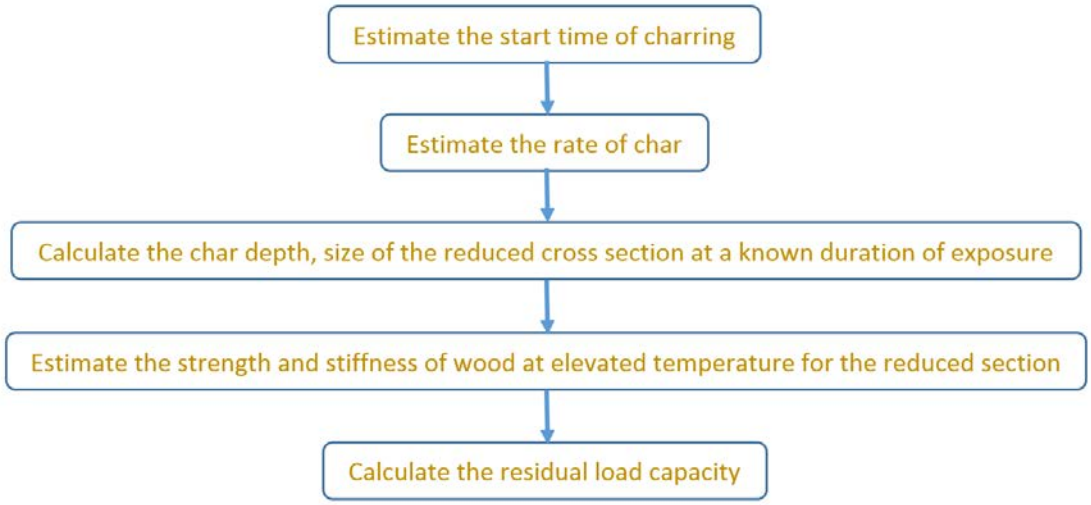

Figure 156 Basic flowchart for calculating load carrying capacity of timber structures

a) Assumptions made

- The building of Configuration I (Type VA) and Configuration III-B (Type VB) including the applied structural loads are code compliant to IBC 2012.
- The sprinkler system in Configuration III-B is assumed to not function.
- Exterior walls of the apartment modeled as shear walls and some internal walls are also modeled as shear walls. All other interior walls are modeled as gravity walls.
- All walls modeled as perforated walls.
- Axial capacity of walls considered as the decision-making factor for propagating the instability of walls (when the capacity is exceeded, loss of wall is assumed).
- Load redistribution is not considered in the RISA-Floor Analysis – The walls that exceed their axial capacity are NOT physically removed (or deleted) from the structural analysis model. However, the effect of load redistribution is considered in RISA-3D analysis of a single apartment floor system.
- Moisture in wood liberates as water vapor at 100 °C; Charring of the wood studs is assumed at a nominal incident temperature of 288 °C (a char layer starts forming on the surface of wood in contact with gypsum board exposed to fire. Charred layer has zero strength and stiffness, but is believed to act as an insulator to prevent further charring).

- Gypsum begins to undergo calcinations at 80 °C (loses chemically bonded water, starts losing strength and stiffness); Absorbed water in Gypsum completely vaporizes at 100 ~ 160 °C; Board undergoes complete contraction at 500-550°C (no more strength and stiffness left).
- Effective char rates are calculated based on NDS Technical Report No. 10 "Calculating the fire resistance of exposed wood members", which is dependent on the time duration after the starting of charring.
- RISA Floor Model: A single apartment, 3 floor stack is modeled using the product RISA-Floor to determine the loss of axial capacity of wall systems due to uniform charring of wood framed wall studs and roof joists. Charring in wall studs is accounted for every 5 minutes in time and 0.25 in. depth of char. (structure is remodeled and run for the reduced cross-section); Charring in floor joists is accounted for every 20 minutes in time and 2 in. depth of char. (structure is remodeled and run for the reduced cross-section). The structural stability analysis is conducted repeated for each reduction of cross-section. **Note: the change in charring depth/time is due to the limitation in the structural analysis software. A separate analysis is conducted in RISA-3D to account for a more accurate analysis.**
- RISA 3D Model: A single apartment floor system is modeled using the product RISA-3D to determine the floor bending capacity due to uniform charring of wood framed wall studs and roof joists. The wall supports are imposed on the model in the form of boundary conditions. Charring in floor joists is accounted for every 5 minutes in time and 0.25 in. depth of char. (structure is remodeled and run for the reduced cross-section). Load redistribution due to the walls losing their axial capacity is considered in this model

  For limitation of the RISA software suite, refer APPENDIX 5.
- No gypsum wallboard or ceiling boards are considered in the structural analysis software. All the interpretations on the loss of gypsum boards are based on the literature and experience with full-scale tests conducted by the author and many other researchers globally.
- A precise estimate of temperature at the surface and the back-face of the gypsum board is adopted from the results obtained from FDS modeling.
- The structure is analyzed for gravity loads only. Lateral loads (e.g., Wind, Earthquake) are not considered in simplified single apartment analysis.
- For RISA-Floor modeling, three levels are considered to represent the structural load carried by the 2 levels above level 1. However, the reduced section analysis is carried out only on level 1.
- For RISA-3D modeling, the floor system of a single apartment is considered.
- Average temperature-time curves are adopted exclusively to obtain the onset time of charring. Once the charring process begins, it is not temperature dependent but time dependent.
- The model for structural analysis is built using wood wall panels using standard dimensional lumber.

b) Relationships between temperature-time curves and different phenomena of GWB and wood studs/joists

Average temperature of gas phase in the compartment and solid phase in the walls/ceiling are needed to analyze the charring process of wood elements.

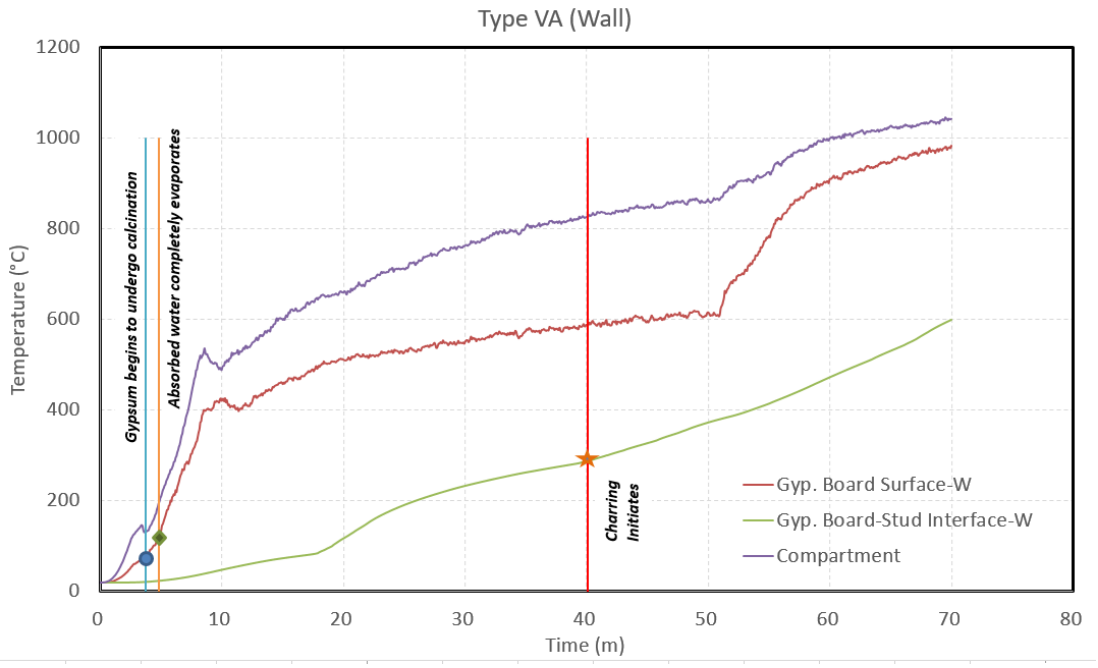

Figure 157 Wall temperature-time curves for building of Configuration I (Type VA Building)

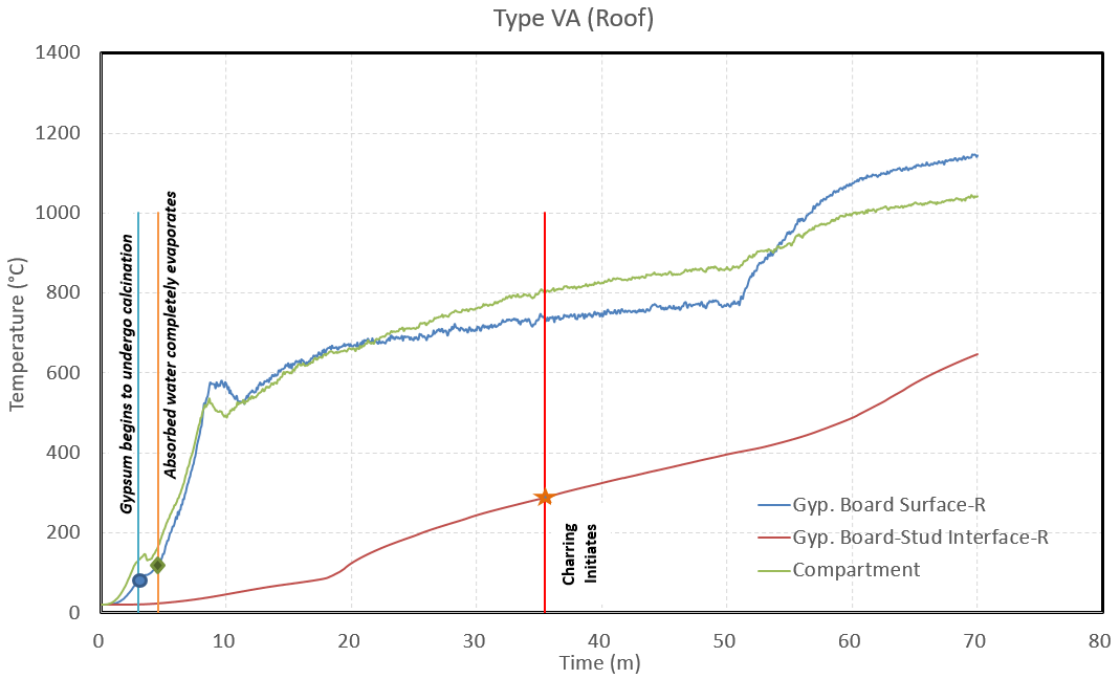

Figure 158 Roof Temperature-time curves for building of Configuration I (Type VA Building)

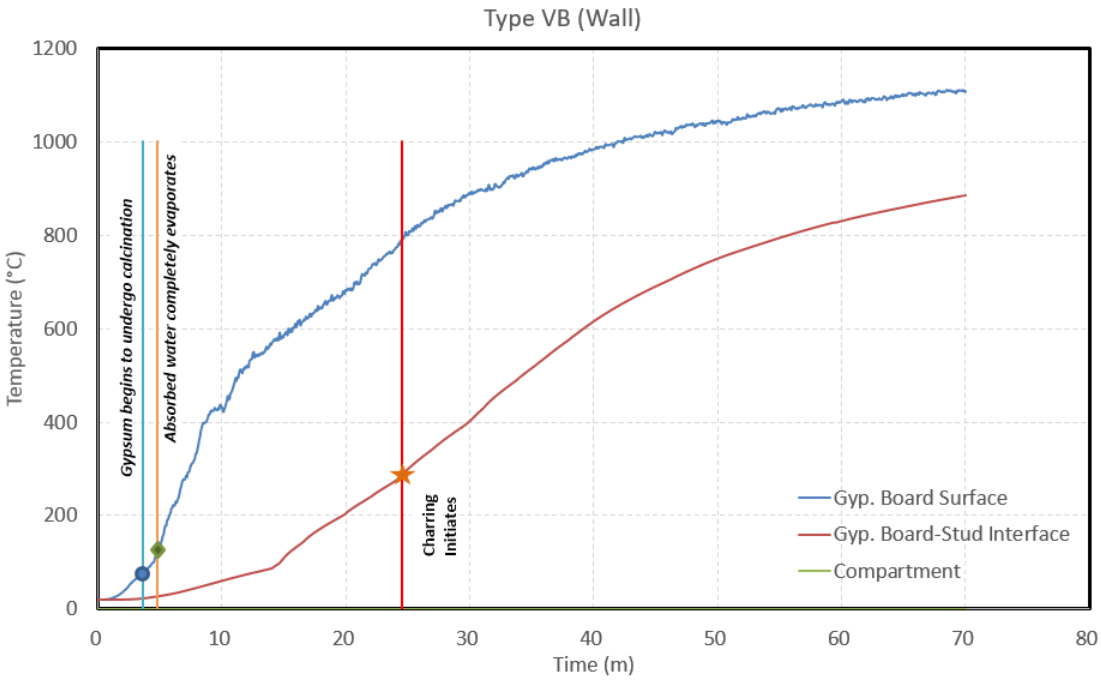

Figure 159 Wall temperature-time curves for building of Configuration III-B (Type VB Building)

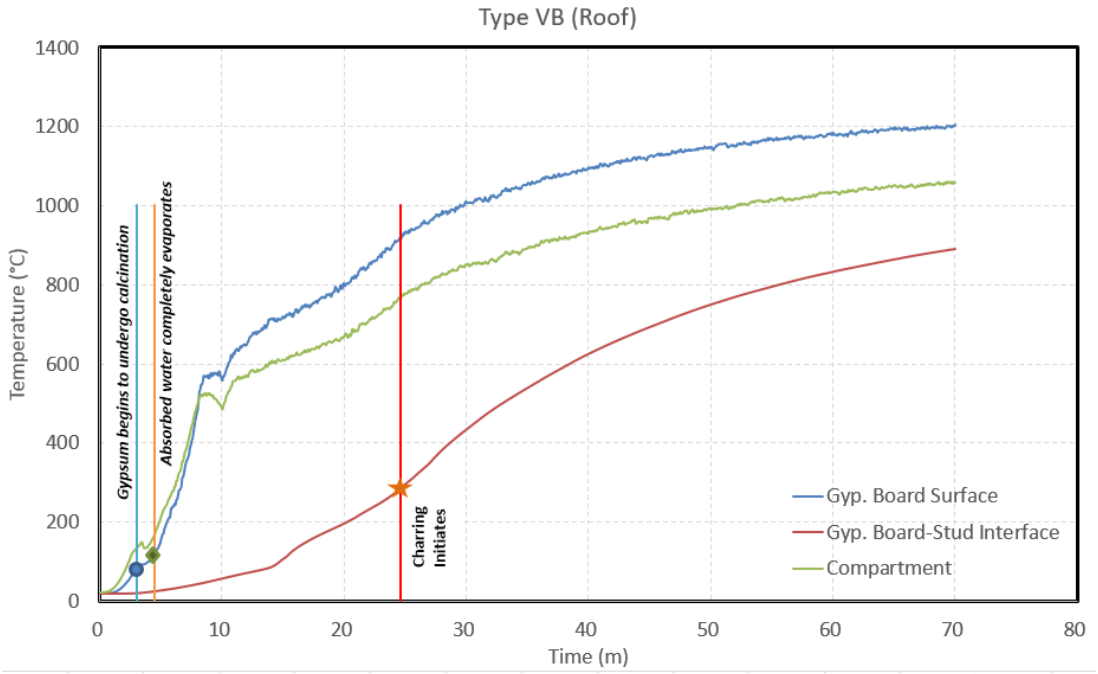

Figure 160 Roof Temperature-time curves building of Configuration III-B (Type VB Building)

These curves in Figure 157 to Figure 160 are obtained by simply averaging all the temperature - time curves gained by running FDS simulations. Different phenomena associated with reactions in gypsum and charring of wood studs/joists are also shown in the figure. The sequence of events are considered in reduced section analysis for wood studs/joists.

c) Charring in Wood Studs/Joists for RISA Floor / RISA-3DModeling

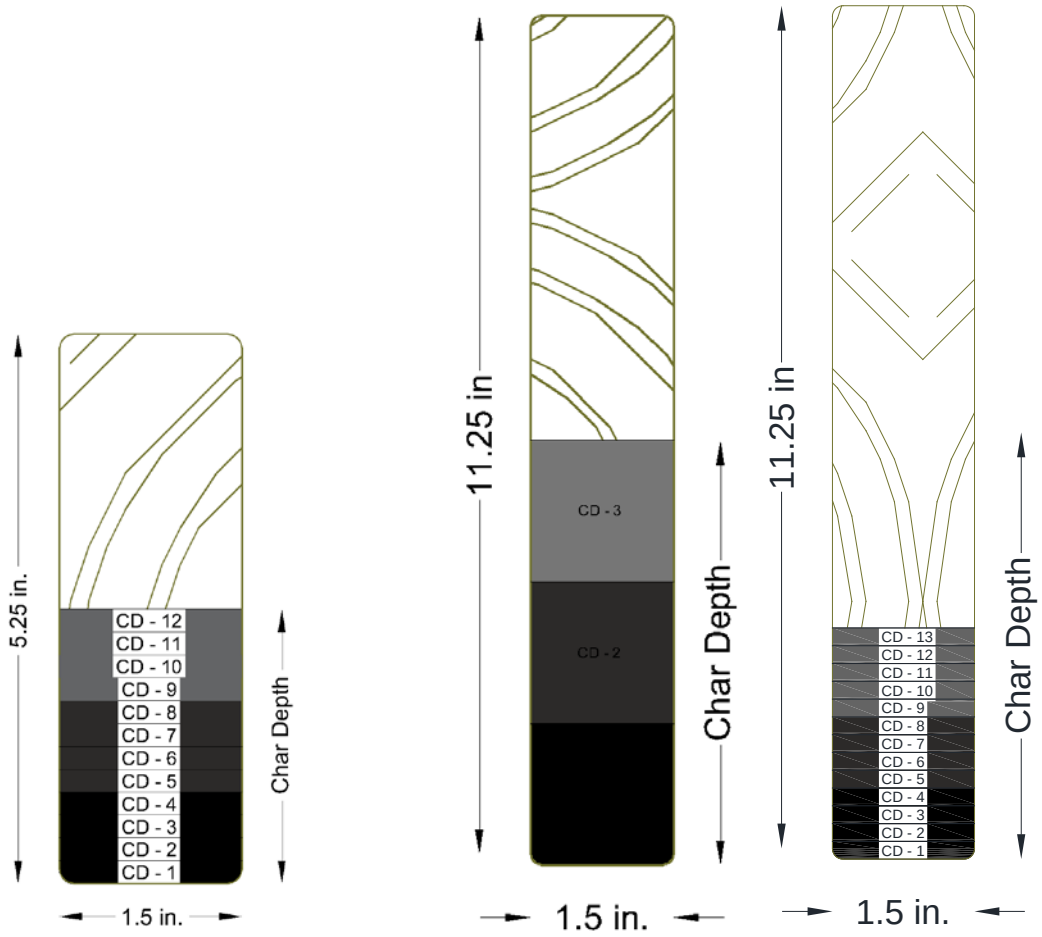

(a) (b) (c)

Figure 161 Char depth in (a) 2x6 wall studs (0.25 in/5 mins. increments): for RISA Floor Model (b) 2x12 floor joists (2 in/20 mins increments): for RISA Floor Model (c) 2x12 floor joists (0.25 in/5 mins increments): for RISA 3D Model

This figure shows the char depths considered for running the analysis on the wood framed apartment models (RISA Floor and RISA-3D) with reduced section. One dimensional charring is considered in both studs and joists since the aspect ratio of the cross-section is high. Charring of wood is considered based on an incident temperature of 288°C at the stud/joist face or at the interface between the gypsum board and stud / joists.

d) RISA Floor + RISA 3D Modeling for Structural Analysis

Structural models are shown in the following figures, Figure 162, Figure 163 and Figure 164:

Figure 162 Floor Plan of a single apartment block

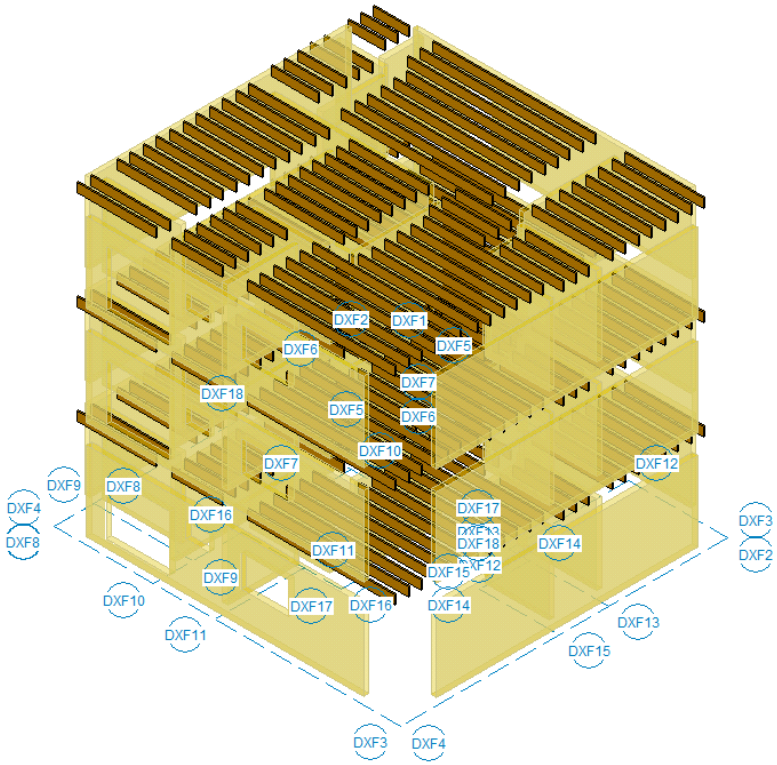

Figure 163 RISA Floor model for 1 apartment block with 3 Levels

(Two levels above are considered to account for the dead and live loads from level 2 and level 3)

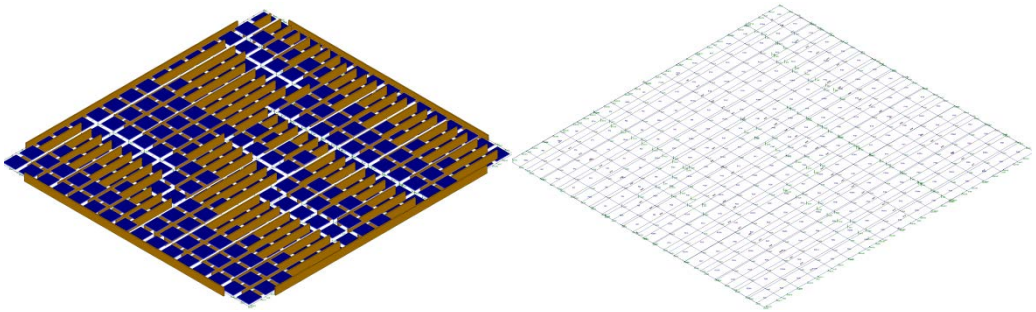

(a) (b)

Figure 164. Isolated model of the single apartment floor with dimensional lumber joist and plywood sub-floor decking (a) Extruded (b) With Plate meshing

4.3.2. Single Apartment Stack Modeling using RISA Floor

a) Modeling steps

The wall panel details such as framing, wall location and wall type are shown in the following table (the labels are marked in Figure 162):

Table 55 Wall Panel Details

Wall Panels	Framing	Location	Type
WP1	2 x 6 @ 16 o.c.	Exterior	Shear Wall
WP2	2 x 6 @ 16 o.c.	Exterior	Shear Wall
WP3	2 x 6 @ 16 o.c.	Exterior	Shear Wall
WP4	2 x 6 @ 16 o.c.	Exterior	Shear Wall
WP6	2 x 4 @ 16. o.c.	Interior	Gravity Wall
WP7	2 x 4 @ 16. o.c.	Interior	Gravity Wall
WP9	2 x 4 @ 16. o.c.	Interior	Gravity Wall
WP10	2 x 4 @ 16. o.c.	Interior	Gravity Wall
WP11	2 x 4 @ 16. o.c.	Interior	Gravity Wall
WP12	2 x 4 @ 16. o.c.	Interior	Gravity Wall
WP11A	2 x 4 @ 16. o.c.	Interior	Gravity Wall
WP12A	2 x 4 @ 16. o.c.	Interior	Gravity Wall
WP13	2 x 6 @ 16 o.c.	Interior	Shear Wall
WP14	2 x 6 @ 16 o.c.	Interior	Shear Wall
WP15	2 x 6 @ 16 o.c.	Interior	Shear Wall
WP16	2 x 6 @ 16 o.c.	Interior	Shear Wall
WP17	2 x 6 @ 16 o.c.	Interior	Shear Wall

The following figure shows the panel layout of the exterior walls

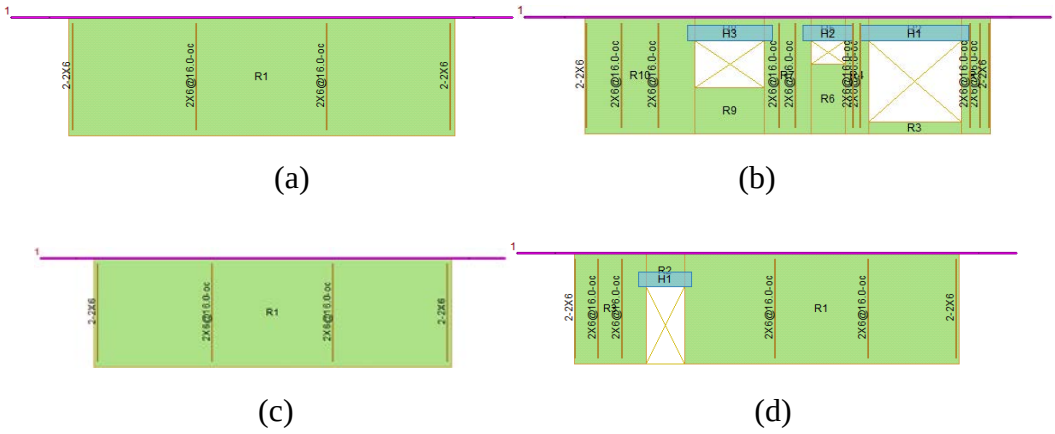

Figure 165 Layout of Exterior Walls (a) WP1, (b) WP2, (c) WP3, (d) WP4

(All exterior walls are made from 2x6 studs arranged 16 in. o.c. with double 2 x 6 top plates and single 2x6 bottom plates)

Once the structural models are established, the following iteration steps can be employed to determine the failure status for each wall:

Step 1: Run the structural analysis / design at ambient temperature. Obtain the results for axial capacity of walls, shear and bending capacity of floor joists.

Step 2: Estimate the time at which the charring on the wood begins from the temperature-time curve. This is the time at which the temperature on the back face of the gypsum equals the charring temperature.

Step 3: Calculate the depth of char based on NDS-2015 technical report 10 using reduced cross-section method.

Step 4: Remodel the single apartment with walls built with reduced cross-section.

Step 5: Run the analysis for updated model with members containing reduced cross-section.

Step 6: Identify the wall panels that fails in maximum shear and bending.

Step 7: Repeat the steps 3) to 6) with further reduction in cross-section until the failure.

b) Quick Results and Comparison

This section shows a quick comparative study on the loss of axial capacity in the walls obtained by running repeated reduced cross-section structural analysis.

Table 56 Structural response of the charred wall stud sections

Depth of Stud Section	Type VA		Type VB	
	Time (min)	% of Walls Exceeding Axial Capacity	Time (min)	% of Walls Exceeding Axial Capacity
	Charring Starts at 40:07		*Charring Starts at 25:30*	
5.25	**40:07:00**	0%	**25:30:00**	0%
5	**45:07:00**	6%	**30:30:00**	6%
4.75	**50:07:00**	6%	**35:30:00**	6%
4.5	**55:07:00**	6%	**40:30:00**	6%
4.25	**60:07:00**	6%	**45:30:00**	6%
4	**65:07:00**	6%	**50:30:00**	6%
3.75	**70:07:00**	35%	**55:30:00**	35%
3.5	**75:07:00**	**53%**	**60:30:00**	**53%**
3.25	**80:07:00**	**65%**	**65:30:00**	**65%**
3	**85:07:00**	**71%**	**70:30:00**	**71%**
2.75	**90:07:00**	**76%**	**75:30:00**	**76%**
2.5	**95:07:00**	**82%**	**80:30:00**	**82%**
2.25	**100:07:00**	**82%**	**85:30:00**	**82%**

This table shows the comparison of structural response of wood wall studs obtained from running reduced section analysis for type VA and Type VB building. Loss of section capacity is color coded where green represents lesser damage and red represents critical damage to wall panels.

It should be noted that the structural analysis is common for both building types due to the fact that the software does not consider use of gypsum wall / ceiling board. FDS simulations are only run for 70 minutes of fire. However the structural analysis was run for a total of 60 minutes from start of charring. The estimated time for charring in Type VA buildings is 40:07 minutes whereas for type VB buildings it is 25:30 minutes

Table 57 Structural response of Type VA building – single apartment unit

Time / Wall Panel	40:07	40:07	45:07	50:07	55:07	60:07	65:07	70:07	75:07	80:07	85:07	90:07	95:07	100:07
WP1	CHARRING in Wall Initiates at 40:06 minutes in the wall and 35:30 minutes in the ceiling	☑	☑	☑	☑	☑	☑	☑	☑	☑	☑	☒	☒	☒
WP2		☑	☑	☑	☑	☑	☑	☑	☑	☑	☑	☑	☑	☑
WP3		☑	☑	☑	☑	☑	☑	☑	☑	☑	☑	☑	☒	☒
WP4		☑	☑	☑	☑	☑	☑	☑	☑	☑	☑	☑	☑	☑
WP6		☑	☑	☑	☑	☑	☑	☑	☑	☑	☑	☑	☑	☑
WP7		☑	☑	☑	☑	☑	☑	☒	☒	☒	☒	☒	☒	☒
WP9		☑	☑	☑	☑	☑	☑	☑	☑	☒	☒	☒	☒	☒
WP10		☑	☑	☑	☑	☑	☑	☒	☒	☒	☒	☒	☒	☒
WP11		☑	☑	☑	☑	☑	☑	☒	☒	☒	☒	☒	☒	☒
WP12		☑	☑	☑	☑	☑	☑	☒	☒	☒	☒	☒	☒	☒
WP11A		☑	☑	☑	☑	☑	☑	☒	☒	☒	☒	☒	☒	☒
WP12A		☑	☒	☒	☒	☒	☒	☒	☒	☒	☒	☒	☒	☒
WP13		☑	☑	☑	☑	☑	☑	☑	☒	☒	☒	☒	☒	☒
WP14		☑	☑	☑	☑	☑	☑	☑	☒	☒	☒	☒	☒	☒
WP15		☑	☑	☑	☑	☑	☑	☑	☑	☑	☒	☒	☒	☒
WP16		☑	☑	☑	☑	☑	☑	☑	☒	☒	☒	☒	☒	☒
WP17		☑	☑	☑	☑	☑	☑	☑	☑	☒	☒	☒	☒	☒

☑ *Axial Capacity Within Required Limits* ☒ *Axial Capacity Exceeds*

Table 58 Structural response of Type VB building – single apartment unit

Time / Wall Panel	25:30	25:30	30:30	35:30	40:30	45:30	50:30	55:30	60:30	65:30	70:30	75:30	80:30	85:30
WP1	CHARRING in Wall Initiates at 25:30 minutes in the wall and 25:38 minutes in the ceiling	☑	☑	☑	☑	☑	☑	☑	☑	☑	☑	☒	☒	☒
WP2		☑	☑	☑	☑	☑	☑	☑	☑	☑	☑	☑	☑	☑
WP3		☑	☑	☑	☑	☑	☑	☑	☑	☑	☑	☑	☒	☒
WP4		☑	☑	☑	☑	☑	☑	☑	☑	☑	☑	☑	☑	☑
WP6		☑	☑	☑	☑	☑	☑	☑	☑	☑	☑	☑	☑	☑
WP7		☑	☑	☑	☑	☑	☑	☒	☒	☒	☒	☒	☒	☒
WP9		☑	☑	☑	☑	☑	☑	☑	☑	☒	☒	☒	☒	☒
WP10		☑	☑	☑	☑	☑	☑	☒	☒	☒	☒	☒	☒	☒
WP11		☑	☑	☑	☑	☑	☑	☒	☒	☒	☒	☒	☒	☒
WP12		☑	☑	☑	☑	☑	☑	☒	☒	☒	☒	☒	☒	☒
WP11A		☑	☑	☑	☑	☑	☑	☒	☒	☒	☒	☒	☒	☒
WP12A		☑	☒	☒	☒	☒	☒	☒	☒	☒	☒	☒	☒	☒
WP13		☑	☑	☑	☑	☑	☑	☑	☒	☒	☒	☒	☒	☒
WP14		☑	☑	☑	☑	☑	☑	☑	☒	☒	☒	☒	☒	☒
WP15		☑	☑	☑	☑	☑	☑	☑	☑	☑	☒	☒	☒	☒
WP16		☑	☑	☑	☑	☑	☑	☑	☒	☒	☒	☒	☒	☒
WP17		☑	☑	☑	☑	☑	☑	☑	☑	☒	☒	☒	☒	☒

☑ *Axial Capacity Within Required Limits* ☒ *Axial Capacity Exceeds*

Table 57 and Table 58 show the progression in the loss of axial capacity of different wall panels in type VA and type VB buildings respectively. Green check boxes with tick mark show that the axial capacity in the walls is within the required limits or in other words, the wall panels are still contributing to support the structural loads. Red check boxes with cross mark show that the axial

capacity in the walls have exceeded the maximum limits or in other words, the wall panels have lost their capacity to support the structural loads.

From **Table 55** to **Table 57** the following observations can be made:

- At 70 minutes into fire, Type VA buildings lost only 35% of the combined wall axial capacity as compared to type VB buildings, where double the axial capacity of the walls was sacrificed (71%).
- At 60 minutes from charring almost all the axial capacity of the walls is lost as the residual sections are too small to carry the structural load.
- It is observed that both building types hold enough structural capacity up to about 50 minutes. Type VB begins to lose its axial capacity ~ 15 minutes earlier than Type VA

4.3.3. Single Apartment Floor System Modeling using RISA 3D

This section presents the modeling plan for the analysis of a single story apartment unit with reduced cross-section to account for load redistribution. Load redistribution governs the overall performance of the building when a wall loses its effective axial capacity. The intent was to simulate the complete loss of wall panels in the existing model and re-run to obtain the results with a 'physically-removed' wall panel.

During the analysis of a three-story apartment building in RISA floor (described in the previous section), it was found that the walls started losing their axial capacity with the increase in the char depth of the framing members on the wall. Figure 166 shows the plan of the apartment building with the damage progression of walls with cross-sectional reduction of walls. Each wall that has lost its axial capacity is shown with a cross (mark) on it. The ID shown on the wall within the brackets next to the cross mark is attached to the degraded cross-section at which the wall loses its axial capacity.

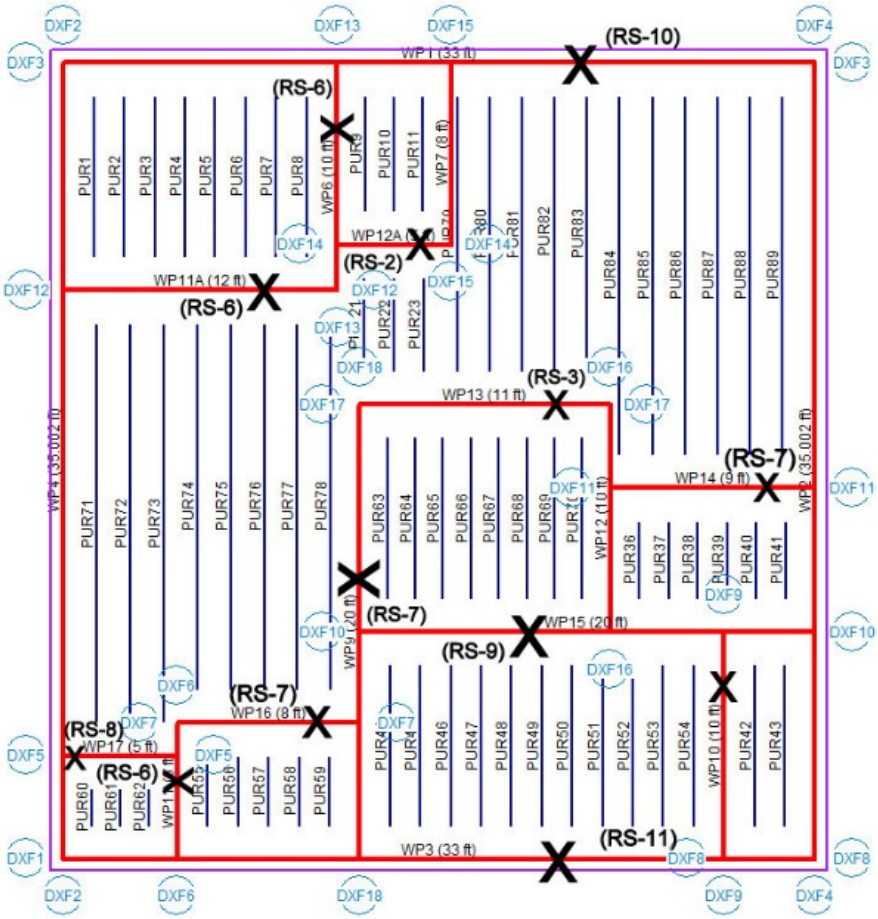

*RS – Reduced section / Reduced Cross-Section

Figure 166. Plan of the single apartment with wall damage progression

However, due to the limitations of RISA floor, the effect of load redistribution could not be captured on the floor system of the single apartment block. In order to simulate the effects of the reduced wall. In an effort to show the effect of load redistribution, the floor system was separately modeled in RISA-3D as a single component, with the appropriate boundary conditions to include the effect of the walls. Refer to APPENDIX 6 for the model attempts conducted to simulate load redistribution.

As shown in Figure 164, the extruded RISA 3D model of the floor for a single apartment is set up to run reduced section analysis. The model was built using standard 2 x 12 dimensional lumber (Doug-Fir) sections for the rim joists and the floor joists and a ¾ in. plywood subfloor decking. Default material properties from RISA material library were used for the Doug-Fir wood. The subfloor deck was modeled using a general plywood material with modified material properties. The plywood decking was also modeled as a plate element sub-meshed with 16 x 16 elements to capture the forces and stresses on the floor system due to the applied loads. The dead and the live loads were applied as the member area loads, that are ideal to capture the plate bending and shear stresses. The load combinations generated according to 2015 IBC ASD. In addition to the distributed dead load, a nominal point load of 240 lbs was applied on the critical floor joist to represent the firefighter load. A moving firefighter load (120 lbs x 2) was also generated on the

same member. A separate load combination was created for combing the moving load with other gravity loads.

13 different models, 1 without reduced cross-section and 12 with reduced cross-sections were setup to run the analyses. In order to simulate the effect of damaged walls, the boundary conditions depicting the walls were deleted using the progression shown in Figure 166. Additionally, **Table 59** (a) and (b) shows the detailed plan for the reduced section analysis for Type VA and Type VB buildings respectively. The first column shows the time interval of 5 minutes from the time at which the charring initiates. The second columns shows the ID assigned for each analysis. Columns three and four show the char depth associated with the time and their respective residual member depth (joist) respectively. The last column shows the wall panels that have lost their axial capacity and hence are removed from the analyses. From the table, it is observed that the charring on the floor joists for type VA building initiates at 35:29 minutes whereas for type VB building, it initiates at 26:30 minutes. The time for charring initiation is based on the temperatures at the back face of the gypsum board reaching the charring temperatures as determined in the FDS simulation for a single apartment block.

Table 59. Reduced section analysis plan for (a) Type VA building (b) Type VB building

(a)

Type VA Time (m)	Label	Char Depth (in)	Member Depth (in)	Wall Panels Lost / Removed
35:29	No RS	0	11.25	-
40:29	RS - 1	0.25	11	-
45:29	RS - 2	0.5	10.75	-
50:29	RS - 3	0.75	10.5	WP 12A
55:29	RS - 4	1	10.25	WP 12A
60:29	RS - 5	1.25	10	WP 12A
65:29	RS - 6	1.5	9.75	WP 12A
70:29	RS - 7	1.75	9.5	WP 12A
75:29	RS - 8	2	9.25	WP 12A, WP 7, WP 10, WP 11, WP 12, WP 11A
80:29	RS - 9	2.25	9	WP 12A, WP 7, WP 10, WP 11, WP 12, WP 11A, WP 13, WP 14, WP 16
85:29	RS - 10	2.5	8.75	WP 12A, WP 7, WP 10, WP 11, WP 12, WP 11A, WP 13, WP 14, WP 16, WP 17
90:29	RS - 11	2.75	8.5	WP 12A, WP 7, WP 10, WP 11, WP 12, WP 11A, WP 13, WP 14, WP 16, WP 17, WP 15
95:29	RS - 12	3	8.25	WP 12A, WP 7, WP 10, WP 11, WP 12, WP 11A, WP 13, WP 14, WP 16, WP 17, WP 15, WP 1
100:29	RS - 13	3.25	8	WP 12A, WP 7, WP 10, WP 11, WP 12, WP 11A, WP 13, WP 14, WP 16, WP 17, WP 15, WP 1, WP 3

(b)

Type VB Time (m)	Label	Char Depth (in)	Member Depth (in)	Wall Panels Lost / Removed
26:38	No RS	0	11.25	-
31:38	RS - 1	0.25	11	-
36:38	RS - 2	0.5	10.75	-
41:38	RS - 3	0.75	10.5	WP 12A
46:38	RS - 4	1	10.25	WP 12A
51:38	RS - 5	1.25	10	WP 12A
56:38	RS - 6	1.5	9.75	WP 12A
61:38	RS - 7	1.75	9.5	WP 12A
66:38	RS - 8	2	9.25	WP 12A, WP 7, WP 10, WP 11, WP 12, WP 11A
70:38	RS - 9	2.25	9	WP 12A, WP 7, WP 10, WP 11, WP 12, WP 11A, WP 13, WP 14, WP 16
75:38	RS - 10	2.5	8.75	WP 12A, WP 7, WP 10, WP 11, WP 12, WP 11A, WP 13, WP 14, WP 16, WP 17
80:38	RS - 11	2.75	8.5	WP 12A, WP 7, WP 10, WP 11, WP 12, WP 11A, WP 13, WP 14, WP 16, WP 17, WP 15
85:38	RS - 12	3	8.25	WP 12A, WP 7, WP 10, WP 11, WP 12, WP 11A, WP 13, WP 14, WP 16, WP 17, WP 15, WP 1
90:38	RS - 13	3.25	8	WP 12A, WP 7, WP 10, WP 11, WP 12, WP 11A, WP 13, WP 14, WP 16, WP 17, WP 15, WP 1, WP 3

4.4. Results and Discussion

Each model was solved for batch and envelope solutions for all the load combinations and results were obtained in the form of member deflections, forces and moments as well as plate forces and moments. A critical member was identified from the first analysis performed on the floor system without any reduced cross-section (No RS) and was monitored in the subsequent analysis. Member M50, was found to be critical in bending and was hence considered to obtain the shear and moment for the reduced sections. However, other members were critical in bending beyond RS-7. Figure 167 shows the member deflections from the results generated in the reduced section analysis plotted against various char depths. It is noted that the download deflection in the member M50 increases gradually up to a char depth of 1.75 in. The deflection however remains under limiting deflection value of L/360. At a char depth of 2 in., that corresponds to a duration of 75:29 from ignition in type VA building and 66:38 minutes in the type VB building, 6 walls lose their axial capacity and hence stop providing

restraints to the members supported on them. This results in excessive deflection in the members, especially at one of the supports. As the char depths increase in both wall studs and the floor joists, more and more walls start losing their axial capacity and hence the members supported by the walls show excessive deflections under the support, which causes excessive deflection as shown in Figure 167. From the figure, it is observed that all the deflections beyond a char depth of 2 in. exceed the limiting deflections. Two main reasons for the excessive deflections are the reduction in load-carrying capacity of the charred floor joists and loss of supports provided to the members due to the damaged walls. Hence, the floor joists fail in bending. This event is detrimental to the overall structural integrity of the floor system, which is used by firefighters to carry out the fire extinguishing and rescue operation. Another important observation is related to the type of the building. The charring initiates in the type VB building ~ 9 minutes earlier than the type VA building, which also confirms that an identical floor system in a type VB building loses its structural integrity sooner than the type VA building.

Figure 168 shows the maximum shear force in the member M50 obtained at different char depths in the floor joists. From the figure, it is observed that the shear force shows a gradual dip up to a char depth of 1.75 in. It shows a slight increment at a char depth of 2 in., after which it decreases. Thereafter, the shear force shows a steep increase at char depths of 2.75 in. The trend shows a clearly shows redistribution of forces, which is influenced by the removal of wall boundary conditions in order to simulate the effect of fire damaged walls. Also, at greater char depths and large value of shear forces at the member ends, the joist members fail the bending checks as they show excessive deflections.

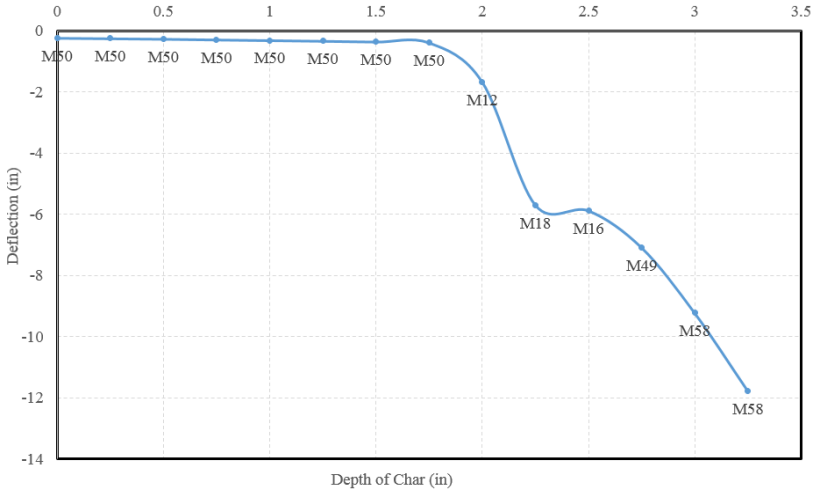

Figure 167. Variation in bending of floor joist (deflection) at different char depths / reduced sections

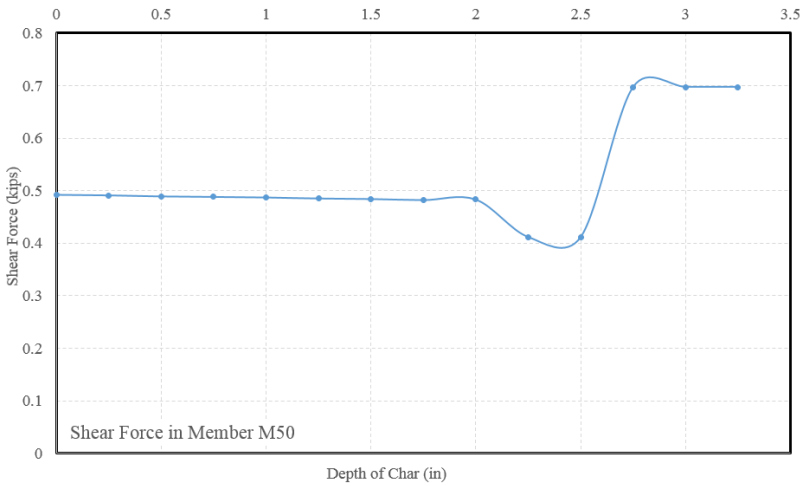

Figure 168. Variation in shear force for the member M50 at different char depths / reduced sections

Figure 169 shows the bending moments in the joist member M50, plotted against various char depths. The char depths correspond to the reduced depth of the member. Unlike the shear force, the bending moment shows a slight increment up to a char depth of 1.75 in and thereafter shows an increase that varies based on the char depths. Similar to the shear force trend, the bending moment trends show an effect of load redistribution as an effect of the removal of wall panels.

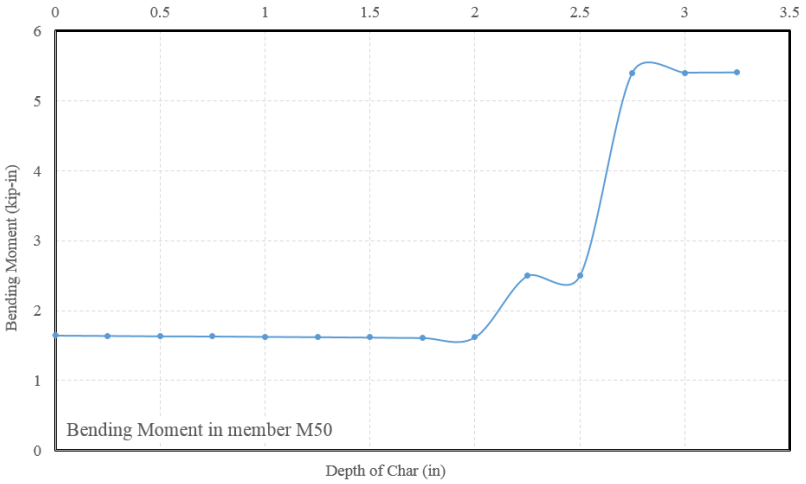

Figure 169.Variation in bending moment for the member M50 at different char depths / reduced sections

In this report, only a typical member identified as a critical member is used to illustrate the effect of load redistribution. However, similar trends were observed in other members that form the floor system of the single apartment unit.

4.4.1. Development of plate forces and stresses in the floor deck

This section presents the plate forces and stress contours obtained for the plywood floor deck modeled on the floor system in RISA-3D. The profiles were obtained in response to the distributed area loads on the floor applied as different load combinations. Figure 170 shows

the von Mises stress (σ_v) profiles of the floor at different char depths of the floor joists. von Mises stresses are the design stresses, used to define the failure of the material. If these stresses exceed the strength of the material, the material fails. The stress profile also considers the loss of wall panels simulated by removed boundary conditions. Stress contours plotted for the actual floor system without the reduced section and with the reduced section are shown in the figure. The stress contours show the maximum stresses concentrated near the wall supports as well as the mid-span of each subpanels. The stresses at the supports are larger than the stresses at the mid-span of the panels. The shades in red display the maximum stresses, yellow shows intermediate stress zones and the blue shades display lower stresses on the floor panel. A slight change in the stress-contours may be observed in the stress profiles up to a char depth of 0.5 in. At the char depth of 0.75 in, it may be observed that the stresses along the member M1, that is the edge supported on the wall panel WP1, starts to extend along the edge of the wall. It is also observed that the stresses at the mid-span at the rear starts to increase. Thereafter the stress intensities may be observed to increase in their intensities shown by the expanding stress contours. At the char depth of 2 inch, the stresses on the surface of the deck are redistributed as the wall panel WP12A fails and is removed from the model. It may be observed that the stresses are redistributed and their intensities change throughout the surface. Most of the stresses are now concentrated in the direction of the removed wall panel. This is because the members supported on the wall panel starts to lose their restraints, due to which the deck supported on the member also deflects. Thereafter, every increment in char depth is followed by the failure of an additional wall panel, which changes the stress contours as the stresses are redistributed due to the load spreading over the remaining wall panels. Loss of every panel induces a sagging effect on the deck, which is evidently seen from the figures. At char depths of 3 and 3.25 in, the exterior walls of the apartment unit are lost and the floor deck is seen to suffer excessive deflections. This is considered as the failure of the floor system due to inadequate supports provided by the wall panels.

Figure 171 shows the development of shear stresses (τ) throughout the floor deck as a result of char depth on the supporting joists and the failure of wall panels supporting the diaphragm. Similar to the von Mises stresses, shear stress profiles for incremental char depths from 0 in to 3.25 in. are shown in the figure. The color coding on the stresses remained the same as that of the von Mises stresses. It is observed that the maximum values of shear stresses are concentrated at the supports of the interior and exterior wall panels. Up to char depths of 1.75 in., minor changes in stress-profiles were detected, mainly at the corner, at the intersection of the members M1 and M2. The removal of wall panel WP 12A resulted in the redistribution of stresses on the deck around that zone. The pattern showed a major shift at a char depth of 2 in., during which more wall panels lost their axial capacity and were removed. A change in the boundary condition resulted in the redistribution of shear stresses throughout the deck. A major shift in the build-up of shear stress is observed. The stresses are observed to be concentrated along the exterior walls of the apartment along the member M1. As more and more walls are removed, the deflection of the diaphragm increases for the applied load and reduced joist members. Thereafter, the diaphragm fails due to excessive deflections.
In conclusion, the stress profiles discussed in this section show the development of weak spots or weak zones. The regions with higher stresses indicates a greater loss in section

capacity and larger deformation of the roof joists. These are possible "*Danger Zones*" for the firefighters. These locations may be identified as potential fall-through hazard spots. Weakening of the floor is quantified by the development of deflections beyond the values of limiting deflections.

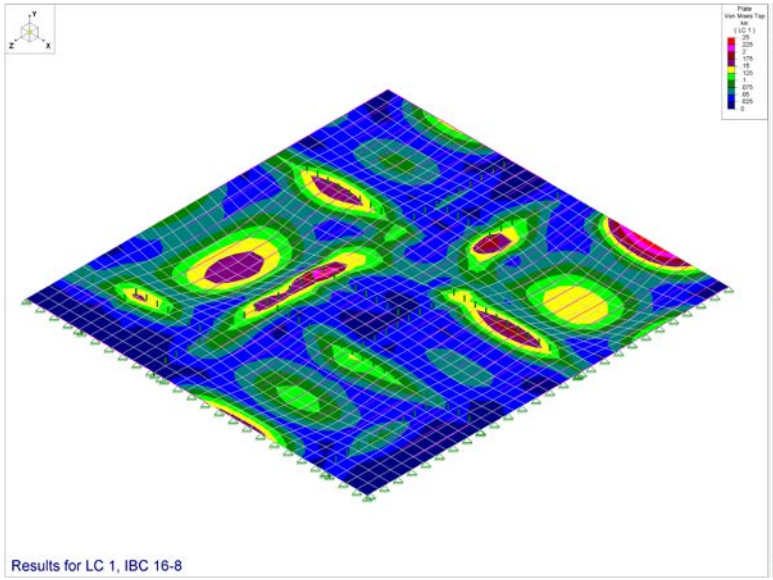

No Section Reduction

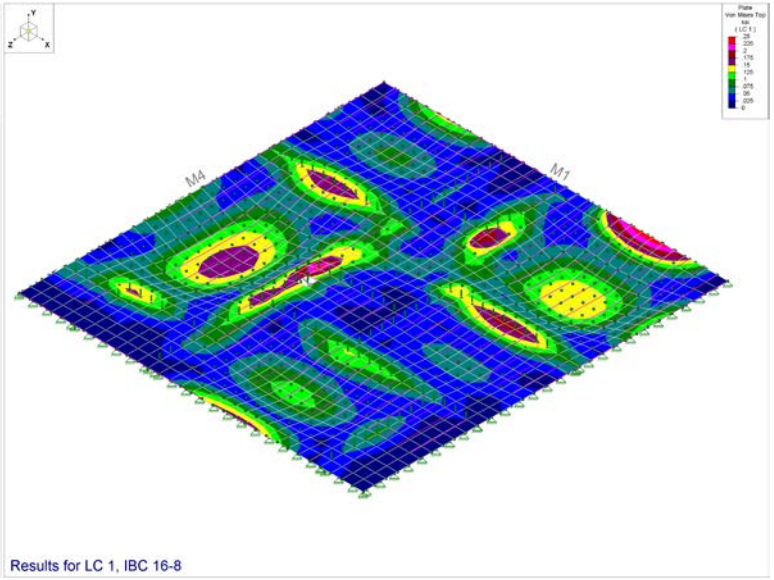

SR1: Char Depth = 0.25 in.

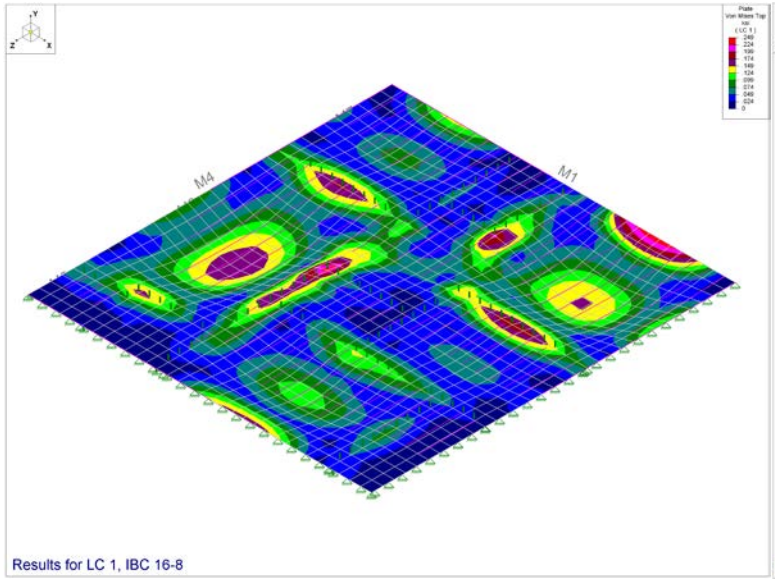

SR2: Char Depth = 0.5 in.

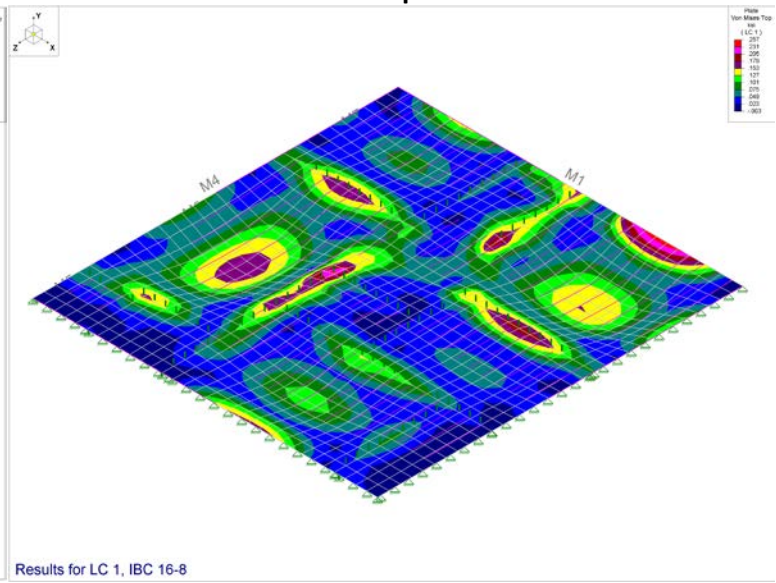

SR3: Char Depth = 0.75 in.

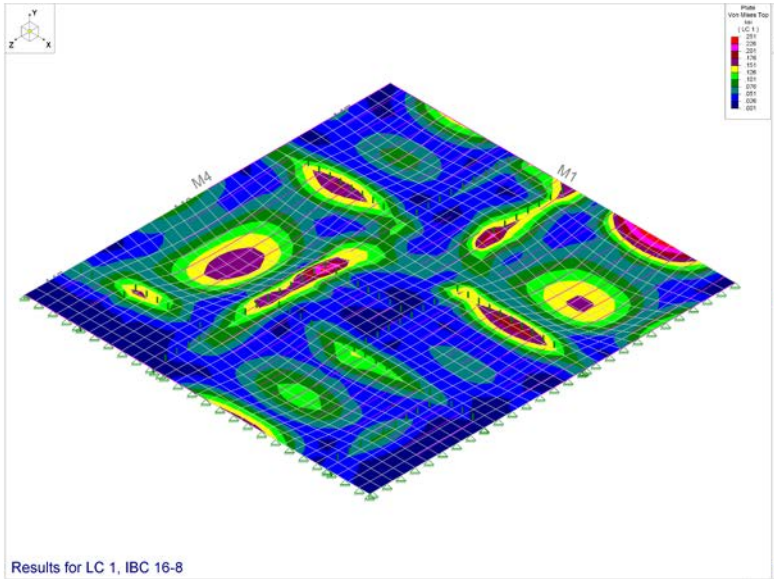

SR4: Char Depth = 1.00 in.

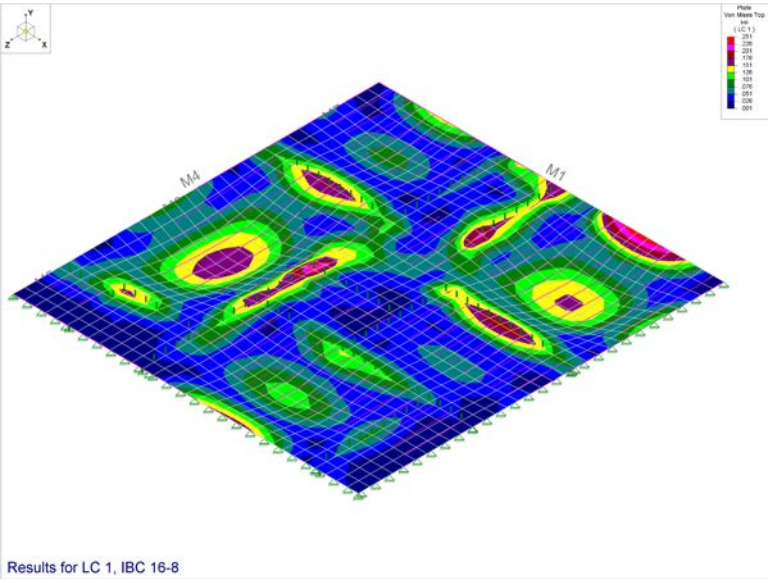

SR5: Char Depth = 1.25 in.

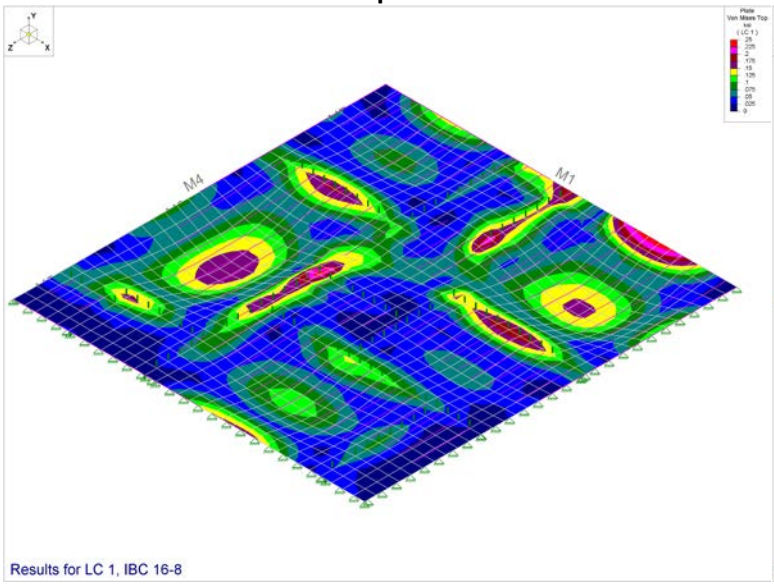

SR6: Char Depth = 1.5 in.

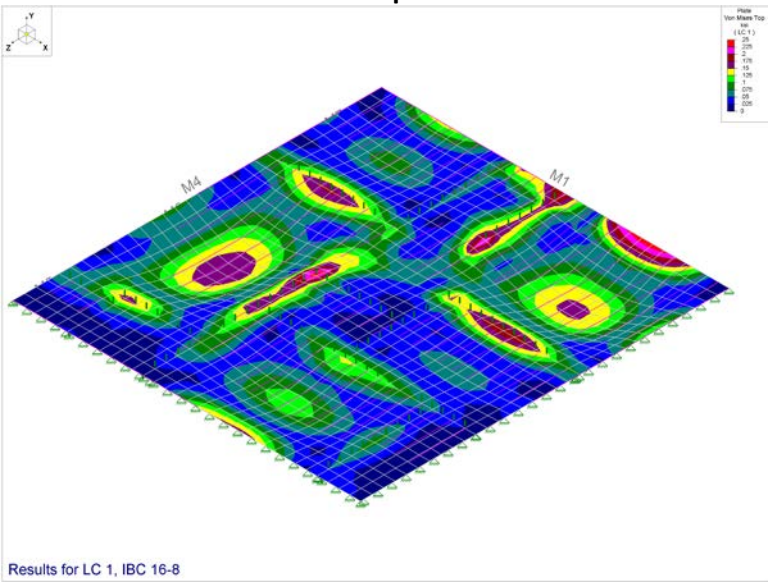

SR7: Char Depth = 1.75 in.

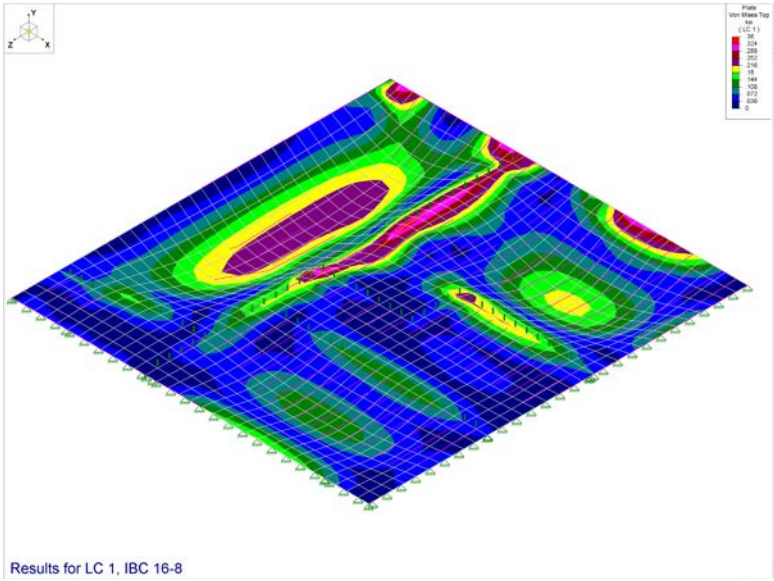

SR4: Char Depth = 2.00 in.

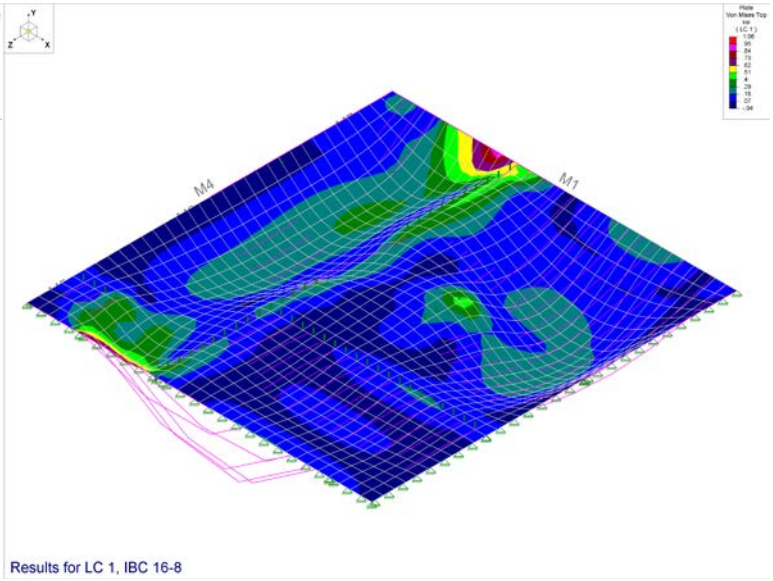

SR9: Char Depth = 2.25 in.

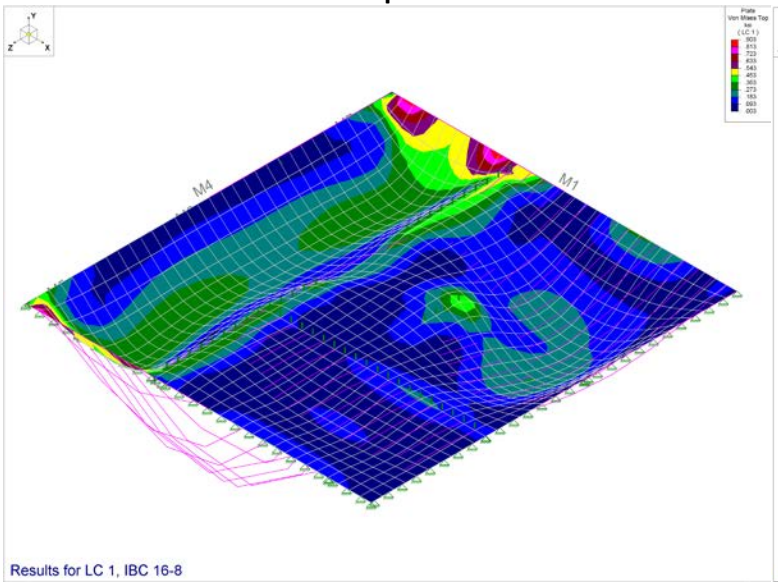

SR10: Char Depth = 2.5 in.

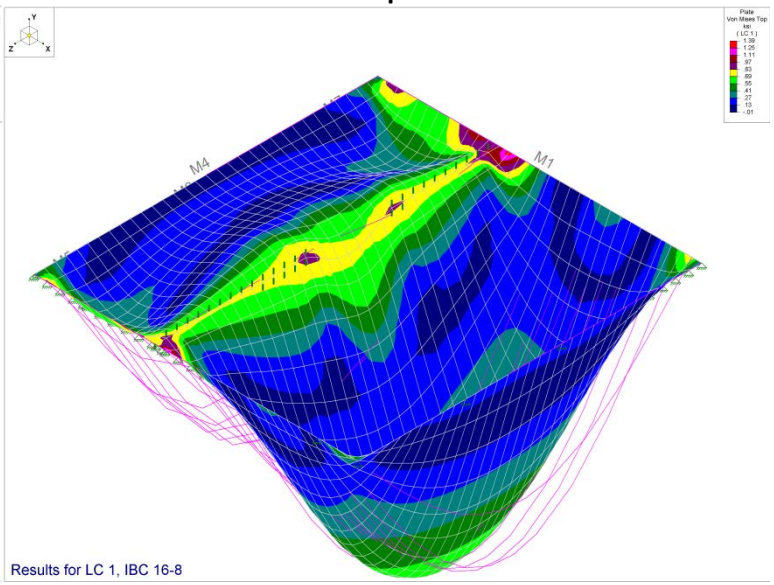

SR11: Char Depth = 2.75 in.

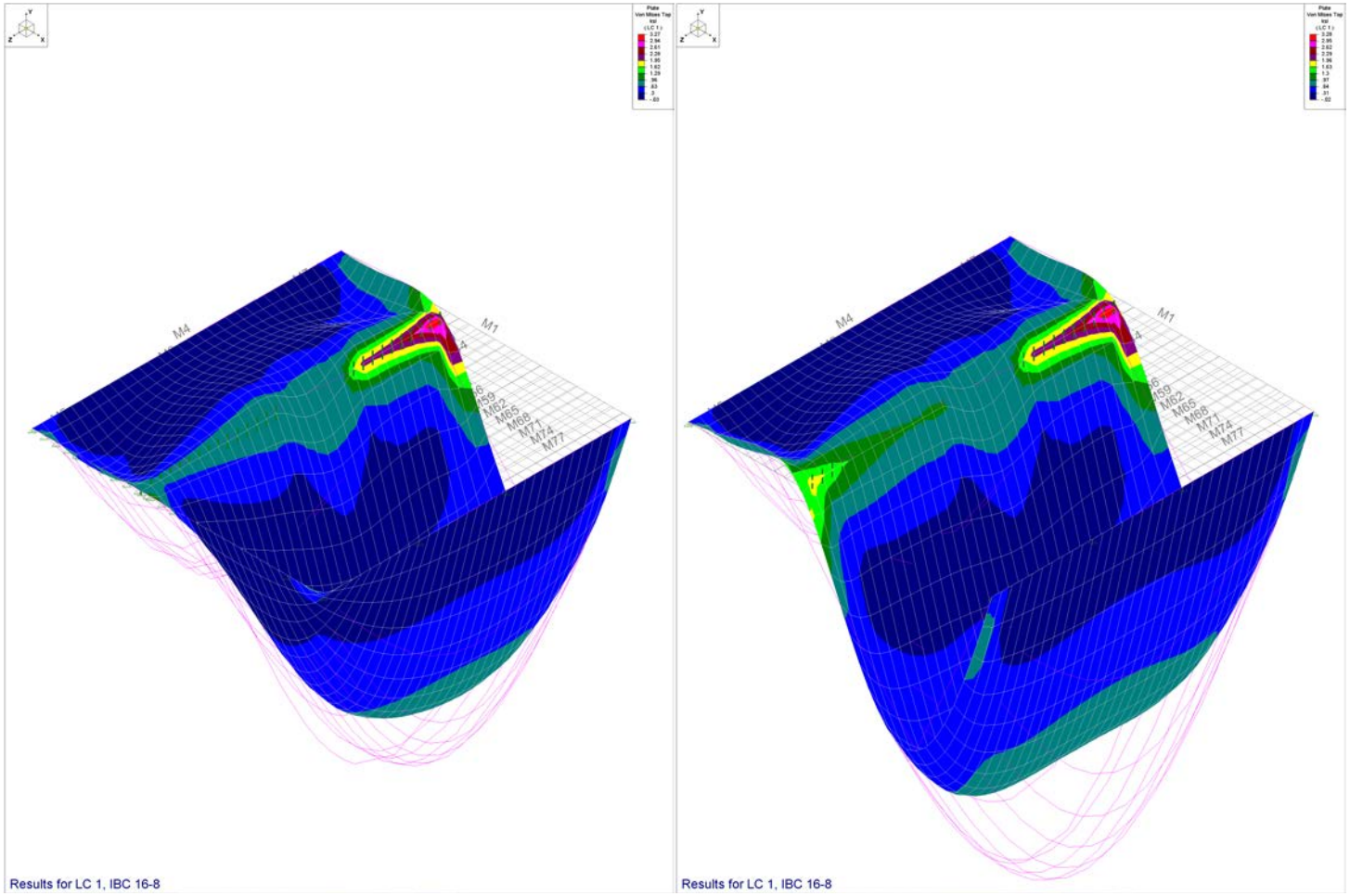

SR12: Char Depth = 3.0 in. **SR13: Char Depth = 3.25 in.**

Figure 170. Development of von Mises Stresses on the single apartment floor due to reduced section and load redistribution

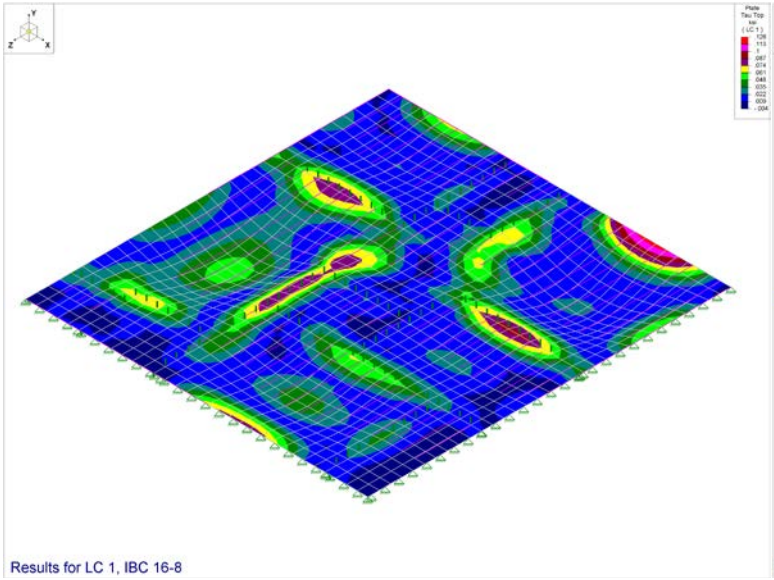

No Section Reduction

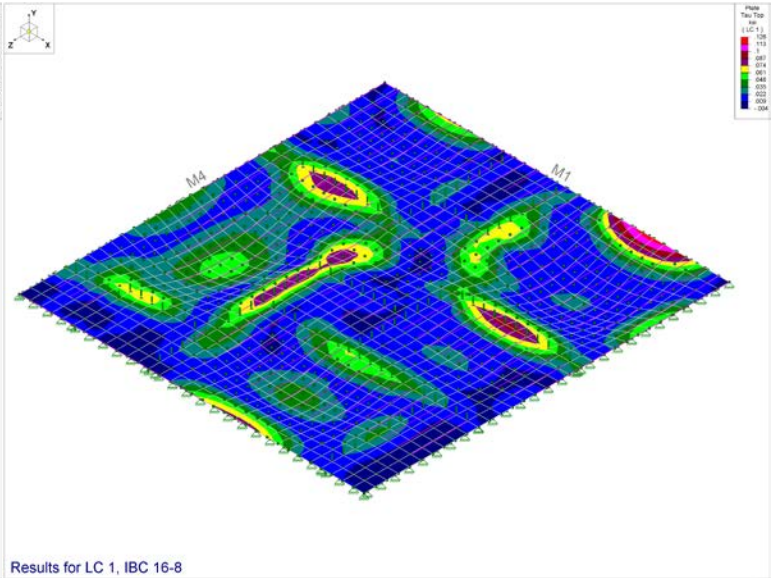

SR1: Char Depth = 0.25 in.

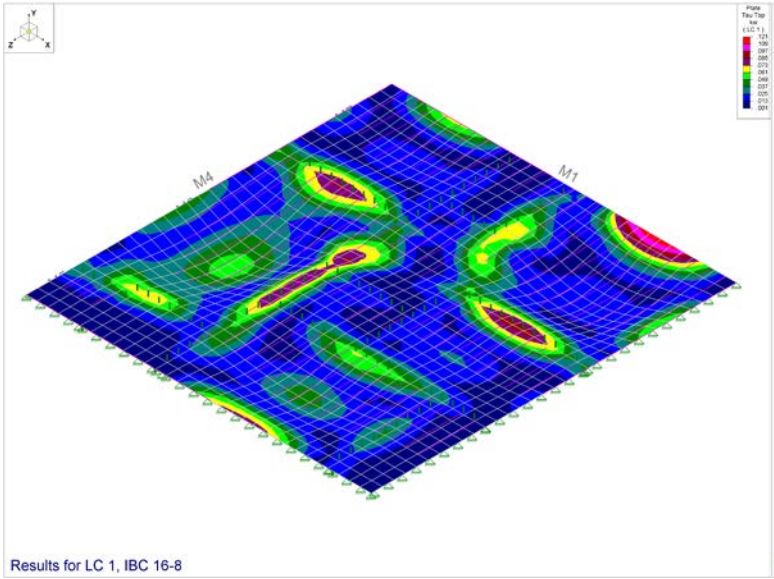

SR2: Char Depth = 0.5 in.

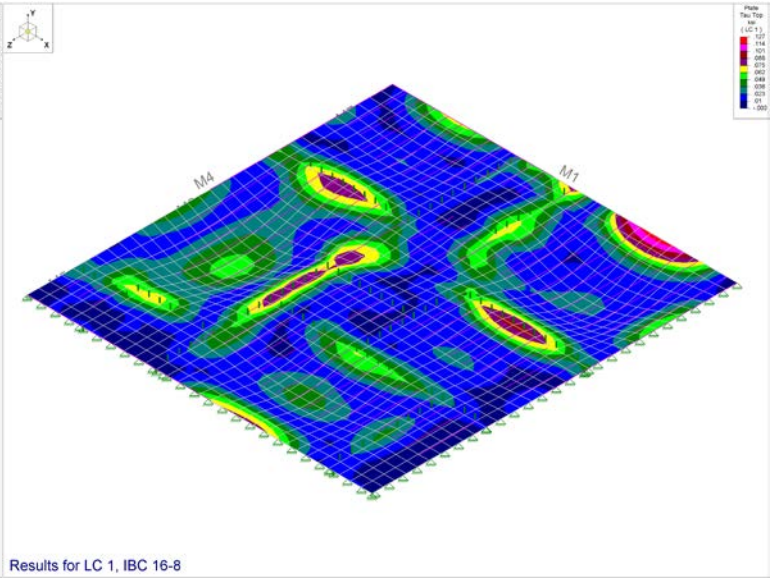

SR3: Char Depth = 0.75 in.

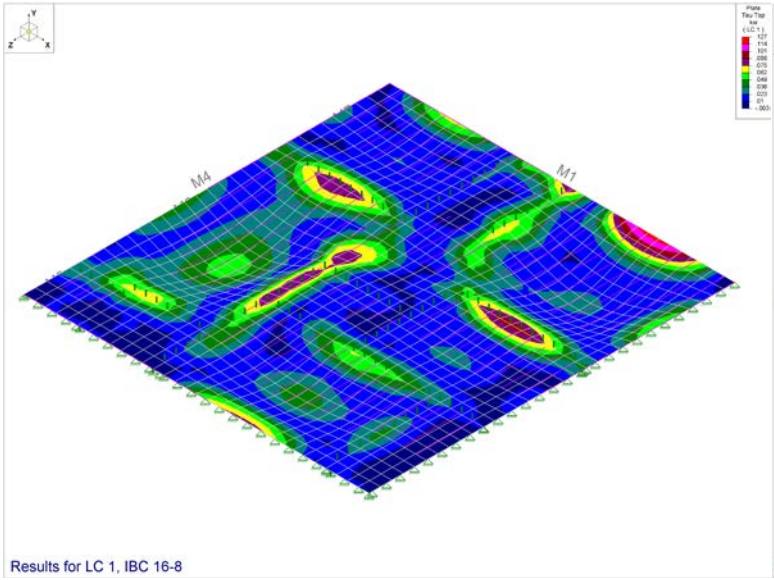

SR4: Char Depth = 1.0 in.

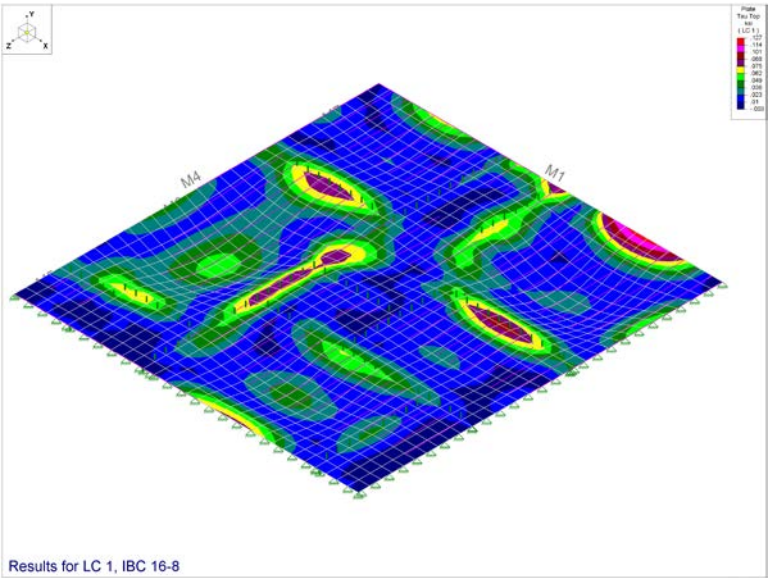

SR5: Char Depth = 1.25 in.

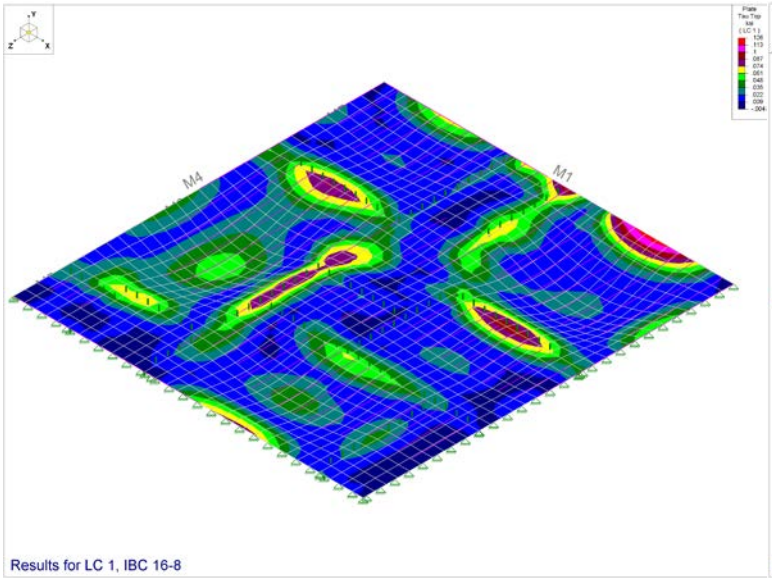

SR6: Char Depth = 1.5 in.

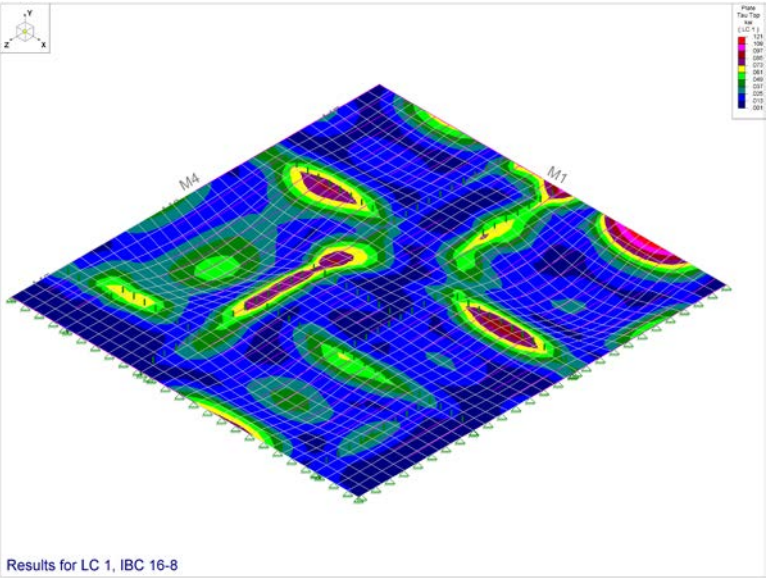

SR7: Char Depth = 1.75 in.

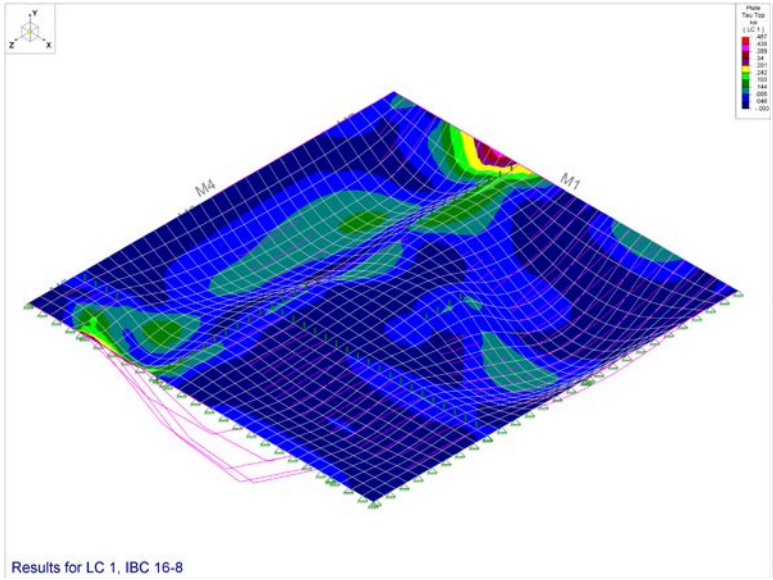

SR8: Char Depth = 2.5 in.

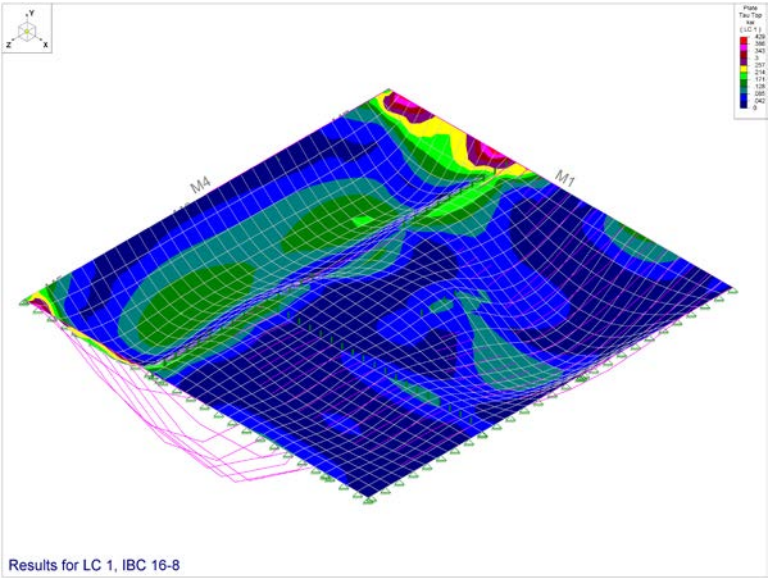

SR9: Char Depth = 2.75 in.

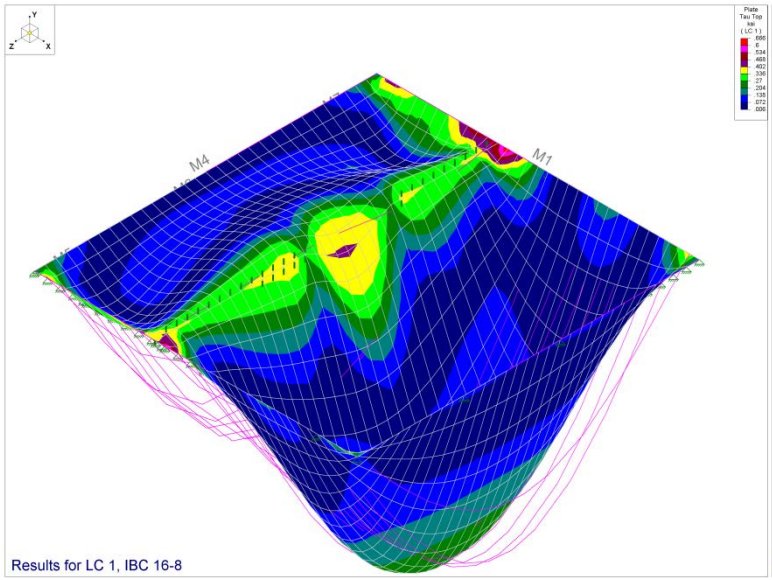

SR10: Char Depth = 2.5 in.

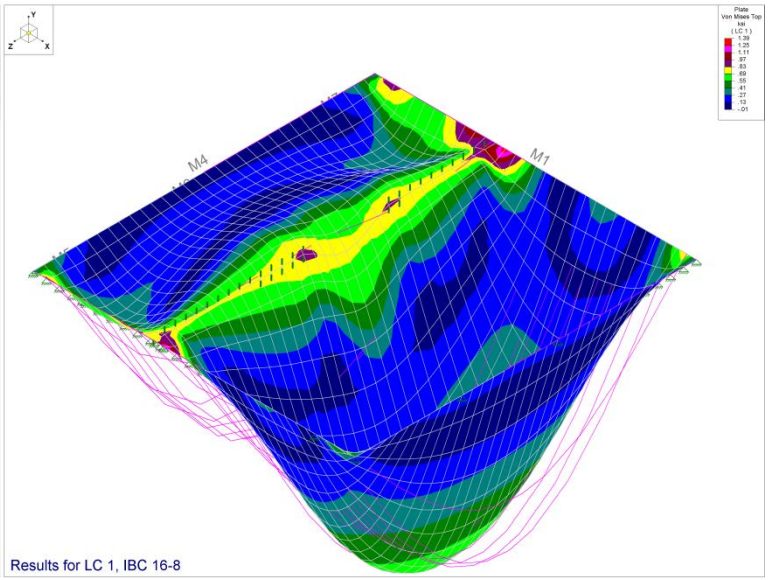

SR11: Char Depth = 2.75 in.

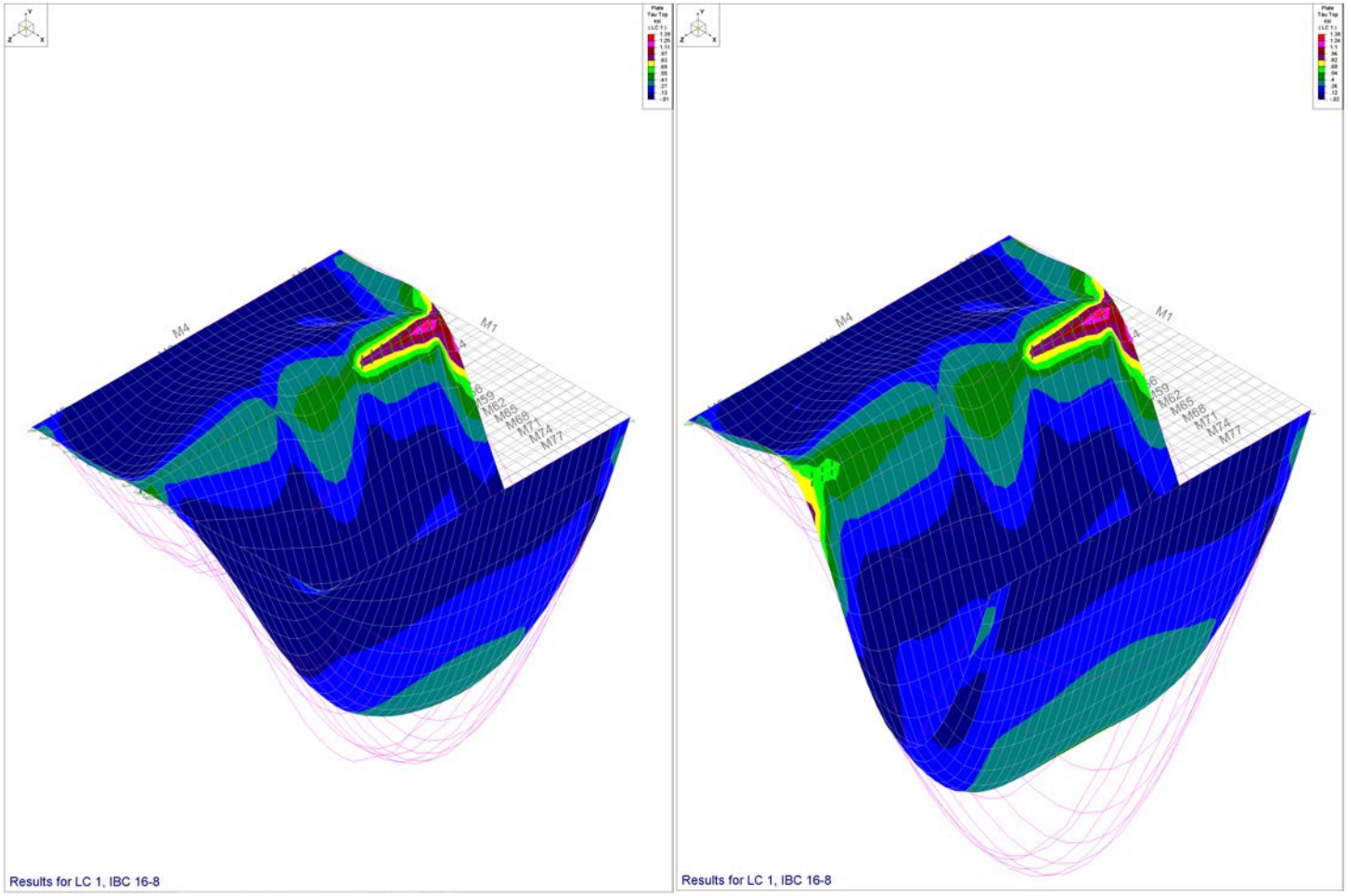

SR12: Char Depth = 3.0 in. **13: Char Depth = 3.25 in.**

Figure 171. Development of Maximum Shear Stresses on the single apartment floor due to reduced section and load redistribution

4.4.2. Isolated Floor Joist FE Analysis

In the real fire events, it is observed that the floor joists undergo differential charring in contrast to the uniform charring assumed in the analysis of the single apartment floor with load redistribution. Post-fire investigations have shown that the differential charring of floor joists is due to the loss of ceiling gypsum board, at which the fire is most severe within the compartment. From one of the tests conducted on a traditional 2 x 4 framed structure constructed using 2 x 12 floor joists made of dimensional lumber, severe charring was observed at the mid-span of the floor joist as shown in Figure 172

To account for this, a simple case of notched floor joist was modeled as a plate element in RISA 3D, the joist dimensions are the same as the identified critical member M50 chosen from the single apartment floor analysis. To keep the analysis simple, a differential charring was assumed in the middle-third of the floor joist. It should be noted that in a real fire event, the location of maximum charring may be concentrated at the supports. The location of the char governs where the maximum floor deflection occurs.

The joist modeled as a plate element is further sub-meshed into quad-elements in order to improve the accuracy of the finite element analysis. The joist is assumed to be made of a Douglas-fir dimensional lumber and assigned properties accordingly. A simply supported boundary condition is imposed on the floor joist as analogous to the full model of the single apartment floor. The joist is loaded with live and dead loads and is assigned a load combination that complied IBC 2015 ASD. A point load of 0.25 kips is also assigned at the mid-depth of the section, which represents the weight of a firefighter. The joist is then solved for different cross-sectional reductions at an increment of char depth of 0.25 in.

Figure 172.Charring at the mid-span of the floor joist

Figure 173 (a-e) shows the deflected shape and stress development in a single joist at different mid-span char depths. It is observed that the mid-span deflection of the member increases with the increase in the char depth with a constant load applied in all the cases. The

region in red in the stress contours show the region with maximum stresses and the region in blue shows lower stresses. As shown in Figure 173 (b), when a notch is introduced in the middle-third section of the joist, the maximum stress region in the mid-span expands. The stress concentration occurs at the mid-span of the notch and at the left support, where pinned end conditions are assigned. As the char depth increases, the stress concentration at the notched section also increases. When the char depth reaches 75% of the original depth of the member, the member fails, which is shown by an excessive deflection in Figure 173 (c). A reversal of stresses may also be observed in Figure 173 (c).

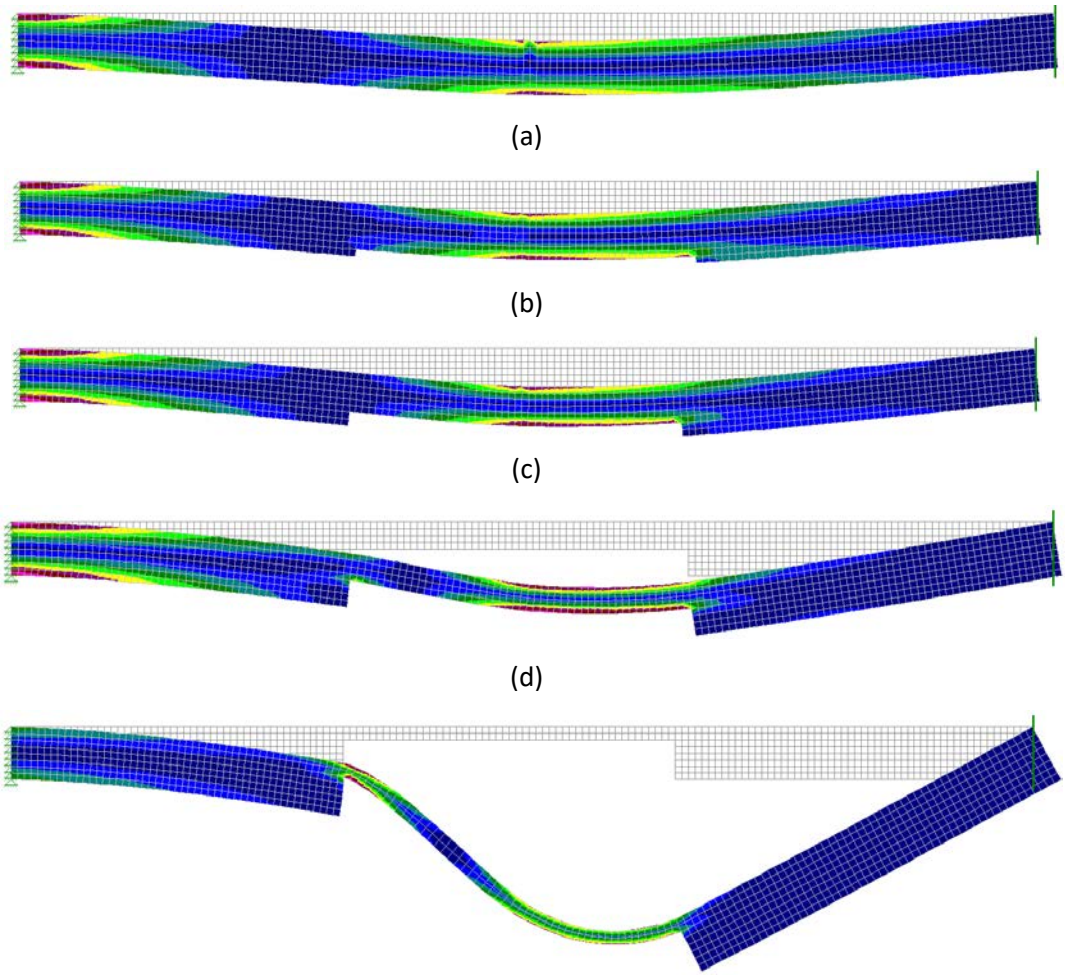

(a)

(b)

(c)

(d)

(e)

Figure 173. FE analysis of single joist for charring simulation: Stress distribution and Shear Deflection (a) Uncharred Section (b) Notched Beam (Char Depth: 1.41 in.) (c) Notched Beam (Char Depth: 2.81 in.) (d) Notched Beam (Char Depth: 5.625 in.) (e) Notched Beam (Char Depth: 8.44 in.)

For additional results from RISA, please refer APPENDIX 7.

4.5. Behavior of small footprint building for assessment of structural integrity due to loss of apartment units with fire progression

4.5.1. Behavior of apartments

In a real fire event, there is a high likelihood of fire spreading into the neighboring apartment units as it grows, which is termed as a traveling fire. A well-contained apartment fire travels from the apartment of fire inception to the other apartments either horizontally or vertically. The horizontal travel path of fire is likely when the exterior walls of the apartment of initiation are consumed in fire whereas the vertical travel path of the fire is likely when the diaphragm in the apartment of fire inception fails. In this study, we are assuming a well contained fire and any fire spread from the external openings of the compartment is neglected. However, in a real building fire, fire spread through exterior openings is a common occurrence. Also, the fire spread is dependent on the type of framing used in the building construction. For example, a balloon-framed construction is vulnerable for vertical fire spread, as there are continuous wall cavities between different floors. The building considered for this study is assumed to have platform-framed apartments and hence does not permit a vertical fire spread through the wall cavities.

Figure 174 shows a hypothetical case of traveling fire considered for this conceptual study. The fire is assumed to start in apartment unit No. 2 and spread to its neighboring apartments, 1 and 3 horizontally and vertically to the apartments 6 and 10.

Figure 174. Plan for progressive analysis of the small footprint building

The overall failure of the building depends on the type of construction and the building's lateral stability. From the analysis of a single apartment building stack conducted in RISA floor and the floor analysis conducted in RISA 3D

For the current study, the fire spread between the apartments is assumed to occur horizontally when the common wall between the two apartment is consumed in the fire and vertically when the floor panel / diaphragm fails when the ceiling joists are consumed in the fire.

The progression of failure of a single apartment is assumed to follow the following steps, which is consistent with the failure patterns observed in the overall single apartment analysis in RISA Floor and single component analysis of the single apartment floor system in RISA 3D.

Step 1: Failure of the common wall between Apartment 1 and Apartment 2, that supports the floor joists on one end.

Step 2: Failure of the common wall between Apartment 2 and Apartment 3, that supports the floor joists on the other end.

Step 3: Failure of the Floor System of apartment 2, with no walls to support the joists on both ends.

From the analysis carried out on the single apartment stack building and the floor of the single apartment building, it is evident that the failure of the walls occur much before the floor system fails. The reduced section of the walls degrade their capacity to carry the structural loads, which results in the load getting redistributed among the remaining walls, which helps the floor to remain supported up to the failure of the exterior wall.

Table 60 shows the comparison of failure progression for the case considered in Figure 174, in type VA and Type VB buildings. The conceptual progression is based on the reduced sections analysis of single apartment wall and floor systems conducted using RISA software suite.

Table 60. Failure Progression for Type VA Building based on the structural analysis for the single apartment:

Sequence	Events	Time at Failure (hrs.)	
		Type VA Building	Type VB Building
1	Fire initiates in Apartment 2.	00:00:00	00:00:00
2	Charring initiates in Apartment 2	00:35:29	00:26:38
3	The wall panel between Apartment 1 and Apartment 2 loses its axial capacity:	01:35:29	01:26:38
4	The wall panel between Apartment 2 and Apartment 3 loses its axial capacity	01:40:29	01:31:38
5	The diaphragm between Apartment 2 and Apartment 6 fails	1:40:29	01:31:38
6	Charring initiates in Apartment 1	02:10:58	01:58:16
7	The east wall of Apartment 1 loses its axial capacity	03:05:58	02:53:16
8	Charring initiates in Apartment 3	02:15:58	02:03:16

9	The east wall panel between Apartment 1 loses its axial capacity	03:05:58	02:53:16
10	The diaphragm between Apartment 6 and Apartment 10 fails:	02:25:58	02:13:16
11	The wall panel between Apartment 3 and Apartment 4 loses its axial capacity	03:10:55	02:57:16

Assumptions:

- The fire is well-contained within the apartment. Any external fire spread is neglected
- The whole apartment experiences a post-flashover fire.
- Inception and growth phase of fire in the travelling apartment is neglected.
- No firefighting / suppression is considered.

4.5.2. Overall behavior of the building

Buildings involved in the event of a fire are likely to undergo a progressive collapse when a primary structural component fails, resulting in the failure of adjoining structural components, which in turn causes further structural failure. Such events are common with tall steel buildings or steel-concrete composite buildings.

As mentioned earlier, the overall performance of the building depends on the type of construction and the building's lateral stability.

The important assumptions related to the building type made in this study are:

1) The building is constructed as a platform construction.
2) All the walls defining the periphery of the apartment are built as shear walls. Although no lateral load is considered to act on the structure.
3) The building is a 3-story structure.

Since the building is a platform type, it resembles modular construction. The apartment units are closely connected to each other and at the same time, it is separated from each other unlike a balloon-framed structure. The Floor system of each apartment is independent and the joists span over both, interior and exterior walls of the apartment. Although the wall supporting the floor joist fails, one of the interior walls of the apartment supports the joist and the floor deck holds the system together and protects it against a complete collapse.

With the structure type and layout considered for this study, a progressive collapse of the building is unlikely.

4.6. Conclusions

The following conclusions are deduced from the reduced section structural analysis on a single apartment building as well as semi-qualitative analysis on the larger multi-apartment building.

1) The overall behavior of the building affected in fire is affected by the following factors: The maximum temperatures generated by the fire, time to achieve charring temperatures on the exposed face of the wood, thickness of the fire separation barrier (gypsum wallboards), charring rates and the loads acting on the structure.

2) The axial capacities of walls of a Type VB building (without operational sprinklers) degrade approximately 15 minutes earlier than a type VA non-sprinklered building. This is attributed to the fact that the thickness of gypsum wallboard in a type VB building is less than the thickness of gypsum wallboard in a type VA building.

3) The Bending capacities of a type VB building (without operational sprinklers) degrade approximately 9 minutes earlier than a type VA non-sprinklered building This is again attributed to the thickness of the gypsum wallboard as mentioned in the previous conclusion.

4) The structural load on the floor is evenly distributed on the internal and external walls of the compartment. Reduction in the cross-section of the wall framing members due to charring deceases the axial capacity on the walls sequentially. The progression is well-captured by the RISA floor analysis set up on a single apartment unit. The loss of axial capacity of some walls redistributes the load among the remaining walls and the failure is said to occur when more than 75% of the walls lose their axial capacity.

5) An independent analysis of the dimensional lumber floor system for a single apartment building modeled in RISA-3D shows that the load-redistribution on some of the members triggered by the failed walls governs the overall failure of the apartment. Excessive deflections are observed in long-span joists due to charred sections of wood reducing the overall depth of cross-section combined with the loss of support conditions from the failing wall panels.

6) The stress concentration on the floor system occurs at different sections, which loses the vertical support from the walls, as they fail due to excessive charring. Redistribution of stresses observed on the subfloor deck is congruent with the load-redistribution.

7) From the results, it is found that the failure of wall panels trigger the overall collapse of the apartment unit rather than the failure of the floor system.

8) Progressive collapse of buildings are not imminent in modular structures due to fewer chances in spread of fire between the apartments. Hence, a platform type framing is preferred over a balloon framing for construction.

9) A detailed FE analysis on the apartment considering differential charring of structural members can improve the results of the analysis and hence predict the failure more accurately.

4.7. **Comments on Code Changes**

Current codes prescribe a 0-hour fire rating (or no fire rating) requirement on a sprinklered, type VB building. However, the FDS simulations in this effort and latest work by the authors on a different project [9] show that the gypsum wallboards underperform in a fire event. In a sprinklered building, this is anticipated in the worst case scenario, where the sprinkler systems are either turned off or malfunction. There is a strong need to reassess this trade-off as in light-wood framing, gypsum boards act as the prime source of fire protection. Similarly, in a non-sprinklered type VA building, the wood surfaces attained charring temperatures much before the code rated value of the gypsum wallboard. In order to address this issue, authors recommend using a performance based approach in design of structure and the fire protection systems for these buildings to clearly show the holistic performance of the building.

Based on the brief study of the multiple apartment buildings, it is found that the type of construction has a major influence on the spread of fire throughout the building, which ultimately governs the overall building performance. Platform framed construction has a key advantage to stop the spread of fire over the balloon framed construction. It is therefore recommended that either the balloon framing be avoided to minimize the risk of fire spread or special fire protection measures be adopted to prevent the fire spread. More work is needed to address the performance of long-span wood framed flooring systems (such as engineered I-joists, wood trusses etc.) in fire. Although this is not addressed in this study, looking at these systems will help to propose new span restrictions on such systems when they are considered as an integral part of 'fail-safe' building systems.

(5) Conclusions and discussions

This report addresses the appropriateness of three major sprinkler trade-offs, namely, Egress, UOA, and FRR. PATHFINDER, FDS and RISA software products are employed in our modeling simulations. The main conclusions are:

5.1. Egress

1) In buildings with sprinkler trade-offs (Configuration II and III-A), the RSET is not sensitive to the availability of the Southeast exit but very sensitive to that of the Northwest exit

2) For our benchmark options (SY=0.052, HRR=0.5MW, Fast fire, all occupants normal, both corridor doors open, zero delay time), the sprinkler trade-offs do not increase the life risk of occupants.

3) The ASETs of buildings with sprinkler trade-offs (Configuration II and III-A) are more sensitive to the change of soot yield than that of buildings without sprinkler trade-offs (Configuration I)

4) As far as the life risk of occupants is concerned, buildings without sprinkler trade-offs outperform that with sprinkler trade-offs when Soot Yield increases.

5) The Southeast and Northeast exits are more sensitive to the increase of HRR than the Northwest and Southwest exits (as results of a doubled HRR achieved in a sprinkler controlled fire, the Southeast exit loses 29.6% of its ASET and the Northeast exit loses 11.6% of its ASET, whereas the Southwest and Northwest exits suffer little).

6) The increase of HRR from 0.5MW to 1MW makes the safety factor of a Configuration II building to decrease by (2.12-1.96)/2.12-1 =7.5%

7) The ASETS of buildings with sprinkler trade-offs are less sensitive to the change of fire growth rate than that of buildings without sprinkler trade-offs.

8) In a fast fire or Ultra-fast fire without any closed corridor doors and any delay times, life risk of occupants in Configuration I buildings is lower than that in Configuration III-A buildings (sprinklers don't function) but higher than that in Configuration II buildings (sprinklers do function). In a slow fire without any closed corridor doors and any delay times, buildings without sprinkler trade-offs performs at least as well as buildings with sprinkler trade-offs do. If the delay time is 90s or more, buildings of both Configuration II and III-A perform better than that of Configuration I, but even so life risk of occupants is of greater concern as compared to when corridor doors are closed.

9) From slow fire to fast fire and Ultra-fast fire, buildings with sprinkler trade-offs gain more benefits than that without sprinkler trade-offs if no corridor doors are closed.

10) Whether corridor doors are mechanically held open or not has very tiny influence on the RSET (<3%) in occupant loads of 200ft2/person.

11) For any delay time, closed corridor doors have very significant effects on the improvement of ASET no matter what type the building is. If one corridor door is closed, buildings

without sprinkler trade-offs are as safe as that with sprinkler trade-offs when sprinklers do function as design but safer when sprinklers do not function as design. . If both corridor doors are closed, buildings without sprinkler trade-offs generally performs much better than that with sprinkler trade-offs, but in each case successful evacuations can be ensured because the safety factors are large enough.

12) The occupants' state has considerable influence on the RSET. When half of the occupants become non-normal, the RSET will on average increase 25%. Consequently all the egress safety factors will on average drop by 20%, indicating high life risks in fast or Ultra-fast fires without closed corridor doors. For a slow fire or non-slow fires but with corridor doors closed, the safety factors are large enough to survive a 20% discount

Two of the most important findings are

1) If no corridor door is closed, although buildings with sprinkler trade-offs generally perform better than buildings without sprinkler trade-offs, the life risk of occupants increases quickly with the delay time.

2) If one corridor door is closed, buildings without sprinkler trade-offs generally performs as same as buildings with sprinkler trade-offs when sprinklers do function as design, but better when sprinklers do not function as design. If both corridor doors are closed, buildings without sprinkler trade-offs generally performs much better than that with sprinkler trade-offs, but in each case successful evacuations can be ensured because the safety factors are large enough.

5.2. UOA

1) Although the enlargement of UOA can increase the effective area of the radiation source, the compartment temperature as a radiation source may drop due to increasingly cooling effects from more entrained air. The combined effects of increased radiation area and decreased radiation temperature depend on which factor dominates the radiation heat transfer in a specific problem.

2) The IBC Code requirements for FSD/UOA pairs are very risky when FSD is short (<3.8ft (1.14m)) and somehow conservative when FSD is long (>10ft (3m)).

3) The construction type has some effects on the radiation heat transfer. A 25% UOA in Type VB building yields a higher radiation heat flux level than a 25% UOA in Type VA building does:

5.3. FRR

1) The overall behavior of the building affected in fire is affected by the following factors: The maximum temperatures generated by the fire, time to achieve charring temperatures on the exposed face of the wood, thickness of the fire separation barrier (gypsum wallboards), charring rates and the loads acting on the structure.

2) The axial capacities of walls of a Type VB building (without operational sprinklers) degrade approximately 15 minutes earlier than a type VA non-sprinklered building. This is attributed to the fact that the thickness of gypsum wallboard in a type VB building is less than the thickness of gypsum wallboard in a type VA building.

3) The Bending capacities of a type VB building (without operational sprinklers) degrade approximately 9 minutes earlier than a type VA non-sprinklered building This is again attributed to the thickness of the gypsum wallboard as mentioned in the previous conclusion.

4) The structural load on the floor is distributed evenly distributed on the internal and external walls of the compartment. Reduction in the cross-section of the wall framing members due to charring deceases the axial capacity on the walls sequentially. The progression is well-captured by the RISA floor analysis set up on a single apartment unit. The loss of axial capacity of some walls redistributes the load among the remaining walls and the failure is said to occur when more than 75% of the walls lose their axial capacity.

5) An independent analysis of the dimensional lumber floor system for a single apartment building modeled in RISA-3D shows that the load-redistribution on some of the members triggered by the failed walls governs the overall failure of the apartment. Excessive deflections are observed in long-span joists due to charred sections of wood reducing the overall depth of cross-section combined with the loss of support conditions from the failing wall panels.

6) The stress concentration on the floor system occurs at different sections, which loses the vertical support from the walls, as they fail due to excessive charring. Redistribution of stresses observed on the subfloor deck is congruent with the load-redistribution.

7) From the results, it is found that the failure of wall panels trigger the overall collapse of the apartment unit rather than the failure of the floor system.

8) Progressive collapse of buildings are not imminent in modular structures due to fewer chances in spread of fire between the apartments. Hence, a platform type framing is preferred over a balloon framing for construction.

9) A detailed FE analysis on the apartment considering differential charring of structural members can improve the results of the analysis and hence predict the failure more accurately.

5.4. Discussion on possible Code changes

1) High reliability of fire doors should be paid more attention even in buildings with sprinklers.

2) The simulation results show that it is reasonable to increase the minimum FSD from 3ft to 6ft.

3) It is recommended that a performance based approach be used to show the holistic performance of the building in terms of active and passive systems and that balloon framing be avoided to minimize the risk of fire spread or special fire protection measures be adopted to prevent the fire spread.

5.5. Note on performance based structural fire engineering

Performance based approach for designing structures for the effect of fire is preferred over the prescriptive approach since the performance of buildings in a real fire event is much different than a standard fire test used to assess the fire rating of panelized wall systems. The international code council's validation committee approved the changes in the structural engineering design standard, "ASCE/SEI 7-16: Minimum Design Loads and Associated Criteria for Buildings and Other Structures" in January 2017. The change includes Appendix E "Performance-Based Design Procedures for Fire Performance of Structures", that gives a recognition and provides relevant design guidance for Structural Fire Engineering. The guidelines are not mandatory and they do not provide standard fire resistance design using prescriptive approaches.

The new guideline addresses:

(i) Identification of the performance objectives

(ii) Quantification of the fuel load

(iii) Identification and evaluation of structural design fires

(iv) Determination of temperature histories of the structural members and connections

(v) Determine the structural response

The prescriptive approach fails in considering disparities in the type of construction, mismatch of the thermal properties of the materials, boundary conditions, thermally induced failure modes, localized effects and holistic building performance. The code makes available the procedure to couple the thermal and the structural behavior to obtain the realistic fire performance. Inclusion of design fire scenarios enables the evaluation of the structures to modern fire loads, which are more accurate than standard fire scenarios used in prescribing the fire resistance ratings in the prescriptive approach.

Further information on the code inclusion are available in McAllister et.al.

APPENDIX 1

Sensitivity analysis on Cell Sizes

This Appendix 1 is designed to find to what extent different cell sizes would affect the results of simulations. Based on the computational domain as shown below, two methods to refine the mesh are adopted: overall refining (mainly for the main mesh including our fire apartment) and localized refining. We begin our simulations from an initial mesh (named as No.1) with a uniform cell size of 0.36x0.40x0.25 for both main mesh and extensional meshes.

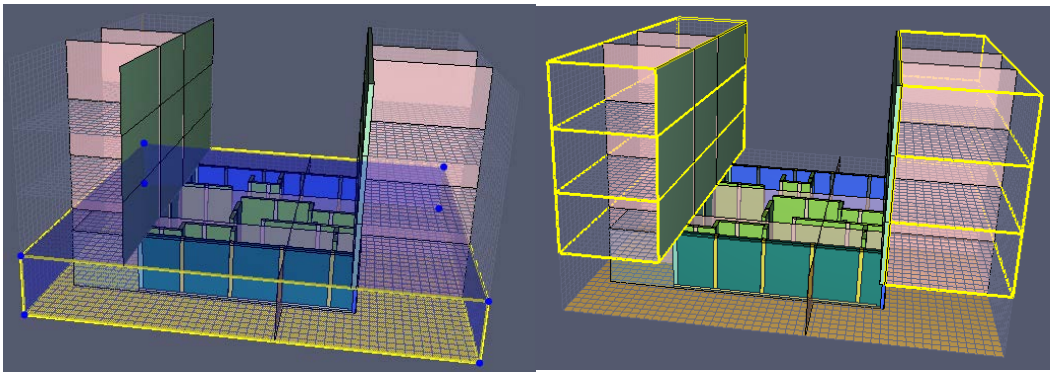

a) Main mesh b) extensional meshes

Figure 175 Computational domain

Following the initial mesh, the overall refining method includes No.R3, No.R4, NO.R5 and No.R6. In No.R3 the mesh is refined only in the Z direction in the main mesh, delivering a cell size of 0.36x0.40x0.125 in the main mesh. In No.R4 the mesh is refined in Z direction for main mesh and in both X and Y directions for all the meshes, delivering a cell size of 0.18x0.20x0.125 in the main mesh and a cell size of 0.18x0.20x0.25 in extensional meshes. In No.R5 the mesh is refined in X direction for all the meshes and Z direction for only the main mesh, delivering a cell size of 0.18x0.40x0.125 in the main mesh and a cell size of 0.18x0.40x0.25 in the extensional meshes. In No.R6 the mesh is refined in X direction for all the meshes and Z direction for only the main mesh, delivering a cell size of 0.24x0.40x0.125 in the main mesh and a cell size of 0.24x0.40x0.25 in the extensional meshes. The localized refining method first divides the main mesh into nine smaller meshes, as shown below:

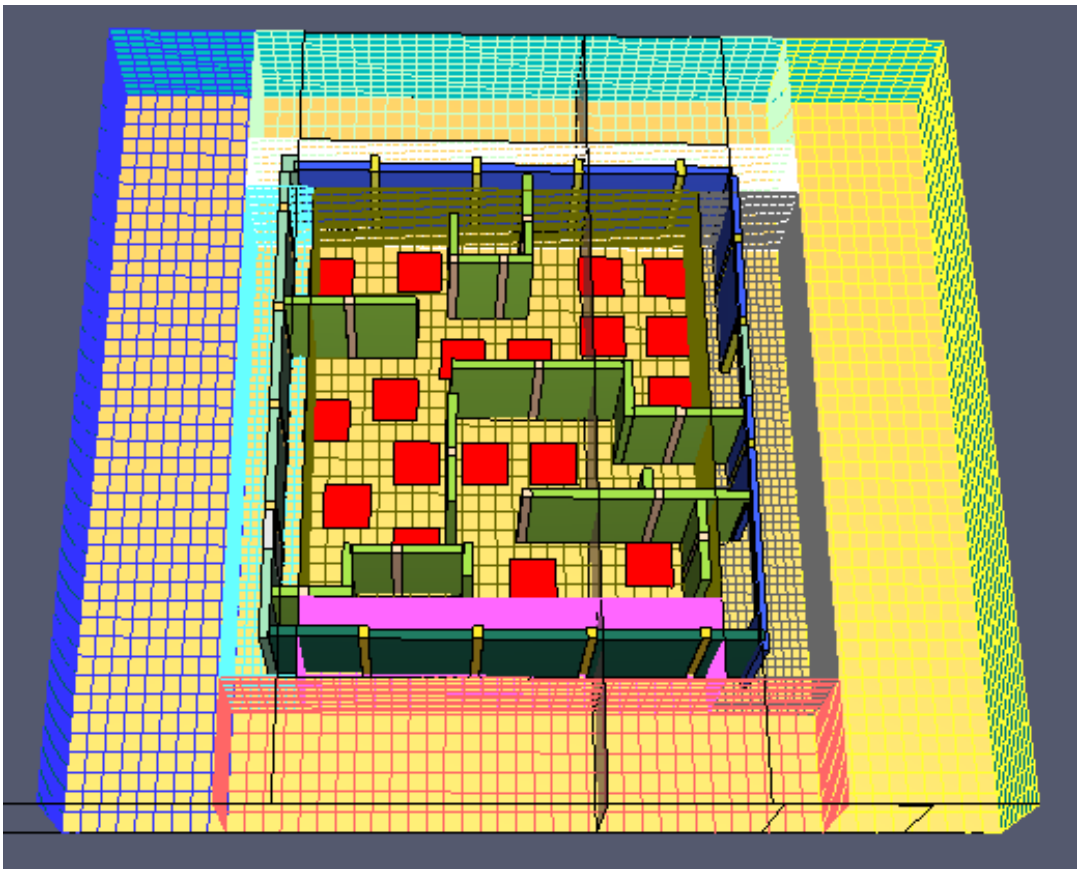

Figure 176 subdivision of the main mesh into nine smaller meshes

There are 3 kinds of meshes in localized refining method: No.2, No.3 and No.4. In No.2, the four meshes having walls and the center mesh are first refined in the Z direction, delivering a cell size of 0.36x0.40x0.125. Then only the meshes engulfing the walls are refined in their normal direction(perpendicular to their surface), delivering a cell size of 0.36x0.20x0.125 close to North and South walls or a cell size of 0.18x0.40x0.125 close to the east and west walls. Based on No.2, in No.3 meshes engulfing walls are further refined in another horizontal directions (X or Y), delivering a cell size of 0.18x0.20x0.125 in all the meshes engulfing walls. Based on No.3, in No.4 the center mesh is further refined in both X and Y direction, delivering a cell size of 0.18x0.20x0.125 for all the four meshes having walls and the center mesh.

Since No.R4 has the finest cell size, the results from it can be deemed as the most accurate data, with which the results from other different cell sizes are compared. Four places possibly having the highest temperature are selected to conduct our comparison, as shown below:

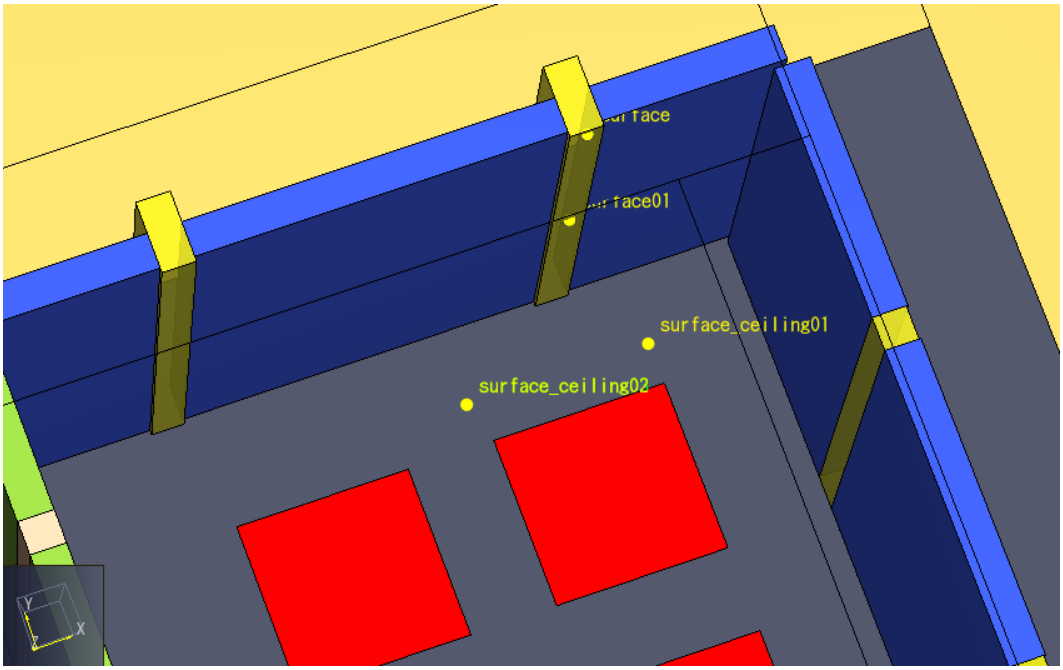

Figure 177 Four locations used for comparison(two are in the stud, the other two are in the ceiling)

The results of comparisons are shown below:

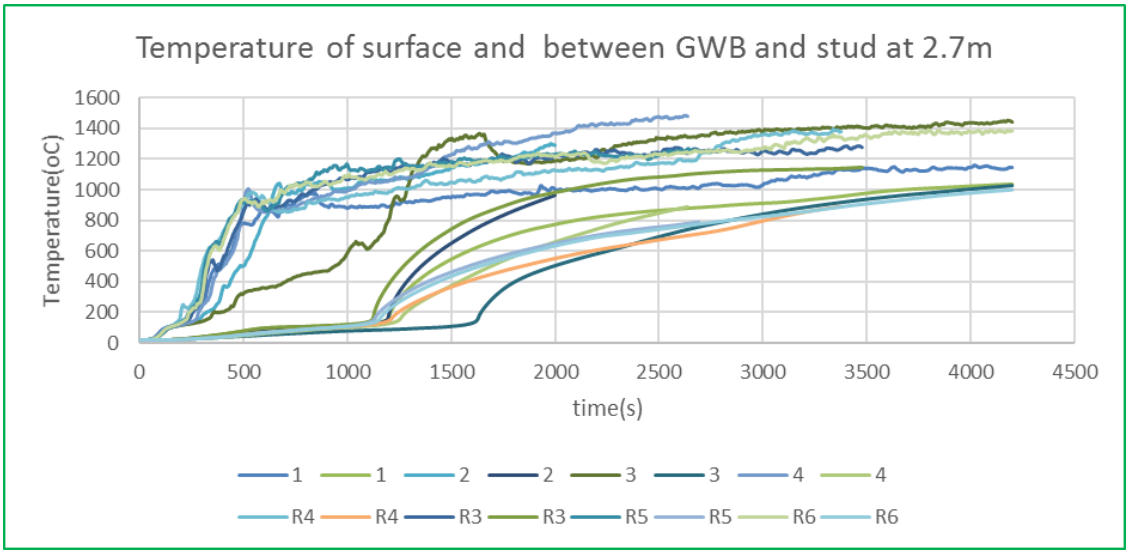

Figure 178 comparison of temperatures developed on/in the wall studs (2.7m) for various mesh models

Results from different refined meshes compared with that from NO.R4 (The location is on the top of the stud, Z=2.71m. there are two classes of curves, one from the surface, the other from the connection of GWB and the wood stud)

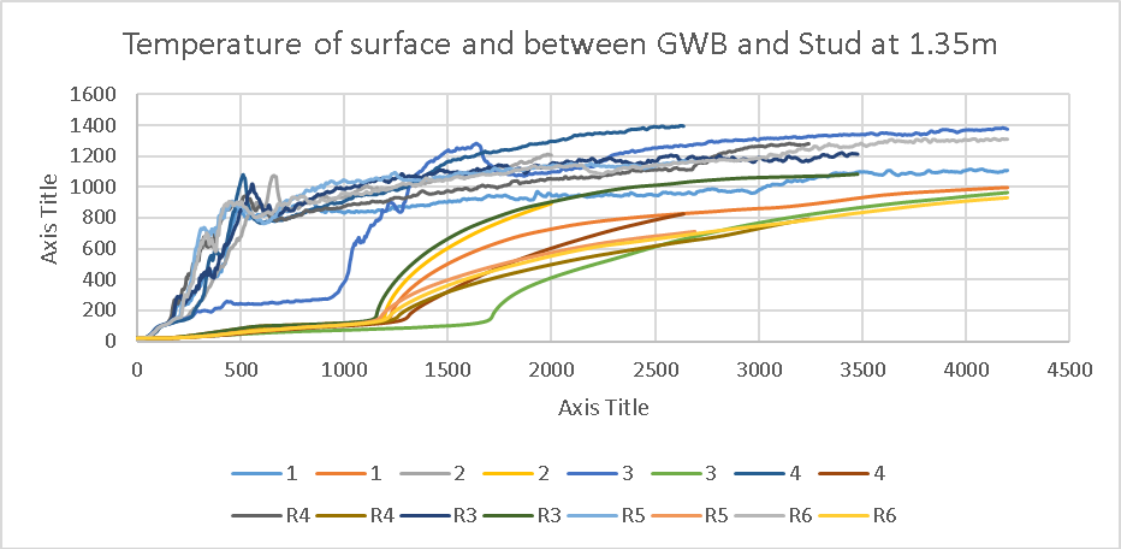

Figure 179 comparison of temperatures developed on/in the wall studs(1.35m) for various mesh models

Results from different refined meshes compared with that from NO.R4 (The location is on the middle of the stud, Z=1.35m. there are two classes of curves, one from the surface, the other from the connection of GWB and the wood stud)

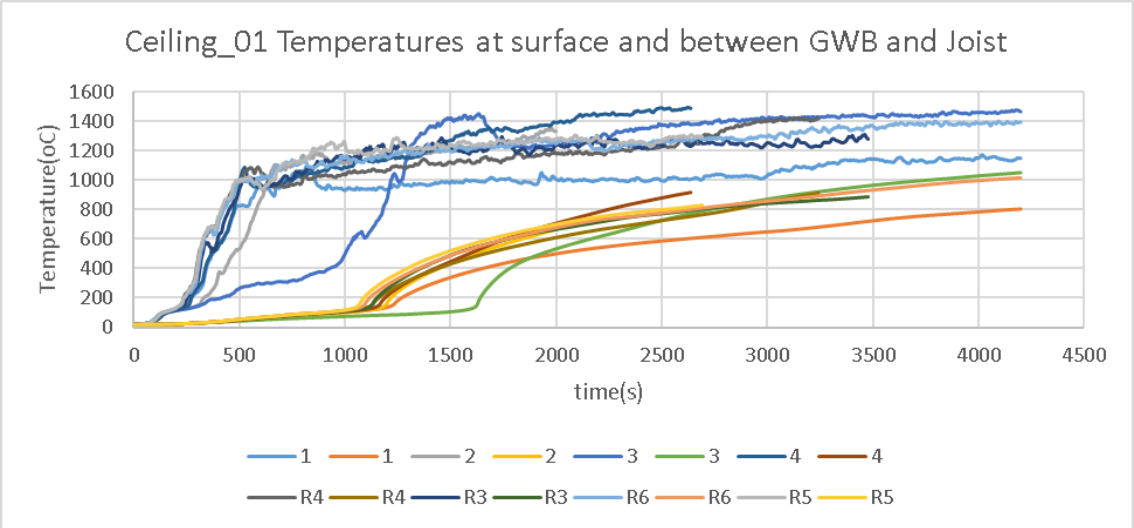

Figure 180 comparison of temperatures developed on/in the ceiling above the first burner for various mesh models

Results from different refined meshes compared with that from NO.R4 (The location is on the ceiling above the first gas burner. There are two classes of curves, one from the surface, the other from the connection of GWB and the wood stud)

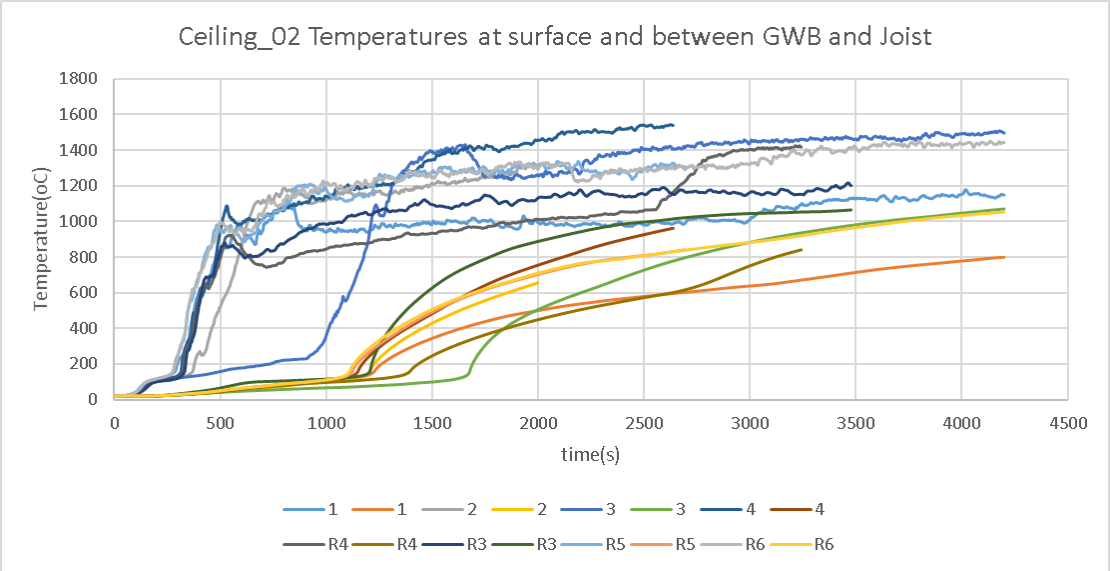

Figure 181 comparison of temperatures developed on/in the ceiling above the second burner for various mesh models

Results from different refined meshes compared with that from NO.R4 (The location is on the ceiling above the second gas burner. There are two classes of curves, one from the surface, the other from the connection of GWB and the wood stud)

The following table shows computational times needed by each case:

Table 61 Times needed for various mesh models

Case No	Number of cells	Running time per 1000s
1	61,490	4 hours
2	82,522	10 hours
3	98,758	15 hours
4	137,720	21 hours
R3	86,086	16 hours
R4	344,344	30 hours
R5	172,172	22 hours
R6	129,129	10 hours

From the figures above, both No.R5 and No.R6 are very close to No.R4, but R6 needs less computational time. Therefore, cell size of No.R6 is selected as base size for the following comprehensive simulations.

APPENDIX 2

Calculation on Sprinkler Activation Time and HRR after activation of one sprinkler

According to NFPA 13 HB 2016, R-2 building is light hazard, therefore for standard sprinklers the maximum spacing distance is 15ft. In our case totally 8 sprinklers are set as shown below:

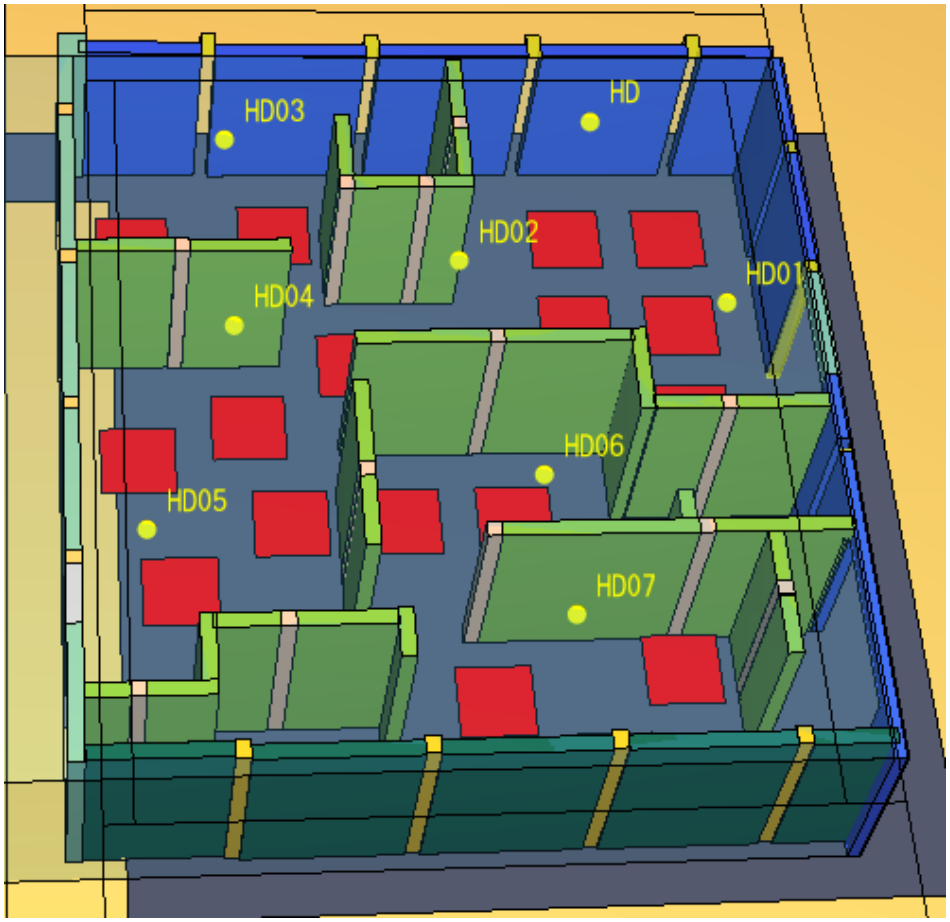

Table 62 Sprinkler layout in the compartment used in this report

Since we ignite a fire from the burner in the Northeast corner of the kitchen, the sprinkler named “HD” will first be activated. We assume the activation of only one sprinkler can control the fire and keep the HRR in a steady state. In the following paragraphs we first calculate the activation time of sprinkler “HD” and then calculate the steady HRR.

The following input data are obtained from the sprinkler layout figure

Radial distance from the center of fire plume to sprinkler “HD”: $r = 1.5m$

Operation temperature of sprinkler $T_{op} = 74^{o}C$

Ceiling Height : $H = 9\,ft = 2.75m$

RTI = $100(m\cdot s)^{1/2}$

Height of fire source: $z_0 = 0.5\,ft = 0.15m$

Gravity acceleration $g = 9.81m/s^2$

Specific Heat capacity of air $C_p = 1.04kJ/(kg\cdot K)$

Density of air $\rho_a = 1.1kg/m^3$

Ambient temperature $t_a = 20 + 273 = 293K$

Convective fraction $\chi = 0.7$

Part 1 Hand calculation

Calculation steps: (SFPH 5th , chapter 40)

(1) The radial distance from the fire axis to a detector:
$r = 1.5m$

(2) Fire growth rate : $a = 1055/t_g{}^2 = 1055/150^2 = 0.0469kW/s^2$

(3) Fist estimation of the operation time is 100s, then

$$\dot{Q} = at^2 = 0.0469\times 100^2 = 469kW$$

$$t_{2f}^* = 0.813\left(1+\frac{r}{H-z_0}\right) = 1.28$$

$$A = \frac{g}{C_p T_a \rho_a} = \frac{9.81}{1.04\times 293\times 1.1} = 0.029$$

$$a_c = \chi a = 0.70\times 0.0469 = 0.0328kW/s^2$$

$$t_2^* = \frac{t}{A^{-1/5}a_c^{-1/5}(H-z_0)^{4/5}} = 11.63$$

$$\frac{u}{u_2^*} = A^{1/5}a_c^{1/5}(H-z_0)^{1/5} = 0.356$$

$$\frac{\Delta T}{\Delta T_2^*} = A^{2/5}\left(\frac{T_a}{g}\right)a_c^{2/5}(H-z_0)^{-3/5} = 1.048$$

$$D = 0.126 + 0.210\left(\frac{r}{H - z_0}\right) = 0.248$$

$$\Delta T_2^* = \left(\frac{t_2^* - t_{2f}^*}{D}\right)^{4/3} = 145.11$$

$$\frac{u_2^*}{\left(\Delta T_2^*\right)^{1/2}} = 0.59\left(\frac{r}{H - z_0}\right)^{-0.63} = 0.832$$

$$\gamma = \frac{3}{4}\sqrt{\frac{u}{u_2^*}}\sqrt{\frac{u_2^*}{\left(\Delta T_2^*\right)^{1/2}}}\frac{\Delta T_2^*}{RTI}\left(\frac{t}{t_2^*}\right)D = 1.261$$

$$\Delta T_d = T_d(t) - T_d(0) = \frac{\Delta T}{\Delta T_2^*}\Delta T_2^*\left(1 - \frac{1 - e^{-\gamma}}{\gamma}\right) = 65.61$$

$$T_d(80) = \Delta T_d + T_d(0) = 85.61^o C$$

(4) Further estimation of the operation time

Since the temperature of the sprinkler after 100s is greater than its operation temperature, namely

$$T_d(100) = 85.61 > 74^o C$$

A less estimation time of 90 s is adopted to calculate the temperature of the sprinkler at this time. Following the same steps as 3), the result is:

$$T_d(90) = 70.22^o C$$

which is less than the activation temperature of 74 °C.

A greater estimation time of 93s is adopted. Following the same steps as 3), the result is

$$T_d(93) = 74.63^o C > 74^o C$$

Which is just a little bit greater than the sprinkler's operation temperature. Therefore the sprinkler will activate at 93s.

Part 2 FDS simulation

By running FDS, the temperature of sprinkler "HD" can be obtained as shown below:

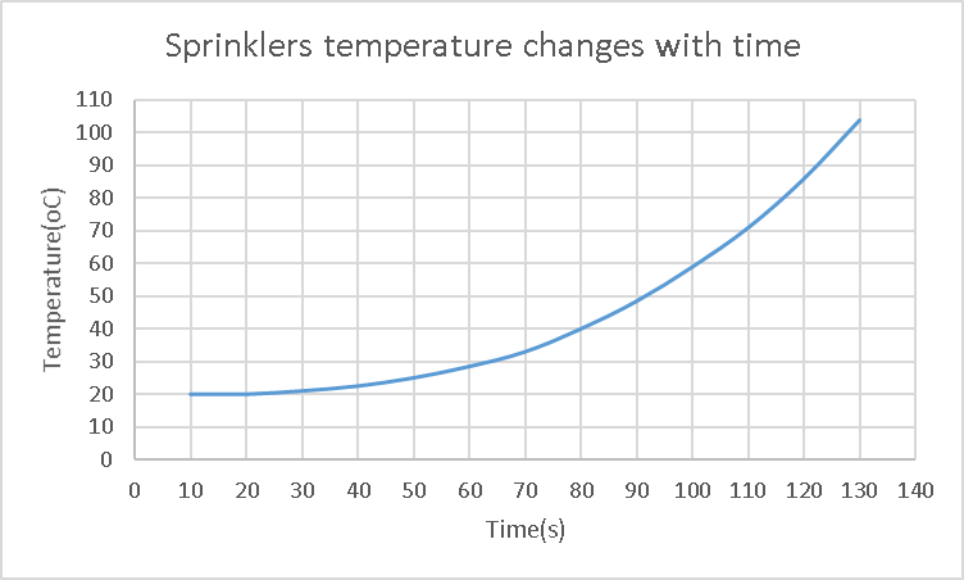

Figure 182 Temperature of the first sprinkler changes with time

At 112s the temperature of sprinkler is 74.5oC, therefore the sprinkler will activate after 112 s.

Based on results from both hand calculation and FDS simulation It seems that the sprinkler's activation time should be within the range of 93s to 112s, which corresponds to a HRR range of 0.384MW((93/150)2) to 0.558MW($(112/150)^2$).

APPENDIX 3

Basic calculations on HRR and fire duration time of a compartment fire

1. About the computational domain

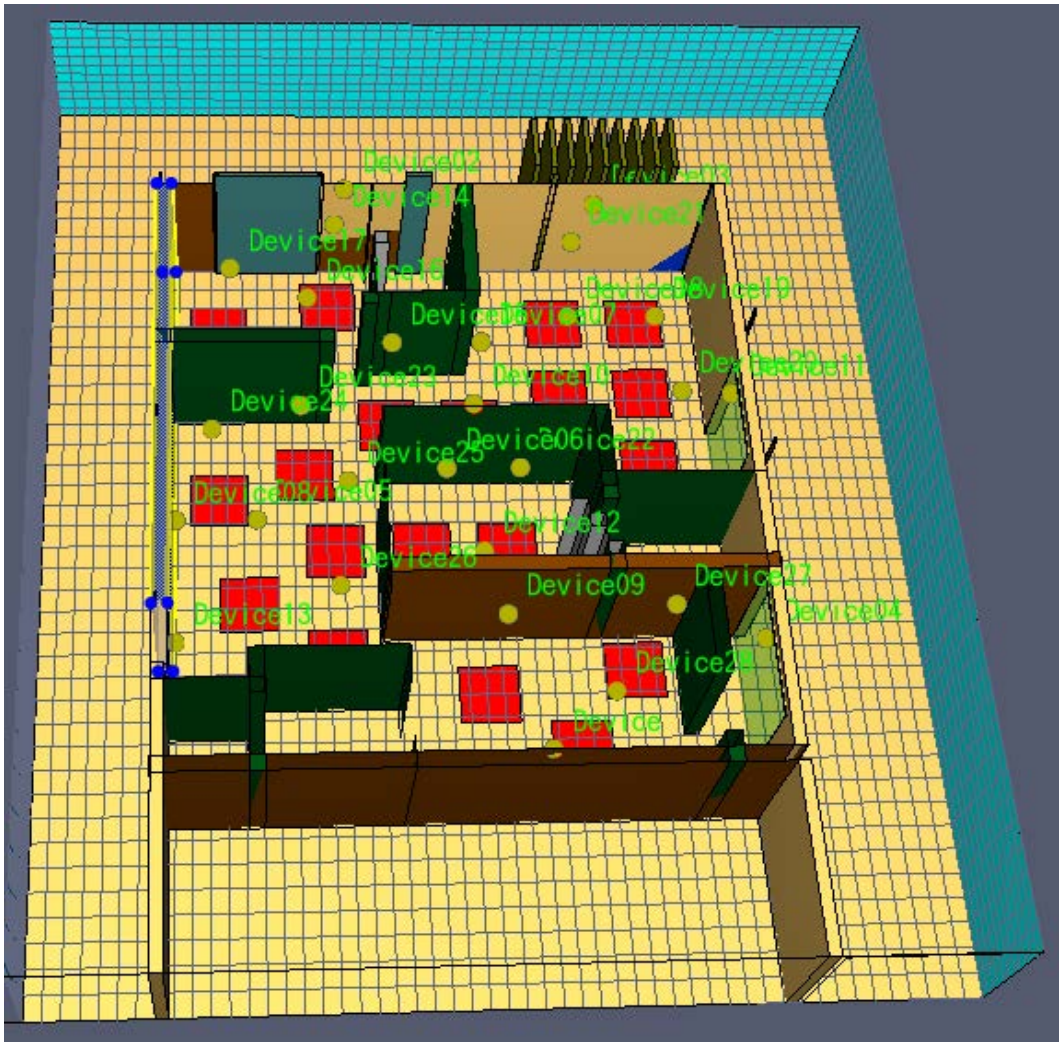

Figure 183 Computational domain of an apartment

The computational domain shown in Figure 183 is around an apartment in a Type V, R-2 building. The area of the apartment (A) is 33ft x 35ft x 0.929=107.3m^2. The corridor door is 1.3m by 2.5m, forming an area (A_d) of 3.25 m^2. The window in the kitchen is 1.8 by 2.5, forming an area (A_w) of 4.5 m^2. The total surface area of the apartment (A_T) is about 308 m^2.

All the gas burners are ramped up to their designated HRRs in a preset time span along a t-squared curve once they are activated. The environment temperature is 20^{o}C.

2. Basic calculations about the HRRs and fire duration time

(1) Minimum HRR needed to achieve flashover in an enclosure

According to Babrauska's method,

$$\dot{Q}_{f/o} = 750 A_o \sqrt{H_o} = 750\left(4.5\times\sqrt{2.5} + 3.25\times\sqrt{2.5}\right) = 9190KW$$

According to Tomas' method,

$$\dot{Q}_{f/o} = 7.8A_T + 378A_o\sqrt{H_o} = 7.8\times 308 + 378\times\left(4.5\times\sqrt{2.5} + 3.25\times\sqrt{2.5}\right) = 7032KW$$

(2) Minimum HRR needed to achieve a ventilation controlled fire in an enclosure

$$\dot{Q}_{v/c} = 1.5A_o\sqrt{H_o} = 1.5\left(4.5\times\sqrt{2.5} + 3.25\times\sqrt{2.5}\right) = 18MW$$

(3) Temperature and duration time of ventilation-controlled fires

The fire temperature in the compartment and fire duration are calculated by "Japanese Method":

$$T_f = 1,280\left(\frac{Q}{\sqrt{A_T\sqrt{k\rho c}}\sqrt{A_o\sqrt{H_o}}}\right)^{2/3} t^{1/6} + T_\infty$$

$$t_D = \frac{1}{60}\frac{F_L A_r}{Q}$$

Where

Q = Heat release rate by combustion (MW)
A_T = Internal surface area of compartment enclosure (m^2)
$\sqrt{k\rho c}$ = Thermal inertia of compartment enclosure ($kW{\cdot}s^{1/2}/m^2{\cdot}K$)
A_o = Area of window opening (m^2)
H_o = Height of window opening (m)
T_∞ = Initial and ambient temperatures (°C)
F_L = Fire load density (MJ/m^2)
A_r = Floor area of the room (m^2)
t_D = Fire duration (min.)

The heat release rate is calculated by the burning type index

$$\chi = \frac{A_o\sqrt{H_o}}{A_{fuel}}.$$

Where

$$A_{fuel} = 0.26F_L^{1/3}A_{room}$$

Then

$$Q = A_{fuel} \times \begin{cases} 1.6\chi & (\chi \le 0.081) \\ 0.13 & (0.081 < \chi \le 0.1) \\ 2.5\chi\exp(-11\chi) + 0.048 & (0.1 < \chi) \end{cases}$$

In our case, a relatively higher fire load is adopted to simulate a worst condition, namely $F_L = 600 + 500 + 130 + 40 = 1270 MJ/m^2$ where 600 is the average contents fire load density, 500 is the standard deviation of contents fire load density, 130 is the average fixed fire load density and 40 is the standard deviation of fixed fire load density [5] .

(1) If only two openings exist (one door and one window) ,

$$F_L = 1270 MJ/m^2, A_r = 107.3 m^2, A_{fuel} = 0.26 F_L^{1/3} A_r = 302.1 m^2,$$

$$\chi = \frac{\sum_{i=1}^{2} A_{0i}\sqrt{H_{0i}}}{A_{fuel}} = \frac{12.25}{302.1} = 0.04 < 0.081, Q = A_{fuel} \times 1.6 \times \chi = 19.6 MW, ,$$

$$t_D = \frac{1}{60} \times \frac{F_L A_r}{Q} = 115.8 \min, T_{f@t_D} = 1115.5^o C$$

(2) If three openings exist (one door and two windows) ,

$$F_L = 1270 MJ/m^2, A_r = 107.3 m^2, A_{fuel} = 0.26 F_L^{1/3} A_r = 302.1 m^2,$$

$$\chi = \frac{\sum_{i=1}^{3} A_{0i}\sqrt{H_{0i}}}{A_{fuel}} = \frac{21.78}{302.1} = 0.072 < 0.081, Q = A_{fuel} \times 1.6 \times \chi = 34.85 MW,$$

$$t_D = \frac{1}{60} \times \frac{F_L A_r}{Q} = 65.2 \min, T_{f@t_D} = 1225.8^o C$$

(3) If four openings exist(two doors and two windows) ,

$$F_L = 1270 MJ/m^2, A_r = 107.3 m^2, A_{fuel} = 0.26 F_L^{1/3} A_r = 302.1 m^2,$$

$$\chi = \frac{\sum_{i=1}^{4} A_{0i}\sqrt{H_{0i}}}{A_{fuel}} = \frac{28.1}{302.1} = 0.093, 0.081 < \chi < 0.1, Q = A_{fuel} \times 0.13 = 39.27 MW,$$

$$t_D = \frac{1}{60} \times \frac{F_L A_r}{Q} = 57.8 \min, T_{f@t_D} = 1195.8^o C$$

Note: the basic calculation in this section only have some referencing meanings since the calculating methods are mainly based on relatively small room tests (<50m2), single opening, single fire source (gas burner), whereas in our case the room (or apartment) floor area is more than 100 m2, the openings are more than one, the fire sources are multiple (20 gas burners). All these differences may have significant effects on the behavior of compartment fire.

APPENDIX 4

Pictures showing the flow of smoke and movement of persons for various scenarios over time

Please see a separate file with the name of “APPENDIX 4 for NASFM’s report”.

APPENDIX 5

Limitations of RISA software suite

Limitations of RISA Floor

RISA Floor is specifically used to design the floor systems and hence it has limited control over the analysis of a typical floor system requiring individual member results.

RISA Floor does not provide detailed set of results such as shear force, bending moment, stress profiles, ability to capture the stresses on the decking member etc.

A single element analysis in RISA floor fails to capture the effect of load redistribution due to the damaged walls.

Limitations of RISA 3D

Removing a wall in RISA Floor creates instability in the model and the analysis quits with an error.

Creating a large opening as a solution to instability increases the shear and bending forces on those walls.

Plywood decking is discontinuous – The decking plywood is not connected to the floor joists and plate analysis neglects axial deflections. Only shear deflections are considered. Hence plate deflections may not be accurate.

Using Moving Loads in combination with other loads does not analyze the decking plywood. The results are accurate for other members though.

Moving Loads can be assigned only it the joints that support a physical member,

APPENDIX 6

Load Redistribution Modelling Attempts

In order to assess the effect of load redistribution due to the walls structurally damaged in fire, the following options were tried to suitably alter the existing reduced section models.

Option 1: Simulating the complete loss of wall by removing it from the apartment

As shown in Figure 184 (a), the apartment wall was deleted from the original reduced section model (eg., RS-6), after wall showed inadequate axial capacity. The floor joists supported by the wall, which caused an instability due to the lack of supporting members were also removed. Under practical conditions, the roof roof joists show an excessive deflection or collapse when the supporting wall fails. In order to bypass the framing problem error, a dummy wall was added in the place of WP 12A. However, the analysis did not show any changes in the values of axial capacity in other walls because of the applied load. This confirms the shortcoming of the software to capture the load redistribution phenomenon.

Option 2: Simulating the degraded wall by modeling it as a wall with large opening

In the second attempt to model the failure of wall panels, the walls having inadequate axial capacity were provided with large openings as Shown in Figure 184 (b). However, the results obtained by running the analysis once again showed no changes from the original (reduced section) model, which was later confirmed that the program only considers the change in the shear capacity of the wall and not the axial capacity.

Hence, the load redistribution effect was unable to be captured by the reduced section models modified to include failure of walls.

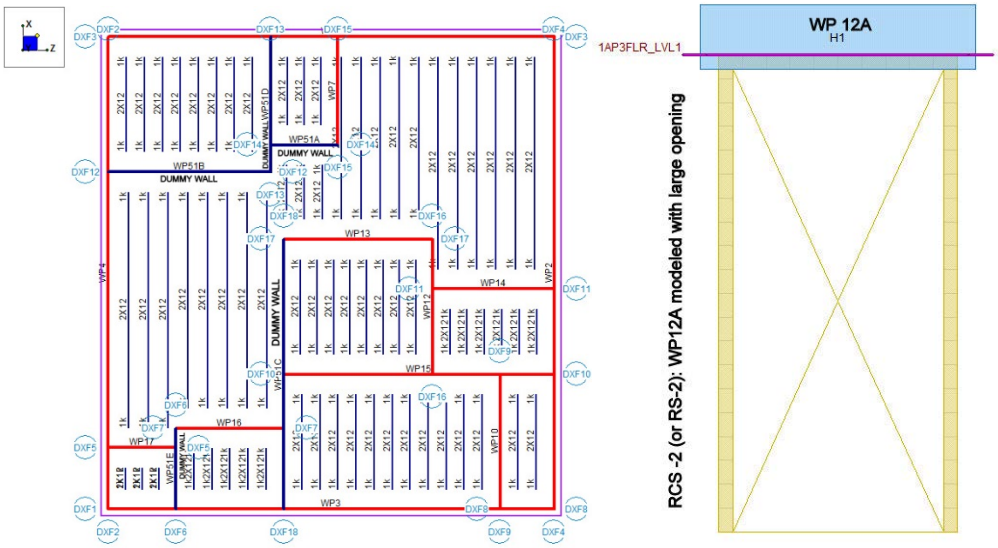

Figure 184. Analysis of a single apartment unit with load redistribution (a) Option 1: Removal of wall panel from the model (b) Option 2: Modeling the wall with a large opening

APPENDIX 7

Additional Results from RISA-3D Analysis – Stress Contours, Shear Forces and Bending Moments

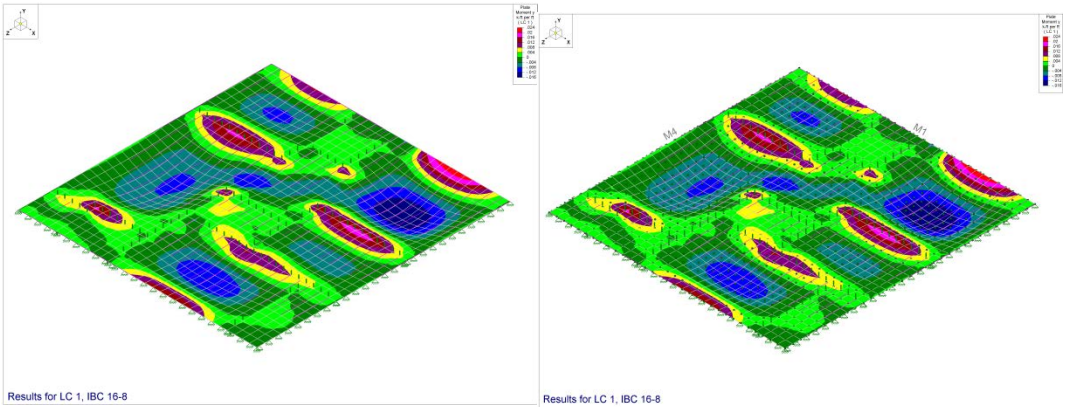

No Section Reduction

SR1: Char Depth = 0.25 in.

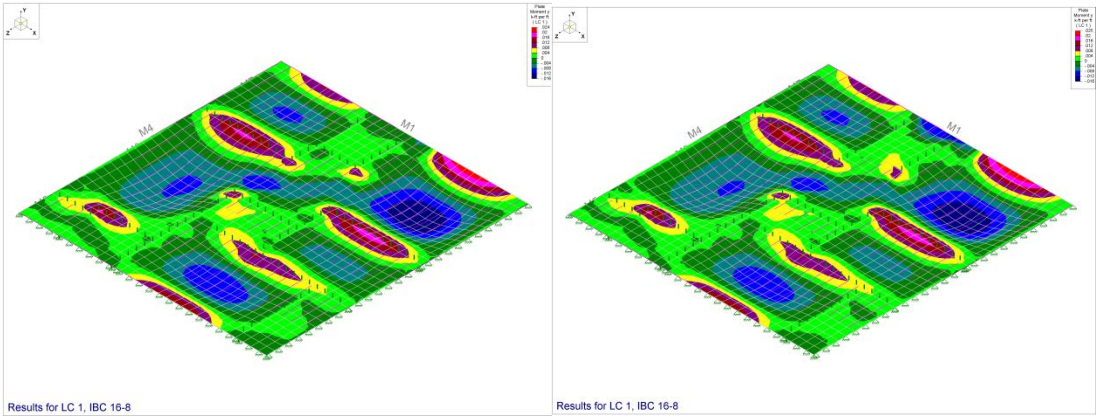

SR2: Char Depth = 0.5 in.

SR3: Char Depth = 0.75 in.

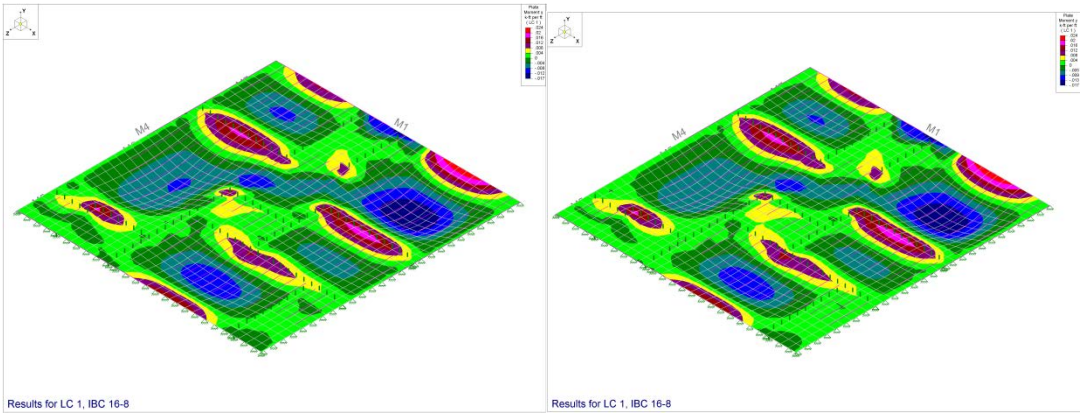

SR4: Char Depth = 1.0 in.

SR5: Char Depth = 1.25 in.

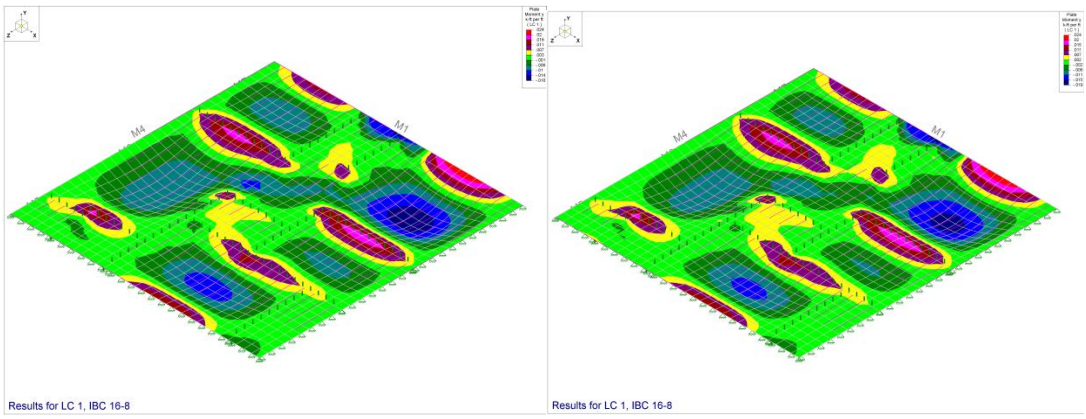

SR6: Char Depth = 1.5 in.

SR7: Char Depth = 1.75 in.

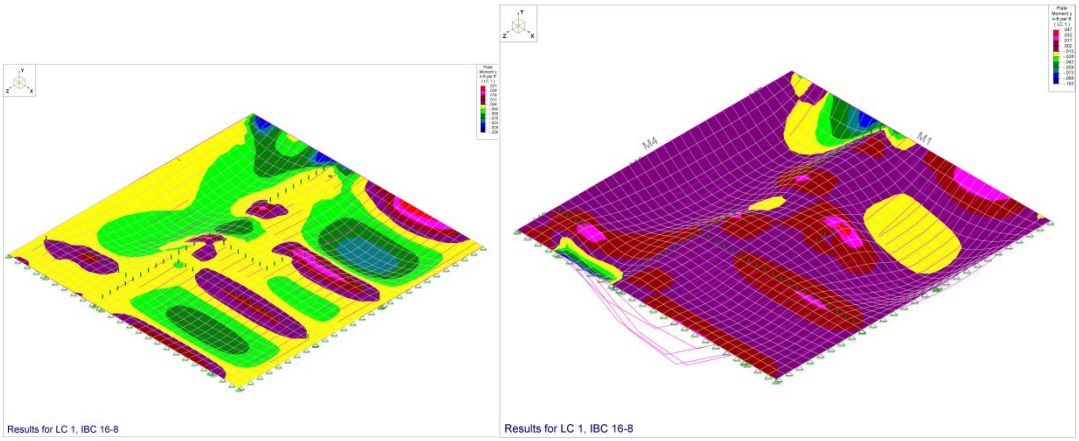

SR8: Char Depth = 2.0 in.

SR9: Char Depth = 2.25 in.

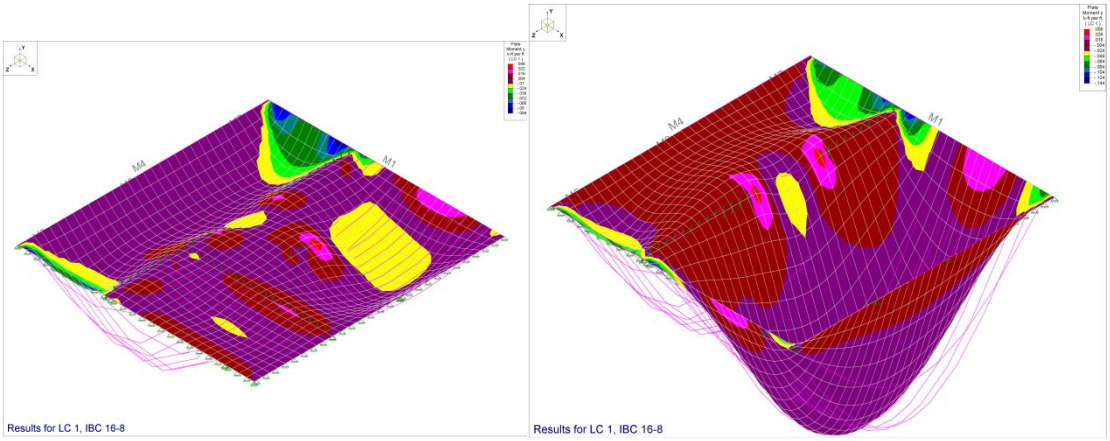

SR10: Char Depth = 2.5 in.

SR11: Char Depth = 2.75 in

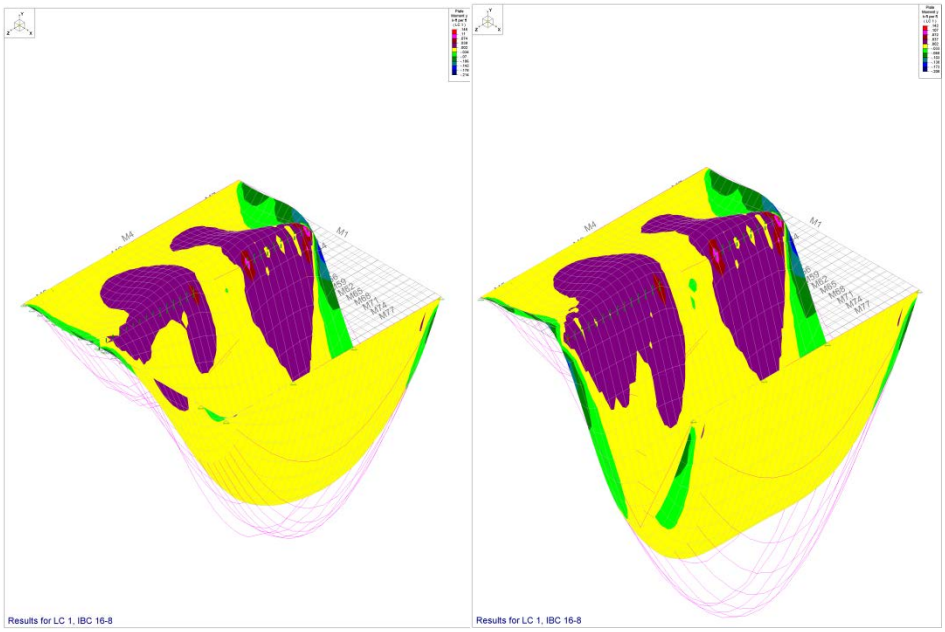

SR12: Char Depth = 3.0 in.

SR13: Char Depth = 3.25 in.

Figure 185. Development of plate moments on the single apartment floor due to reduced section and load redistribution

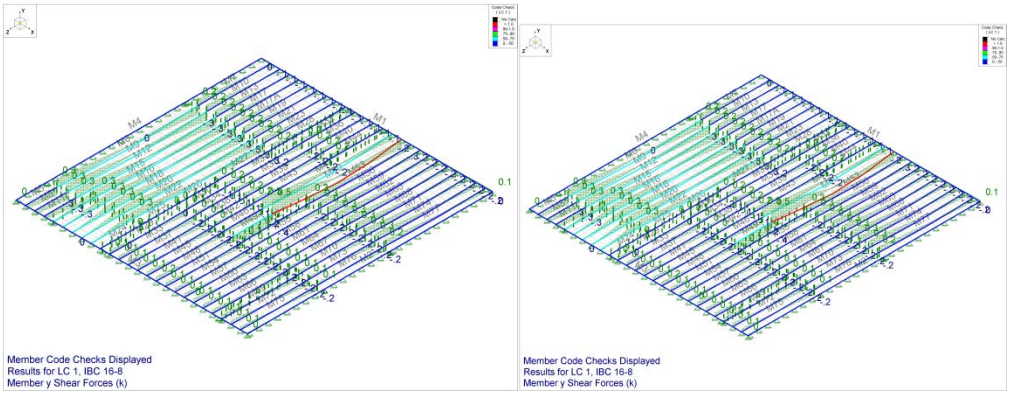

No Section Reduction

SR1: Char Depth = 0.25 in.

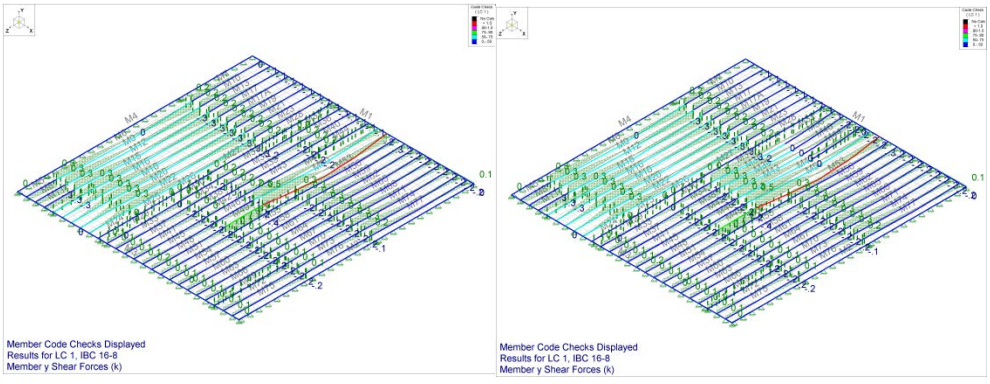

SR2: Char Depth = 0.5 in.

SR3: Char Depth = 0.75 in.

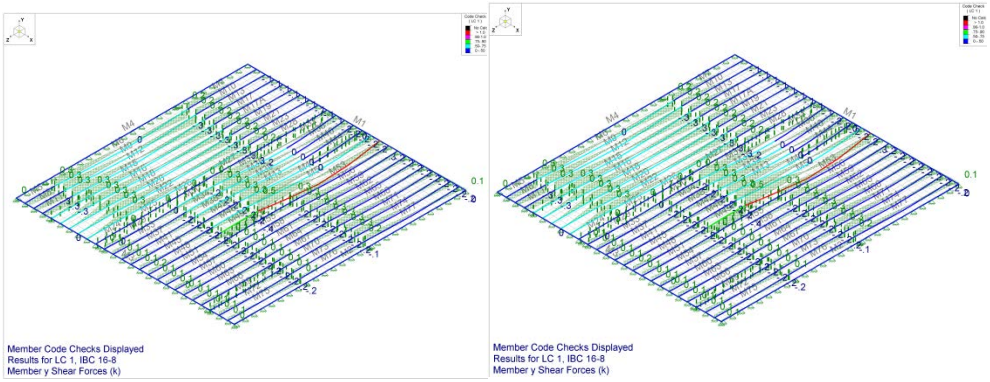

SR4: Char Depth = 1.0 in.

SR5: Char Depth = 1.25 in.

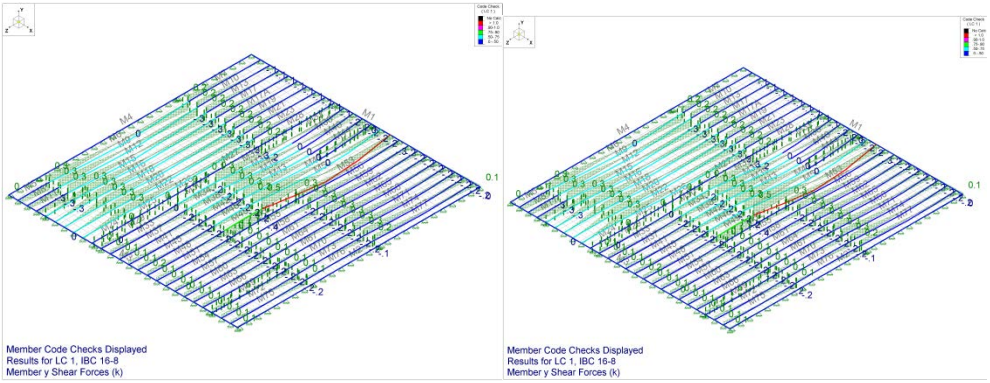

SR6: Char Depth = 1.5 in.

SR7: Char Depth = 1.75 in.

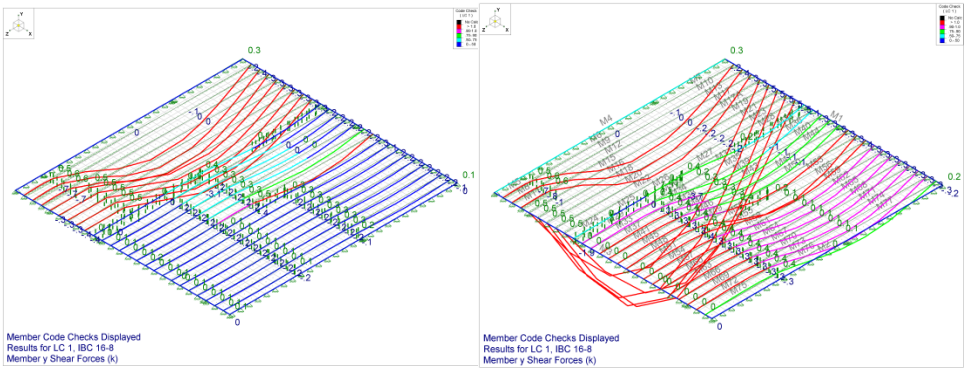

SR8: Char Depth = 1.25 in.

SR9: Char Depth = 1.75 in.

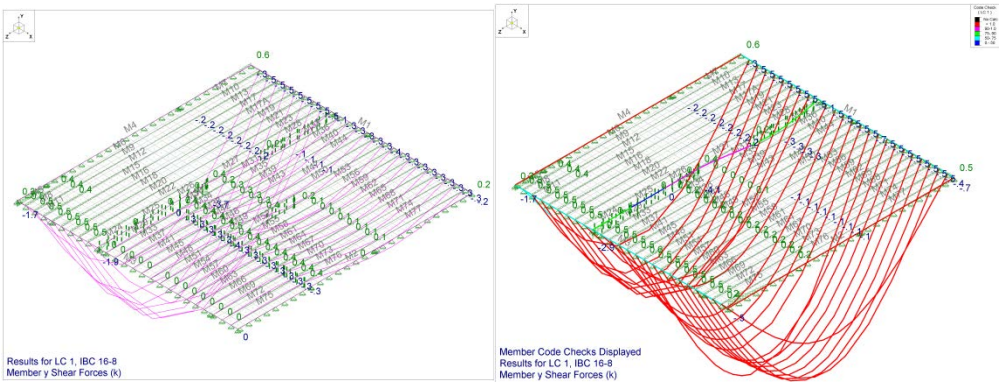

SR10: Char Depth = 2.0 in.

SR1: Char Depth = 2.25 in.

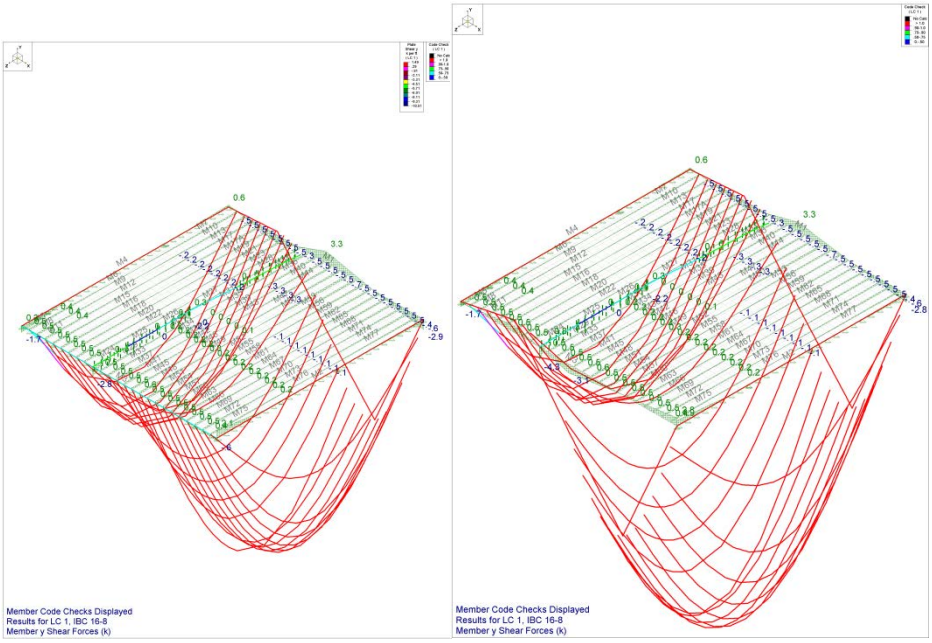

SR12: Char Depth = 0.5 in.

SR13: Char Depth = 0.75 in.

Figure 186. Shear forces single apartment floor due to reduced section and load redistribution

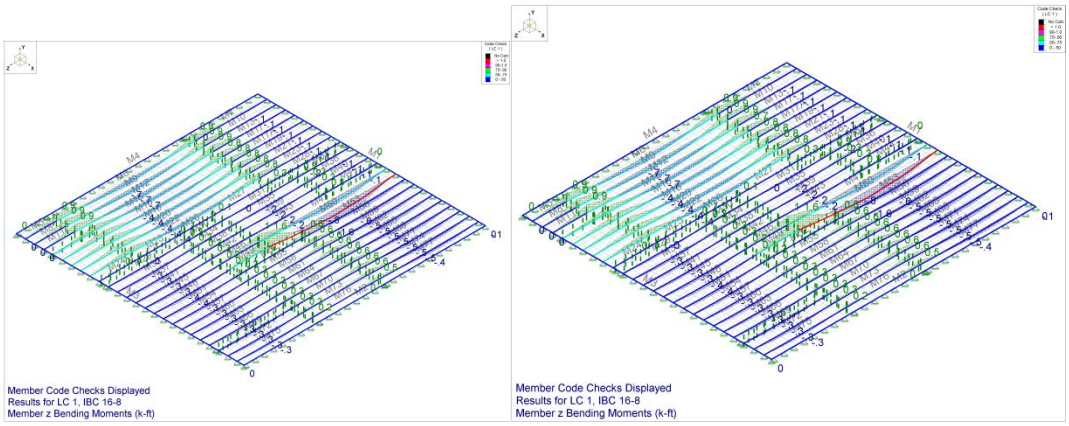

No Section Reduction

SR1: Char Depth = 0.25 in.

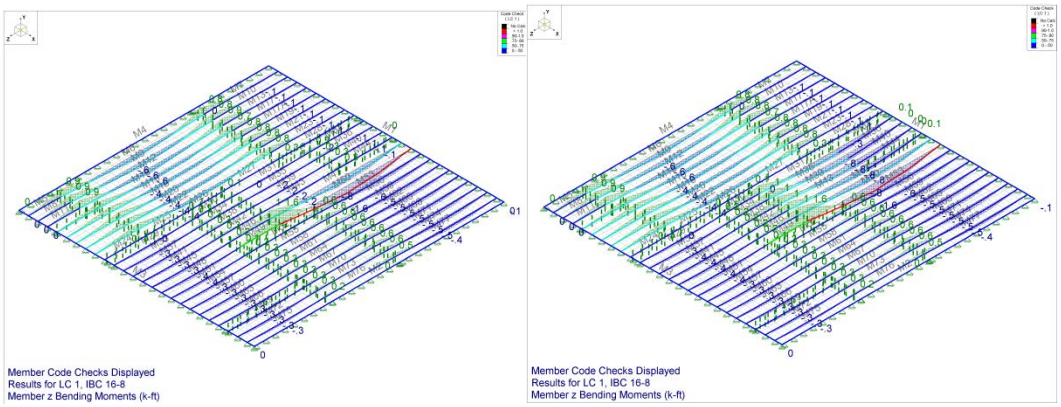

SR2: Char Depth = 0.5 in.

SR3: Char Depth = 0.75 in.

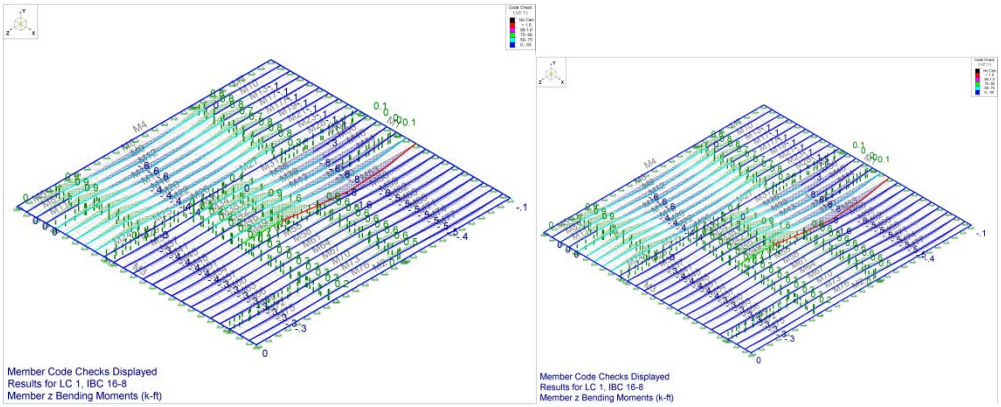

SR4: Char Depth = 1.0 in.

SR5: Char Depth = 1.25 in.

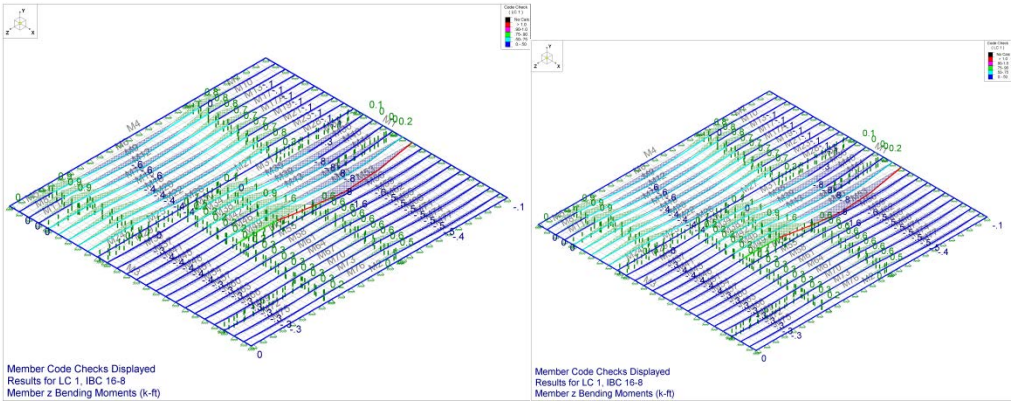

SR6: Char Depth = 1.5 in.

SR7: Char Depth = 1.75 in.

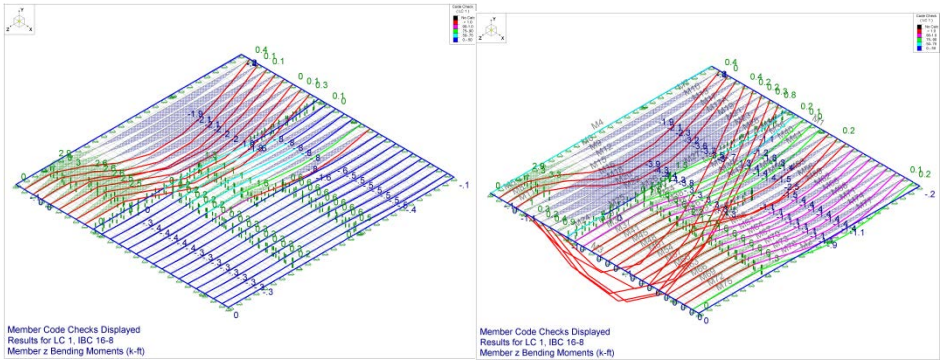

SR8: Char Depth = 2.0 in.

SR9: Char Depth =2.25 in.

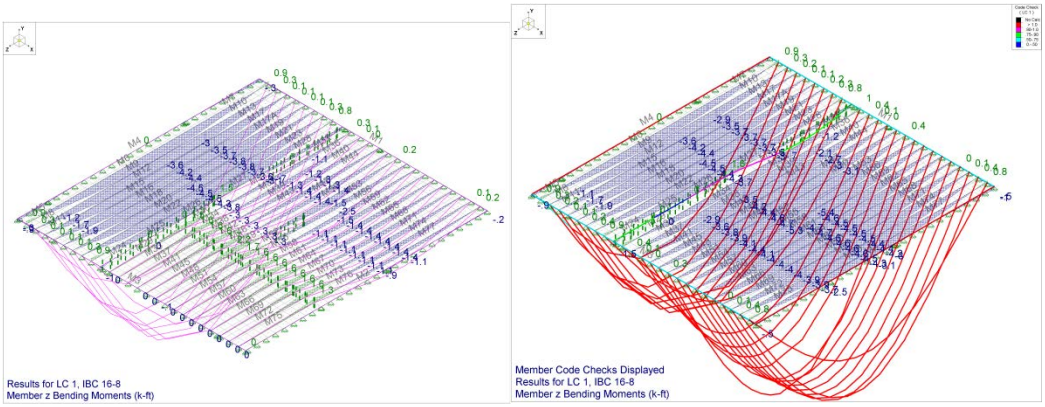

SR10: Char Depth = 2.5 in.

SR11: Char Depth = 2.75 in.

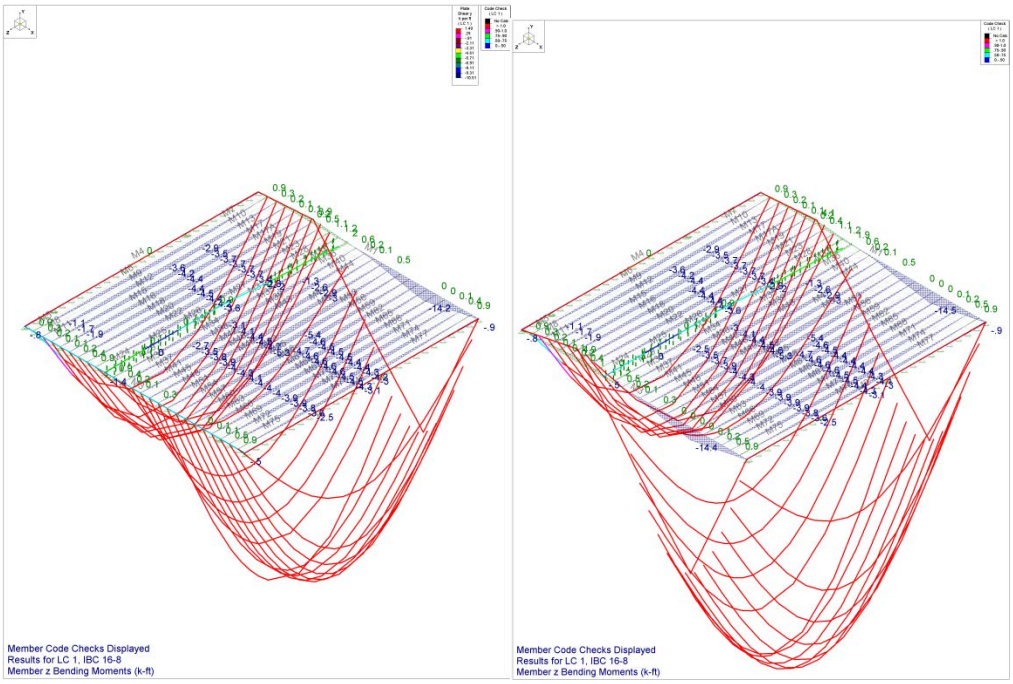

SR12: Char Depth = 3.0 in.
SR13: Char Depth = 3.75 in.

Figure 187. Bending Moments in the single apartment floor due to reduced section and load redistribution

REFERENCE

[1] RISA Technologies, Inc., RISA Software Suite, Verison 15.0.2 ed., Foothill Ranch, CA: RISA Technologies, Inc., 2016

[2] RISA Technologies, Inc., RISA Floor, Version 11.0.2 (64-bit) ed., Foothill Ranch, CA: RISA Technologies, Inc., 2016

[3] RISA Technologies, Inc., RISA-3D, Version 15.0.2 (64-bit) ed., Foothill Ranch, CA: RISA Technologies, Inc., 2016.

[4] Springer. SFPE Handbook of Fire Protection Engineering, Springer 5th edition, Page 3234, 2015

[5] NFPA, Standard for Determination of Fire Loads for Use in Structural Fire Protection Design (NFPA 557), 2016

[6] Springer. SFPE Handbook of Fire Protection Engineering, Springer 5th edition, chapter 64, 2015

[7] Jamie Vistnes, etc., 2005, IAFSS, A Stochastic Approach to Occupant Pre-movement in Fires

[8] NFPA, Standard for Fire Doors and Other Opening Protectives (NFPA 80), 2016

[9] B. J. Meacham, N. A. Dembsey, P. Kamath, M. J. Gollner, A. W. Marshall and P. Maisto, "Quantification of Green Building Features on Firefighter Safety: Final Report (Year 3 and Year 4) - EMW-2012-FP-01336," Worcester Polytechnic Institute, Worcester, MA, 2017